

Development and Performance Evaluation of an Adaptive MAC Protocol for MC-CDMA Wireless LANs with QoS Support

Von der Fakultät für Elektrotechnik und Informationstechnik der
Rheinisch-Westfälischen Technischen Hochschule Aachen zur Erlangung
des akademischen Grades eines Doktors der Ingenieurwissenschaften
genehmigte Dissertation

vorgelegt von

Diplom-Ingenieur
Georgios Orfanos

aus Athen

Berichter: Universitätsprofessor Dr.-Ing. Bernhard Walke
 Universitätsprofessor Dr. Petri Mähönen

Tag der mündlichen Prüfung: 19. Juni 2006

AACHENER BEITRÄGE ZUR MOBIL- UND TELEKOMMUNIKATION

Herausgeber:
Universitätsprofessor Dr.-Ing. Bernhard Walke

Bibliografische Information Der Deutschen Bibliothek

Die Deutsche Bibliothek verzeichnet diese Publikation in der Deutschen Nationalbibliografie; detaillierte bibliografische Daten sind im Internet über <http://dnb.ddb.de> abrufbar.

© 2006 Georgios Orfanos

1. Auflage 2006
ISBN: 3-86130-931-9
Aachener Beiträge zur Mobil- und Telekommunikation; Band 52

Wissenschaftsverlag Mainz
Süsterfeldstr. 83, 52072 Aachen
Telefon: 02 41 / 2 39 48 oder 02 41 / 87 34 34
Fax: 02 41 / 87 55 77
www.verlag-mainz.de

Herstellung: Druckerei Mainz GmbH,
Süsterfeldstr. 83, 52072 Aachen
Telefon 02 41 / 87 34 34; Fax: 02 41 / 87 55 77

Gedruckt auf chlorfrei gebleichtem Papier

"D82 (Diss. RWTH Aachen)"

To my parents
Kostantina and Ioanni

ABSTRACT

The Institute of Electrical and Electronics Engineers, Inc. (IEEE) standards 802.11a,e are currently established as worldwide standards for Wireless Local Area Networks (WLANs). Applying Carrier Sense Multiple Access with Collision Avoidance (CSMA/CA), the Distributed Coordination Function (DCF) and Enhanced Distributed Coordination Function (EDCF) protocols deploy minimum complexity in Medium Access Control (MAC), while the use of Orthogonal Frequency Division Multiplex (OFDM) in Physical layer (PHY), promises high data rates of up to 54 Mbit/sec.

The system throughput at MAC layer is though reduced both, from the overhead and in so called hot spot scenarios by the high number of collisions which limit the system's performance and consequently its Quality of Service (QoS) achievements. A possible improvement, is the application of a new multiple access method, namely Multi-Carrier Code Division Multiple Access (MC-CDMA). MC-CDMA is a novel, high capacity, multi-carrier modulation scheme, which is developing to a key radio transmission technology for future WLANs.

Besides the fact that its Bit Error Rate (BER) performance (in fully loaded indoor communication systems) is due to the spreading gain better than that of Orthogonal Frequency Division Multiple Access (OFDMA), when low or no mobility scenarios are considered, MC-CDMA can reduce the probability of collisions, due to its inherent characteristic of operating parallel, from spreading sequences distinguished, channels in the same frequency channel. Thus the system throughput enhances and the delay reduces. The system throughput profits further as spreading improves the ratio of frame length to guard intervals, thus implicitly reducing the overhead.

This thesis provides an overview of the MC-CDMA technique, and a performance evaluation in real multiuser transmission channel conditions. Further, the MC-CDMA is applied in the PHY of the IEEE 802.11a system. Accordingly, the needed modifications to the MAC protocol are done. In this respect, a new DCF for the MAC protocol is presented and evaluated, optimized for the multi channel structure of a MC-CDMA network, called Coded-Distributed Coordination Function (C-DCF), which achieves high

efficiency.

However in adhoc Code Division Multiplex Access (CDMA) networks near-far effects can block a receiver due to high interference. These effects occur when a receiving station is closer to an interferer than to its corresponding transmitter. Accordingly, the receiver cannot detect the intended signal out of the received one and the data transmission fails.

Therefore the distributed, WLAN, MAC protocol presented in this thesis is enhanced by adaptation algorithms, which mitigate the effects of the near-far problem, and allow WLANs to improve significantly their performance and achieve high efficiency even under heavy multiuser interference, as is typical for ad-hoc operation.

KURZFASSUNG

Die Standards 802.11a,e des Institute of Electrical and Electronics Engineers, Inc. (IEEE), sind heute als weltweite Standards für Wireless Local Area Networks (WLANs) etabliert. Die Anwendung von Carrier Sense Multiple Access with Collision Avoidance (CSMA/CA), minimiert sowohl bei Anwendung in Form des Distributed Coordination Function (DCF) als auch des Enhanced Distributed Coordination Function (EDCF) Protokolls, die Komplexität des Medium Access Control (MAC) Protokolls, wobei mit dem Orthogonal Frequency Division Multiplex (OFDM) Verfahren im Physical layer (PHY) Datenraten bis 54 Mbit/sec erreicht werden können.

Der Systemdurchsatz wird erheblich durch den grossen Overhead Anteil und (in hot spot Szenarien) durch die grosse Anzahl von Kollisionen von Paketübertragungsversuchen beschränkt. Dies limitiert die Leistung des Systems und seine Möglichkeiten Dienstgüte zu unterstützen erheblich. Eine mögliche Verbesserung stellt die Anwendung eines neuen Vielfachzugriffverfahrens dar: Multi-Carrier Code Division Multiple Access (MC-CDMA). MC-CDMA ist ein Multiträgerverfahren, das mit seiner grossen Kapazität erwarten lässt eine wichtige Technik für zukünftige WLANs zu werden.

Die Leistung des neuen Verfahrens in der physikalischen Schicht ist wegen des Spreizgewinns (unter voller Last in einem stationären oder quasi-stationären Kommunikationssystem) besser als Orthogonal Division Multiple Access (OFDMA). Ausserdem hat MC-CDMA die Fähigkeit, die Kollisionswahrscheinlichkeit zu senken, weil es den Frequenzkanal in mehrere parallele, im Codebereich von einander getrennte Kanäle teilt und Kanalzugriffe parallelisiert, wodurch der Systemdurchsatz erhöht wird. Der Durchsatz steigt ausserdem, weil das Spreizverfahren das Verhältnis von Rahmenlänge zu den Schutzzeiten des Protokolls verbessert, was eine implizite Verkleinerung des Overhead bedeutet.

Diese Arbeit liefert einen Überblick vom MC-CDMA, und eine Leistungsbewertung des Verfahrens unter realistischen Betriebsbedingungen mit mehreren gleichzeitigen Übertragungen verschiedener Nutzer. MC-CDMA wird in der physikalischen Schicht eines IEEE 802.11a Systems angewendet, wobei die nötigen Modifikationen im MAC Protokoll gemacht werden. Es wird eine neue DCF für das MAC Protokoll präsentiert, nämlich

die Coded-Distributed Coordination Function (C-DCF), die für die Multi-kanalstruktur des MC-CDMA Netzes optimiert ist und eine hohe Effizienz erzielt.

In verteilten adhoc Code Division Multiplex Access (CDMA) Netzen können near-far Effekte einen Empfänger blockieren. Diese Effekte treten auf, wenn eine Empfangsstation näher zu einer interferierenden Station liegt als zu ihrem korrespondierenden Sender. Dementsprechend, kann die Empfangsstation das beabsichtigte Signal aus dem Empfangssignal nicht dekodieren und die Datenübertragung scheitert.

Um dieses Problem zu beseitigen, wird das verteilte WLAN MAC Protokoll, das in dieser Arbeit vorgestellt wird, um Adaptivitätsregeln erweitert, die die Effekte des near-far Problems mässigen, und dem drahtlosen System ermöglichen, seine Leistung bedeutend zu verbessern, sodass eine hohe Effizienz, auch unter hoher Multiuser-Interferenz, erreicht werden kann.

CONTENTS

| | |
|---|------------|
| Abstract | v |
| Kurzfassung | vii |
| 1 Introduction | 1 |
| 1.1 Motivation and Objectives | 1 |
| 1.2 Outline | 3 |
| 1.3 Contributions Made by this Thesis | 5 |
| 2 IEEE 802.11a | 7 |
| 2.1 MAC Protocol | 8 |
| 2.1.1 Interframe Spaces | 9 |
| 2.1.2 Distributed Coordination Function | 9 |
| 2.1.3 Collision Avoidance | 10 |
| 2.1.4 Acknowledgement and Collisions | 10 |
| 2.1.5 The RTS/CTS Handshake | 11 |
| 2.1.6 Hidden and Exposed Mobile Stations | 12 |
| 2.1.7 Synchronization over Beacons | 14 |
| 2.1.8 Point Coordination Function | 14 |
| 2.1.9 MAC Frame Formats | 15 |
| 2.2 OFDM PHY Layer | 17 |
| 2.2.1 IEEE 802.11a PHY Layer Parameters | 19 |
| 2.2.2 PHY Frame Format | 20 |
| 3 Multi-Carrier Code Division Multiple Access | 21 |
| 3.1 Multiple Access Schemes | 21 |
| 3.2 Direct Sequence-Code Division Multiple Access | 23 |
| 3.3 Multi-Carrier CDMA Schemes | 25 |
| 3.4 Principles of MC-CDMA | 26 |
| 4 Evaluation of the MC-CDMA Physical Layer Performance | 31 |
| 4.1 Calculation of SINR | 32 |
| 4.2 An Upper Bound for PER | 34 |

| | | |
|----------|--|-----------|
| 4.2.1 | Symbol Error Rate | 34 |
| 4.2.2 | Bit Error Rate | 35 |
| 4.2.3 | Packet Error Rate | 35 |
| 4.3 | Simulation Results | 37 |
| 4.4 | Conclusion | 40 |
| 5 | C-DCF: cch selection on Connection Basis | 43 |
| 5.1 | Protocol Description | 43 |
| 5.1.1 | The Codechannel | 44 |
| 5.1.2 | Selection of a Cch | 44 |
| 5.1.3 | Medium Sensing | 45 |
| 5.1.4 | Collision Avoidance | 46 |
| 5.1.5 | The RTS/CTS Handshake Extension | 46 |
| 5.1.6 | Asynchronous Packet Transmission | 47 |
| 5.1.7 | Collisions | 49 |
| 5.2 | Transmit Power Control | 49 |
| 5.2.1 | Interference Estimation Algorithm | 50 |
| 5.2.2 | Extended Frame Formats | 51 |
| 5.2.3 | Power Adjustment Algorithm | 52 |
| 5.3 | Improved Handshake - Adaptation to Suitable Cch | 55 |
| 5.4 | Frequency adaptation - 2nd adaptation method | 59 |
| 5.4.1 | The Frequency Adaptation Algorithm | 61 |
| 5.5 | Performance Analysis and Comparison with the Standard DCF | 64 |
| 5.5.1 | Performance analysis in a wideband channel | 67 |
| 6 | The MACNET2 Simulation Tool | 71 |
| 6.1 | SDL Modules - Protocol Specification | 72 |
| 6.2 | SPEETCL | 73 |
| 6.3 | C++ Modules | 73 |
| 6.3.1 | Traffic Load Generators | 74 |
| 6.3.2 | Interference Calculation | 74 |
| 6.4 | Validation | 76 |
| 7 | C-DCF Performance Evaluation: cch selection on Connection Basis | 79 |
| 7.1 | Basic MAC | 79 |
| 7.1.1 | Basic MAC queueing delay evaluation in a wideband channel | 88 |

| | | |
|-----------|---|------------|
| 7.2 | Transmit Power Control Analysis | 89 |
| 7.3 | Improved Handshake - Adaptation to Suitable Cch | 97 |
| 7.4 | Frequency Adaptation - Adaptation to Suitable Frequency Channel | 107 |
| 7.5 | Conclusion | 116 |
| 8 | C-DCF: cch selection on Frame Basis | 119 |
| 8.1 | Parallel Backoff | 121 |
| 8.2 | Smart Backoff | 124 |
| 8.3 | Performance Evaluation | 126 |
| 8.4 | Prioritized Access | 132 |
| 8.5 | Conclusion | 135 |
| 9 | Cross Layer Optimization of the C-DCF | 137 |
| 9.1 | Isochronous Packet Transmission | 137 |
| 9.2 | Performance Evaluation | 139 |
| 9.2.1 | The impact of cross layer synchronization in larger scenarios | 144 |
| 9.3 | Conclusion | 147 |
| 10 | MAC Extensions for Multihop | 149 |
| 10.1 | Multihop MAC Protocol | 150 |
| 10.1.1 | SDL specification of multihop extensions to C-DCF | 152 |
| 10.2 | Performance Evaluation | 156 |
| 10.2.1 | The Bottleneck Case | 156 |
| 10.2.2 | Multihop Network Performance Study | 159 |
| 10.2.3 | Simulative Comparison with IEEE 802.11 DCF | 164 |
| 10.3 | Conclusion | 166 |
| 11 | Centralized Mode of the C-DCF | 171 |
| 11.1 | The Contention Free Period | 171 |
| 11.2 | Capacity Analysis and Comparison with IEEE 802.11e | 174 |
| 11.3 | Performance Evaluation | 178 |
| 11.4 | Conclusion | 183 |
| 12 | Conclusion | 185 |
| A | Derivation of a Closed Form Expression for the Demodulator Out- puts | 189 |

| | |
|--------------------------------------|------------|
| List of Figures | 191 |
| List of Tables | 201 |
| Glossary | 203 |
| Nomenclature | 205 |
| List of Abbreviations | 209 |
| List of Unpublished Documents | 213 |
| Bibliography | 215 |
| Index | 223 |
| Curriculum vitae | 229 |
| Acknowledgement | 231 |

Introduction

Content

| | |
|---|---|
| 1.1 Motivation and Objectives | 1 |
| 1.2 Outline | 3 |
| 1.3 Contributions Made by this Thesis | 5 |

1.1 Motivation and Objectives

A mobile adhoc network, is a system of autonomous mobile terminals connected by wireless links. Being independent of any infrastructure, these networks have the ability to be deployed easily, fast and cost efficient. The objective of this thesis is to exploit the advantages of the application of *Code Division Multiple Access* (CDMA) in the lower layers of such networks.

In next generation mobile networks (beyond 3G, 4G), it is expected that traffic will be a mixture of diverse traffic classes, such as data and multimedia, each posing different *Quality of Service* (QoS) demands. Adhoc wireless networks should be able to deal with all these traffic classes efficiently and achieve high capacity. Due to this variability of demands on the network, new adaptive *Medium Access Control* (MAC) protocols appear necessary to be developed, taking into consideration the peculiarities of adhoc networks. Such networks are self organizing and independent from the support of central controlling instances.

Currently, the worldwide standards for decentralized *Wireless Local Area Network* (WLAN)s are IEEE 802.11a [802.11A /D7 (1999)] and IEEE 802.11g [802.11G (2003)], operating in 5 and 2.4 GHz, respectively. They have dominated the market for WLANs and gained a lot of attention from the research community. Depending on the link quality, the channel throughput can be up to 54 Mbit/sec. Realistic values though, in multiuser scenarios are limited by the interference below 36 Mbit/sec.

Besides that, the throughput at MAC level is limited by the high overhead, the guard intervals and collisions of frames. The practically achievable efficiency is therefore further lowered. In order to meet the future demands of delay sensitive applications and provide enough capacity to support many users, enhancements are needed.

Based on a combination of *Time Division Multiple Access* (TDMA) and *Frequency Division Multiple Access* (FDMA), IEEE 802.11a applies *Orthogonal Frequency Division Multiplexing* (OFDM) in the *Physical Layer* (PHY) layer to achieve a high spectral efficiency. Although *Multi-Carrier* (MC) based transmission systems are known for years [LINDNER (1996)], OFDM has only been recently accepted for WLANs as a high capacity modulation scheme, which can mitigate inter-symbol interference, caused by the high bit-rates of modern telecommunication systems.

Another efficient approach used in 3G systems is CDMA. A technique, where the frequency channel is divided in many parallel subchannels, separated from each other by orthogonal spreading sequences, called *code channels* (cchs). The energy of the transmitter is spread over the whole system bandwidth, either in time domain using narrow pulses (*Wideband-Code Division Multiple Access* (W-CDMA)), or in the frequency domain using a set of subcarriers for the parallel transmission of the chips belonging to the same modulated symbol, known as *Multi-Carrier Code Division Multiple Access* (MC-CDMA).

In adhoc CDMA networks, *Mobile Stations* (MSs) transmit at the same time over the same frequency band, without the need of synchronization among the different transmitters, or central control of resources. A receiving station correlates the wideband received signal with the spreading code identifying the signal from the intended transmitter and gets the narrowband information signal. The rest is considered as *Multiple Access Interference* (MAI).

CDMA is an interference limited system, meaning that there can exist parallel transmissions, until the energy of the received narrowband signal is well above the interference level, for the detector to correctly detect the encoded information. For this reason and in order to maximize the capacity, a good power control scheme and a *Multiuser Detector* (MUD) are needed. Power control is needed for minimizing the emissions in the channel and MUD to suppress MAI.

Since it has been shown that MC-CDMA can outperform OFDM [LINDNER (2001)] in link level, it is a promising candidate for future WLANs.

Further, MC-CDMA provides one more degree of freedom, the code domain, which can be used to optimize the performance of the network. These advantages of MC-CDMA are deployed in this thesis for the design of a suitable adaptive MAC protocol for the next generation of WLANs.

1.2 Outline

This thesis is outlined as follows. Chapter 2 presents an overview of the IEEE 802.11a WLAN. Its *Distributed Coordination Function* (DCF) is the basis for the suggested protocols in this thesis. Additionally a short description of OFDM modulation is given, as an introduction to multi-carrier modulation and MC-CDMA.

In Chapter 3, the MC-CDMA scheme is described. After a brief introduction on different variations of MC-CDMA, the basic characteristics of the scheme used in this thesis are discussed. Further, the performance of MC-CDMA is evaluated in Chapter 4, under real channel conditions, while the parameters of the IEEE 802.11a [802.11A /D7 (1999)] and a *Minimum Mean Square Error* (MMSE) MUD are assumed.

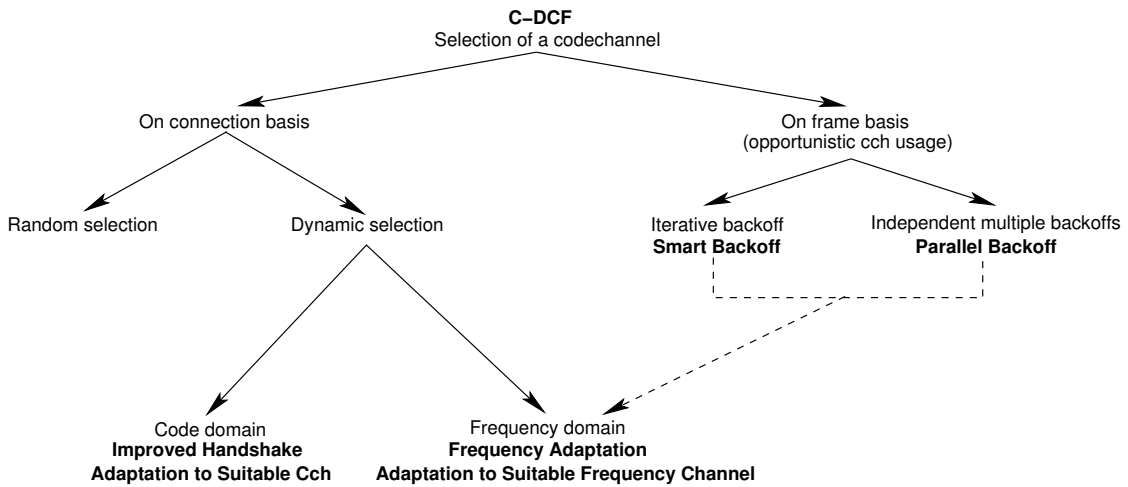


Figure 1.1: Overview of the C-DCF functions for codechannel selection.

The main functionality of the proposed modified DCF with support for the MC-CDMA PHY layer, namely *Coded-Distributed Coordination Fun-*

tion (C-DCF), can be divided in two categories, according to the transmitter's selection of a *code channel* (cch) for establishing the connection:

- Selection of a cch on connection basis.
- Selection of a cch on frame basis.

An overview of the C-DCF functionality for codechannel selection is given in Fig. 1.1.

A detailed presentation of the C-DCF functionality for the case of cch selection on connection basis is given in Chapter 5. The DCF is extended to support the multi-channel structure of the spread spectrum system and is enhanced with *Transmit Power Control* (TPC). An improved handshake procedure introduced in this chapter, constitutes the first improvement in form of a code adaptation function of the proposed protocol, which allows the coexistence of many high capacity connections in one frequency channel by avoiding large MAI. Another improvement is introduced, in terms of a second adaptation rule of the suggested protocol, consisting of frequency divergency for connections blocked by near-far problems. Additionally, a theoretical analysis and comparison with the OFDM based system is provided.

Chapter 6 gives a description of the event driven simulation tool used for the performance evaluation of the suggested protocols. The results of analysis and simulations for the protocols in Chapter 5 are discussed in Chapter 7.

The C-DCF functionality is extended in Chapter 8 for cch selection on frame basis (see Fig. 1.1). New backoff algorithms, optimized for a multi-channel WLAN are presented, evaluated and compared.

Protocol's performance in large multi user scenarios is further enhanced by applying cross layer optimization of the C-DCF protocol, as presented and discussed in Chapter 9.

In Chapter 10, the proposed protocol is extended with relaying functionality for the operation under multihop transmission, while Chapter 11 presents a further extension of the proposed protocol, namely a centrally controlled operating mode, for the efficient support of *Access Points* (APs). The final chapter of the thesis draws the conclusions.

1.3 Contributions Made by this Thesis

The goal of this thesis is to conduct research in new fields of wireless communications, such as MAC protocols for MC-CDMA based WLANs and provide solutions to some of existing impairments in this area. Following goals have been achieved:

- In Section 5.5, the benefits of spread spectrum application in high capacity WLANs are shown. Spreading effectively reduces overhead, by expanding the duration of data packets. Further, contention among *Mobile Station* (MS)s is substantially reduced, since MSs are distributed to more than one channel.
- The multi-channel structure of the MC-CDMA PHY layer, is used advantageously in Chapter 8, where the newly developed Parallel Backoff and Smart Backoff algorithms provide both, prioritized access to some MSs and load smoothing among cchs.
- The phenomenon of blocked connections due to high MAI, especially in ad-hoc WLANs, is also addressed in this thesis. Two solutions for avoiding blocking, consisting of different adaptation functions are proposed and investigated. The improved handshake and frequency adaptation functions enable the support of QoS even under high MAI.
- By proper choice of the protocol's parameters, the performance can be optimized. In Chapter 9, the proposed parameter setup enhances system's synchronization. The applied MUD benefits from reduced timing misalignments of different users' signals, and MAI is reduced, thus network performance enhances.
- The availability of multiple cchs in conjunction with MS prioritization (Smart Backoff) has been used for realization of effective, layer-2, forwarding techniques. The proposed protocols show good performance in multihop environments exploiting low transmission latency.
- In Chapter 11, a centralized mode for the proposed system is presented. The newly introduced medium sharing between *Contention Period* (CP) and *Contention Free Period* (CFP) in time and code domain, improves the coexistence of these operating modes. The network capacity during CFP is higher than in CP, due to less overhead and a better QoS can be achieved there. Capacity is further increased by introducing application data oriented requests of MSs that replace the request per data packet. Consequently, cumulative packet access

grants are used by the *Access Point* (AP), set per cch, that include consideration of forthcoming data frame transmissions.

The applicability of the above achievements, is not restricted to MC-CDMA based systems. Many of the proposed protocol aspects can be combined with other *Spread Spectrum* (SS) techniques, resulting to equivalent achievements. Additionally, many of the proposed protocols, can be applied, with some modifications, to other WLANs with multi-channel structure, which does not necessarily emerge from a spread spectrum based PHY layer.

IEEE 802.11a

Content

| | |
|--------------------------|----|
| 2.1 MAC Protocol | 8 |
| 2.2 OFDM PHY Layer | 17 |

The standard IEEE 802.11 was published in 1997 from the IEEE Computer Society, specifying the MAC and PHY layer of a WLAN, aiming at providing wireless connectivity within a local area. The standard supports both, ad hoc and infrastructure based networks, with associated low mobility MSs. Its architecture is hierarchical with basic element the *Basic Service Set* (BSS), consisting of several MSs, operating according to one of the two specified coordination functions. The elementary BSS is called *Independent Basic Service Set* (IBSS) and comprises at least two MS operating in adhoc mode.

It is possible that MSs within a BSS are also parts of a distributed system, which is not specified in the standard. Those MSs, called APs, are operating as connection nodes between different BSSs, over the distribution system. The interconnected BSSs form consequently an *Extended Service Set* (ESS).

The standard defines the functionality of MSs in the MAC sublayer of the *Data Link Control* (DLC) layer and of PHY layer. The reference model is given in Fig. 2.1.

The MAC sublayer functionality is described mainly by the two coordination functions, namely DCF and *Point Coordination Function* (PCF). The PHY layer is divided in the *Physical Layer Convergence Protocol* (PLCP) and *Physical Medium Dependent* (PMD) sublayer. Latter, provides means of transmitting and receiving data over a channel between two or more MSs. The PLCP sublayer constitutes a convergence sublayer, which allows the MAC to operate with minimum dependence on the PMD sublayer. This functionality in the sublayer simplifies the PHY service interface to the MAC services.

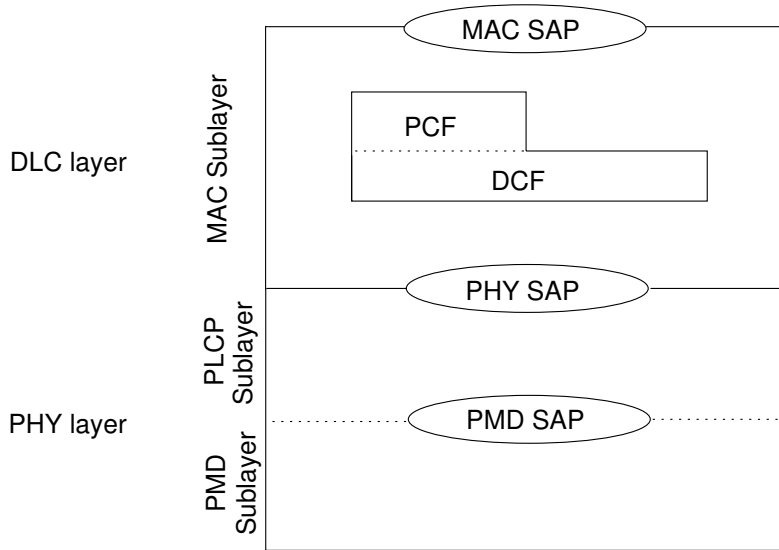


Figure 2.1: ISO/OSI equivalent of IEEE 802.11.

The standard [802.11 (1999)] specifies the use of *Frequency Hopping-Spread Spectrum* (FH-SS) and *Direct Sequence-Spread Spectrum* (DS-SS) in the 2.4 GHz *Industrial Scientific and Medical bands* (ISM), which allows a maximum transmission ratio of 2 Mbit/sec.

In order to meet the demands of new applications for higher transmission rates, a revised version of the standard [802.11 (1999)] together with the specification of a high-speed PHY layer in the 5 GHz *Unlicensed-National Information Infrastructure* (U-NII) band [802.11A /D7 (1999)] is available since 1999. The PHY layer characteristics of the IEEE 802.11a standard, were later used for the definition of a further higher data rate extension in the 2.4 GHz band, forming standard IEEE 802.11g [802.11G (2003)]. A brief description of the standard is given in the following sections.

2.1 MAC Protocol

The rules of medium access are described in two functions. The DCF for distributed systems and asynchronous data transfer, and PCF for contention free frame transfer. PCF is an optional operating mode for QoS support, based on the DCF (Fig. 2.1), which was not implemented by the industry, due to its higher complexity.

The MAC protocol is based on TDMA and prioritization on medium access is achieved by the use of different *InterFrame Spaces* (IFS).

2.1.1 Interframe Spaces

The time interval between two subsequent frames is called IFS. Four different types of IFS are defined, which provide different priority for channel access. Their duration is given in the following for the IEEE 802.11a protocol.

1. The reply by a MS to a previously received frame follows after *Short InterFrame Space* (SIFS), the shortest IFS. Its duration is $16 \mu\text{sec}$ and is mainly defined by the transceiver turnaround time, the *Radio Frequency* (RF) and MAC processing delay.
2. The second IFS used is *Distributed Coordination Function InterFrame Space* (DIFS), with duration $34 \mu\text{sec}$. It comprises mainly the time needed for the sensing mechanism to determine whether the channel is free or not. The SIFS period is shorter than DIFS in order to give MSs, which respond to a prior frame reception, a higher priority for channel access, compared to MSs that initiate a data packet transfer.
3. The interval *Point Coordination Function Interframe Space* (PIFS) is used by stations operating under the PCF. With a duration of $25 \mu\text{sec}$, PIFS allows them to gain prioritized access to the medium, to be able to control a CFP.
4. The *Extended InterFrame Space* (EIFS) is used in DCF instead of DIFS, when a frame at a MS was received with an incorrect *Frame Check Sequence* (FCS) sequence. The EIFS duration of about $200 \mu\text{sec}$ gives other MSs a higher priority for channel access before the affected MS is permitted to initiate a transmission. The reception of a correct frame terminates the EIFS.

2.1.2 Distributed Coordination Function

Under DCF operation, MSs apply *Carrier Sense Multiple Access with Collision Avoidance* (CSMA/CA), a nonpersistent CSMA technique [TANENBAUM (1996)], as a channel access procedure. A MS ready to transmit monitors the channel for the time duration DIFS in order to determine whether it is free or not. In OFDM networks, channel sensing is equal to measurements of the channel's signal strength level. Should the detected

level not exceed the threshold of $-88dBm$ for the duration of DIFS, the channel is concluded by a MS to be idle. The MS initiates the Collision Avoidance (CA) procedure. In order for two or more MSs, to avoid a collision, a MS is not allowed to start a transmission immediately after the medium is detected idle, but after a randomly chosen time duration, called backoff time.

If the medium is detected as busy, the MS has to wait until the channel becomes idle again.

2.1.3 Collision Avoidance

The collision avoidance procedure is based on the so called backoff procedure. After detecting the medium as idle, the MS defers for a random backoff interval. The duration of this interval is calculated by the product of a random integer number and the slot duration, which is set to $9\mu sec$. The random number is drawn from the interval $[0, CW]$, where CW is the Contention Window (CW) size, maintained at each MS separately. The starting value of CW is $CW_{min} = 7$. After every collision, the value of CW is increased. Its values are "sequentially ascending integer powers of 2, minus 1" [802.11 (1999)], with maximum value of $CW_{max} = 1023$. After a collision resolution, CW is set again to CW_{min} .

If during the backoff countdown, carried out in steps of $9\mu sec$, of MS 1 another MS 2 starts a transmission, then the countdown at MS 1 is interrupted. MS 1 defers until the end of any other transmissions, and after detecting the medium idle again, continues its countdown for the remaining backoff interval (Fig. 2.2).

2.1.4 Acknowledgement and Collisions

A received data frame is acknowledged in case of correct reception by an Acknowledgement (ACK) frame, sent from the receiver with a delay SIFS after reception's end. Even if a MS doesn't have any other data packets in the queue waiting for transmission, after the reception of ACK it initiates a backoff procedure. This backoff is referred to as "post-backoff" [MANGOLD (2003)] and guarantees that any frame, with the only exception of the first data packet of a burst arriving in a MS in idle state, will be transmitted after a backoff procedure. "Post-backoff" enhances the system's fairness, and improves the service time in networks with lower load.

Should two or more stations access the same frequency channel at the same time, a collision occurs. A retransmission attempt in each collided MS is started after backoff. Depending on the frame size, the number of retransmission attempts is limited. For data frames, shorter than an implementation dependent threshold, the *Short Retry Counter* (SRC) is used to denote the number of unsuccessful transmissions for the same data frame, including the unsuccessful transmissions of *Ready To Send* (RTS) frames. The maximum value of SRC is 7. For long data frames respectively, the *Long Retry Counter* (LRC) with maximum value 4 is applied. After a successful transmission both these counters are reset.

Figure 2.2 gives an example of data transfer based on DCF. MS 1 transmits a data frame after a backoff of 3 time slots, while MS 2 defers after counting down one of its four time slot long backoff. It continues its count-down after the medium is detected idle for time DIFS, and wins the contention with MS 1. In the last transmission of the example in Fig. 2.2, the same backoff duration at MS 1 and MS 3 leads to a collision of transmitted data frames.

2.1.5 The RTS/CTS Handshake

The DCF allows optionally the use of a handshake between transmitter and receiver, before the transmission of the actual data frame. If the data

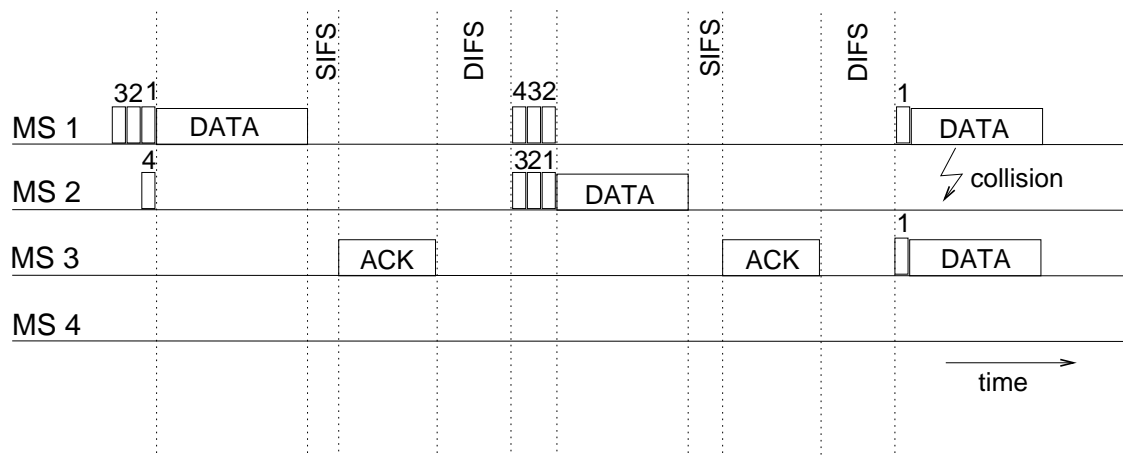


Figure 2.2: Distributed Coordination Function.

frame is larger than a certain threshold, which is not defined in the standard and is therefore implementation depended, the transmitting MS transmits a RTS frame when backoff reaches zero. This frame informs both, the intended receiver and MSs in the neighborhood of the transmitter about the coming data frame. Upon receiving a RTS, MSs which are not the intended receivers, interrupt their backoff countdowns and set their *Network Allocation Vector* (NAV) (Fig. 2.3) according to the duration encoded in the RTS frame. The NAV denotes the time a MS must defer from the medium in order not to interfere with an ongoing transmission.

The intended receiver, if idle i.e. able to receive data, responds to the RTS frame with a *Clear To Send* (CTS) frame, after time SIFS. The CTS frame informs the neighboring MSs to the receiver about the pending data transmission, which set their NAV as well. With the successful reception of the CTS frame at the transmitter the handshake is finished. The data frame is then transmitted after SIFS.

2.1.6 Hidden and Exposed Mobile Stations

The RTS/CTS handshake provides a solution to the so called hidden station problem. In wireless communication networks, where the MAC protocol relies on carrier sensing, it is possible that two MSs start concurrent transmissions to the same receiver, or to adjacent ones, when one MS cannot sense the transmission of the other, leading to a collision. This case is presented in Fig. 2.4.

In Fig. 2.4, MS 2 is in the transmission range of both, MS 1 and MS 3, which are not in the transmission range of each other. The transmission

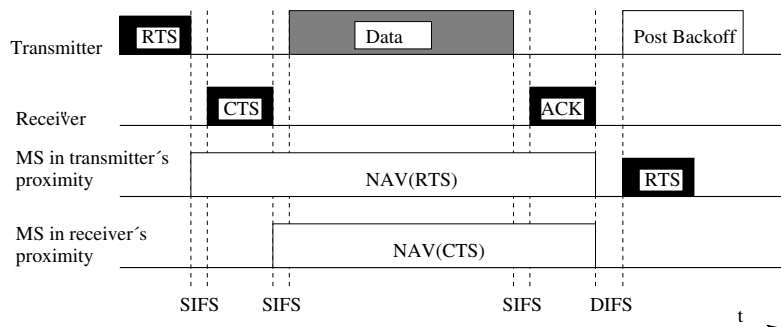


Figure 2.3: Setting NAV according to RTS/CTS control frames.

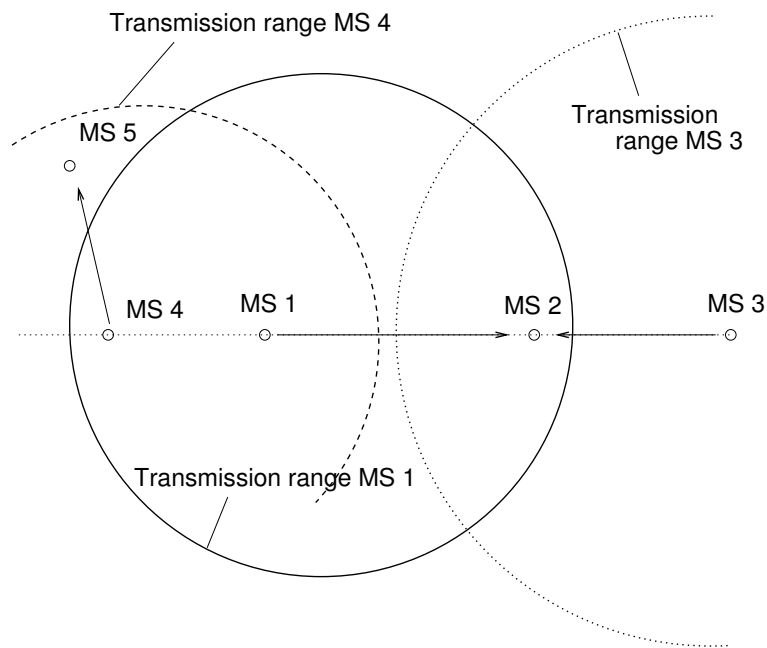


Figure 2.4: Hidden and exposed station problem in IEEE 802.11a.

range, is the distance at which the signal transmitted from a MS can be received with power no less than -86 dBm, which is necessary for the proper reception of the lowest applicable PHY mode. This might result in MS 1 initiating a transmission to MS 2, that MS 3 is not aware of, so that MS 3 during the ongoing transmission between MS1 and MS 2 might start a transmission to MS 2 or any other of its neighbors. A collision at MS2 will result from this. The RTS/CTS handshake between MS 1 and MS 2 would prevent MS 3 from starting a transmission to MS 2, as MS 3 will defer upon receiving the CTS frame from MS2.

In case that both transmitting MSs initiate their transmissions with short time difference, where a collision is inevitable, only the short RTS frames will be affected and not the longer data frames, if the handshake is being used. Thus the two way hand shake enhances the system's performance, by reducing probability of collision of data frames.

Although the hidden station problem is mitigated by the RTS/CTS handshake, another issue not treated by the standard appears, the so called exposed station problem. The exposed station (in Fig. 2.4 MS 4) is blocked

by the RTS frame sent by MS 1, although its transmission (to MS 5) will not interfere with an ongoing data transfer between MS 1 and MS 2.

2.1.7 Synchronization over Beacons

All MSs within a single BSS, according to the standard, are synchronized to a common clock. For this purpose each MS uses a local timer. Local timers are synchronized by the *Time Synchronization Function* (TSF) with the use of periodically transmitted beacon frames by the AP. The time when the next beacon frame will be transmitted is encoded in the current beacon and called *Target Beacon Transmission Time* (TBTT). Each MS in the BSS should not initiate any further transmissions when TBTT is approaching to allow an interference free transmission of the new beacon. Ongoing transmissions though should be finished, which inevitably leads to short delays in beacon transmissions.

In an IBSS the TSF is implemented in a distributed manner, where each MS participating in the BSS is transmitting beacons. Upon reaching TBTT all MSs try to transmit a beacon frame after an interval PIFS and back-off according to the rules of DCF. When one MS succeeds in transmitting a beacon, all the others stop their attempts. Like in data transfer with DCF, beacons might also collide. Since the standard does not foresee acknowledgements for the beacon transmission, the MS which transmitted the beacon is not aware of its success. Collided beacons are consequently not retransmitted.

In an IBSS, synchronization is achieved by broadcasting the TSF values in the beacons. A MS which receives the beacon will update its TSF timer, in case the time stamp in the beacon frame has a lower value than the own timer. The outcome is a synchronization of all clocks with the slowest running one.

2.1.8 Point Coordination Function

The PCF is an optional access method, which is usable only in infrastructure network configurations using an AP. Designed to support delay sensitive applications, the PCF has higher priority over the DCF, and allows a MS, the *Point Coordinator* (PC), to gain temporarily control of the medium and coordinate the data exchange within the BSS.

The time between two successive beacons is called in IEEE 802.11 su-

perframe. A superframe is typically divided into two periods when at least one PC is active in the BSS:

1. The CFP, where the medium is controlled by the PC. The PC, which is normally the AP, gains control of the medium by transmitting the beacon after detecting the channel idle for time PIFS. All other MSs set their NAV for the duration of CFP, which is announced in the beacon frame. During the CFP the PCF is used. The PC polls the MSs with a poll frame and the polled MS replies after time SIFS. Should the PC have data to transmit, then it can use a combined Data and Poll frame for higher efficiency. In case a polled MS doesn't reply to a poll after time SIFS, the PC gains control of the medium after a time interval PIFS. The CFP ends after a time specified in the beacon, with the PC transmitting the *Contention Free* (CF)-End control frame.
2. During the CP all MSs participating in a BSS have the same priority. Medium access follows the rules of DCF as described above (Section 2.1.2). It is mandatory that the duration of CP is long enough to allow at least one data packet transfer.

An example of the PCF operation [HETTICH (2001)] is given in Fig. 2.5.

2.1.9 MAC Frame Formats

In the following, a brief description of the mostly used MAC frames of IEEE 802.11a is given. The beacon, RTS, CTS and Data frames are depicted in Figs. 2.6, 2.7, 2.8 and 2.9 respectively.

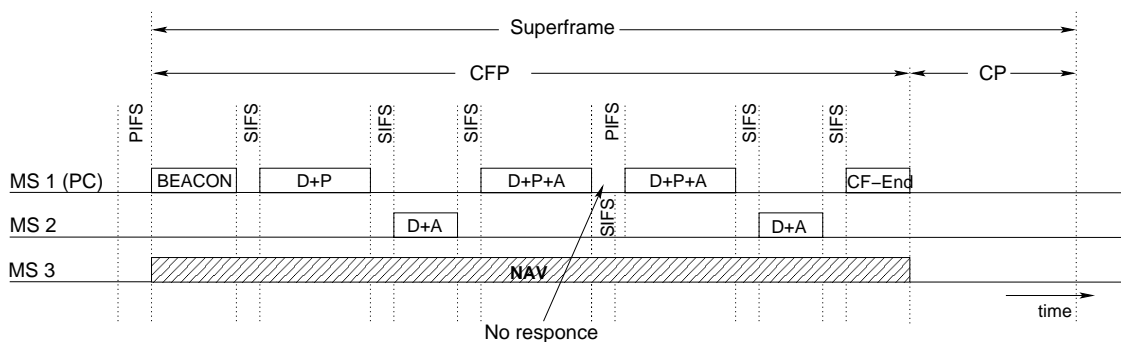


Figure 2.5: Point Coordination Function.

All MAC frames start with the frame control field, with general information such as the protocol version, the frame type (control, data, management), indication of a frame retransmission, and a fragmented *Service Data Unit* (SDU), etc [802.11 (1999)]. All frames conclude with the FCS field, containing a 32bit-*Cyclic Redundancy Check* (CRC) code for detection of erroneous frames.

In DCF operation, the Duration Field in the RTS and CTS frame is of great importance, since it denotes the time in microseconds, after the end of the current frame, which is needed to complete one transmission cycle, and is used from other MSs to set their NAV timer. A transmission cycle comprises a RTS (optionally), a CTS (optionally), a data or management frame, an ACK, one DIFS and three SIFS intervals between consecutive frames.

The address fields are 6 byte long. In the beacon frame they consist of the *Destination Address* (DA), *Source Address* (SA) and *Basic Service Set Identification* (BSSID). The RTS frame contains the transmitter and immediate receiver addresses, while CTS contains one address, that of the immediate receiver. In a data frame the four addresses represent the final receiver (address 1), the initiator of the data transfer (address 2), the current transmitter of the frame (address 3) and the immediate receiver (address 4) to support multihop.

The sequence control field contains the sequence number of the transmitted SDU and the fragment number in case the SDU is part of a bigger data unit.

The beacon body contains information about the TSF of the MS sending

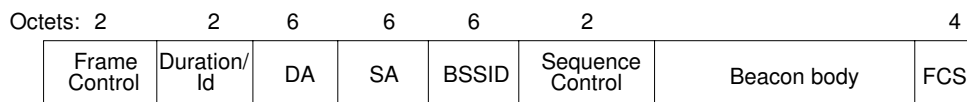


Figure 2.6: Beacon frame format.

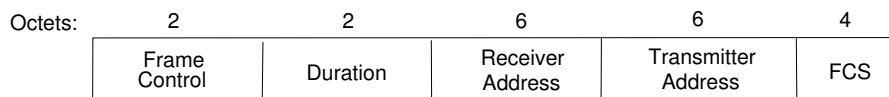
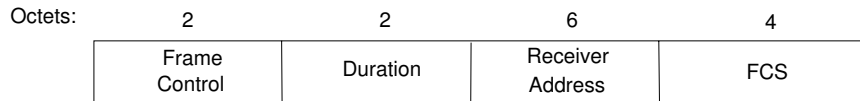
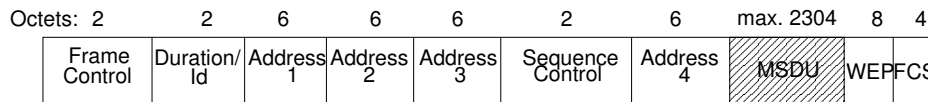


Figure 2.7: RTS frame format.

**Figure 2.8:** CTS frame format.**Figure 2.9:** Data frame format.

the beacon, the TBTT, *Service Set Identification* (SSID), the supported PHY rates and other parameters necessary to support the operation of PCF.

2.2 OFDM PHY Layer

Contemporary WLANs aim in expanding or even substituting wired systems. To achieve this, high capacity is needed in order to support both, a big number of users and applications with high throughput requirements like video streams. The demand for higher throughput is mainly translated to broader frequency channels. Those channels allow the use of shorter symbols for modulation, which suffer, in multipath environments, from *Inter-Symbol Interference* (ISI), as successive symbols are overlapping to a great extent at the receiver. Additionally, the use of broader channels enhances the system throughput but the spectral efficiency remains mostly the same.

OFDM is a modulation technique that deals with both problems. The wide channel is thereby divided in many (M_s) narrow subchannels. Instead of transmitting M_s short sequential symbols in the wide channel in time T , now M_s longer symbols are transmitted in time $M_s T$, each in one of the parallel subchannels. Assuming the same multipath channel, the multipath delay spread remains the same, while now the symbol duration is longer and the probability of two symbols overlapping, or the percentage of overlapping is greatly reduced.

OFDM is an especially efficient to implement modulation technique. The spectrum representation of a rectangular pulse with duration $[0, T_b]$ is a sinc function with zero crossings at multiples of $1/T_b$. Having M_s parallel sub-

channels each modulated by a rectangular pulse, the spectrum of an OFDM modulated signal consists of M_s spectra, with the shape of a sinc function, each centered at one subcarrier center frequency, as depicted in Fig. 2.10. The spectrum of neighboring subcarriers can overlap in a way that the peak of each subcarrier's spectrum overlays with the zero crossings of other subcarriers, if the subcarrier separation frequency is a multiple of $1/T_b$. This attribute of spectrum overlapping improves the spectral efficiency, increases however the complexity, as the orthogonality of the subcarriers must hold to avoid *InterCarrier Interference* (ICI).

The multi-carrier OFDM symbol, can be easily modulated with the use of an *Inverse Fast Fourier Transform* (IFFT). The symbols are first serial to parallel converted in groups with population size equal to the amount of data subcarriers of the system, M_s . The IFFT modulates each subcarrier with one data symbol and converts the M_s complex values from frequency domain to M_s complex values in time domain, which are summed in one multi-carrier symbol. Both, frequency and time representation of the signal contain exactly the same information.

For further enhancement, the multi-carrier symbol is expanded prior to

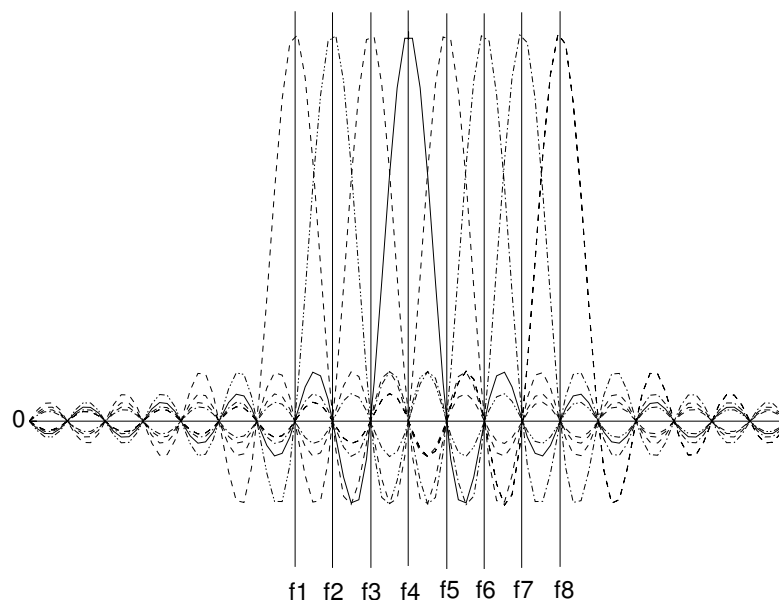


Figure 2.10: Frequency representation of orthogonal, unmodulated OFDM subcarriers.

its transmission with a cyclic prefix, a copy of the last part of the symbol added to its beginning, which is discarded at the receiver. If its duration is longer than the delay spread of the channel, the transmission is not distorted from ISI.

The received signal is sampled at the rate $1/T_b$. The receiver needs therefore to synchronize with the transmitted symbol. In IEEE 802.11, synchronization is done over the PLCP preamble send at the beginning of each frame. Its duration consists of $16\mu\text{sec}$ in the IEEE 802.11a standard. In DCF mode, asynchronous transmissions are supported, and synchronization is crucial for the prompt reception of the frame. The time domain samples are converted in frequency domain with a *Fast Fourier Transform* (FFT). Its output represents the received subcarrier symbols, input to the demodulator.

2.2.1 IEEE 802.11a PHY Layer Parameters

The PHY layer parameters applied in the IEEE 802.11a are summarized in Table 2.1.

Table 2.1: IEEE 802.11a PHY layer parameters.

| Parameter | Value |
|----------------------------|--------------------|
| Number of data subcarriers | 48 |
| Pilot subcarriers | 4 |
| Subcarrier spacing | 0.3125 MHz |
| Channel bandwidth | 20 MHz |
| Noise figure | -93 dBm |
| FFT length | 64 |
| FFT period | $3.2\mu\text{sec}$ |
| Guard interval | $0.8\mu\text{sec}$ |
| Symbol interval | $4\mu\text{sec}$ |
| Preamble length | $16\mu\text{sec}$ |

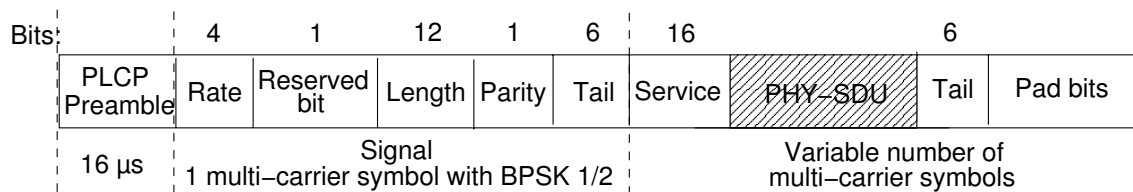
The OFDM PHY layer, allows transmission speeds of up to 54 Mbit/sec in the 20 MHz channel. Depending on the center carrier frequency, different transmission power levels are allowed in the U-NII band, see Table 2.2.

Table 2.2: U-NII Frequency bands and allowed emissions.

| Frequency band | Maximum transmission power [mW] |
|----------------|-------------------------------------|
| 5.15 - 5.25 | 50 |
| 5.25 - 5.35 | 250 |
| 5.725 - 5.825 | 1000 |

2.2.2 PHY Frame Format

The MAC frames described above, arrive at the PHY layer over the PHY *Service Access Point* (SAP). Prior to transmission, the PHY SDU is supplemented with PHY overhead as depicted in Fig. 2.11, and pad bits in order to map its content to a whole multiple of multi-carrier symbols. The overhead comprises the PLCP preamble used for receiver synchronization and the signal field with general information about the transmission, such as the applied transmission rate and SDU length. The 16 bit long service field contains 7 null bits for initialization of the scrambler and 9 reserved bits for future use.

**Figure 2.11:** PHY frame format.

Multi-Carrier Code Division Multiple Access

Content

| | |
|---|----|
| 3.1 Multiple Access Schemes | 21 |
| 3.2 Direct Sequence-Code Division Multiple Access | 23 |
| 3.3 Multi-Carrier CDMA Schemes | 25 |
| 3.4 Principles of MC-CDMA | 26 |

Recently, "CDMA technique has been considered a candidate to support multimedia services in mobile radio communications" [PRASAD (1996)]. It allows the operation of many transmitters in parallel, on one frequency band, and is applied in 3G wireless communication systems. In *Universal Mobile Telecommunication System* (UMTS), *Direct Sequence-Code Division Multiple Access* (DS-CDMA) is used to achieve high capacity and support for many users. In high speed WLANs though, DS-CDMA cannot be used, since other conditions are posed from the frequency channel, such as larger bandwidth. The large channel bandwidth, used to achieve high capacity, enforces the use of multi-carrier modulation in order to mitigate the effects of multipath. Thus OFDM is adopted in contemporary systems [802.11A /D7 (1999), 802.11E /D9 (2004), HIPERLAN2 (1999)]. For WLANs, MC-CDMA, which combines CDMA with multi-carrier modulation, has been found to be a suitable spread spectrum scheme.

MC-CDMA is a digital modulation technique where a single data symbol is transmitted at multiple narrowband subcarriers, with each subcarrier encoded with a phase offset 0 or π based on a spreading code [YEE and LINNARTZ (1994a)].

3.1 Multiple Access Schemes

In communication systems, one user rarely needs the whole system bandwidth over a longer period of time. In order to achieve high efficiency and

support for many users, the communication channel is divided in smaller subchannels which are associated with one user. This division takes place in one of the four main dimensions of a communications system, namely frequency, time, code and space, leading to the *Frequency Division Multiplex* (FDM), *Time Division Multiplex* (TDM), *Code Division Multiplex* (CDM) and *Space Division Multiplex* (SDM) schemes [WALKE (2000)] respectively. The first three of them are depicted in Fig. 3.1.

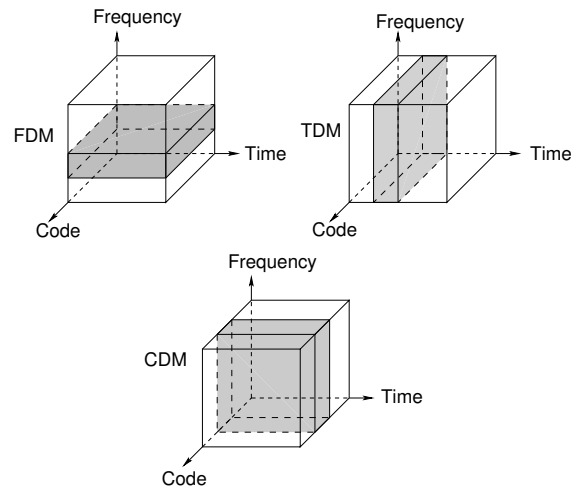


Figure 3.1: Multiplex schemes.

In FDM many simultaneous, continuous channels are derived out of the system bandwidth by assigning to each of them a fraction of the available spectrum. For the proper operation, guard bands are added between the channels, to compensate for imperfections of filters.

TDM allows different users to communicate in the same broad frequency channel. As the channel capacity is bigger than the one needed by one connection, the medium is divided into sequential intervals, with one connection periodically using one interval. In this case guard intervals are applied as well, which compensate the transmission delay between different users and avoid overlapping of information transmitted as a data burst in a time slot, with bursts of adjacent time slots.

In CDM the division of the channel is done in code domain. Each sub-channel is defined by a spreading sequence, which is used for spreading the

information symbols in a bandwidth larger than the one needed for transmission without spreading, while keeping the same symbol energy. The outcome is a broad frequency channel with low spectral energy, which allows concurrent transmissions of low spectral energy on the same frequency band, at the same time. Different channels are distinguished by different spreading sequences.

Each of the above schemes, can be further combined with each other and enhanced with SDM, which uses antenna arrays for the spatial division of different communication streams. In this thesis the focus is on CDM and the corresponding multiple access technique CDMA.

3.2 Direct Sequence-Code Division Multiple Access

The *3rd Generation Partnership Project* (3GPP) group developed the UMTS standard [25.301 (2002)], for 3G wireless networks in Europe to support high data rates for multimedia applications. In PHY layer the standard applies one variation of CDMA as multiplex scheme, namely W-CDMA. W-CDMA is a *Direct Sequence* (DS) technology, spreading transmissions over a 5 MHz wide carrier.

DS-CDMA is one of the first spread spectrum techniques used primarily for military services. As shown in Fig. 3.2, each symbol of the original data stream is spread in time domain by representing it as a sequence of N_c pulses. Each pulse, also called chip, has a much shorter duration than the pulse representing the original data bit, thus more spectral content. The pulse sequence is unique for each active user and is usually a *Pseudo Noise* (PN) sequence. Alternatively, sequences from the orthogonal Walsh-Hadamard family can be used. In this case there is no randomness and the spreading sequence repeats itself. Since the spreading sequences are orthogonal there is no mutual interference between different user signals, in the ideal case. The PN sequence has a long period that is much longer than the period of the signal pulse. Therefore, it is expanding over a wide range of symbols and is repeated periodically. The orthogonal sequences on the other hand, have the length of the applied *Spreading Factor* (SF) and are consequently repeated in every symbol.

The capability of suppressing multiuser interference is determined by the crosscorrelation characteristic of the spreading codes. The capability of distinguishing one component from other components in the composite

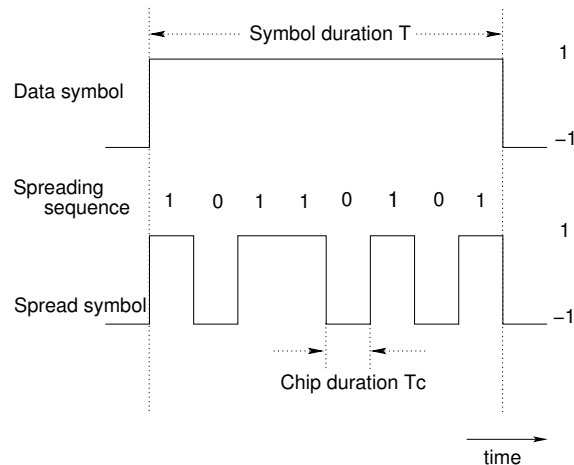


Figure 3.2: Direct Sequence-Code Division Multiple Access.

receiver signal is determined by the auto-correlation characteristic of the spreading codes. The *Bit Error Rate* (BER) depends on the number of RAKE fingers at the receiver. In a DS-CDMA using RAKE receivers, the system capacity is limited by self-interference and multiple access interference MAI, which result from the imperfect auto-correlation characteristic and imperfect cross-correlation characteristic of spreading codes, respectively.

Main advantages of DS-CDMA are its robustness to jamming and low intercept probability. A narrowband jamming signal will be correlated at the receiver with the spreading sequence of the corresponding transmitter which results in spreading the jamming signal over a wider bandwidth. The spectral energy of the interferer, in the observed bandwidth, is then reduced. Additionally, the spreading sequence used, lowers the intercept probability since interception is only possible when the spreading sequence used by the transmitter is known to the intercepting MS.

Further advantages, compared to FDMA and TDMA techniques, are the lower spectral power density and transmission power since the subscribers can transmit permanently over the whole channel bandwidth [HEIER (2003)]. As for the system's drawbacks, most important is the imperfect autocorrelation and crosscorrelation of the spreading sequences under imperfect transmission conditions, leading to MAI at the receivers. To compensate MAI, complex receiver architectures are required.

3.3 Multi-Carrier CDMA Schemes

The multi-carrier CDMA schemes are categorized mainly into two groups [HARA and PRASAD (1997)]. One spreads the original data stream using a given spreading sequence and then modulates a different subcarrier with each chip. The other, converts the data stream from serial to parallel and applies consequently spreading to each of the parallel streams before modulating the subcarrier. In a way the first method, MC-CDMA, applies spreading in frequency domain, whilst the latter method, *Multi-Carrier Direct Sequence Code Division Multiple Access* (MC DS-CDMA) combines multi-carrier modulation with spreading in time domain.

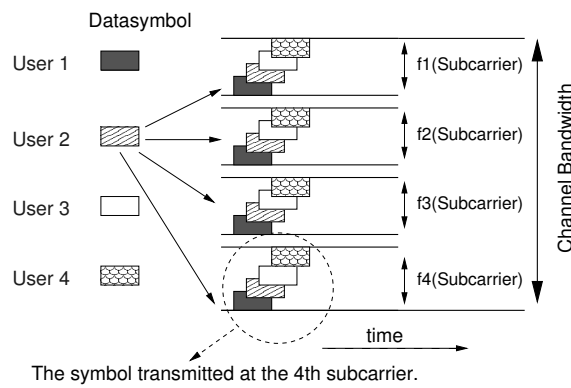


Figure 3.3: Multi-Carrier Code Division Multiple Access.

In MC-CDMA, each symbol of the output data stream of a user is multiplied by each element of the user's spreading code. The MC-CDMA chips are formed in this way and placed via IFFT in several narrow band subcarriers as shown in Fig. 3.3. Multiple chips are transmitted in parallel on different subcarriers [NASSAR et al. (2002)]. The spectra of different subcarriers are overlapping like in OFDM and the system achieves high capacity as well.

From the system's point of view, one subcarrier carries a fraction of the user's symbol, and can therefore carry additional load, coming from symbols of other users. At the end the symbol that is transmitted in one subcarrier consists of the sum of e.g. 4 fractions of 4 symbols that belong to 4 different users (Fig. 3.3).

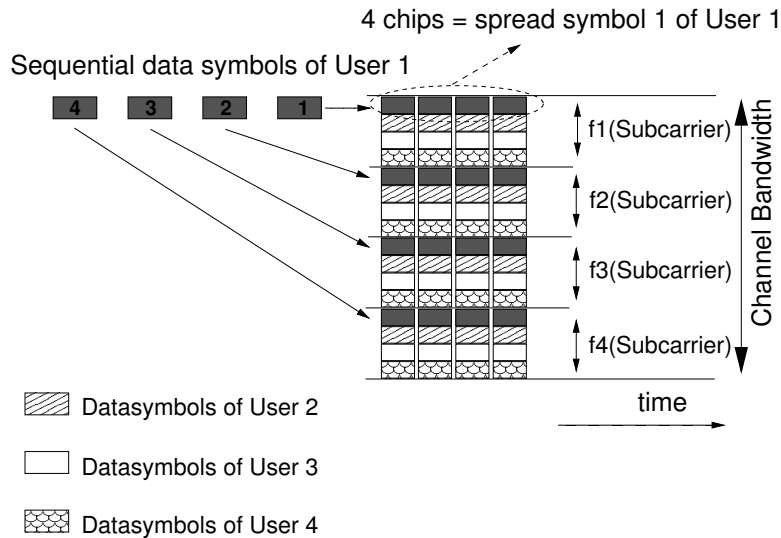


Figure 3.4: Multi-Carrier DS-CDMA.

In MC DS-CDMA the data stream of each user is first converted from serial to parallel. Each of the parallel data symbols is spread in time domain [PERSSON (2002)] according to the DS-CDMA scheme, resulting in a chip sequence for each symbol, which afterwards modulates a subcarrier as depicted in Fig. 3.4. In contrast to MC-CDMA the information of an original data symbol is now spread in different subsequent data chips transmitted on the same subcarrier, whilst in MC-CDMA chips of the same symbol are transmitted over different subcarriers.

When setting the number of subcarriers to 1, the MC DS-CDMA scheme is the same as DS-CDMA, and MC-CDMA falls back to OFDM when applying a SF of 1 in the system.

3.4 Principles of MC-CDMA

In conventional DS-CDMA, each user symbol is transmitted in the form of many sequential chips, each of which is of short duration and has a wide bandwidth. In contrast to this, due to the FFT associated with OFDM, MC-CDMA chips are long in time duration, but narrow in bandwidth [LINNARTZ (2001)]. Consequently inter-chip interference is reduced, and synchronization is easier compared to other spread spectrum techniques. Furthermore,

the DS-CDMA receiver cannot always employ all the energy scattered in time domain, whereas the MC-CDMA receiver can effectively combine the frequency scattered signal energy [HARA and PRASAD (1999)].

Compared to MC DS-CDMA, MC-CDMA exploits frequency diversity as different chips of the same symbol are transmitted in parallel over different subcarriers, while in MC DS-CDMA systems time diversity enhances performance. In aspects of processing gain and required bandwidth both systems are equivalent [HARA and PRASAD (1997)]. In this respect the focus in this thesis is on MC-CDMA.

The transmitter diagram of MC-CDMA is shown in Fig. 3.5 [YEE et al. (1993)], and can be easily realized with an IFFT. According to the transmitter modules, a mathematical equivalent of the transmitted signal in each subcarrier can be calculated, assuming perfect synchronization among the different users.

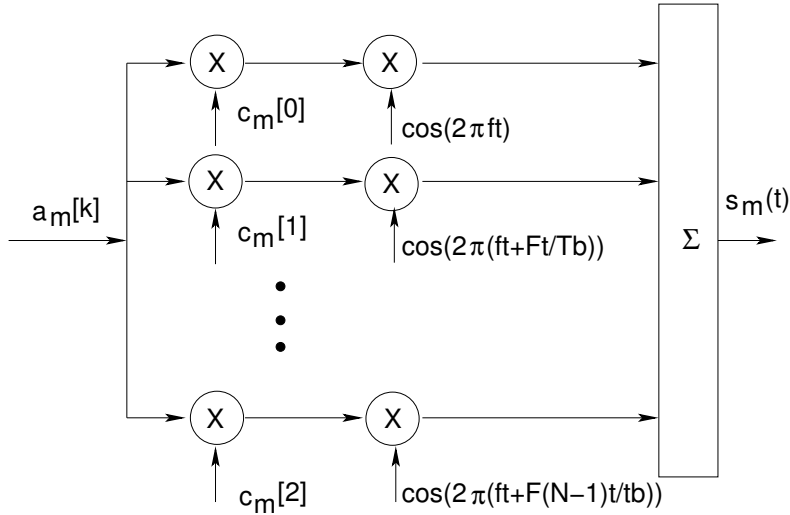


Figure 3.5: MC-CDMA transmitter.

Let the matrix $\mathbf{B}_{N \times 1}$ denote the i -th symbols of N different users, and matrix $\mathbf{C}_{N \times N}$ the spreading matrix. Each column of the matrix $\mathbf{C}_{N \times N}$ describes one spreading sequence. The equivalent discrete vector representation of the transmitted MC-CDMA signal, according to the transmitter in Fig. 3.5, is formed by the multiplication of the two matrices,

$\mathbf{C}_{N \times N} \mathbf{B}_{N \times 1} = \mathbf{S}_{N \times 1}$. The phase at each subcarrier corresponds to one element of the spreading sequence [YEE and LINNARTZ (1994b)].

$$\mathbf{B} = \begin{bmatrix} b_0(i) \\ b_1(i) \\ \dots \\ b_{N-1}(i) \end{bmatrix} \quad (3.1)$$

$$\mathbf{C} = \begin{bmatrix} c_0(0) & c_1(0) & \dots & c_{N-1}(0) \\ c_0(1) & c_1(1) & \dots & c_{N-1}(1) \\ \dots & \dots & \dots & \dots \\ c_0(N-1) & c_1(N-1) & \dots & c_{N-1}(N-1) \end{bmatrix} \quad (3.2)$$

$$\mathbf{S} = \begin{bmatrix} c_0(0)b_0(i) & c_1(0)b_1(i) & \dots & c_{N-1}(0)b_{N-1}(i) \\ c_0(1)b_0(i) & c_1(1)b_1(i) & \dots & c_{N-1}(1)b_{N-1}(i) \\ \dots & \dots & \dots & \dots \\ c_0(N-1)b_0(i) & c_1(N-1)b_1(i) & \dots & c_{N-1}(N-1)b_{N-1}(i) \end{bmatrix} \quad (3.3)$$

$$\mathbf{S} = \begin{bmatrix} s_0 \\ s_1 \\ \dots \\ s_n \end{bmatrix} \quad (3.4)$$

Each row of matrix $\mathbf{S}_{N \times 1}$ represents the signal transmitted at one subcarrier, which is a composite signal of all users' symbols. The contribution of a user's symbol to the signal transmitted at the m -th subcarrier is defined by the m -th element of the user's spreading code. It can be seen from the above equations, that for this ideal case of synchronous users (down-link), MC-CDMA is equal to multiplying an *Orthogonal Frequency Division Multiple Access* (OFDMA) stream with a spreading matrix.

Figure 3.6 depicts the corresponding receiver diagram, which is easily implemented with an FFT [LIU (2003a)].

The transmitted MC-CDMA symbol is enhanced with a *Cyclic Prefix* (CP) similar to OFDM, to mitigate the ISI caused from multipath, and hold the orthogonality among the subcarriers, which applies in the MC-CDMA scheme as well.

Additionally, when orthogonal spreading codes are used, the orthogonality of the codes must be kept. Oscillator frequency offsets and asynchronous

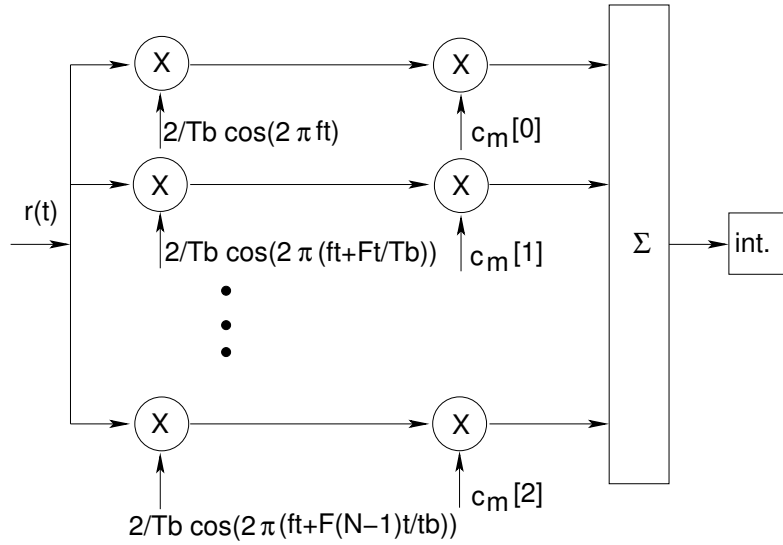


Figure 3.6: MC-CDMA receiver.

transmissions with different spreading sequences, lead to imperfect correlations at the receivers and consequently to MAI. The first problem can be solved with oscillators of good quality, where the normalized frequency offset is kept low. Throughout this thesis it is assumed that the oscillators' offset is very low. The effect of timing mismatch between different users' transmissions can be improved with a MUD. The benefits of MUD applied at the receivers' side are discussed in Chapter 4.

In the proposed system a SF of 4 is chosen, thus the symbol of one user is transformed into 4 chips and each of them is transmitted in parallel in 4 different subcarriers. Since the assumed channel utilizes 48 data subcarriers, another $(48-4)/4=11$ symbols of the same user can be transmitted in parallel to use the complete channel bandwidth. Apparently, other SFs and number of subcarriers per channel could be used reaching comparable results.

Evaluation of the MC-CDMA Physical Layer Performance

Content

| | |
|----------------------------------|----|
| 4.1 Calculation of SINR | 32 |
| 4.2 An Upper Bound for PER | 34 |
| 4.3 Simulation Results | 37 |
| 4.4 Conclusion | 40 |

In this chapter, the physical layer performance of MC-CDMA is analyzed. For this purpose, a model is provided for the estimation of *Signal to Interference and Noise Ratio* (SINR) at the detector, for MC-CDMA based asynchronous packet radio transmissions. In a multiuser MC-CDMA system, each receiver receives multiple wideband signals and uses the code assigned to a particular cch, to extract the original signal from the received one. Signals from all other cchs will appear as noise after decorrelation, thus the power of other users' signals will determine the noise level at the detector [JANKIRAMAN and PRASAD (2000)]. Furthermore, in asynchronous multiuser environments, such as in a distributed adhoc network, the received signal consists of all active users' information spread on all subcarriers with timing misalignment. This timing mismatch destroys the orthogonality among different subcarriers and different users' spreading codes [WANG et al. (2001)], resulting mainly in MAI.

For this reason a linear MUD [VERDU (1986)] [POOR and VERDU (1997)] is applied at the receiver's side, based on the MMSE criterion, which has the ability to suppress the MAI. MUD techniques improve the performance of MC-CDMA uplink significantly, increasing though the complexity at the receiver [COSOVIC (2005)]. An MMSE receiver combines both, good performance and simplicity of implementation, compared to other MUDs.

4.1 Calculation of SINR

An asynchronous multiuser MC-CDMA System is considered. Let b_k be the k -th user's binary symbol, which is transmitted in parallel over M_s ($=$ SF) subcarriers in form of chips. Each chip is multiplied by a different element c_{km} of the spreading sequence. The spreading sequences used, belong to the family of orthogonal Walsh-Hadamard codes and are given for SF=4 as rows of the Walsh w_4 matrix:

$$\begin{bmatrix} 1 & 1 & 1 & 1 \\ 1 & -1 & 1 & -1 \\ 1 & 1 & -1 & -1 \\ 1 & -1 & -1 & 1 \end{bmatrix} \quad (4.1)$$

The choice of Walsh-Hadamard codes is justified from their orthogonality property and from their performance in a fully loaded system (all spreading codes are used by different users), concerning both, the worst-case and lowest median peak-factor. In [HANZO et al. (2003a)], it has been shown that Walsh-Hadamard codes outperform other families of orthogonal spreading sequences, with respect to the peak factor of a MC-CDMA signal.

In this model it is assumed that each subcarrier experiences frequency non-selective but time-varying fading, and further that the speed of MSs is limited to pedestrian levels. Latter imposes negligible influence of Doppler frequency shift, which can under circumstances degrade the MC-CDMA system's performance [HANZO et al. (2003b)]. During the transmission of one multi-carrier symbol though, fading is assumed to be constant. Under these conditions the received signal can be given from the following equation:

$$r(t) = \sum_{k=1}^K \sqrt{a_k} b_k(i) \sum_{m=1}^{M_s} c_{km} h_{km} e^{j2\pi(t-\tau_k)m/T} p(t - \tau_k) + \eta(t) \quad (4.2)$$

where K is the maximum number of active users, a_k the transmission power of the k -th user's i -th symbol $b_k(i)$, M_s the number of subcarriers used for the transmission of one symbol, $p(t)$ a rectangular pulse over $[0, T]$, T the symbol duration, τ_k the delay of the k -th user and $\eta(t)$ denotes the additive white Gaussian noise. The Rayleigh fading process for the m -th subcarrier and the k -th user is given by:

$$h_{km} = \beta_{km} e^{j\phi_{km}} \quad (4.3)$$

with β_{km} a Rayleigh distributed and ϕ_{km} a uniform over $[0, 2\pi)$ distributed random variable.

For the following part of the calculation the focus, without loss of generality, is on the signal of user 1, therefore τ_1 is zero. The delays τ_k are all relative to τ_1 , and can be considered as uniformly distributed random variables in $[0, T)$, with $\tau_1 = 0 \leq \tau_2 \leq \tau_3 \leq \tau_4$.

After discarding the cyclic prefix, the received signal is fed to a FFT where multi-carrier demodulation takes place, [HARA and PRASAD (1997)]. The signal, received at the n -th subcarrier equals to:

$$y_n = \int_T^{(i+1)T} r(t) e^{-j2\pi nt/T} dt \quad (4.4)$$

In Appendix A a closed form expression for Eq. (4.4) is developed which is used for the implementation of the model in the simulation tool (Chapter 6).

When a linear MUD is employed, the demodulator outputs y_n are multiplied by the weights w_m , which is used for the optimization of the detector's decision on the transmitted symbol and can mitigate the effects of the channel. Accordingly, the output of the linear MUD is [STUEBER (2001)]:

$$b'_k = \mathbf{W}^H \mathbf{y} \quad (4.5)$$

where \mathbf{y} denotes the matrix of subcarrier signals at the detector, after integration. The optimum weight matrix $\mathbf{W}_{M \times 1}$, for a given set of delays τ_k and fading parameters β_{km} , is selected to minimize the MMSE at the detector:

$$MSE(\tau\beta) = E\{(\mathbf{W}^H \mathbf{y} - b_k)^2\} \quad (4.6)$$

Under these conditions, the SINR at the detector for the observed user 1 can be calculated from the following equation [WANG et al. (2001), YI et al. (2003), STUEBER (2001)]:

$$SINR = \frac{|\sqrt{a_1} \mathbf{W}^H \mathbf{p}_{K+1}|^2}{\mathbf{W}^H \mathbf{\Gamma} \mathbf{W} + |\mathbf{W}^H \mathbf{p}_{K+1} \mathbf{A}_{K+1}|^2} \quad (4.7)$$

where the matrices \mathbf{P} , \mathbf{p} are obtained from Eq. (4.4) as derived in [WANG et al. (2001), YI et al. (2003)]. The first term in the denominator of Eq. (4.7) expresses the contribution of noise and the second the contribution of MAI to total interference.

In [WANG et al. (2001)], the optimum weights are calculated in order to minimize the gradient of Eq. (4.7) with respect to \mathbf{W} , leading to the maximum achievable SINR (MSINR):

$$MSINR = a_1 \mathbf{p}_{K+1}^H (\mathbf{P}_{K+1} \mathbf{A}_{K+1}^2 \mathbf{P}_{K+1}^H \Gamma)^{-1} \mathbf{p}_{K+1} \quad (4.8)$$

At this point the importance of the cyclic prefix for the calculation of the SINR should be considered. In order to avoid ISI and to maintain orthogonality between the subcarriers in a time dispersive medium, a cyclic prefix is added to the multi-carrier modulated symbol of duration T_s . ISI is avoided if the length of the cyclic prefix T_{CP} is selected large enough to exceed the maximum path delay of the multipath channel. For the calculations in this thesis, a cyclic prefix of $800\mu sec$ is applied, as proposed in [802.11A /D7 (1999)], which has been proven to be sufficient, especially in indoor wireless propagation channels. Since the receiver uses only the energy received during the symbol duration discarding the cyclic prefix, a power reduction factor a_{CP} should be considered between the received power before and after integration [TUFVESSON (2000)], depending on the relative length of the cyclic prefix to the total symbol duration:

$$a_{CP} = \frac{T_s}{T_s + T_{CP}} \quad (4.9)$$

4.2 An Upper Bound for PER

In this section a calculation of an upper bound for the Packet Error Rate (PER) of a received frame is presented, based on the previous estimation of the SINR and a convolutional decoder with generator polynomials:

$$g_1 = 133_8, g_2 = 171_8. \quad (4.10)$$

The calculation applies to both, OFDM and MC-CDMA systems.

4.2.1 Symbol Error Rate

After the SINR is estimated, the symbol error probability for M-ary Quadrature Amplitude Modulation (QAM) can be calculated [PROAKIS (2001)]:

$$P_{SER, M-QAM} = 1 - (1 - P_{\sqrt{M}})^2 \quad (4.11)$$

with:

$$P_{\sqrt{M}} = 2\left(1 - \frac{1}{\sqrt{M}}\right)Q\left(\sqrt{\frac{3}{M-1} \frac{E_{av}}{N_0}}\right) \quad (4.12)$$

The Q-function is defined in [PROAKIS (2001)] and E_{av}/N_0 is the average signal to noise ratio per symbol. The latter is estimated according to the calculation in Section 4.1. For *Quaternary Phase Shift Keying* (QPSK) and *Binary Phase Shift Keying* (BPSK) the *Symbol Error Rate* (SER) is given by:

$$P_{SER,QPSK} = 2Q\left(\sqrt{\frac{E_{av}}{N_0}}\right)\left[1 - \frac{1}{2}Q\left(\sqrt{\frac{2E_{av}}{N_0}}\right)\right] \quad (4.13)$$

$$P_{SER,BPSK} = Q\left(\sqrt{\frac{2E_{av}}{N_0}}\right) \quad (4.14)$$

4.2.2 Bit Error Rate

In the IEEE standard for OFDM physical layer [802.11A /D7 (1999)], Gray coded constellation mapping is proposed. Thus the BER for both, QAM and QPSK (M=4) modulation, can be calculated from the SER:

$$P_b = \frac{1}{\log_2(M)} P_{SER,M} \quad (4.15)$$

For BPSK the BER is the same as the SER.

4.2.3 Packet Error Rate

The evaluation of the packet error probability is complicated by the fact that the bit errors in the decoder output stream are not independent. As described in [FRENGER et al. (1999)] errors occur in bursts at the output of the Viterbi decoder, even if the errors at the decoder's input are independent. Thus an upper bound for the packet error probability is used, which in this work is the tight bound derived in [FRENGER et al. (1999)]:

$$P_e^m(L_b) \leq 1 - (1 - P_u^m)^{8L_b} \quad (4.16)$$

where L_b is the number of information bits in the packet and P_u^m , the union bound of first event error probability is given by:

$$P_u^m = \sum_{d=d_{free}}^{\infty} a_d P_d \quad (4.17)$$

with d_{free} being the minimum free distance of the convolutional code for the given code rate, a_d the total number of errors with weight d [STUEBER (2001)], [TUFVESSON (2000)] and P_d the probability of error in the pairwise comparison of two paths which differ in d bits. The values for a_d are obtained from the transfer function of the convolutional code [ORFANOS et al. (2005b)] and represent the number of paths of distance d from the all-zero path. For the encoder used in this work the values are given in Table 4.1.

Table 4.1: Distance spectra.

| Distance d | a _d | | |
|-------------------|----------------|-------------------------|---------------|
| | code rate 1/2 | code rate 2/3 | code rate 3/4 |
| d_{free} | 11 | 1 | 8 |
| $d_{free} + 1$ | 0 | 16 | 31 |
| $d_{free} + 2$ | 38 | 48 | 160 |
| $d_{free} + 3$ | 0 | 158 | 892 |
| $d_{free} + 4$ | 193 | 642 | 4512 |
| $d_{free} + 5$ | 0 | 2435 | 23307 |
| $d_{free} + 6$ | 1331 | 6174 | 121077 |
| $d_{free} + 7$ | 0 | 34705 | 625059 |
| $d_{free} + 8$ | 7275 | 131585 | 3234886 |
| $d_{free} + 9$ | 0 | 499608 | 16753077 |
| $d_{free} + 10$ | 40406 | values not relevant: | |
| $d_{free} + 11$ | 0 | $a_d P_d \rightarrow 0$ | |
| $d_{free} + 12$ | 234969 | | |
| $> d_{free} + 12$ | | | |

In case of hard decision decoding, the probability P_d can be calculated from the following equations [PROAKIS (2001)]:

$$P_d = \begin{cases} \sum_{k=\frac{(d+1)}{2}}^d \binom{d}{k} P_b^k (1 - P_b)^{d-k} & d = \text{odd}, \\ \sum_{k=\frac{d}{2}+1}^d \binom{d}{k} P_b^k (1 - P_b)^{d-k} + \binom{d}{\frac{d}{2}} \frac{P_b^{d/2} (1 - P_b)^{d/2}}{2} & d = \text{even} \end{cases} \quad (4.18)$$

Instead of the above expressions, the Chernoff upper bound can be used,

leading to the following bound for the calculation of P_d .

$$P_d < [4P_b(1 - P_b)]^{\frac{d}{2}} \quad (4.19)$$

4.3 Simulation Results

In this section the results of the previously presented analysis are presented using different modulation and coding schemes. For that purpose the most common used PHY modes have been chosen, proposed for OFDM based standards of *Institute of Electrical and Electronics Engineers* (IEEE) [802.11A /D7 (1999), 802.11E /D9 (2004)] and the *European Telecommunications Standards Institute* (ETSI)/*Broadband Radio Access Network* (BRAN), [HIPERLAN2 (1999)]. An overview of the used PHY modes and their basic characteristics is given in Table 4.2. Further parameters of the proposed MC-CDMA system are kept close to the values of the OFDM based WLAN standard [802.11A /D7 (1999)] and can be taken from Table 4.3.

Table 4.2: PHY modes.

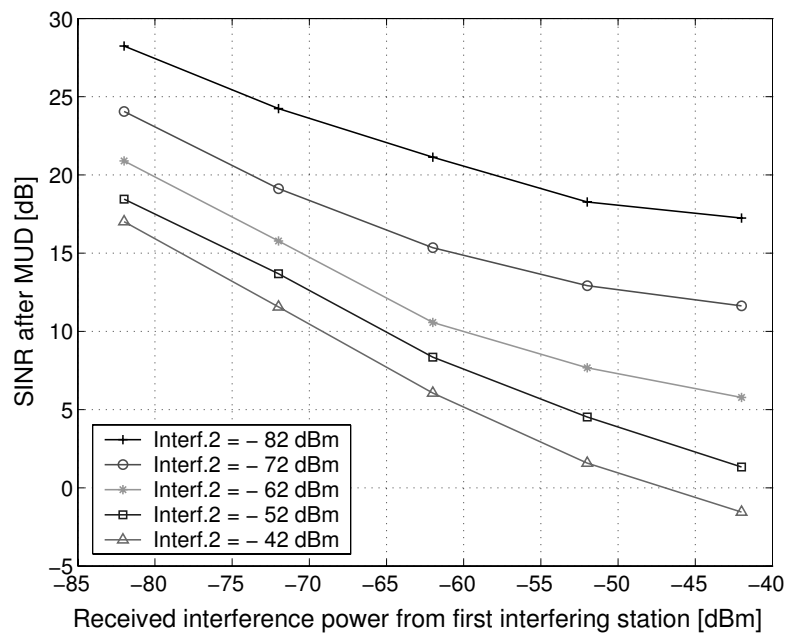
| PHY mode m | Modulation | Code rate | Data bits per multi-carrier symbol | d_{free} |
|--------------|------------|-----------|------------------------------------|-------------------|
| 1 | BPSK | 1/2 | 24 | 10 |
| 2 | BPSK | 3/4 | 36 | 5 |
| 3 | QPSK | 1/2 | 48 | 10 |
| 4 | QPSK | 3/4 | 72 | 5 |
| 5 | 16QAM | 1/2 | 96 | 10 |
| 6 | 16QAM | 3/4 | 144 | 5 |
| 7 | 64QAM | 2/3 | 192 | 6 |
| 8 | 64QAM | 3/4 | 216 | 5 |

For the results presented here, the assumption is made that the maximum excess delay of the radio channel is smaller than the 800ns cyclic prefix duration, thus ISI does not occur.

In the following the performance of the MUD for different values of MAI is analyzed. Simulations, based on Matlab, were performed with 4 active

Table 4.3: PHY layer parameters.

| Parameter | Value |
|-----------------------|--|
| Spreading factor | 4 |
| Number of subcarriers | 48 Data + 4 Pilot |
| Subcarrier spacing | 0.3125 MHz |
| Channel bandwidth | 20 MHz |
| Carrier frequency | 5.25 GHz |
| Noise level | -93dBm |
| Symbol interval | $4\mu\text{sec} = 3.2\mu\text{sec} + 0.8\mu\text{sec}$ |
| Guard interval | $0.8\mu\text{sec}$ |
| Preamble length | $16\mu\text{sec}$ |

**Figure 4.1:** MUD performance with 4 active users and $SF = 4$.

users, modelling one carrier and 3 interfering signals. Two parameters are constant; the received carrier strength is set to -60dBm and the power of the third interferer is assumed -55dBm. Noise power level is assumed -93dBm. The interference power received from the other interferers varies between

-82dBm (sensing range) and -42dBm. Figure 4.1 presents the SINR at the detector with the power of the first interferer for five different values of the second interferer's power. The SINR value on the diagram is the average over 10,000 runs with different delays τ_k . The graphs show that performance decreases almost linearly with the interfering power. One important observation is that the MUD manages to provide a positive SINR even in the case when all the three interfering signals are 5dB higher than the carrier strength. This demonstrates the interference suppression ability of the detector in the presence of high MAI.

The following figures depict the dependency of the MUD's performance from the relative delays τ_k of active users. Figure 4.2 presents the SINR at the detector with the relative delay of the interferer, for two active users. Both, the carrier strength P_c , and the interference at the receiver, P_I , comprise -68dBm. For small relative delay, the output SINR reaches the maximum of 31dB, which corresponds to the theoretical maximum: Assuming no fading and perfect interference suppression, $P_I=0$ after applying multiuser detection. The noise level for a 16.25 MHz channel and receivers with similar noise figure as the one defined in [802.11A /D7 (1999)], is approximately -93dBm.

$$SINR = \frac{P_c}{N_0} + G_{sp} = 31$$

where G_{sp} is the spreading gain in dB:

$$G_{sp[dB]} = 10\log(SF) = 10\log 4 \simeq 6dB$$

For larger relative delays the performance of the MUD degrades and reaches a minimum for a delay of half the multi-carrier symbol duration. As the delay increases more, the detector synchronizes with the next symbol, thus the output SINR increases.

Figure 4.3 presents the PER versus E_{av}/N_0 for 1514 byte long frames. The solid lines refer to multi-carrier systems with a power loss due to the cyclic prefix of 20%, compared to a single carrier system without cyclic prefix (dashed lines in Fig. 4.3). The performance of the multi-carrier system is 1dB worse. This loss is compensated both, from the mitigation of the multipath effects by the cyclic prefix and the higher capacity of multi-carrier systems. It is interesting to observe the performance of the BPSK 3/4 PHY mode in comparison to QPSK 1/2, which are very close. Thus it is

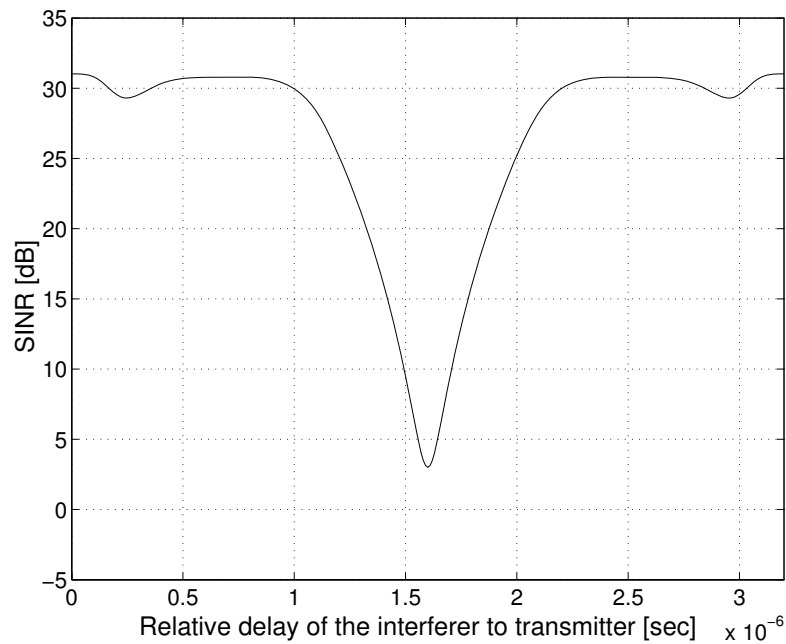


Figure 4.2: SINR at the detector vs. relative delay of interferer to transmitter and spreading factor 4.

better to use the QPSK 1/2 mode since more data bits are transmitted per symbol (Table 4.2). In Fig. 4.4 the PER versus E_{av}/N_0 is given for frame lengths of 48, 512, 2304 byte and different PHY modes. The maximum frame length used is 2304 byte, which is the maximum payload of IEEE 802.11a. The diagrams show that the PER is growing with the packet size.

4.4 Conclusion

In this chapter a model has been presented estimating the PHY layer performance of a MC-CDMA based WLAN. After computing the SINR at the detector, the model provides a calculation of a bound on the packet error probability for a packet radio system that employs convolutional encoding and hard decision Viterbi decoding. Calculations are done by taking into account the channel characteristics, parameters of the multi-carrier spread spectrum technique as well as different modulation and coding schemes. This simple model is aimed to represent the link characteristics on packet

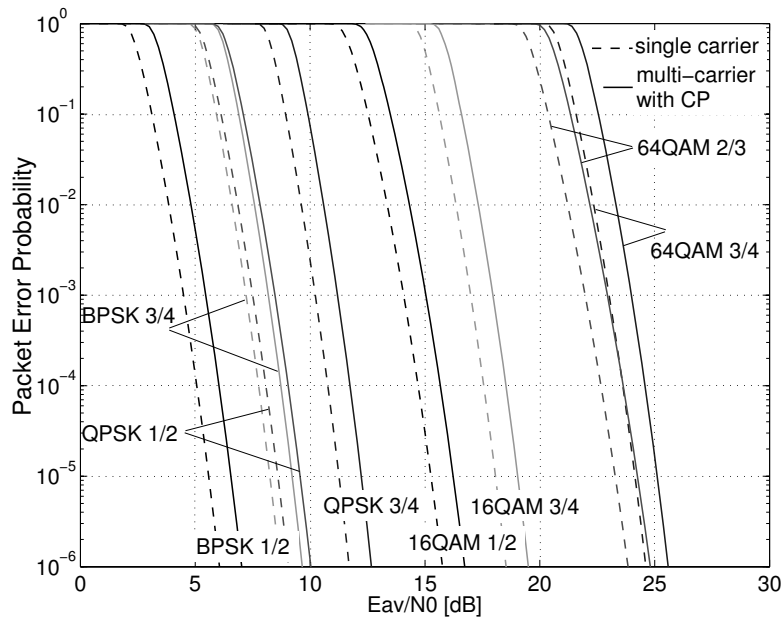


Figure 4.3: Theoretical PER for a 1514 byte long packet. The solid lines refer to a multi-carrier system with $a_{CP} = 80\%$. Dashed lines refer to a single carrier system without cyclic prefix.

transmission and has been implemented in the MACNET-2 simulation tool, that models a MC-CDMA WLAN based on the IEEE 802.11 MAC protocol [ORFANOS et al. (2004a)], see Chapter 6.

More complex models, which address several issues of the MC-CDMA PHY layer have been recently developed and solutions proposed: In [COSOVIC (2005)], an analytical model of the uplink MC-CDMA PHY layer is derived, and countermeasures for the oscillator frequency offset and channel estimation problem are suggested. It is shown that with combined pre- and post- equalization in presence of frequency interleaving, the performance of an uplink MC-CDMA system under full load, is only 1-1.5 dB worse than the single user bound.

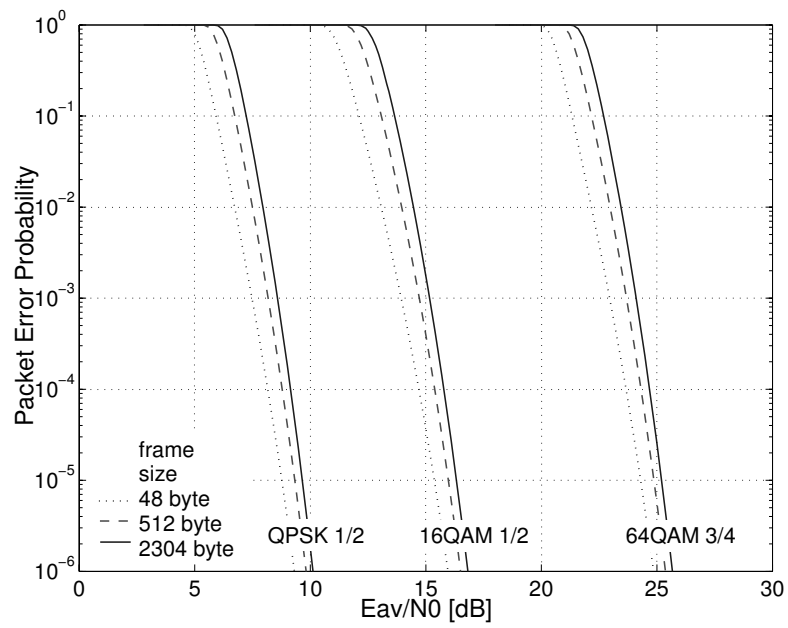


Figure 4.4: PER vs. E_{av}/N_0 for different packet sizes.

C-DCF: cch selection on Connection Basis

Content

| | |
|---|----|
| 5.1 Protocol Description | 43 |
| 5.2 Transmit Power Control | 49 |
| 5.3 Improved Handshake - Adaptation to Suitable Cch | 55 |
| 5.4 Frequency adaptation - 2nd adaptation method | 59 |
| 5.5 Performance Analysis and Comparison with the Standard DCF | 64 |

In this chapter, the functionality of a Modified Distributed Coordination Function is analyzed, namely C-DCF, which constitutes the main MAC protocol of the MC-CDMA WLAN. The main difference compared to DCF of the standard [802.11A /D7 (1999)], is the coordination of frequency channels both, in time and code domain. This two dimensional approach raises the protocol complexity but provides another dimension in protocol design to optimize the system's performance.

In the following, the functions and features of the protocol are described, assuming a selection of the applied spreading sequence per transmitter on connection basis (see Fig. 1.1). An analytical performance evaluation and comparison with the standard DCF is given in the last section of this chapter. It must be noted, that throughout this work all MSs are assumed to be equipped with one transceiver and thus transmitting and receiving at the same time is not possible.

5.1 Protocol Description

The MAC protocol of the proposed system is based on the MAC protocol of the IEEE 802.11a WLAN. Its main functionality is similar to DCF, with some modifications needed to support the MC-CDMA PHY layer. In this case the frequency channel is divided into 4 parallel cchs ($SF = 4$), showing a multi-channel structure which should be taken into account by the MAC protocol. Each MS uses C-DCF to access one cch and initiate a data trans-

fer. The low complexity of DCF is slightly increased due to the need for coordination of multiple channels, which is compensated by the enhanced performance (Section 5.5).

5.1.1 The Codechannel

In the proposed protocol, a spreading factor of four is used. The spreading factor is small compared to other spread spectrum systems but it is best suited for WLANs at 5GHz. The main problem besides the higher complexity of a system with higher spreading factor is the service time, especially in scenarios with many active MSs. Spreading the transmitted symbols by a factor of four makes each packet 4 times longer, thus the service time increases. A higher spreading factor would be acceptable if the transmission rate of the channel would increase enough to compensate for the spreading delay.

In order to avoid wide subcarriers and have a measure for direct comparison with the IEEE 802.11a system, in PHY layer of the MC-CDMA system, the same parameters are being used. From the 48 data subcarriers consequently, a symbol spread with factor four occupies only 4 subcarriers. The remaining 44 subcarriers are modulated with 11 more symbols of the same users, each spread with the same spreading code of length 4, in order to fill one 48-multi-carrier symbol.

Unlike UMTS, where each transmitter uses a unique spreading sequence, in the proposed system that uses four spreading sequences, this is not feasible. Therefore, the concept of a cch is introduced in this thesis. A cch is a spreading sequence, that is not explicitly assigned to a MS, but shared among a number of MSs. Each MS considers each spreading sequence as a subchannel of the frequency channel. Consequently, the frequency channel is divided (logically) by the four spreading sequences into four subchannels, the cchs. The cch is defined by a spreading sequence and the center frequency of a frequency channel. Therefore a hybrid medium access control function is required, which controls both, the distribution of transmitters to the different cchs and the resource sharing inside the same cch among MSs.

5.1.2 Selection of a Cch

A MS ready to transmit has to select one or more cchs [LIU (2003b)]. This means practically that the information transmitted for this MS will

be spread using one particular spreading code of the four spreading codes available in the system. For this selection two methods are possible [ORFANOS et al. (2004b)]:

- The first consists in selecting a cch before every frame transmission. Initially this selection is done randomly. For subsequent transmissions, the MS does not select cchs, which have already been reserved by other MSs (according to the standard the considered MS has set a NAV for an occupied channel). This is an opportunistic usage of the cchs (Fig. 1.1), and will be discussed in Chapter 8.
- The second method consists of selecting the cch with the least traffic load, according to an initial channel monitoring, and keeping this cch for the entire duration of the session, see Fig 1.1. This method is followed in this chapter.

The first method can only be applied if an idle receiver is able to monitor all four cchs. For the second method, a small simplification is suggested. All MSs are initiating a transmission in the first cch and can afterwards negotiate the channel to be used for further transmissions.

Both methods perform well in scenarios with an average traffic load. The advantage of the first is the achievement of load balance among the cchs while a static allocation of cchs can be better used from adaptive resource allocation methods that optimize the network's performance. Adaptive methods divert the connection to a cch with more favorable conditions for the data transfer. The impact of both methods on the system's performance will be analyzed in the following chapters where extensions of the MAC protocol will be discussed.

5.1.3 Medium Sensing

After having selected the cch, the MS applies carrier sensing, according to DCF. The MS needs to sense the medium for a continuous time duration of DIFS as idle in order to detect a free channel. In this work it is assumed that a MS can monitor all cchs when being idle or being receiving. For this purpose four correlators (one for each cch) per receiver are assumed existent.

In contrast to OFDM networks, in CDMA networks sensing cannot be based on received spread power level measurement of the frequency carrier. In case the intended cch is idle, while all other cchs are occupied by ongoing

transmissions, a power level measurement and comparison to some threshold would result in an "occupied" channel. Thus, the decision on the state (idle, occupied) of the medium is made by analyzing the signal level after the MUD, where the different cchs are separated. Should the signal level of a cch exceed -82dBm [MANGOLD (2003)], the channel is assumed busy and the MS is not allowed to initiate a transmission. The -82dBm threshold is an implementation depended parameter.

5.1.4 Collision Avoidance

As specified in the standard IEEE 802.11a, a backoff procedure at every MS prior to a transmission is required to protect a frame from immediate collision. The backoff procedure provides in general means to avoid collisions, but its effectiveness in scenarios with many active MSs is limited and collisions become the determining factor for achieved throughput and delay. The reason for this is mainly the next transmission of a MS, after a successful one, that always starts with the lowest CW size, meaning highest contention level. In [SONG et al. (2003)], it has been proposed to reduce the CW by half, instead of resetting it to CW_{min} after a successful transmission of a collided frame. This method has proven to adopt the CW size to a proper value, according to the number N of active MSs.

This modification to the MAC protocol, proposed in this section, has an advantage in the MC-CDMA system. Since each frequency channel is divided in SF parallel cchs, and only N/SF MSs compete against each other in accessing the medium, contention is reduced by a factor SF and collision probability is therefore reduced. Consequently, a lower value for CW_{min} can be applied, leading to shorter backoff times and shorter data packet transmission delays.

5.1.5 The RTS/CTS Handshake Extension

In C-DCF the RTS/CTS handshake is used, prior to the transmission of every data packet. In addition to its main functionality to protect the data transmission and prevent from hidden stations, the two way handshake (RTS/CTS) provides means to optimize the MS parameters for the data transmission. TPC and dynamic frequency channel selection are two extensions of the protocol contained in the enhanced standard IEEE 802.11h 802.11H /D2.0 (2003). In this work, both enhancements are used, however

new algorithms have been developed, that best fit the used MC-CDMA PHY layer. They both are based on information exchanged over the RTS/CTS control frames preceding data transmission.

For the MC-CDMA protocol, the assumption is made that MSs are equipped with four correlators and can thus monitor all four cchs in idle state or during the reception of a frame. This means, consequently, that in each MS four NAV timers are administered, one per cch.

5.1.6 Asynchronous Packet Transmission

Data packets are transmitted after a successful two way handshake. An example is given in Fig. 5.1 where MS 1 and MS 3 are transmitting to MS 2 in cch 3 and MS 4 in cch 4, respectively. After a backoff of 3 time slots, MS 1 initiates a transmission with an RTS frame. Consequently, all other MSs mark cch 3 as busy, and only after the successful reception of RTS, MS 2 interrupts its 6 slot backoff timer on cch 1, in order to prepare the transmission of CTS frame. MS 4 is the only station setting a NAV on cch 3 after decoding the RTS frame of MS 1. The duration of the NAV is taken from the field duration in the RTS frame. MS 3, although sensing cch 3 as busy, cannot set the NAV timer on cch 3, since its own backoff down count reaches zero before finalizing the reception of RTS from MS 1, and initiates another transmission on cch 4. This transmission is immediately sensed by MS 2 and MS 4, which mark cch 4 as busy, and after the transmission's end of RTS at MS 1, this station marks also cch 4 as busy. MS 4 replies after SIFS with a CTS frame on cch 4 while MS 1 is transmitting its data packet on cch 3. Since both, MS 1 and MS 2, are not in receiving mode throughout the transmission duration of the CTS frame from MS 4, they cannot set their NAV for cch 4, but continue marking the channel as busy, as it has not been sensed idle for a time duration equal to DIFS.

In this example, it is assumed that both data frames are received successfully. The NAV timer of MS 4 for cch 3 expires after the specified occupancy time has elapsed. The channels marked as busy in all MSs are set to idle after they have been monitored for a time duration DIFS with power level lower than the given threshold. In the MC-CDMA system this is not happening immediately after the completion of an ongoing transmission, but, as visible for cch 3 of MS 3 in the given example, a certain delay until rating an unused cch idle might occur. This delay results from the ongoing transmission of MS 3 in cch 4, which has to be finished before MS 4

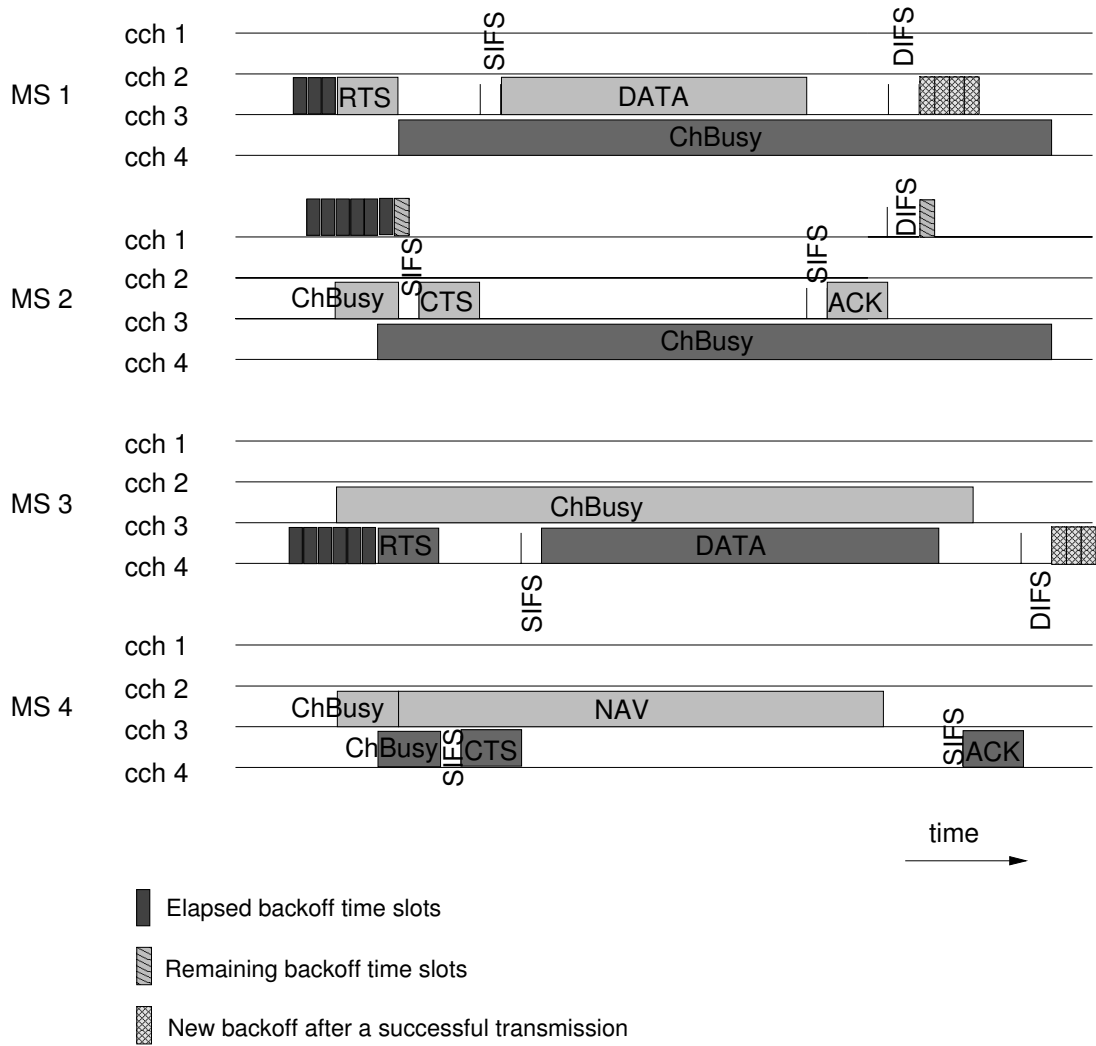


Figure 5.1: CSMA/CA on four cchs.

can sense the cchs' status. This situation occurs, because MSs are assumed to be equipped with only one transmitter each, so that transmitting and either receiving or monitoring the cchs at the same time is impossible.

After successful transmissions, MS 1 and MS 3 start new backoff timers for the next data transfer. MS 2 continues with the interrupted backoff in cch 1.

5.1.7 Collisions

A collision occurs when a receiver cannot decode correctly the received frame. In contrast to OFDM, collisions in the MC-CDMA protocol are mainly not direct, due to concurrent transmissions in the same channel, as the contention for accessing a cch is lower than the contention of accessing a frequency channel, but indirect, owing to MAI.

The MUD at the receiver's side can suppress interference from transmissions in other cchs, up to a certain degree only. The nature of asynchronous transmissions, leading to some orthogonality loss among the spreading codes, and the nature of ad-hoc networks, where transmissions in other cchs from adjacent MSs can lead to much higher power level than that of the cch carrying the intended receive signal, make MAI suppression a difficult task. Generally, the MAI suppression by the MUD is sufficient for low PHY modes. For higher modes, where a higher SINR is required for correct signal decoding, the problem is overcome by applying adaptation rules and crosslayer optimization as discussed in the following chapters of this thesis.

5.2 Transmit Power Control

Besides reducing energy consumption, efficient TPC is essential for a good performance of wireless networks. This applies especially to CDMA systems, where the capacity is limited by receiver's ability to extract the intended signal from the received one.

One way to save power is to force MSs to enter a "sleep mode", as suggested in [SIMUNIC et al. (2000)] and [JUNG and VAIDYA (2002)]. Another approach for power saving is to adaptively adjust the power by a MS for its frame transmissions to the same destination. A reduced overall interference is achieved by this. In [AGARWAL et al. (2001)], an algorithm is suggested, where the transmit power of data frames is adjusted with the help of an enhanced RTS/CTS handshake. [EBERT and WOLISZ (2001)],

propose a power saving method that both, adjusts the transmission power of data frames and their size. The method of [AGARWAL et al. (2001)] is further developed in [QIAO et al. (2003)], where TPC combines with link adaptation.

In this work, the TPC method proposed in [AGARWAL et al. (2001)] is extended and applied in a MC-CDMA network. Information needed for TPC is exchanged in the RTS/CTS frames [SIRIN (2004)]. The key idea is to use the MUD output signal at the receiver to establish an accurate interference estimate, instead of measuring the power level during idle times. This has the advantage of a fast transmission power adjustment, according to a good estimate of the interference level at the receiver, which can boost the networks performance.

5.2.1 Interference Estimation Algorithm

An optimum TPC can be achieved, if MSs are able to estimate the interference upon frame reception, and use this estimate for power adjustment of their future transmissions. One possible way to achieve this, is to estimate the expected interference for the next reception, according to an estimate of interference, calculated during the reception of previous frames (P_{MeanIF}). Each time a MS receives a frame correctly, its interference estimate is updated according to Eq. (5.1). In case the MS operates in many cchs, one interference estimate is built for all channels.

$$P_{MeanIF} = \begin{cases} P_{LastIF} & , P_{MeanIF} = 0 \\ (1 - a_{IF}) \cdot P_{MeanIF} + a_{IF} \cdot P_{LastIF} & , P_{MeanIF} \neq 0 \end{cases} \quad (5.1)$$

with

| | |
|--------------|---|
| P_{LastIF} | Interference value of last received frame |
| P_{MeanIF} | Mean interference estimate of the MS |
| a_{IF} | Weight for the contribution of the latest interference estimate to total estimate of a MS |

The value of the mean interference during the reception of one frame can be calculated by the MSs from an estimate of the SINR. The estimate can be calculated with the help of the MUD scheme, that jointly detects the signals of all active users [DUEL-HALLEN et al. (1995)]. After receiving the composite MC-CDMA signal, the receiver simultaneously detects and

sorts the information from various users. An analysis of its functionality has been provided in Section 4.1. Based on Eq. (4.8) (and the analysis in Appendix A), a MS using four correlators is able to calculate an SINR estimate, by measurements of the power received at each cch. From the SINR the MS can estimate the mean interference during frame reception for a known reception power.

The interference during the last received frame, is weighted with a_{IF} [ORFANOS et al. (2005a)]. In this work, the focus is on *Small Office/ Home Office* (SOHO) scenarios with low or no mobility of MSs, and therefore TPC should be immune to high interference peaks. Accordingly, the latest interference estimate contributes to the SINR estimate of a MS only to a certain percent. The choice of the weight directly impacts the TPC procedure.

5.2.2 Extended Frame Formats

In order to make the exchange of the interference status information between MSs possible, that is needed for TPC, RTS and CTS frames need to be extended by two more fields, TxPow and IfPow, as depicted in Figs. 5.2 and 5.3. In the field TxPow the transmit power used for the current frame is encoded by a MS and IfPow carries the estimated mean interference power at this station. Each field is one byte long. All other frames have the same format as specified in IEEE 802.11a (Section 2.1.9).

Alternatively, the TPC relevant information could be transmitted in the data and ACK frames, which then would have to be extended with the two fields TxPow and IfPow. In the data frame, the information should be

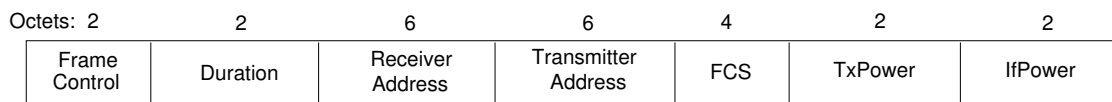


Figure 5.2: Extended RTS frame format.

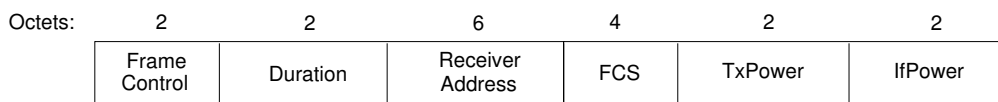


Figure 5.3: Extended CTS frame format.

encoded in the MAC header. Depending on the payload length of the data frame and the applied PHY mode, the amount of multi-carrier symbols to be transmitted may remain the same, as without TPC information. However, the PHY header is filled with information, to cover an integer number of multi-carrier symbols. The addition of two byte for TPC would require an extra multi-carrier symbol increasing consequently, the overhead.

The protocol's efficiency is not much affected by the way selected for exchanging TPC information. No safe conclusion on the most efficient way of transmitting TPC information can be made. Throughout this thesis the TPC information will be send as part of the RTS/CTS control frames.

5.2.3 Power Adjustment Algorithm

Setting a large value for a_{IF} , TPC becomes more sensible to interference fluctuations, adapting fast the transmission power. As a consequence, all other MSs sense higher interference levels and adopt their transmission power to the new status. Accordingly, the interference at the receiver of the first MS raises, and it increases its transmission power. The outcome is a vicious circle resulting in MSs reaching maximum transmission power.

On the contrary, a small a_{IF} value results in slower Transmit Power (TP) adjustments. The power control in this case doesn't respond immediately to an increase on sensed interference, but adopts the transmission power in smaller steps, requiring many interference estimates, with big deviation to the current estimate of one MS, for a big increase in the transmission power.

This technique, combined with an adaptation function, like the one proposed in Section 5.4, is more appropriate for an ad-hoc network able to provide transmission opportunities to all MSs, even under heavy interference.

Figure 5.4 provides an overview of the TPC algorithm. MS 1 transmits a RTS frame, using the extended frame format of Fig. 5.2. In the frame transmitted by MS1 the current values of its transmit power P_{TX}^{S1} and interference power P_{IF}^{S1} are communicated. MS 2 receives the RTS frame with power level P_{RX}^{RTS} and decodes the values of P_{TX}^{S1} and P_{IF}^{S1} . MS2 can now calculate the pathloss L between MS 1 and MS 2:

$$L = P_{TX}^{S1} - P_{RX}^{RTS} \quad (5.2)$$

MS 2 can also calculate the minimum needed receive power for MS 1

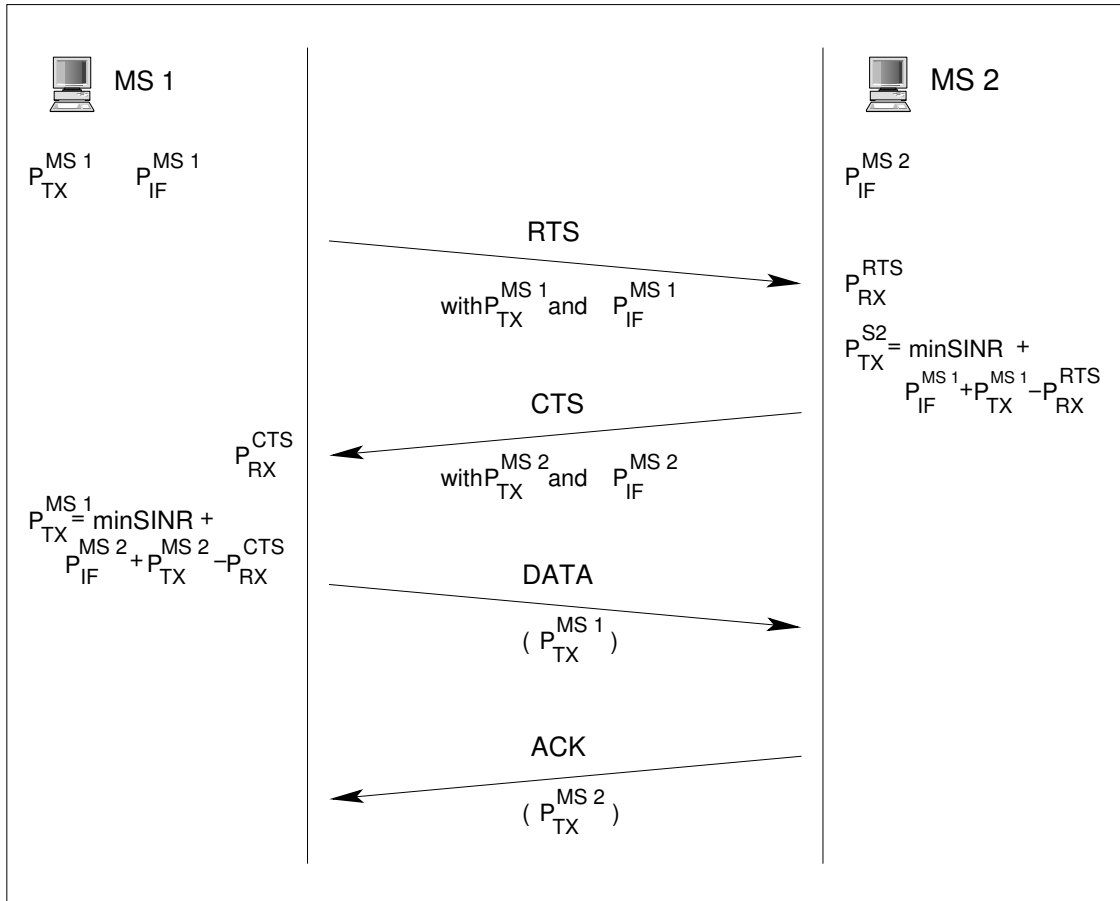


Figure 5.4: The TPC method.

taking the actual mean interference estimate P_{IF}^{S1} at MS 1 into account, assuming a threshold value minSINR :

$$\text{min}P_{RX}^{S1} = \text{minSINR} + P_{IF}^{S1} \quad (5.3)$$

From Eqs. (5.2), (5.3) the minimum needed Tx-Power for MS 2 is:

$$P_{TX}^{S2} = \text{min}P_{RX}^{S1} + L \quad (5.4)$$

This Tx-Power is saved in MS 2 and used for future transmissions to MS 1 (and will be communicated in the extended CTS frame).

It is worth noting that a MS needs to adopt its transmission power only when the newly calculated one differs at least by 1dBm from the previous Tx-Power value. Such a stepwise adjustment simplifies implementation and provides means to reduce jitter of the received power. If the minSINR threshold is 2dB higher than the value needed to achieve the QoS aimed at with the current PHY mode, both, the stepwise adjustment of transmission power and possible short fading phenomena during reception, can be compensated in many cases.

The minSINR value used, is the same for both, the control and data frames, although control frames are always transmitted with a robust PHY mode, which requires lower SINR for reception. If different values of minSINR would be used, the big difference in power adjustment between control and data frame transmission would lead to large interference fluctuations and instability in the network. Additionally, since control frames are mainly used to prevent collisions, they should use a high transmission power to cover a big range.

If MS 1 receives the CTS frame in Fig. 5.4 with Rx-Power P_{RX}^{CTS} and decodes from the frame the values of P_{TX}^{S2} and P_{IF}^{S2} , MS 1 can calculate the pathloss between MS 1 and MS 2

$$L = P_{TX}^{S2} - P_{RX}^{CTS} \quad (5.5)$$

and the minimum needed Rx-Power for S2

$$\text{min}P_{RX}^{S2} = \text{minSINR} + P_{IF}^{S2} \quad (5.6)$$

From Eqs. (5.5), (5.6), the Tx-Power needed for MS 1 can be calculated

$$P_{TX}^{S1} = \text{min}P_{RX}^{S2} + L \quad (5.7)$$

This Tx-Power value is saved in MS 1 and used for future transmissions to MS 2. After receiving the data frame, MS 2 transmits the ACK with the Tx-Power calculated before. It is though possible that MS 2 cannot receive correctly either the RTS or the data frame (no CTS or ACK arrives in MS 1) due to high interference. In this case, MS 1 repeats the transmission with double Tx-Power

$$P_{TX}^{S1} = P_{TX}^{S1} + 3dB \quad (5.8)$$

The successful reception of a frame follows an update of PMeanIF.

5.3 Improved Handshake - Adaptation to Suitable Cch

Before a data transmission starts, a handshake (RTS/CTS) between sender and receiver takes place so that the medium can be reserved and the transmission will be protected from collisions with frames of other terminals transmitting in overlap. This is a precaution for the data transfer, but the RTS and CTS frames are only protected against collision by the CA mechanism of the CSMA/CA protocol.

In cases, where the reception of RTS is not possible at the receiver, although there is no concurrent transmission in the channel, but high interference from adjacent channels at the receiver, repeated transmissions of the RTS frames will result in repeated collisions. Consequently the connection is blocked or at least suffers from a very high delay. In communication systems, using more than one channel simultaneously, like the proposed one, that have free capacity in some channels available, this problem can be solved efficiently, if a retransmitted RTS frame is send in another channel [ORFANOS et al. (2005f)]. Figure 5.5 shows the effectiveness of an improved handshake, when applied to the proposed system with 4 cchs. The improved handshake constitutes the first adaptivity function of the proposed MAC protocol.

According to the given example, MS 1 and MS 2 initiate transmissions on cch 2 and cch 4 respectively. Transmissions are not synchronized, but overlap to some degree. Due to the assumed proximity of MS 2 to MS 3, the latter cannot decode the signal from MS 1 and a collision occurs (Fig. 5.6). In static and low mobility scenarios, where MSs don't change their relevant positions frequently, collisions like the one described, will repeat. MS 1 will not manage a successful transmission to MS 3 unless it uses a more robust

PHY mode.

Alternatively, MS 1 may change the cch and initiate a transmission in another one. If MS 1 changes to cch 4, where the connection between MS 2 and MS 4 is operated, then the two previously interfering stations will share the same cch in a time basis, which allows them a collision free operation. The selection of the new cch is proposed to be done randomly and in worst case it might take up to 3 channel changes until MS 1 might find cch 4 as usable.

Depending on the relative position of MS 4 to the other stations, MS 2 might also not be able to successfully transmit its data to MS 4. Such a

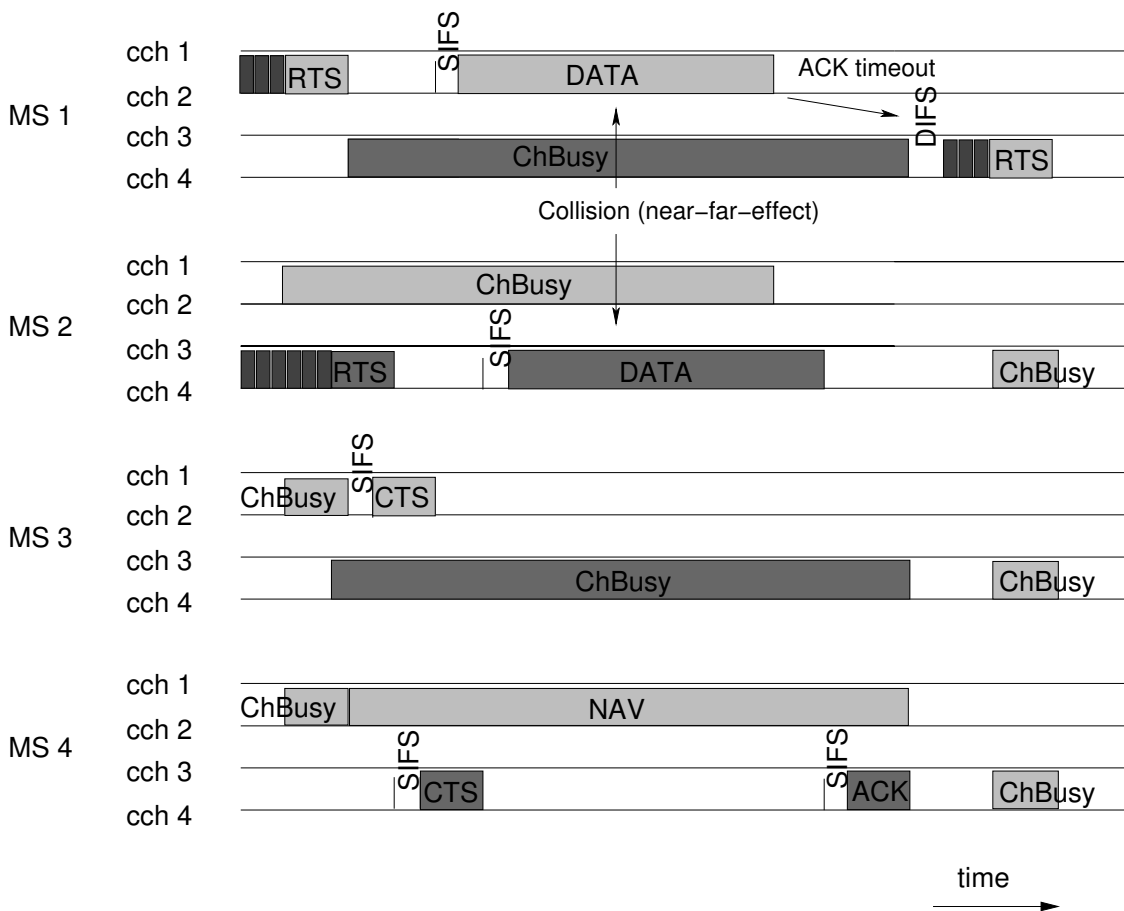


Figure 5.5: Selection of another cch, after collision, increases the possibility of successful retransmission.

situation is shown in Fig. 5.6. The improved handshake can be used also to resolve collisions owing to hidden stations or caused by a great number of MSs operating in the same cch.

When an initiated transmission (RTS or data) fails (CTS, respectively ACK is missed), the MS proceeds with the retransmission according to the algorithm shown in Fig. 5.7, where an overview of the algorithm is provided, for the case of a missed CTS. The functionality is the same for a missing ACK.

According to the algorithm, the transmitting MS doubles the transmission power and CW value to be used for the retransmission, in case their values do not exceed the maximum specified ones. Additionally, every time a frame is received or missed, the station updates its transmission history, which holds the results of the last five transmission attempts. When the improved handshake is enabled and two initiated transmissions in a row, or three out of the last five transmissions have failed (`aDecision=true`) the MS decides that the actual cch is currently not useable. This decision control contributes much to make the algorithm more robust against random transmission errors. A second decision is needed in order for the MS to differentiate between:

- **case 1:** a generally not useable channel (`GoodChannel=false`) where most of the last five transmission attempts were unsuccessful and
- **case 2:** a generally usable channel (`GoodChannel=true`), where previous transmissions were mainly successful.

In both cases, depending on a list of cch idle times, supervised by MSs that monitor all cchs, the MS will switch first (Fig. 5.5) to the cch with the largest idle time. Such a cch change is performed with a certain probability, which is 100% for case 1 (MS is completely blocked) and variable for case 2, in order to avoid a cch change of all interfering MSs at the same time.

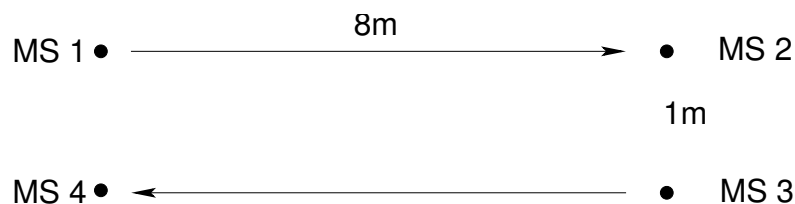


Figure 5.6: Practical application scenario of the improved handshake.

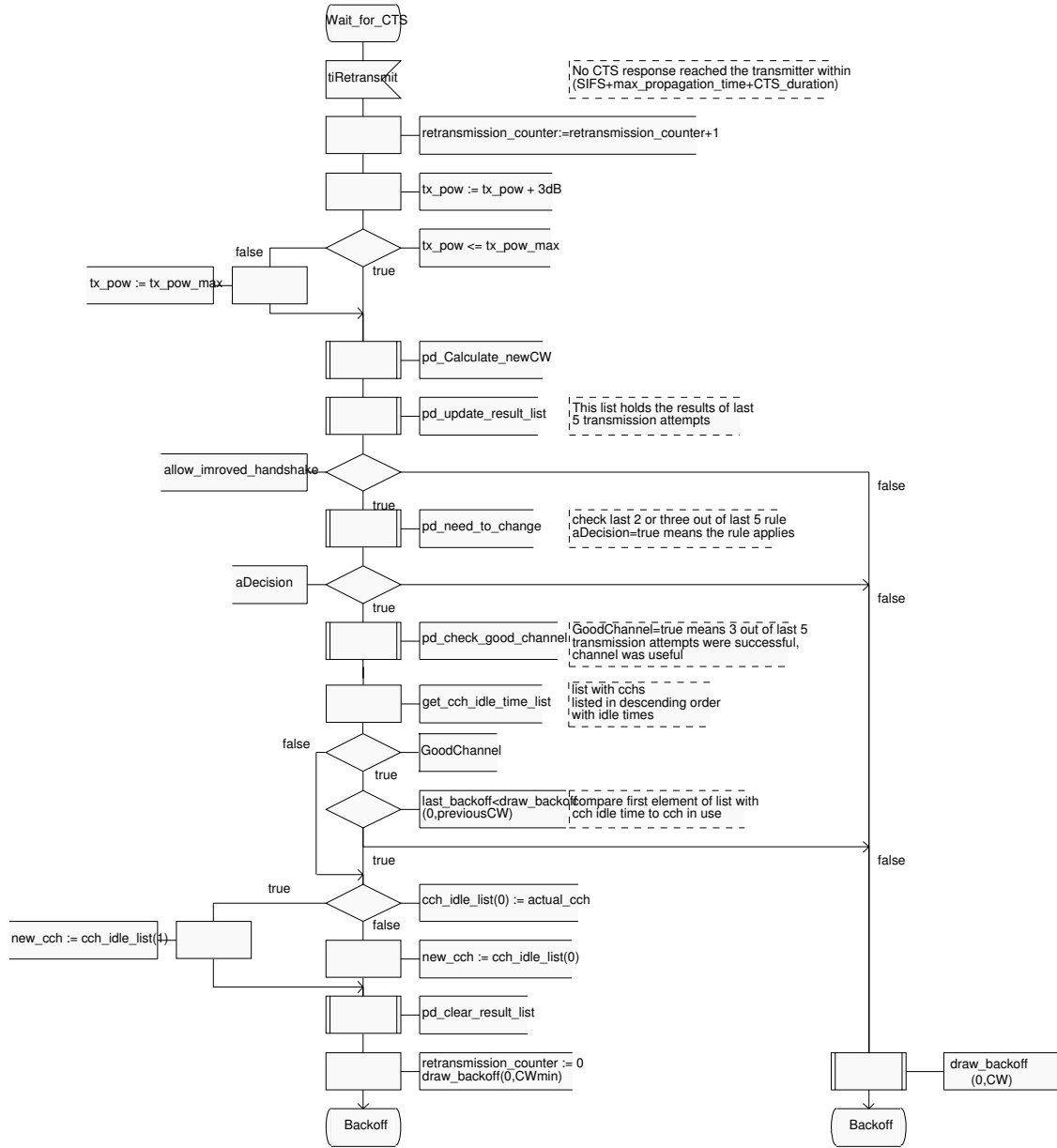


Figure 5.7: Improved handshake algorithm. The SDL diagram shows the case for a missing CTS, but applies equally to a missing ACK.

In the proposed system the probability for changing the cch in case 2 is relying on the backoff time length prior to the transmission of the collided frame. Each MS, switches its cch with a probability equal to the quotient of the number of backoff time slots B_{TS} and the actual value of CW. This method provides fairness, since MSs with longer backoff periods are more likely to change the channel and increase thereby their probability of correct transmission.

Additionally, in extensions of the DCF, like the *Enhanced Distributed Channel Access* (EDCA) used in standard IEEE 802.11e [802.11E /D9 (2004)], MSs of high priority with short CW, will be prioritized in channel change as well.

Referring once again to Fig. 5.5, MS 1 has waited for a backoff time duration of 3 time slots whereas MS 2 has waited for 6 time slots. Assuming a CW of 7 for both stations (the previous data frames of both stations did not collide), MS 1 changes its channel with probability $3/7$ and MS 4 with probability $6/7$.

The MSs keep switching their cch until a useable cch is found. A cch is decided useable as long as the "last two or three out of five" criterion is not met. A single failed transmission only leads to an increase of the CW as described in Chapter 2.

5.4 Frequency adaptation - 2nd adaptation method

In Section 5.3, the ability of improved handshake to limit the effects of MAI is analyzed. Its performance is limited since one or two cchs in general might not be able to fulfill the QoS demand of a connection. A longer connection for instance, in an environment with shorter connections, will suffer from MAI that can not always be kept sufficiently low. Especially, in adhoc CDMA networks near-far effects can block a receiver due to high interference. These effects occur when a receiving station is closer to an interferer than to its corresponding transmitter. Accordingly, the receiver cannot detect the intended signal out of the received one and the data transmission fails.

Depending on the applied receiver architecture, the system is resistant up to a certain degree against near-far problems. For the MMSE detector assumed in this work, its theoretical near-far resistance is derived in [XI-AODONG and FAN (2004)]. The results show that the MMSE detector can

in general cope with near-far-problems when BPSK modulation is applied. There is a tradeoff though, between the number of active users and the near-far ratio. The resistance becomes very poor in a fully loaded system when a near-far ratio of 20dB, with respect to received power, occurs.

In [WANG et al. (2001)] and [YI et al. (2003)] a partial sampling MMSE and an adaptive minimum BER detector is presented. With BPSK, coderate 1/2 and less than the maximum number of cchs used, the above solutions show a good performance. Furthermore in [ANDREWS and MENG (2004)] and [DENG and LEE (2003)] complex receiver architectures are analyzed and their performance with BPSK 1/2 is proven to approach the ideal maximum SINR receiver with perfect channel knowledge.

Besides the MMSE detector, interference cancellation has also been discussed, as a possible solution for near-far problems. In [BENVENUTO and BISAGLIA (2003)], the impact of *Successive Interference Cancellation* (SIC) and *Parallel Interference Cancellation* (PIC) detectors is discussed. The robustness of the detectors to near-far-problems is investigated, when QPSK modulation is applied. Simulations show that the SIC receiver outperforms the PIC receiver, but the performance of both degrades with the number of users. The complexity of this approach is high and the latency times of a SIC receiver in a fully loaded system could be a drawback for delay sensitive traffic.

In general, contemporary work focuses on PHY layer solutions for the near-far problem and the robust *Phase Shift Keying* (PSK) PHY modes. These PHY modes though, don't have the capacity to support heavy load or a big number of users in the network. Under these conditions, the application of QAM PHY modes is unavoidable, which is then reducing much the receivers' ability to cope with near-far problems. Therefore, an approach to the solution of this problem from the MAC layer is required.

In this Section, another enhancement of the basic protocol (Section 5.1) is presented, namely a frequency adaptation function. The new protocol has the ability to overcome the near-far-problem by employing a frequency adaptation method. The key of the proposed method is the interference estimate built at each receiving MS. Aided by its estimate, a MS can calculate whether the QoS expectations of the incoming connection can be accomplished. If the interference is too high, the receiving MS initiates a frequency channel change and informs the corresponding transmitter by means of the control frames about the Id of the new channel.

5.4.1 The Frequency Adaptation Algorithm

An overview of the frequency adaptation algorithm is given in Fig. 5.8. Like in the TPC procedure, the receiver (MS 2 in this case) calculates the maximum SINR ($maxSINR$) which is possible to achieve during reception, according to its current interference (P_{IF}^{MS2}) status and the maximum allowed transmit power in the network ($maxP_{TX}$). MS 2 can now decide whether the data packet transfer can take place under the current conditions [ORFANOS et al. (2005e)].

Two cases are possible:

1. $maxSINR \geq minSINR$, where $minSINR$ denotes a set threshold needed, according to the used PHY mode, for the reception of the data frame with PER of, say, less than 3%. The aimed PER value can be different, depending on the application and supported QoS. The data transfer can take place in the current frequency channel. MS 2 sends an extended CTS frame, as shown in Fig. 5.3, with the actual values of P_{TX}^{MS2} and P_{IF}^{MS2} .

Should the CTS frame be received correctly, MS 1 will transmit the actual data packet according to the C-DCF protocol. In case of erroneous reception, the RTS retransmit timer of the MAC protocol in MS 1 will reach zero and MS 1 will start a retransmission attempt with a new RTS frame, after having increased the CW by a factor of two.

2. $maxSINR < minSINR$. In this case MS 2 changes the frequency channel with a certain probability, which in this work is set to 50%. The selection of the new frequency channel is done randomly out of the set of the system's available channels.

The probabilistic change of the frequency channel is needed in order to prohibit unnecessary frequency changes and collisions owing to possible near-far-problems in the new frequency channel [BUTSCH (2004)]: In scenarios with heavy load, it can occur that more than one receiver are blocked by other transmissions or are even blocking each other. If a connection is diverted to another frequency channel, the interference situation is changed at once, and it might be then possible for all other receivers to communicate with much less near-far-problems. If this is not the case, other MSs will have to change the frequency channel, too.

The frequency channel change probability is set to 50%. Larger values

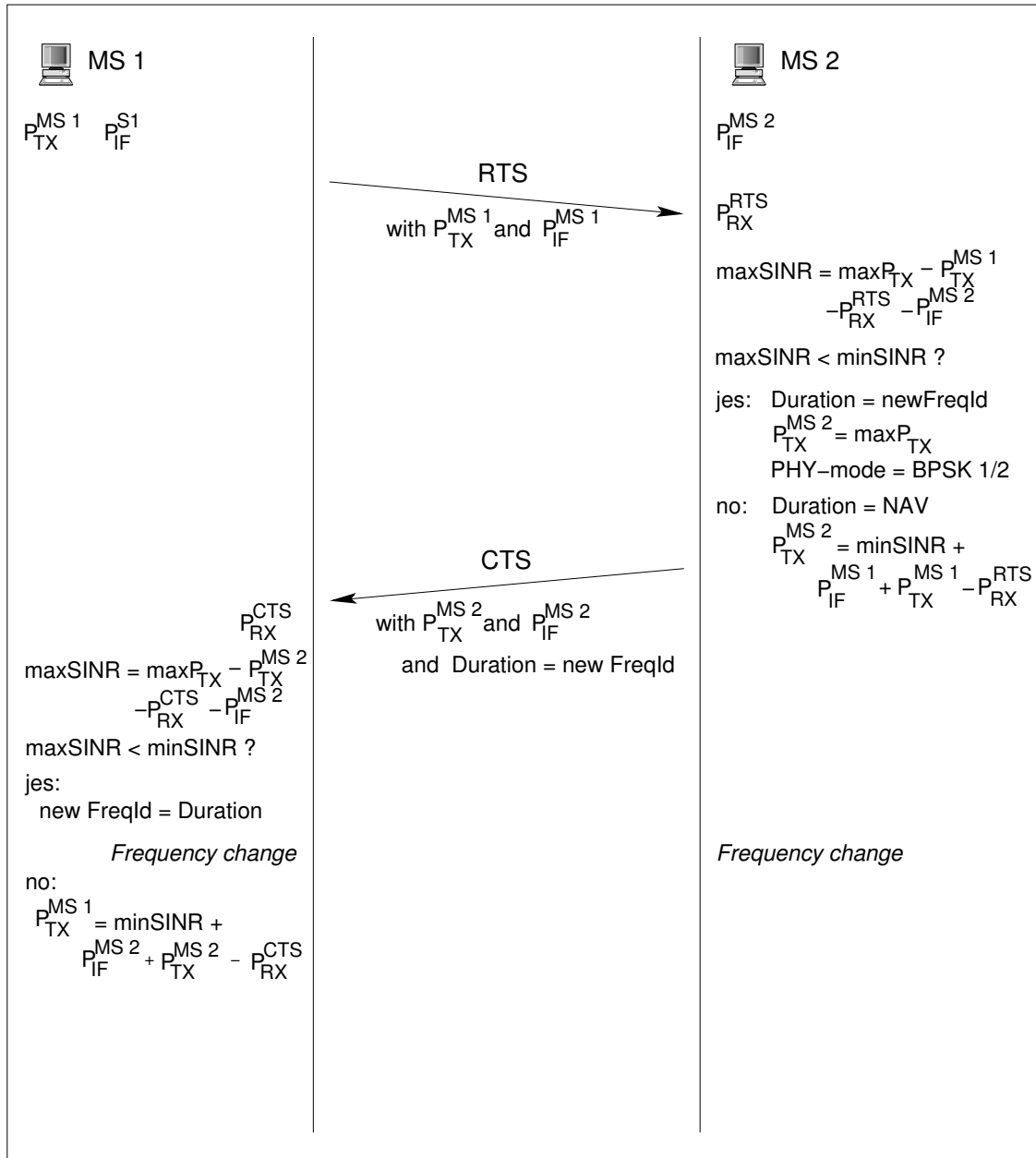


Figure 5.8: The frequency adaptation algorithm.

lead to more frequent channel changes since all MSs with mutual blocking connections will change the frequency channel and again might not be separated, which was the original intention of the algorithm. How-

ever, lower values than 50% for the frequency channel change probability lead to inertia on channel switching, which has a direct impact on the system's throughput.

The extended CTS frame (Fig. 5.3) is send to MS 1 using $maxP_{TX}$ and the robust BPSK 1/2 PHY mode to ensure the correct reception. The fields P_{TX}^{MS2} and P_{IF}^{MS2} are filled with the current values available at MS 2.

The Duration Field of the CTS frame (Fig. 2.8) is used in the IEEE 802.11 standard to denote the duration of the data transfer after the end of the current control frame, in microseconds. In case of a frequency change, MS 2 can use the Duration Field to denote a frequency change and to encode there the new frequency channel *Identification* (ID). This does not create inconsistencies to the receiver of the frame, since the small duration values in Duration Field do not make sense according to the standard. After the transmission of the CTS frame, MS 2 changes to the new frequency channel and resets all its transmission relevant parameters:

$$\begin{aligned} P_{TX}^{S2} &= startP_{TX} \\ P_{IF}^{S2} &= -93dBm = N_0 \end{aligned}$$

MS 1 receives the CTS frame with Rx-Power P_{RX}^{CTS} and decodes from the frame the values of P_{TX}^{S2} and P_{IF}^{S2} . Accordingly, MS 1 calculates the pathloss between MS 1 and MS 2:

$$L = P_{TX}^{S2} - P_{RX}^{CTS} \quad (5.9)$$

and the maximum achievable SINR under the current interference situation:

$$maxSINR = maxP_{TX} - L - P_{IF}^{S2} \quad (5.10)$$

MS 1 compares the values of $maxSINR$ and $minSINR$ to decide about a frequency change. This operation is not really necessary since the information about the frequency change is also available from the Duration Field of the extended CTS frame transmitted by MS 2, but it provides an additional control mechanism for the algorithm. MS 1 changes to the new frequency channel and resets its relevant parameters:

$$\begin{aligned} P_{TX}^{S1} &= startP_{TX} \\ P_{IF}^{S1} &= -93dBm = N_0 \end{aligned}$$

Afterwards, MS 1 initiates a new transmission with a RTS frame in the new frequency channel after monitoring the channel for at least a period of five DIFS intervals in order to gain a picture of the interference situation in the new frequency channel.

5.5 Performance Analysis and Comparison with the Standard DCF

Considering a complete transmission cycle, such as the one shown in Fig. 5.9, a comparison between the maximum achievable throughput of the MC-CDMA and the OFDM based system can be carried out. The time needed for a complete data packet transfer Δt in IEEE 802.11a, ignoring collisions and considering the average backoff interval, can be calculated as:

$$\Delta t = DIFS + t_{RTS} + SIFS + t_{CTS} + SIFS + t_{DATA} + SIFS + t_{ACK} + 3.5 * aSlotTime \quad (5.11)$$

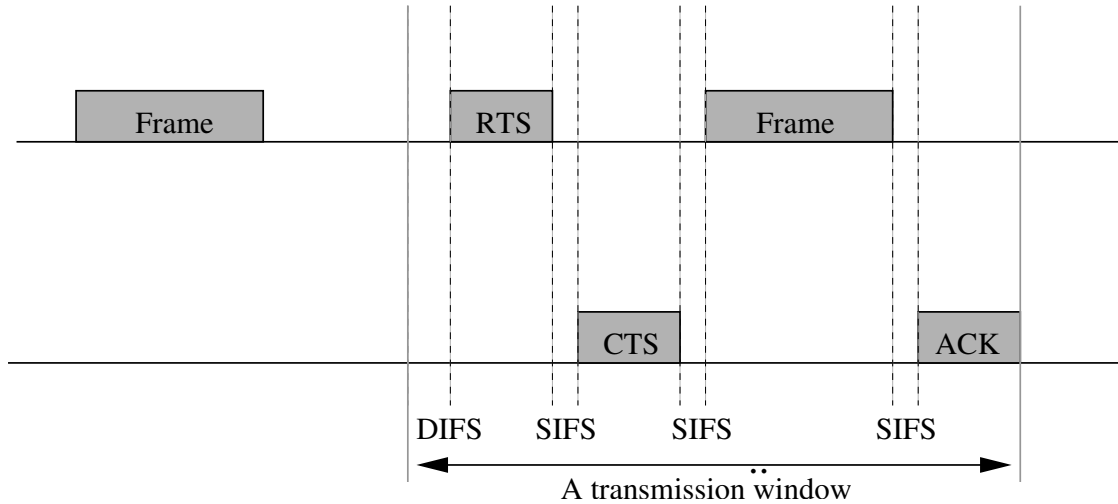


Figure 5.9: A transmission window.

Taking into account the number N_b of information bits per multi-carrier symbol for the applied PHY mode (Table 4.3), the number of multi-carrier

symbols N_s required for the transmission of a frame with L bits is given by Eq. (5.12):

$$N_s = \lceil \frac{L \cdot SF}{N_b} \rceil \quad (5.12)$$

Assuming a MAC-SDU of 1024 byte and considering the 336 bits MAC and 22 bits PHY overhead, the number of multi-carrier symbols, required for the transmission of each frame in the transmission window with the OFDM, as well as with the MC-CDMA system with $SF = 4$, is given in Table 5.1. For the transmission of control frames the QPSK 1/2 PHY mode is used. The interframe space durations and the slot length are taken from the IEEE 802.11a standard and are summarized in Table 5.2.

Given the length of one symbol which is $4\mu sec$ for both systems and that in each frame a $16\mu sec$ preamble and a $4\mu sec$ signal field are added [802.11A /D7 (1999)], it can be found:

$$\Delta t_{OFDM} = 393.5\mu sec \quad (5.13)$$

$$Throughput_{OFDM} = 1024 * 8 / 393.5\mu sec = 20.82 Mbit/sec \quad (5.14)$$

$$\Delta t_{MC-CDMA} = 1037.5\mu sec \quad (5.15)$$

$$Throughput_{MC-CDMA} = 4 * 1024 * 8 / 1037.5\mu sec = 31.58 Mbit/sec \quad (5.16)$$

The MC-CDMA system can theoretically achieve 51.68% higher efficiency than OFDM with the highest, 64QAM3/4 PHY mode.

Table 5.1: Number of multi-carrier symbols per frame.

| Frame type | OFDM | MC-CDMA |
|----------------|------|---------|
| RTS | 4 | 16 |
| CTS | 3 | 12 |
| DATA QPSK 1/2 | 179 | 713 |
| DATA 64QAM 3/4 | 40 | 159 |
| ACK | 3 | 12 |

Table 5.2: Durations.

| Parameter | Duration |
|-----------|-------------|
| SIFS | $16\mu sec$ |
| DIFS | $34\mu sec$ |
| aSlotTime | $9\mu sec$ |

For the $QPSK1/2$ PHY mode respectively, the following throughput is calculated:

$$\Delta t_{OFDM} = 915.5\mu sec \quad (5.17)$$

$$Throughput_{OFDM} = 1024 * 8 / 915.5\mu sec = 8.95 Mbit/sec \quad (5.18)$$

$$\Delta t_{MC-CDMA} = 3253.5\mu sec \quad (5.19)$$

$$Throughput_{MC-CDMA} = 4 * 1024 * 8 / 3253.5\mu sec = 10.07 Mbit/sec \quad (5.20)$$

According to the above results, the protocol efficiency in this case is 12.51% higher for MC-CDMA.

Figure 5.11 presents the results of a direct comparison for both systems for different data packet sizes while Fig. 5.10 gives the comparison results for different PHY modes. In both cases the MC-CDMA system achieves higher MAC protocol efficiency, compared to the OFDM system. The MAC protocol efficiency is defined as the percentage of net MAC throughput to the channel capacity at the PHY mode used for data frame transmission. The difference increases with the PHY mode and drops with data packet size, from MC-CDMA point of view.

The main advantage of MC-CDMA compared to an OFDM based system in MAC level, is the longer duration of frames. Spreading the symbols by a factor of four, increases the size of frames by four, while the preamble and guard intervals (SIFS, DIFS) remain constant. This results in a reduction of the relative overhead needed for the transmission of a data packet, thus the MAC protocol efficiency improves. For further reductions

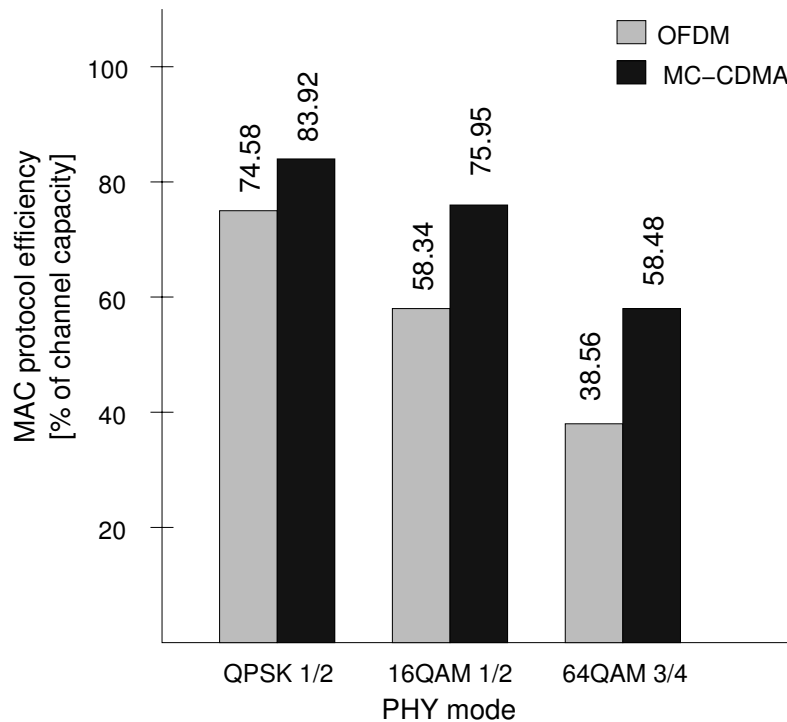


Figure 5.10: MAC protocol efficiency comparison for different PHY modes. The MAC protocol efficiency is defined as the percentage of net MAC throughput to the channel capacity at the PHY mode used for data frame transmission

of overhead, a higher Spreading Factor SF could be applied in channels with higher capacity, where the higher transmission rate would compensate for the higher service time introduced by spreading.

5.5.1 Performance analysis in a wideband channel

Recently, the research project *Wireless Gigabit with Advanced Multimedia Support* (WIGWAM) [www.wigwam-project.de] is working towards the design of a system for wireless data transmission with speeds up to 1 Gbit/sec. For the Home and Office WLAN networks, which are the focus of this thesis, the WIGWAM project proposes the use of 100 MHz wide frequency channels at the 5.25 GHz frequency band. Further parameters of the suggested wideband channel are given in Table 5.3. Under these conditions, the maximum achieved data rate at the channel, assuming the 64QAM 3/4 PHY

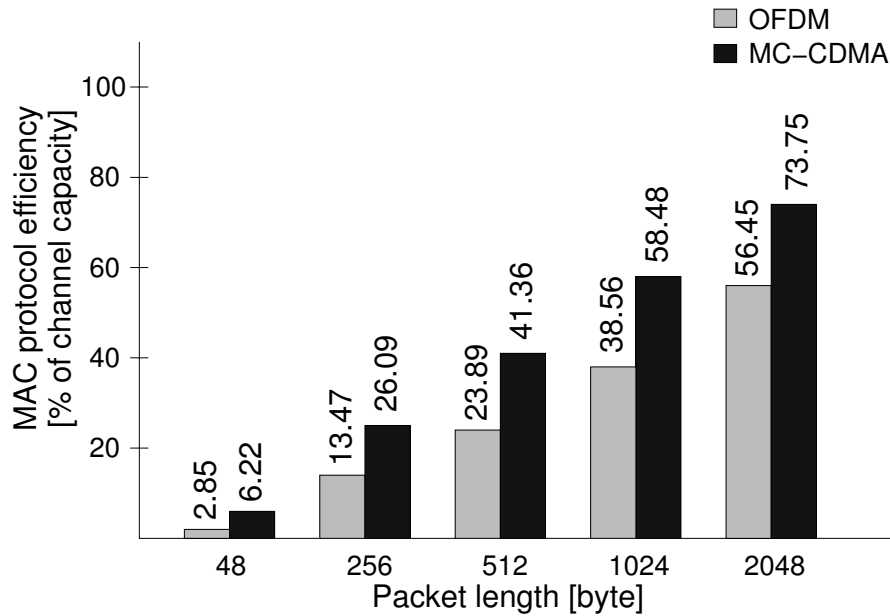


Figure 5.11: MAC protocol efficiency comparison for different data packet sizes.

mode, is 394.41 Mbit/sec.

In order to calculate the throughput of C-DCF under these conditions, the time needed for a complete data frame transfer should be calculated, that is given from Eq. (5.11). The needed parameters for the calculation have the following values:

Table 5.3: Parameters of the wideband channel for high speed WLANs at 5.25 GHz.

| Parameter | Value |
|-----------------------|--|
| Symbol interval | $6.8\mu\text{sec} = 6.4.2\mu\text{sec} + 0.4\mu\text{sec}$ |
| Guard interval | $0.4\mu\text{sec}$ |
| Number of subcarriers | 596 Data + 20 Pilot |
| Subcarrier spacing | 0.15625 MHz |
| Channel bandwidth | 100 MHz |
| Carrier frequency | 5.25 GHz |

- The synchronization preamble has a duration of $16\mu\text{sec}$ [802.11A /D7 (1999)].
- The RTS, CTS frames have the extended frame format described in Section 5.2.2.
- The format of data and ACK frames is the same as described in Section 2.1.9.
- PHY layer frames are build according to the format described in Section 2.2.2.
- The signal field of the PHY layer frame has a length of 24 bits [802.11A /D7 (1999)] and is transmitted with the BPSK 1/2 PHY mode. Consequently, it covers in DCF a complete multi-carrier symbol [802.11A /D7 (1999)] and in C-DCF with SF=4, the same field (4x24 bits=96 chips) covers 4 multi-carrier symbols. When the wideband channel is used for C-DCF, the 96 chips of the signal field fit in one multi-carrier symbol with $6.8\mu\text{sec}$ duration.

From the above parameter values, Eqs. (5.11) and (5.12), the duration for a complete data frame transfer can be calculated for different PHY modes and data packet sizes and therefrom the throughput at MAC layer. The results are presented in Fig. 5.12 in form of MAC protocol efficiency. Optionally, the wideband IFS values of Table 5.4 can be used to increase further the throughput.

From Fig. 5.12 the advantage of spreading, through the application of MC-CDMA, is obvious for all the analyzed cases. The C-DCF achieves higher MAC protocol efficiency, that depending on the applied setup is up to 281% higher than the OFDM based DCF.

Table 5.4: Values of interframe spaces adopted to the wideband channel.

| Parameter | Value |
|-----------|------------------|
| aSlotTime | $4\mu\text{sec}$ |
| SIFS | $4\mu\text{sec}$ |
| DIFS | $8\mu\text{sec}$ |
| Preamble | $4\mu\text{sec}$ |

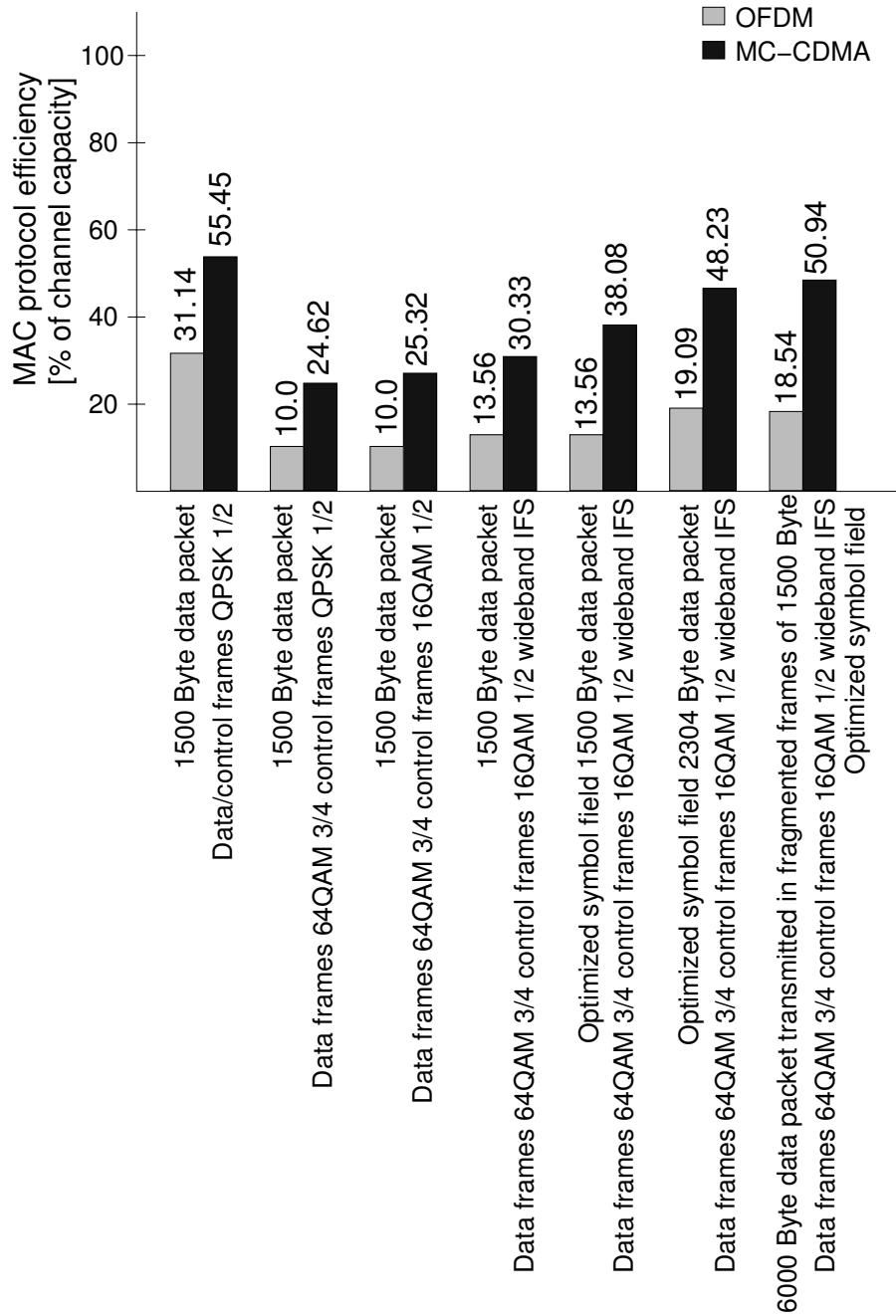


Figure 5.12: MAC protocol efficiency comparison for different data packet sizes and PHY modes.

The MACNET2 Simulation Tool

Content

| | |
|--|----|
| 6.1 SDL Modules - Protocol Specification | 72 |
| 6.2 SPEETCL | 73 |
| 6.3 C++ Modules - Interference Calculation - PER | 73 |
| 6.4 Validation | 76 |

MACNET2 stands for Multihop Ad Hoc Network Simulator for HiperLAN2 and IEEE 802.11a. This event driven simulation tool was originally developed in [PEETZ (2003)], for the performance evaluation of the HiperLAN/2 MAC protocol. The protocol is implemented in *Specification and Description Language* (SDL) as graphical representation, and translated to C++ with the SDL2SPEETCL [AIXCOM (2002)] translation tool.

Besides the SDL graphical implementation, MACNET2 comprises several C++ modules, which either act as support for the SDL functionality in form of *Abstract Data Types* (ADT) or stand for the channel model, traffic load generator and simulation control.

An overview of the simulation tool is given in Fig. 6.1.

In this thesis, the MACNET2 simulator has been extended with the functionality of a MC-CDMA based, distributed WLAN. On MAC level, the modules of the C-DCF MAC protocol have been added and a detailed MC-CDMA model is implemented in the PHY layer.

Extensions are performed to the channel model. The multi-channel structure of spread spectrum systems, with users active in parallel, and the distributed channel access of the new protocol compared to the centralized control in the HiperLAN2 system, require different approach, especially for the interference modelling and calculation. Besides adjacent channel interference, MAI from different cchs is taken into account for all the asynchronous transmissions running in parallel.

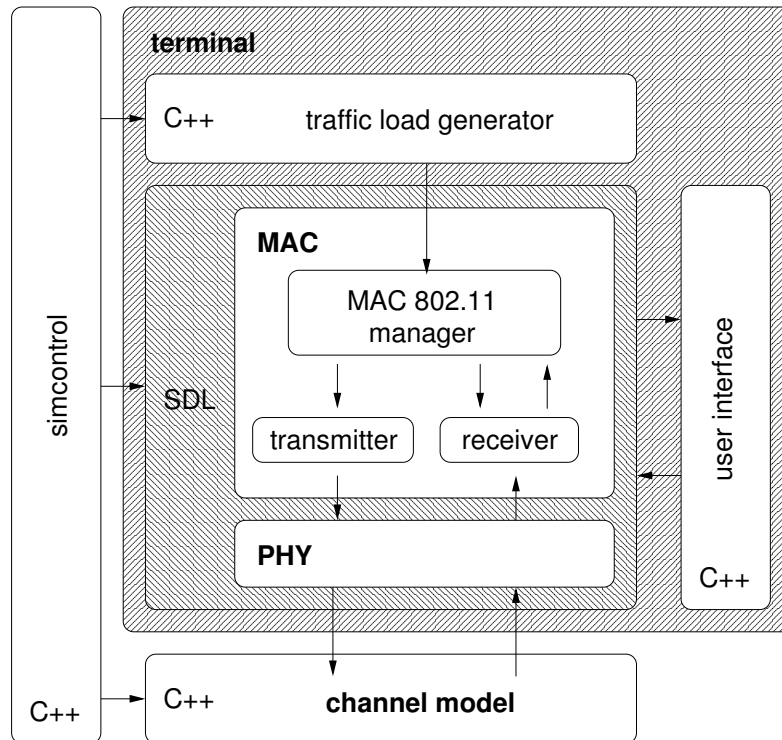


Figure 6.1: The MACNET2 simulation tool.

6.1 SDL Modules - Protocol Specification

The new developed algorithms, together with the C-DCF, have been specified in SDL. The implementation comprises four processes: the MAC IEEE 802.11 manager, the transmitter and receiver and the process to represent the functionality of the PHY layer. The MAC IEEE 802.11 manager interfaces to the MAC layer and the traffic load generators implemented in C++. It is also responsible for the communication between transmitter and receiver and the distribution of incoming signals among them.

The initialization of backoff procedure, the transmission of frames and the evaluation of queueing delay are done at the transmitter process. The receiver module provides the functionality needed for the reception of the frames and performs the evaluation of the service time duration.

Coding and mapping of the information bits into modulated symbols take place in the transmitter part of the PHY layer. In addition, MC-CDMA spreading is performed, the coded OFDM symbols are created and

the cyclic prefix added. Adequate functions for the reverse operations exist at the receiver part.

6.2 SPEETCL

For a detailed implementation according to the *International Standards Organization* (ISO)/ *Open Systems Interconnection* (OSI) model and the performance evaluation of the protocol, *SDL Performance Evaluation Tool Class Library* (SPEETCL) [AIXCOM (2002)] is attached to the MACNET2 simulation tool. The SPEET library provides classes for an accurate modelling of telecommunication entities and the communication between both, corresponding entities and neighboring layers of the ISO/OSI model.

Furthermore, SPEETCL contains powerful functions for statistical performance evaluation of the results. Especially for the evaluation of data packet delay, besides the calculation of the mean, variance, and moments of higher order, the library provides means for calculating the *Cumulative Distribution Function* (CDF) of random variables. This functionality is especially applied for estimating the CDF of data packet queueing delay.

6.3 C++ Modules

The C++ modules comprise the simulation control, user interference calculation and channel modelling.

The simulation control section manages initialization and control of both, the simulation run and the event driven scheduler of the simulator. It is also responsible for the assignment of the user specified values to the system parameters, and the periodic update of the simulation output files.

The user interface consists of C++ procedures, which are called from the SDL modules in form of ADT. Here the *Protocol Data Unit* (PDU) and SDU classes are build, with the needed functions for parsing information to their variables and for retrieving it.

The channel module is used to represent logical connections of different MS entities. It contains functions for the calculation of path loss as given in Eq. (6.1), provides models for measurements of the received power and the interferences at the receivers and contains detailed functionality model

of both, the MMSE MUD and the convolutional encoder.

$$L = -10\log g_t - 10\log g_r - 20\log \frac{\lambda}{4\pi} + 10\gamma\log d \quad (6.1)$$

6.3.1 Traffic Load Generators

The traffic load generators, offer traffic defined by type, data packet length and mean interarrival time. These parameters can be set for each MS individually. In order to evaluate the QoS achieved under different load conditions, three types of traffic load generators are implemented in MACNET2: Poisson, constant bitrate and *Moving Picture Experts Group* (MPEG). With the Poisson and the constant bitrate generators the data packet length is constant and defined in the ini-file, while the MPEG traffic load generators deliver data packets of variable length according to MPEG-4 loaded H.263 video traces as defined in [FITZEK and REISSLEIN (2001)].

6.3.2 Interference Calculation

In multiuser scenarios a complex interference model is used. Since packet switching is used, users in the same frequency channel can be affected by fluctuating interference levels [AKYILDIZ et al. (1999)]. In simulations performed for this thesis, all alien transmissions contribute to MAI, namely other transmissions on the same cch and transmissions on other cchs. The SINR is calculated according to the model provided in Section 4.1 and takes into account not only the transmission powers in all cchs, but also relative delays of all transmissions interfering to the observed one.

Since the interference is not constant during frame reception, event driven simulation is applied in the channel model. The signals startReceive and endReceive, sent (simulator internally, not via a cch) by the transmitter of a frame to all stations mark the start and end of a frame as depicted in Fig. 6.2. Upon receiving these signals, MSs who are not the intended receivers of the frame, update their interference estimates. The interference and consequently the SINR calculation, is thus divided into intervals with a constant interference level. For all intervals, SINR values are calculated in each receiver and at the end of the reception they are averaged resulting in a mean SINR value, Fig. 6.3. Should one of the intermediate SINR values, at a receiver be smaller than 0dB, the frame is discarded.

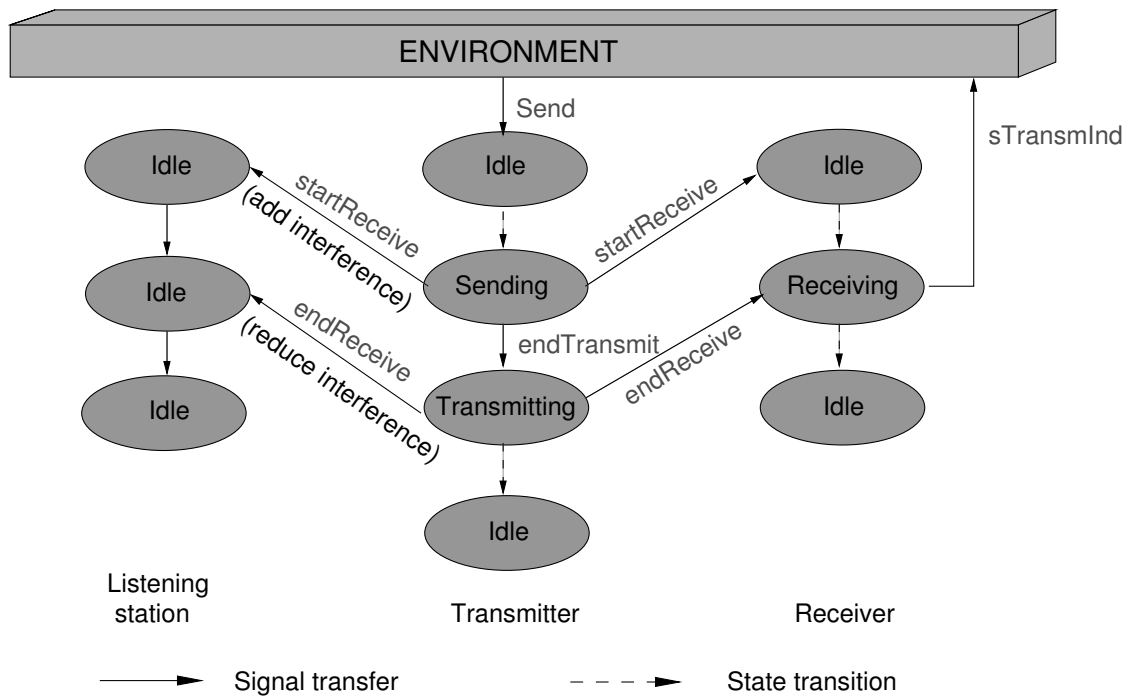


Figure 6.2: Event driven channel model for interference calculation.

The average PER for a packet is calculated based on the above mentioned estimation of the mean SINR assuming the convolutional decoder with generator polynomials $g_1 = 133_8$ $g_2 = 171_8$. Optionally, an upper limit for the tolerable PER value can be specified, resulting in discarding all frames with higher PER.

6.4 Validation

The simulation tool has been validated with respect to its results in terms of throughput and delay by the analytical modelling approach presented in Section 5.5.

Figure 6.4 presents the network and cch throughput as a function of the offered load for the 64QAM 3/4 PHY mode. The data PDUs are 1024 byte long and the scenario consists in this case of two terminals using all four cchs in parallel to exchange information with each other. Both, ana-

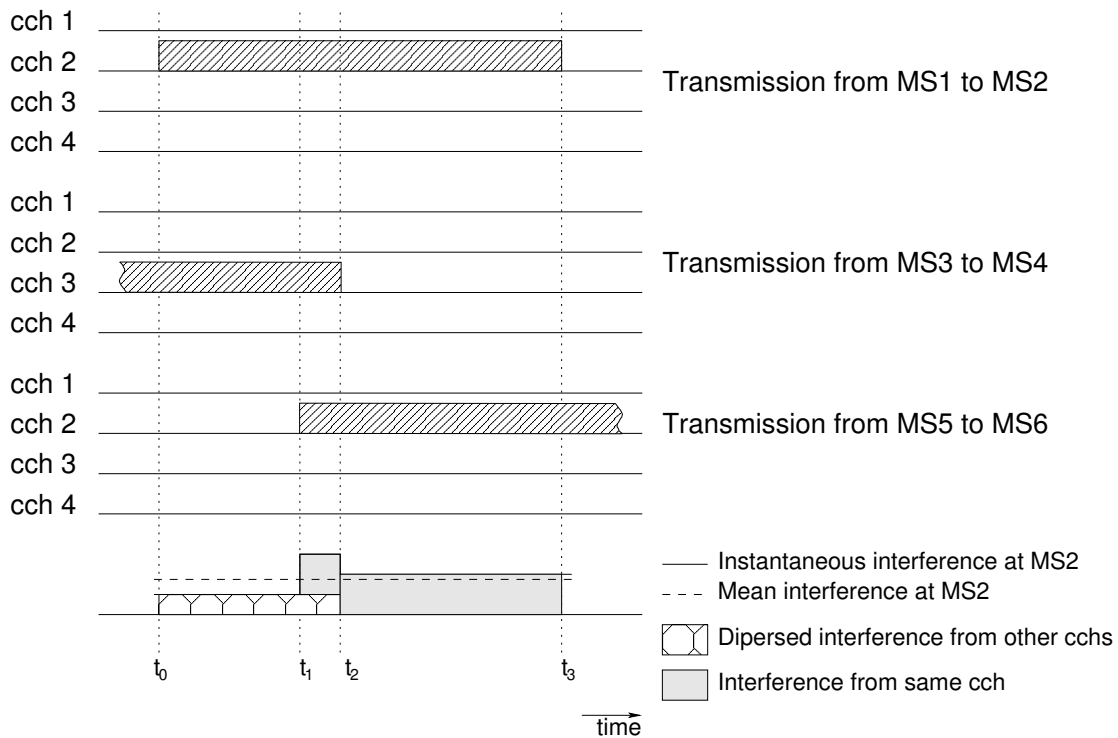


Figure 6.3: Mean interference calculation.

lytical (markers) and simulated results (lines), show the same performance characteristics. The service time consists in both cases of about $1,03ms$, complying with the one previously calculated, see Section 5.5.

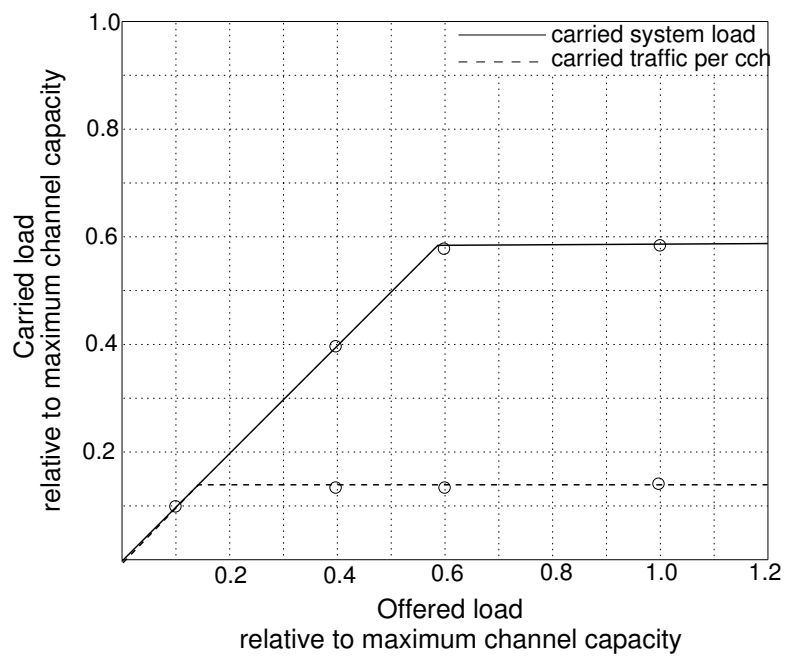


Figure 6.4: Simulated and analytically calculated throughput.

C-DCF Performance Evaluation: cch selection on Connection Basis

Content

| | |
|---|-----|
| 7.1 Basic MAC | 79 |
| 7.2 Transmit Power Control Analysis | 89 |
| 7.3 Improved Handshake - Adaptation to Suitable Cch | 97 |
| 7.4 Frequency Adaptation - Adaptation to Suitable Frequency Channel | 107 |
| 7.5 Conclusion | 116 |

This chapter introduces simulation results for the new MAC protocol described in Chapter 5. Divided in five sections, the results comprise the performance evaluation of the C-DCF, the enhancements from the application of power control and the benefits of the first and second adaptation method. In the last section, conclusions are drawn.

The parameter values used in the simulations are shown in Table 7.1.

7.1 Basic MAC

In order to measure the practically achievable throughput of the proposed C-DCF for operation on 4 MC-CDMA cchs, the scenario shown in Fig. 7.1 is simulated at first. It describes a typical SOHO scenario, which is the focus of this thesis, comprising 10 terminals operating 5 connections in a 8mx8m area. This elementary scenario is used for simulations at first, in order to deploy the protocol's features and limits, where MSs experience low distortion from MAI. Simulations of complex scenarios will follow in next sections of this chapter.

Simulations are performed with the QPSK 1/2 PHY mode used for both, control and data frames, in all connections. For these simulations a CW_{min} size of 7 is used to allow a direct comparison with the mathematical analysis results given in Section 5.5. In general, due to contention reduction by

Table 7.1: Simulation parameters.

| Parameter | Value |
|------------------------------|---|
| max. TxPower | 17dBm |
| start TxPower | 6dBm |
| Spreading Factor | 4 |
| CW_{min} | 7 slots (Data QPSK 1/2) 15 slots (Data 64QAM 3/4) 31 slots (>20 MSs and multihop) |
| CW_{max} | 1023 slots |
| Number of subcarriers | 48 Data + 4 Pilot |
| Subcarrier spacing | 0.3125 MHz |
| Channel bandwidth | 20 MHz |
| Carrier frequency | 5.25 GHz |
| Noise level | -93dBm |
| Pathloss factor | 3.5 |
| TxRate Data | 12/54 Mbit/sec |
| TxRate Control | 6/12 Mbit/sec |
| RTS/CTS | enabled |
| Symbol interval | $4\mu sec = 3.2\mu sec + 0.8\mu sec$ |
| Guard interval | $0.8\mu sec$ |
| Preamble | $16\mu sec$ |
| Max. propagation delay | $0,370\mu sec$ |
| MAC SDU length | 1024 Byte |
| SIFS | $16 \mu sec$ |
| DIFS | $34 \mu sec$ |
| PIFS | $25 \mu sec$ |
| aSlotTime | $9 \mu sec$ |
| Frequency change probability | 50% |
| target SINR | 25dB (64QAM 3/4) 10dB (QPSK 1/2) |
| TPC fading margin | 2.5dB (included in target SINR) |
| Number of Frequency Channels | 2 |
| a_{IF} | 0.25 |
| Offered load distribution | Poisson (default) MPEG CBR |
| LRE confidence interval | 5% |

operating four parallel cchs in the same frequency channel, a smaller CW_{min} can be used. Poisson traffic load generators are applied with normalized mean interarrival time equal to the average transmission window size for MC-CDMA (Eq. (5.19)), as calculated in Section 5.5. Mean interarrival time is scaled to the offered traffic load parameter.

The selection of the cchs is done randomly for all connections, and does not change throughout the connections running time. Before the first transmission of a data packet in each connection, the RTS frame is transmitted in all 4 cchs, in order for the transmitter to inform the receiver about the cch to be used.

Figures 7.2 and 7.3 show the simulated system throughput and throughput per cch versus the offered load for 512 and 1024 byte long *MAC sublayer Service Data Unit* (MSDU)s respectively. Simulation results show that the proposed C-DCF achieves a total throughput close to the theoretical maxi-

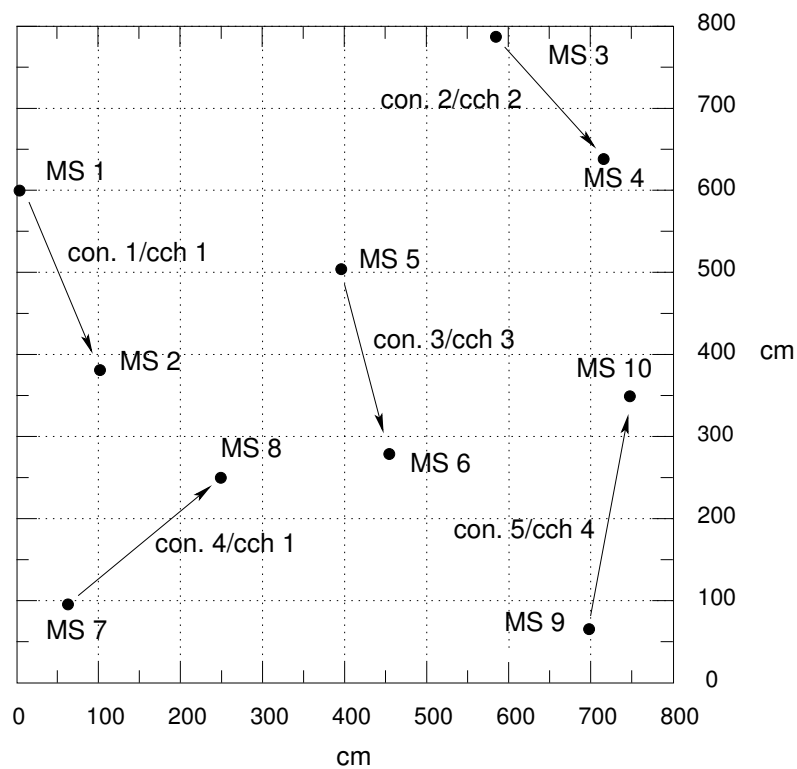


Figure 7.1: Elementary simulation scenario.

mum (Eq. (5.20)), for high offered load. This is 8.75 Mbit/sec in case of 512 byte long MSDUs with the QPSK PHY mode. For the case of 1024 byte long MSDUs, the system throughput approaches under saturation (with an offered load greater than 10 Mbit/sec) a maximum of 83% of the frequency channel capacity, corresponding to 10.05 Mbit/sec.

In the simulated scenario saturation is reached at an offered load exceeding 25% the analytically calculated maximum throughput value. Taking as example the case of 1024 byte long data packets, saturation is reached when all resources are utilized, thus each cch carries 2.5 Mbit/sec of traffic. Assuming that offered load is same for all MSs, saturation is reached when 2.5 Mbit/sec/con. offered load is applied (which equals to 5×2.5 Mbit/sec = 12.5 Mbit/sec offered load in the system), in order to saturate each cch. As a result, the offered load in cch 1 carrying two connections sums to 5 Mbit/sec.

From the two figures 7.2 and 7.3, the dependency of the system throughput on data packet size is obvious. The reason for this is the growing payload with data packet size, whereas the size of control frames, the duration of guard intervals and different sublayers' overhead remains the same.

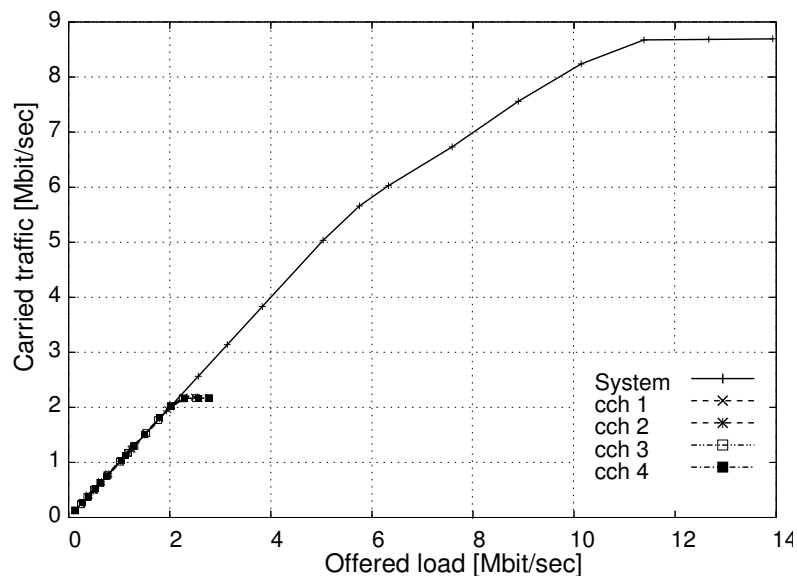


Figure 7.2: Achievable system throughput and throughput per cch for 512 byte long data packets, applying the QPSK 1/2 PHY mode for both control and data frames.

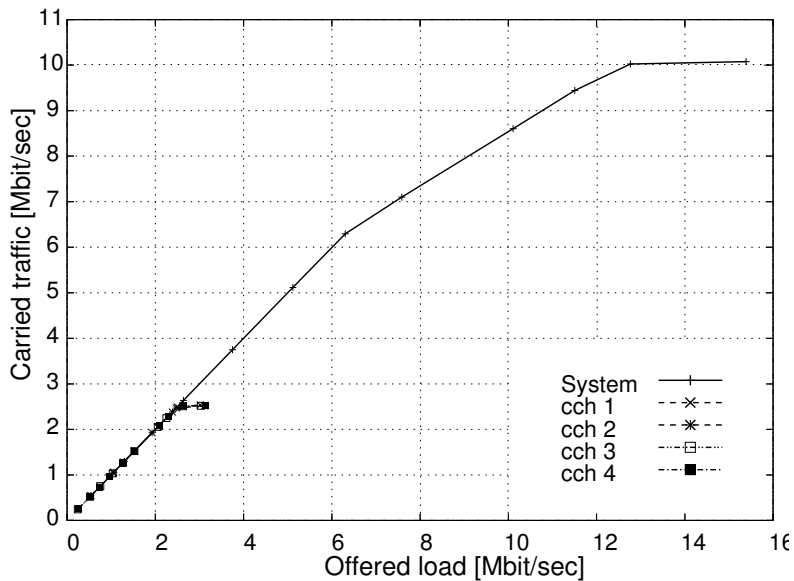


Figure 7.3: Achievable system throughput and throughput per cch for 1024 byte long data packets, applying the QPSK 1/2 PHY mode for both control and data frames.

In Fig. 7.3 system throughput raises linearly with offered load, up to a value of 6.25 Mbit/sec. At this point, each of the 5 connections is offered 1.25 Mbit/sec Poisson load in average and cch 1 carrying 2 connections, reaches its maximum throughput of 2.5 Mbit/sec (see Section 7.3). As a result, for values of offered load higher than 6.25 Mbit/sec, only the three other cchs, that are not yet saturated, can raise their amount of carried traffic. Consequently, system throughput raises with offered load, from this point on, with a gradient of 0,75 until saturation. The system throughput curve for 512 byte long data packets in Fig 7.2 has similar characteristics.

Figure 7.4 shows the measured mean queueing delay over all transmitted data packets with offered load, for 512 and 1024 byte long MSDUs. Queueing delay denotes the duration for which a data packet waits for transmission in the queue. The results in Fig. 7.4 show a progressive increase of the queueing delay with offered load, after the saturation point of cch1 that serves two connections.

In Fig. 7.5 the mean queueing delay per connection with offered load is presented, for both cases of 512 and 1024 byte long data packets. When

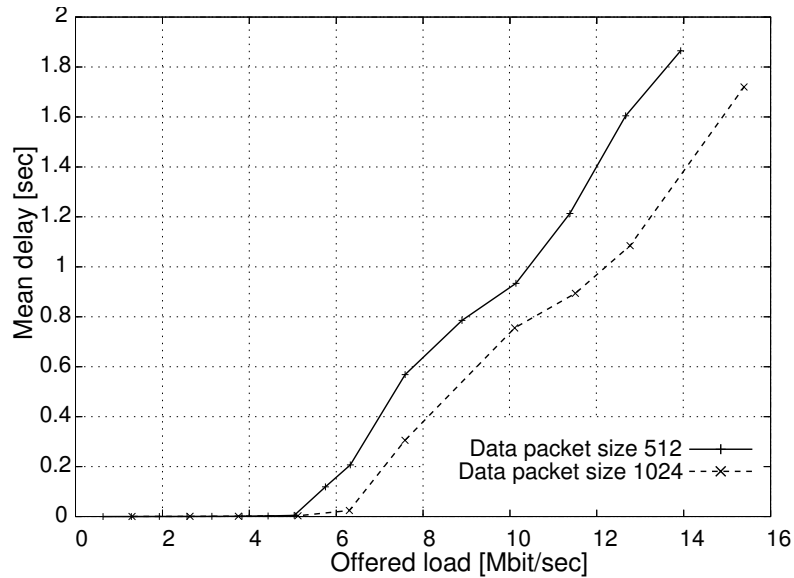


Figure 7.4: Mean queueing delay over all transmitted data packets for 512 and 1024 byte long data packets, applying the QPSK 1/2 PHY mode for both control and data frames.

load does not exceed the saturation point of the particular connection, that as discussed before depends on the number of concurrent connections per cch, the mean queueing delay is below 10 msec, which is an acceptable value for wireless data transmission.

The mean service time over all transmitted data packets with offered load for both, 512 and 1024 byte long MSDUs is shown in Fig. 7.6. The service time is defined as the time between the first transmission attempt of a RTS for a data packet and the reception time of the corresponding ACK. The measured service time is on average 1.8 and 3.4msec, respectively, latter corresponding well to the value of Eq. (5.19), and are for both cases constant and independent of the offered load. The service time could be affected from collisions, especially under higher load. Collisions lead to repetitive transmissions of the same frame after some backoff periods for the previously collided MSs. The simulation results give evidence to the assumption that the proposed protocol avoids collisions during contention periods, at least for the limited number of connections in the SOHO environment studied. This is a benefit of the parallel cchs used, since each station has now fewer

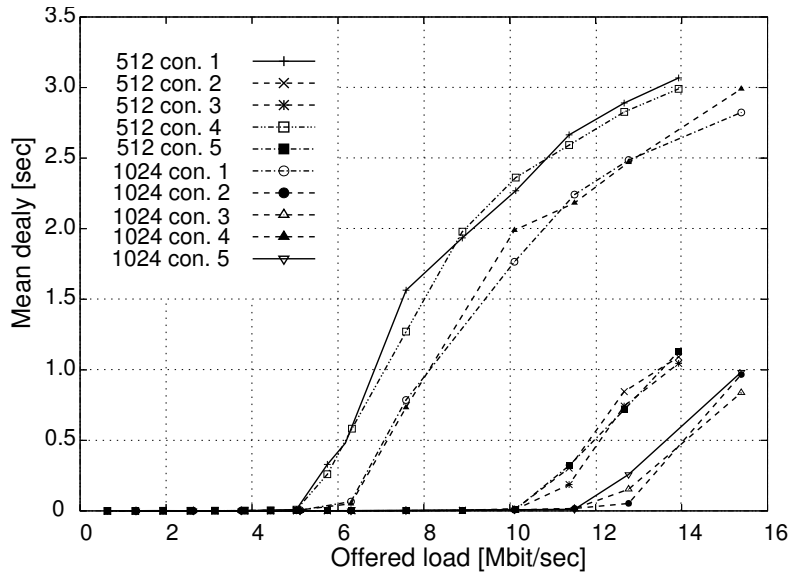


Figure 7.5: Mean queueing delay per connection for 512 and 1024 byte long data packets, applying the QPSK 1/2 PHY mode for both control and data frames.

competitors for medium access. Another proof of the efficient use of the available resources is the mean idle time, of all cchs, which has been found under full load in the simulation to be 5,79%.

In Figs. 7.7 and 7.8 the CDF of the measured delay in the example scenario is presented for different types of load.

In Fig. 7.7 the CDF for data packet queueing delay is shown for different data packet sizes, traffic source types and load intensities. Comparing the results for load 1.0, it is observed that for Poisson traffic sources both, the probability of no queueing delay and the maximum queueing delay value are higher, compared to the *Constant Bit Rate* (CBR) source. This results from the occasional burstiness of data packets from the Poisson traffic source, which consequently leads to higher delay of data packets. Unlike Poisson, the CBR traffic source is non-bursty in traffic, but with the same load, any erroneous frame results in queueing delay for all the following frames. The queueing delay's CDF for large data packets appears to be similar to that for short data packets (512 byte), with the difference that shorter data packets face shorter queueing delay, in general.

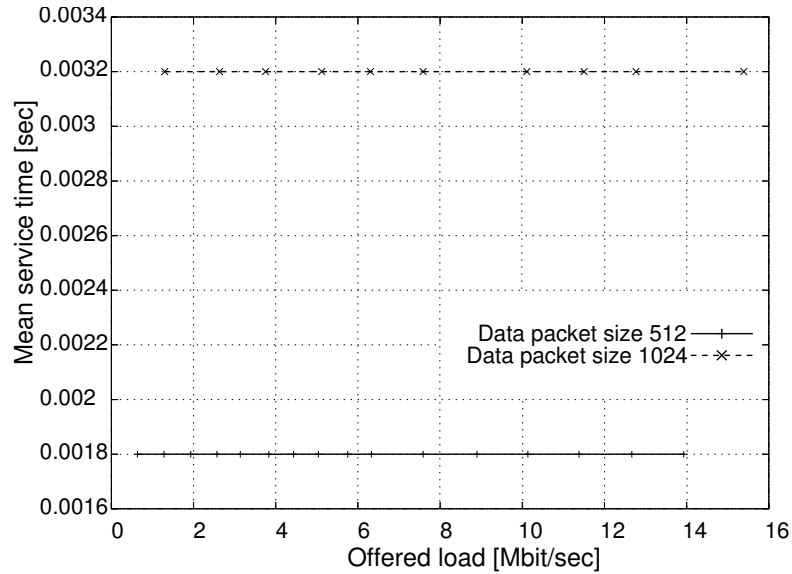


Figure 7.6: Mean service time over all transmitted data packets for 512 and 1024 byte long packets, applying the QPSK 1/2 PHY mode for both control and data frames.

Under lower offered load the measured queueing delay reduces. For offered load of 75% and Poisson traffic, the maximum queueing delay is about 6.2msec, corresponding to the transmission window size of 2 data frames.

Figure 7.8 presents the CDF of data packet queueing delay at MS 7 (see con. 4 in Fig. 7.1), with two MPEG streams in parallel, each offered 280 kbit/sec load. Other connections carry Poisson traffic with average intensity of 600 kbit/sec. The queueing delay is provided for 512 and 1024 byte long MSDUs and has an average value of 0.7msec and 0.25msec, respectively. Both graphs show that transmitted data packets experience very low queueing delay with high probability, while a small amount of data packets only face higher but still small queueing delay. These data packets are reaching the destination MS after a retransmission, caused by frame corruption in the channel.

For 512 byte long MSDUs, the amount of data packets experiencing higher queueing delay is bigger. Since in both simulations the same MPEG trace file is used, the amount of data to be transmitted is the same, and

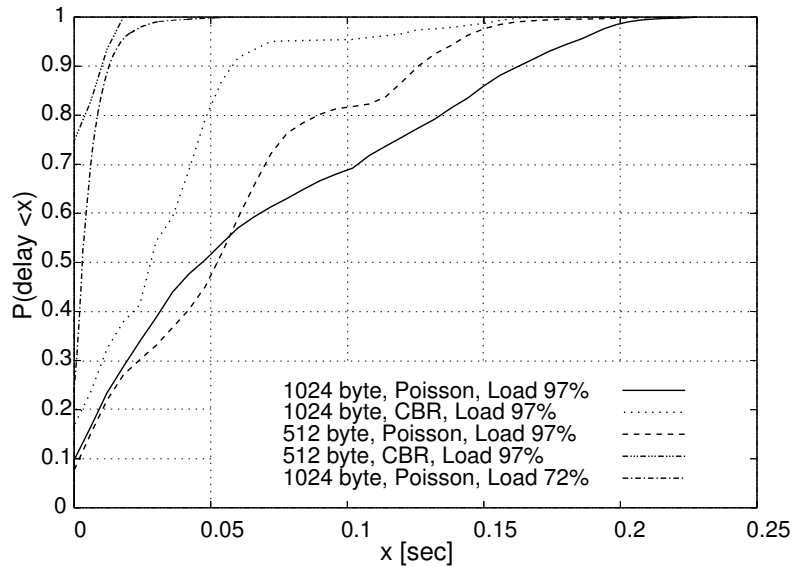


Figure 7.7: CDF of data packet queuing delay in the network at different load. The applied PHY-mode is QPSK 1/2 for both control and data frames.

the amount of transmitted MSDUs is doubled, when 512 instead of 1024 byte long MSDUs are transmitted as the payload. For the same channel conditions, the amount of corrupted frames is approximately doubled, too. This explains also the higher peak value of the queuing delay for 512 byte long data packets. The probability that a data frame at the beginning of a burst is corrupted is higher, and its retransmission affects the queuing delay of all the other data frames of the burst. In general, a small data packet size increases the average queuing delay as a result of additional control frames and both, MAC and PHY overhead.

Summarizing, the network's performance for MPEG load is very good, due to the cchs. MSs don't compete for the whole channel, but for a fraction of it, namely one cch. In the following chapters, the advantages of the new proposed protocol will be shown in larger scenarios, with data transmissions at higher PHY modes. In the current scenario, each transmitting MS is attached to one cch, and can completely utilize its resources for transmission, leading to short queuing delay. This can be considered as a form of bandwidth reservation for the transmitting MS. The network could con-

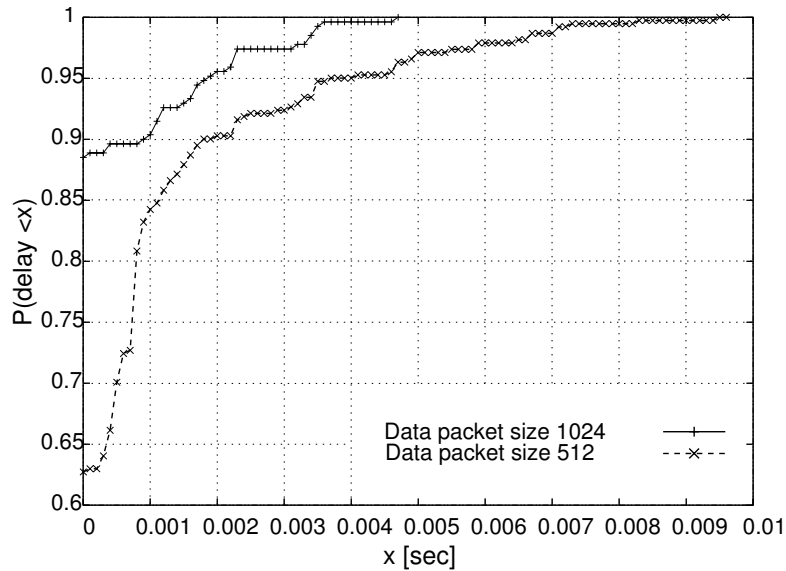


Figure 7.8: CDF of data packet queueing delay at MS 8 with two MPEG streams. The applied PHY-mode is QPSK 1/2 for both control and data frames.

sequently support more reservations if the number of spreading sequences would increase, which is feasible with broader bandwidth channels.

7.1.1 Basic MAC queueing delay evaluation in a wideband channel

The scenario of Fig. 7.1 is used for comparison of queueing delay performance of C-DCF in both, the IEEE 802.11a 20 MHz channel and the wideband (100 MHz) channel suggested in project WIGWAM. The MAC protocol efficiency has been compared in Fig. 5.12, where the ability of C-DCF to achieve high efficiency in wideband channels was shown.

Figure 7.9 presents the CDF of queueing delay for data packets transmitted in con. 2, in both cases, of the 20 MHz and 100 MHz channel applied. Data packets are 1500 Bytes long and the applied PHY-mode is 16QAM 1/2 for control and 64QAM 3/4 data frames (3rd case in Fig. 5.12). Poisson traffic load generators are used that offer load with average intensity equal to 95% of MAC level throughput. The queueing delay measured with both channels is very small, with transmissions in the wideband channel experiencing 5 times lower delay. Since the offered load and the protocol

(C-DCF) are the same in both cases, the queueing delay in the wideband channel profits from the effectively smaller overhead. In case a transmission error or collision occurs and a retransmission is needed, the duration of a complete frame transmission is $953.5\mu\text{sec}$ in the 20 MHz channel, whereas in the 100 MHz channel $494.3\mu\text{sec}$ are required for a complete transmission.

The CDF estimation in the results of Fig. 7.9 was done by the *Limited Relative Error* (LRE) algorithm [SCHREIBER (1988)] with a confidence interval of 5%. Other CDF estimations in this thesis are based on simpler algorithms (measurements of relative frequency of a value.), as they serve the comparison among both, different simulation setups and proposed functions of the C-DCF MAC protocol.

7.2 Transmit Power Control Analysis

In wireless networks, it is always beneficial to keep interference low. Especially in systems where MAI occurs, each transmitter should use the minimum possible transmission power, which ensures both, correct reception

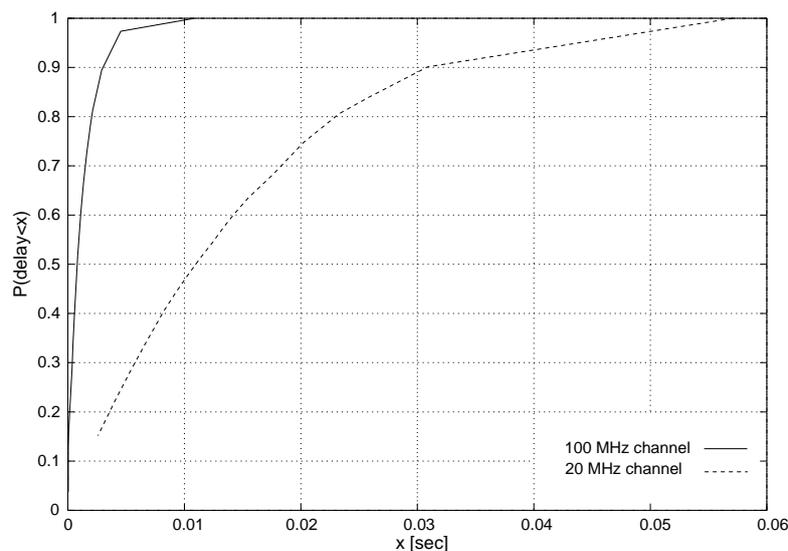


Figure 7.9: CDF of data packet queueing delay for con. 2 in the wideband channel, built by LRE algorithm. The applied PHY-mode is 16QAM 1/2 for control and 64QAM 3/4 data frames.

at the corresponding receiver and produces the least MAI to concurrent transmissions. In the following, power control is analyzed, according to simulation results based on the scenario of Fig. 7.10, where longer connections coexist with shorter ones in the same frequency channel, using different cchs.

Connections from MS 1 to MS 2 and MS 9 take place in cch 1, the connection from MS 3 to MS 4 in cch 2, connection from MS 5 to MS 6 in cch 3 and connection from MS 7 to MS 8 takes place in cch 4. The minSINR value is set to 12dB. For the QPSK 1/2 PHY mode and the used data packet length, a SINR value of 9.5dBm is sufficient for the PER to be close to zero. A 2.5dB margin is added in order to mitigate the effects of short term fading. Offered load follows the Poisson distribution and is a fraction of the cch maximum capacity at MAC layer, as calculated in Section 5.5.

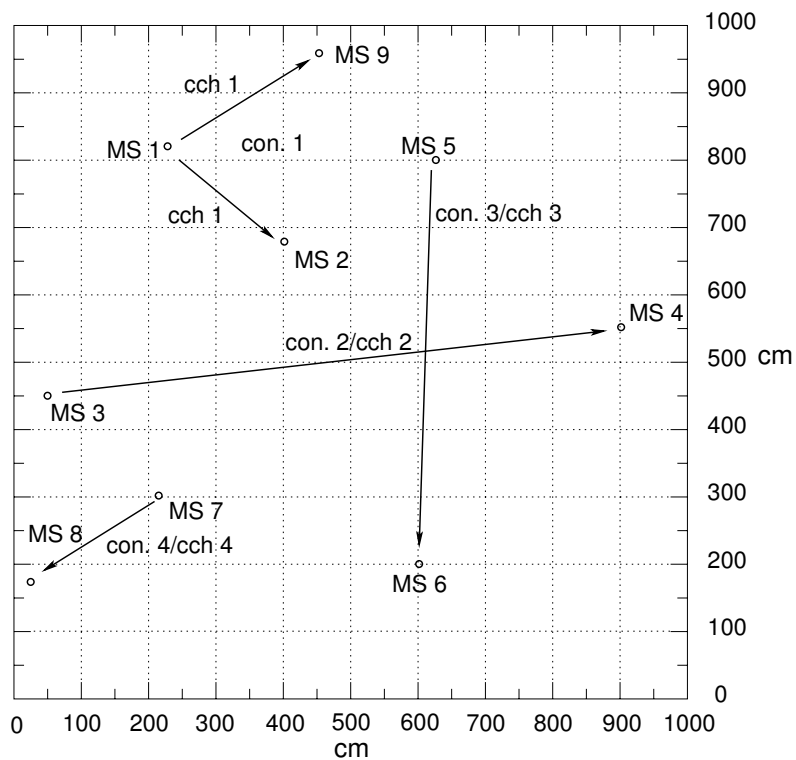


Figure 7.10: Simulated scenario for TPC analysis.

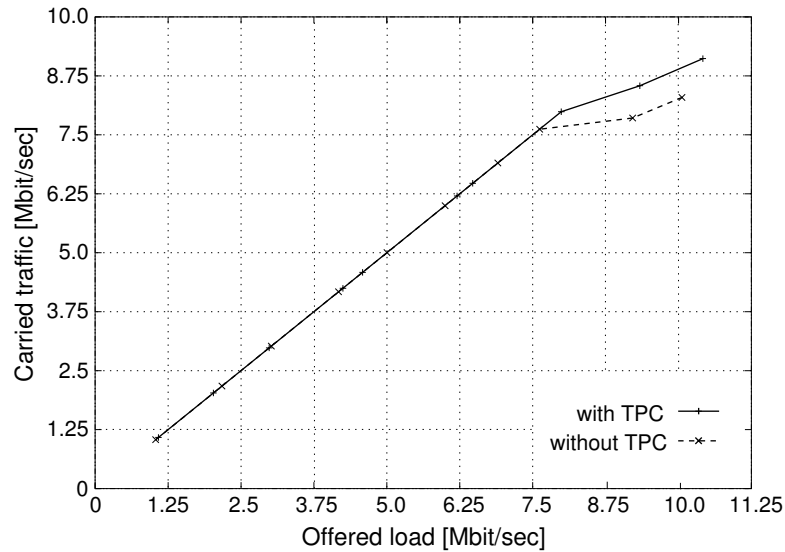


Figure 7.11: System throughput **with** and **without** TPC. The applied PHY-mode is QPSK 1/2 for both control and data frames.

In Fig. 7.11, the carried system traffic versus the offered load is given for both, activated and deactivated TPC. It can be seen from the figure that under high load the system's performance with TPC is better than without. In this case the maximum achieved throughput is 9.1 Mbit/sec. This corresponds to 91.2% of the theoretical maximum (Section 5.5). The throughput gain, when TPC is activated, is a result of the lower interference from ongoing transmissions, in other cchs.

The contribution of TPC to reduce interference, is better visible from Figs. 7.12 and 7.13. Figure 7.12 gives the carried traffic per cch without TPC. All MSs use the maximum transmit power of 50mWatt (17dBm). In this case, the long distance transmission, from MS 3 to MS 4, suffers under high load from high interference generated by MS 1, MS 5 and MS 7. Even with the robust QPSK 1/2 PHY mode, few data packets only can be transmitted on this connection when the other MSs are very active. For offered load less than the maximum cch capacity, MS 3 manages data transmissions on the idle time of its interferers. Short distance connections run without problems, and, as can be seen from the diagram, the corresponding cchs (cch 1, cch 2 and cch 4) achieve almost the maximum throughput (each about a quarter of the system throughput).

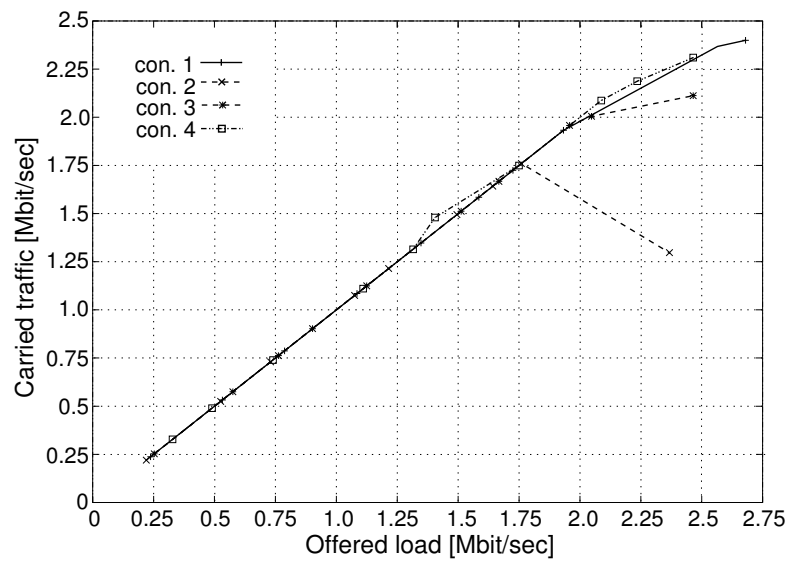


Figure 7.12: Throughput per cch **without** TPC. The applied PHY-mode is QPSK 1/2 for both control and data frames.

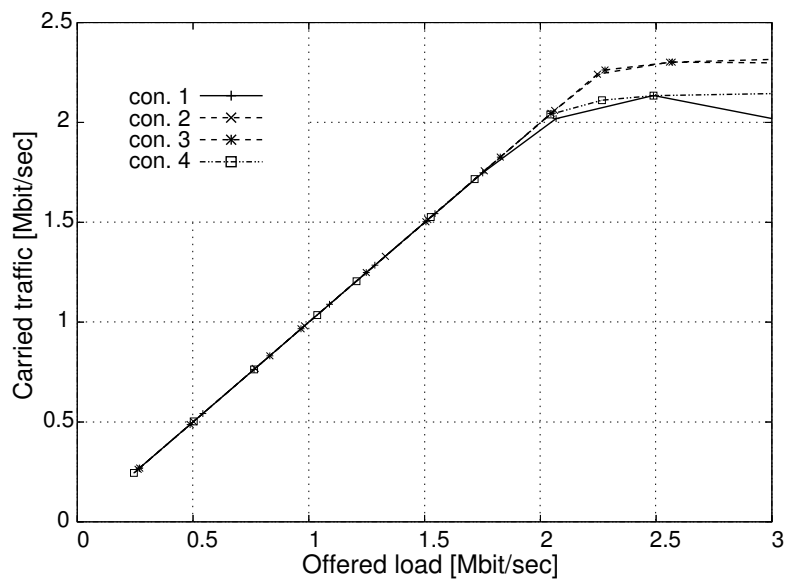


Figure 7.13: Throughput per cch **with** TPC. The applied PHY-mode is QPSK 1/2 for both control and data frames.

Figure 7.13 presents the carried traffic per cch over the offered load with TPC activated. The output powers of the transmitting stations are now adjusted by the TPC, algorithm to the algorithm in Fig. 5.4, to the following values:

MS 1: -18.5dBm
 MS 3: 0.2dBm
 MS 5: -5.7dBm
 MS 7: -10.7dBm

It can be seen from Fig. 7.13, that with these power arrangements no connection is blocked and the system achieves in every cch high throughput capacity. The major benefit of TPC, however, is the reduction of queueing delay, for connections that without TPC are under high load (partially) blocked from high interference, like con. 2 (between MS 3 and MS 4). In Figs. 7.14 and 7.15, the mean queueing delay (of all successfully transmitted data packets) is shown over the offered load. Without TPC, the operation for con. 1, con. 3 and con. 4 is ideal and the achievable queueing delay low. Queueing delay of data packets from MS 3 is low, for low offered load, but raises rapidly when the offered load exceeds 65% of the cch capacity, as offered load in concurrent connections reduces the chance for occurrence of low interference intervals, that MS 3 could use to transmit its data. The situation improves with TPC, Fig. 7.15, where the transmission power is reduced to the necessary level. For offered load up to 2.1 Mbit/sec/con., the queueing delay of previously blocked MS 3 does not exceed 50msec, and reaches 100msec for a fully loaded network (2.5 Mbit/sec/con.). Thereby, the mean queueing delay of other MSs improves, too.

Figures 7.16 and 7.17 present the mean service time of successfully transmitted data packets per MS over the offered load, for both cases of deactivated and activated TPC, respectively. Without TPC, con. 2 suffers higher average service time than other connections, that raises up to 6.5msec for a high offered load. This service time value equals to double the transmission window size (Eq. (5.11)), which corresponds to one erroneous frame transmission per data packet. With activated TPC, the service times reduce much, while their increase with offered load is limited to 0.7msec, reaching a maximum of 4msec.

For an offered load of 1.0, Fig. 7.18 shows the CDF of queueing delay in the network. The application of TPC lowers slightly the probability of low queueing delay, but improves the network's performance drastically

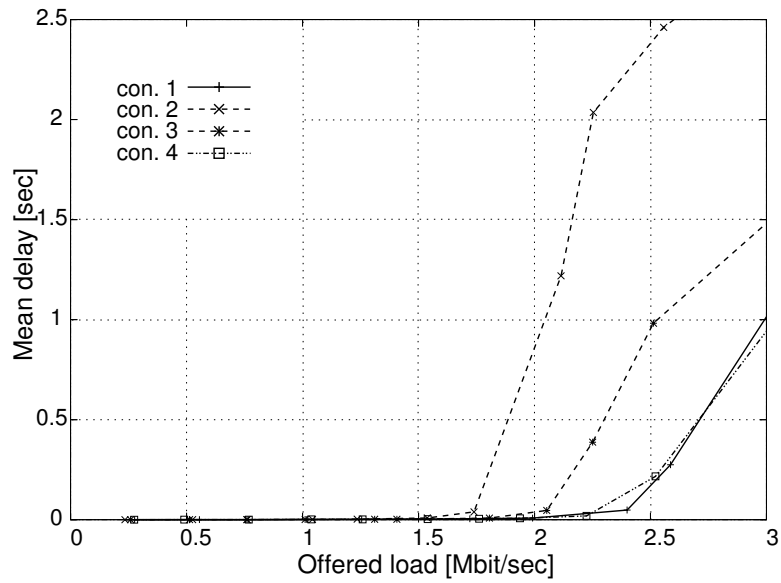


Figure 7.14: Mean queueing delay per transmitting MS **without** TPC. The applied PHY-mode is QPSK 1/2 for both control and data frames.

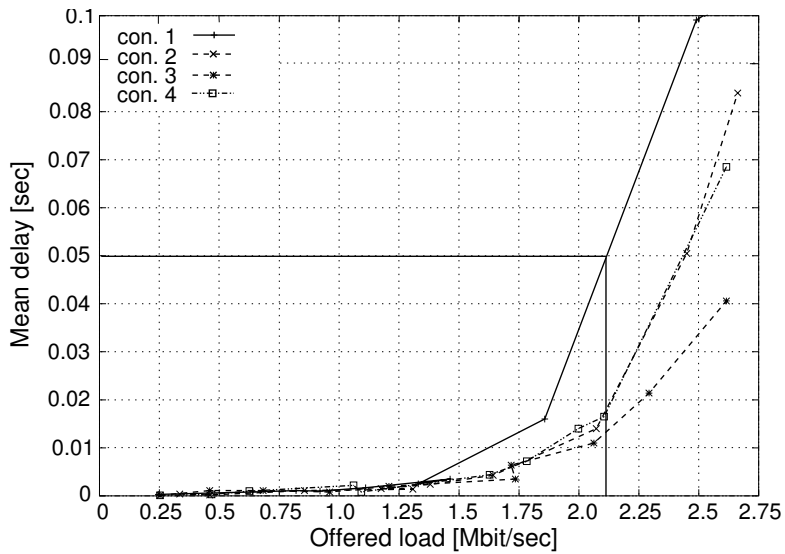


Figure 7.15: Mean queueing delay per transmitting MS **with** TPC. The applied PHY-mode is QPSK 1/2 for both control and data frames.

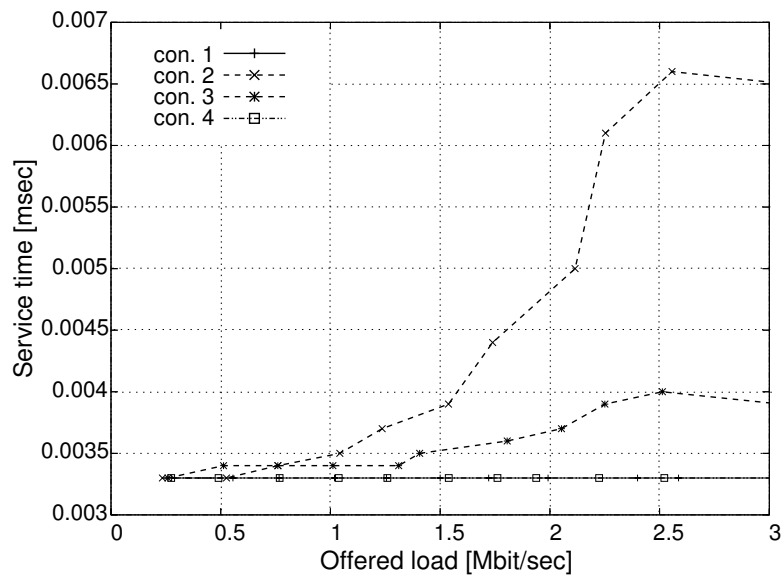


Figure 7.16: Mean service time per transmitting MS **without** TPC. The applied PHY-mode is QPSK 1/2 for both control and data frames.

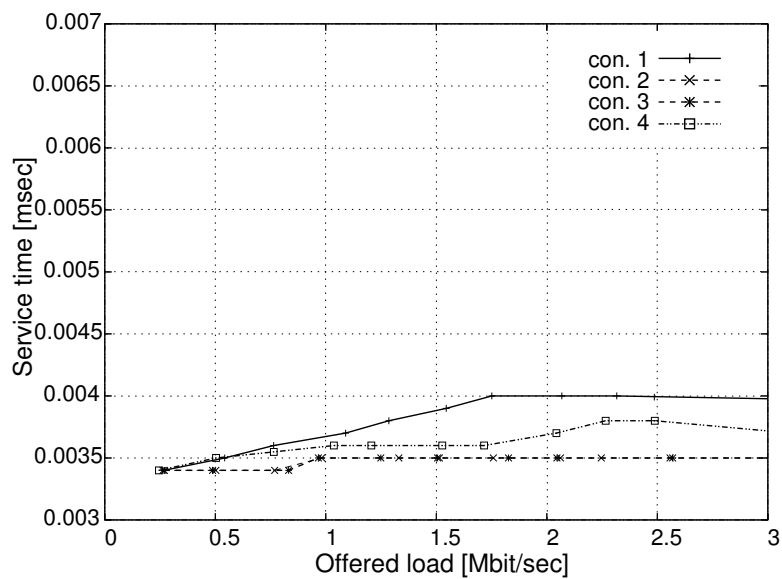


Figure 7.17: Mean service time per transmitting MS **with** TPC. The applied PHY-mode is QPSK 1/2 for both control and data frames.

with respect to the maximum measured queueing delay, reaching 0.25sec in the considered scenario. Without TPC (see Fig. 7.14) the maximum measured queueing delay approaches 0.9sec. Apparently, TPC reduces the interference to con. 2 substantially.

The proposed TPC method is based on estimating interference at the receiver, that is updated after a successful transmission, see Fig. 5.4. The most recent interference value measured contributes to the mean interference estimate with a weight factor a_{IF} . The influence of the weight factor on the queueing delay CDF is shown in Fig. 7.19. The worst performance is achieved with $a_{IF} = 1.00$. In this case only the most recent interference value is taken into account for estimating the mean interference at the receiver, leading to an overreacting power adjustment on the link and poor network performance. Best performance is achieved for $a_{IF} = 0.75$, allowing sufficient reactive power adjustment. For $a_{IF} = 0.25$ and $a_{IF} = 0.50$ the queueing delay performance is worse, with $a_{IF} = 0.25$ achieving the second best CDF. Since the considered scenario is non-representative for all possible set-ups of MSs, the weighting factor will have to be optimized scenario specific. The benefits of TPC will be exploited in the following in

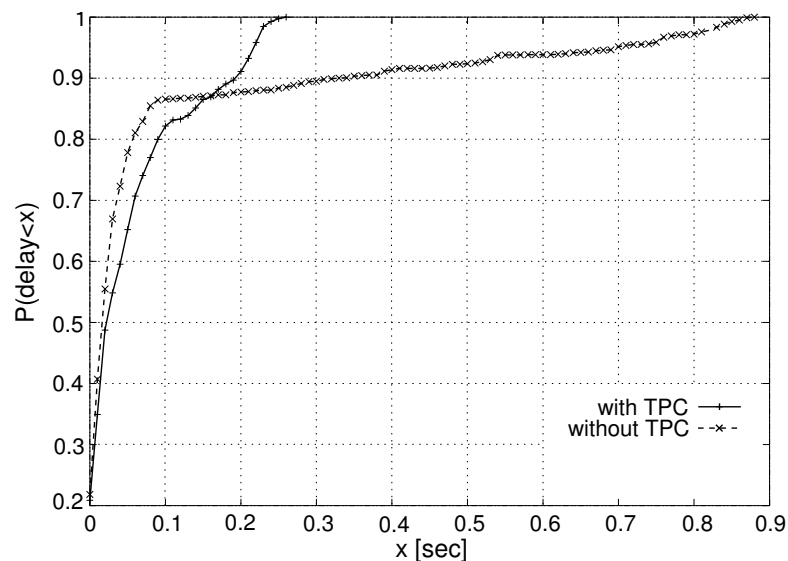


Figure 7.18: CDF of queueing delay **with** and **without** TPC. The applied PHY-mode is QPSK 1/2 for both control and data frames.

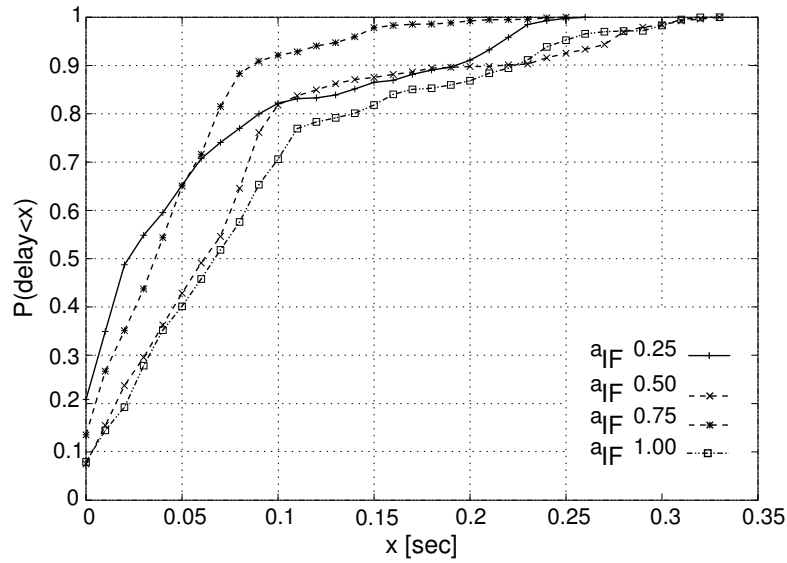


Figure 7.19: CDF of queuing delay for different weights in mean interference calculation. The applied PHY-mode is QPSK 1/2 for both control and data frames.

other scenarios, under heavy MAI and data transmission using higher PHY modes.

7.3 Improved Handshake - Adaptation to Suitable Cch

It has been shown in the previous section that TPC is beneficial in a wireless network where longer connections coexist with shorter ones. In decentrally controlled networks, it is not always possible to adjust the transmission power in a way that the intended receiver can achieve the demanded performance (especially when a higher PHY mode is required for the connection), while the interference generated at neighboring MSs is kept low. In centrally controlled systems, appropriate scheduling of uplink transmissions at the AP can overcome this problem.

In the proposed decentrally controlled system, the improved handshake (described in Section 5.3) provides means to operate concurrent connections in the same cch, separated in time domain, that cannot coexist in different cchs (due to MAI). In Fig. 7.20 a scenario relevant to the described problem

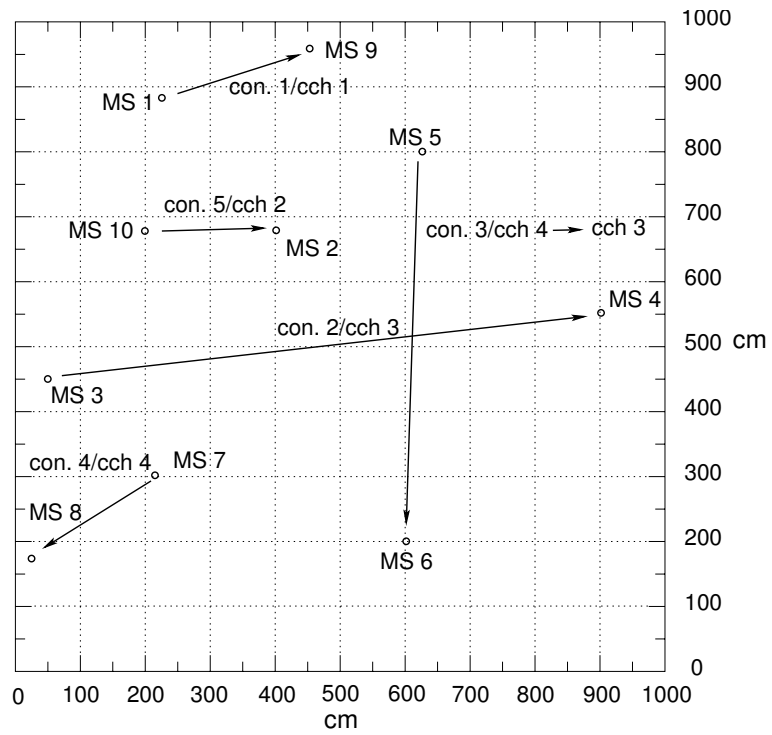


Figure 7.20: Simulation scenario for the **improved handshake** evaluation.

is presented, which is used for evaluation of the performance contribution of the proposed improved handshake algorithm. The applied values of the simulation parameters can be taken from Table 7.1. The minSNR value is set to 25dB. For 64QAM 3/4 as the user data PHY mode considered and the 1024 byte data packet length used, a value of 22.5dB is sufficient for a PER of 3% [ORFANOS et al. (2005b)]. The 2.5dB margin is added in order to mitigate the effects of short term fading. At transmitting MSs, Poisson load generators of variable intensity are used.

The cch 1 is assigned to con 1 from MS 1 to MS 9, while cch 2 is used by con. 5 (MS 10 to MS 2), cch 3 is allocated to con. 2 (MS 3 to MS 4) and cch 4 is assigned to con. 4, between MS 7 and MS 8. Connection 3 selects randomly after network initialization cch 4 for transmission, and applying the improved handshake algorithm searches for a more suitable cch, stabilizing in cch 3, where its major interferer (con. 2) is placed.

Figure 7.21 presents the system throughput versus the offered load. When the cch-adaptation algorithm is disabled, the system throughput reaches a maximum of about 26 Mbit/sec in overload, which corresponds

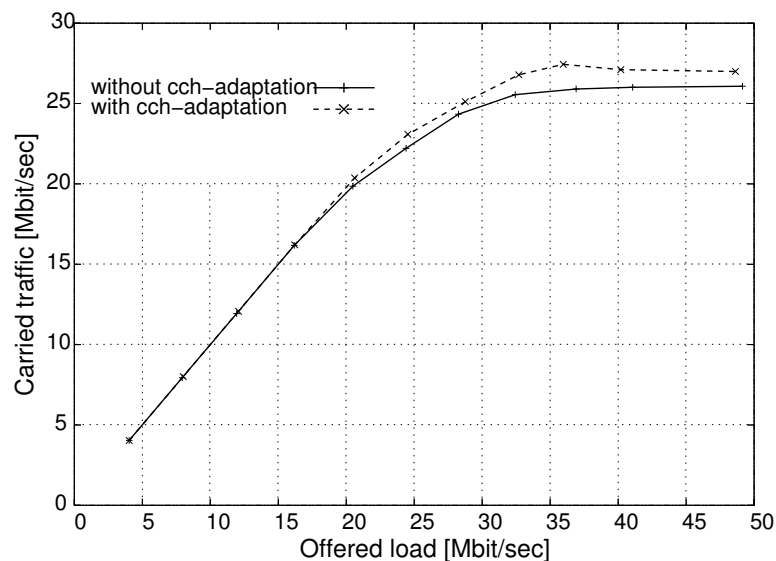


Figure 7.21: System throughput **with** and **without** adaptation to suitable cch vs. offered system load. The applied PHY mode is 64QAM 3/4 for data frames and QPSK 1/2 for control frames.

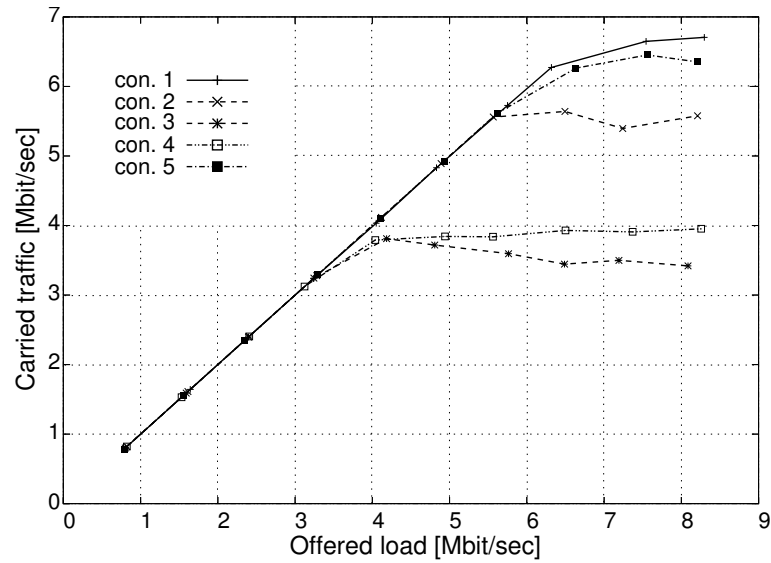


Figure 7.22: Throughput per connection **without** cch-adaptation vs. offered load per connection. The applied PHY mode is 64QAM 3/4 for data frames and QPSK 1/2 for control frames.

to 82.5% of the theoretical maximum (Section 5.5). This is due to high MAI, as can be seen from Fig. 7.22 presenting the carried traffic per connection without cch-adaptation. Due to high interference from con. 3, con. 2 achieves only a fraction of the available capacity in cch 3, namely 5.5 Mbit/sec instead of 7.895 Mbit/sec maximum cch capacity (see Section 5.5). Additionally, con. 3 itself is also distorted, achieving lower throughput than expected. Connection 4 reaches maximum throughput, that is approximately 4 Mbit/sec, since it is almost equally sharing the cch with con. 3.

When applying the proposed cch-adaptation, the situation improves. The graph in Fig. 7.21 shows a rise of the network throughput versus the offered load, up to a maximum of 27.5 Mbit/sec. Figure 7.23 presents the carried traffic of each connection, that now rises almost linearly to 4 Mbit/sec for con 2 and con. 3 sharing the same cch 3 and up to 6.8 Mbits/sec for the other connections. Compared to the case without adaptation (Fig. 7.22), con. 1 and con. 5 increase further their throughput, while con. 3 utilizes half of the resources in cch 3. cch 3 is shared among con. 3 and con.

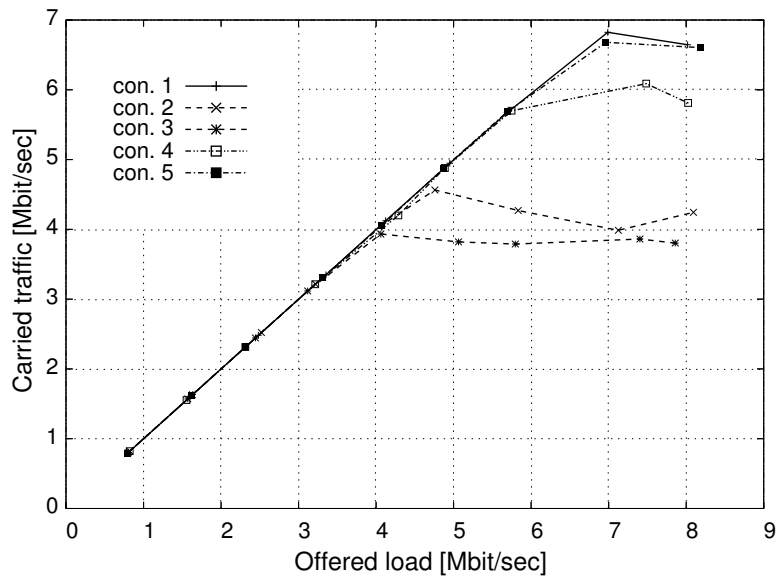


Figure 7.23: Throughput per connection **with** cch-adaptation vs. offered load per connection. The applied PHY mode is 64QAM 3/4 for data frames and QPSK 1/2 for control frames.

2 almost equally. For medium load, the carried traffic of con. 2 raises 10% to 20% higher than that of con. 3. This effect owes to con. 3 operating for some periods of time on cch 4, where its other major interferer is placed, namely con. 4. Carried traffic at con. 4 is 25% below the cch throughput, as a result of MAI from con. 2.

From Figs. 7.22 and 7.23 another important observation can be made. Without cch-adaptation, con. 3 chooses randomly cch 4 for transmission, where con. 4 operates. This limits the capacity for con. 4 to half the capacity of one cch. Accordingly, when cch-adaptation is applied, con. 3 is diverted to cch 3, limiting now the capacity of con. 2, sharing the same cch, with a direct impact on its achieved throughput (Figs. 7.22 and 7.23). Consequently, the cch-adaptation algorithm should only be applied, if the addition of a connection in the network does not limit the performance of existing connections, below their QoS bounds.

The contribution of the cch-adaptation algorithm, with regards to the achieved throughput is small from a somewhat lower MAI. The benefits

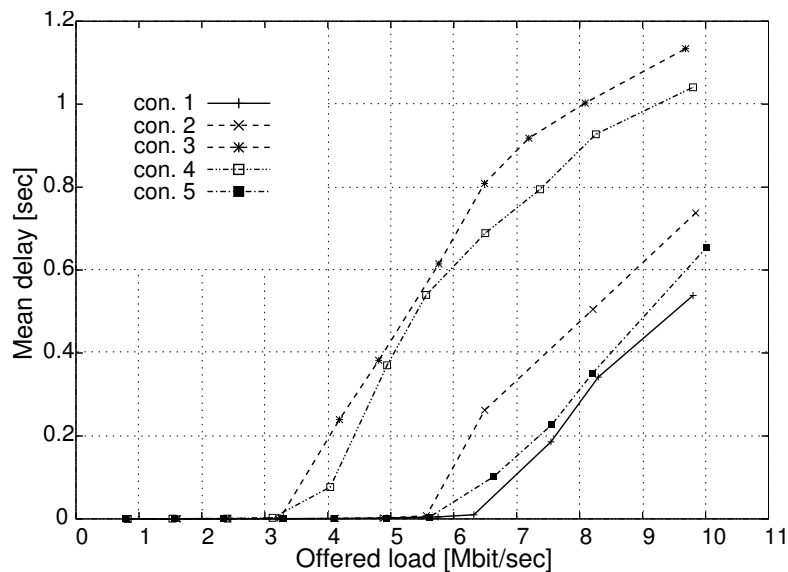


Figure 7.24: Mean queueing delay of successfully transmitted data packets per connection vs. offered load per connection, **without** cch-adaptation. The applied PHY mode is 64QAM 3/4 for data frames and QPSK 1/2 for control frames.

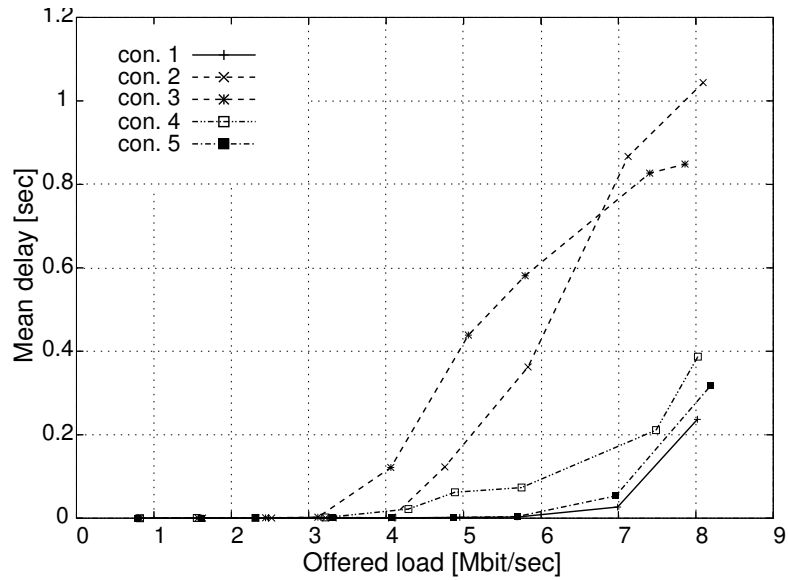


Figure 7.25: Mean queuing delay of successfully transmitted data packets per connection vs. offered load per connection, **with** cch-adaptation. The applied PHY mode is 64QAM 3/4 for data frames and QPSK 1/2 for control frames.

of the cch-adaptation algorithm become more evident when observing the results for queueing delay. Figure 7.24 depicts the mean queueing delay for all successfully transmitted data packets per connection, without cch-adaptation. For small offered load the queueing delay is low, but rises rapidly with increased offered load (more than 6Mbit/sec/cch), as a result of high MAI. For higher offered load, the mean queueing delay of all connections quickly grows up to 0.2sec, making the support of delay sensitive traffic impossible.

In Fig. 7.25 the corresponding results under cch-adaptation are presented. For offered load less than 7Mbit/sec, for con. 1, con. 4 and con. 5 operating in a cch each, and less than 3.5Mbit/sec, for con. 2 and con. 3 sharing the same cch, the queueing delay is very low, thus high QoS can be achieved.

Figures 7.26 and 7.27 present the service time of the connections with offered load. In both cases the mean service time grows for all connections from the initial theoretical value of $1037.5\mu\text{sec}$ (Section 5.5, Eq. (5.15)) up

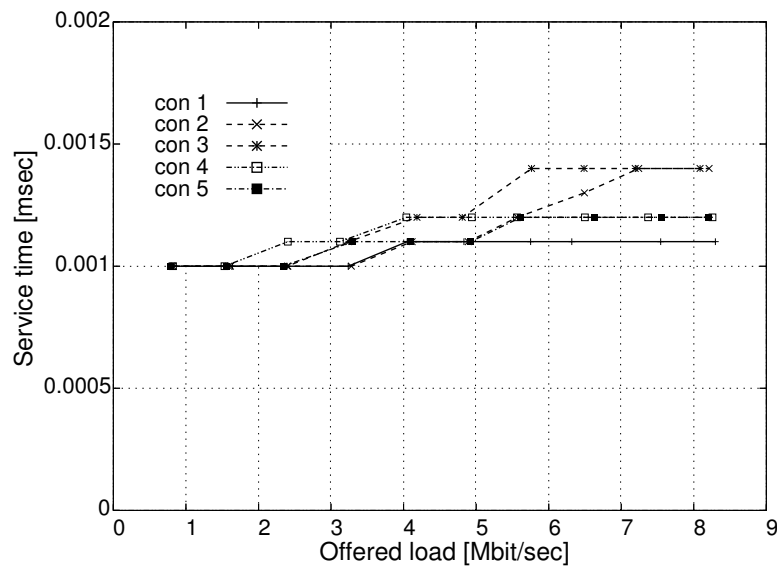


Figure 7.26: Mean service time of successfully transmitted data packets per connection vs. offered load per connection, **without** cch-adaptation. The applied PHY mode is 64QAM 3/4 for data frames and QPSK 1/2 for control frames.

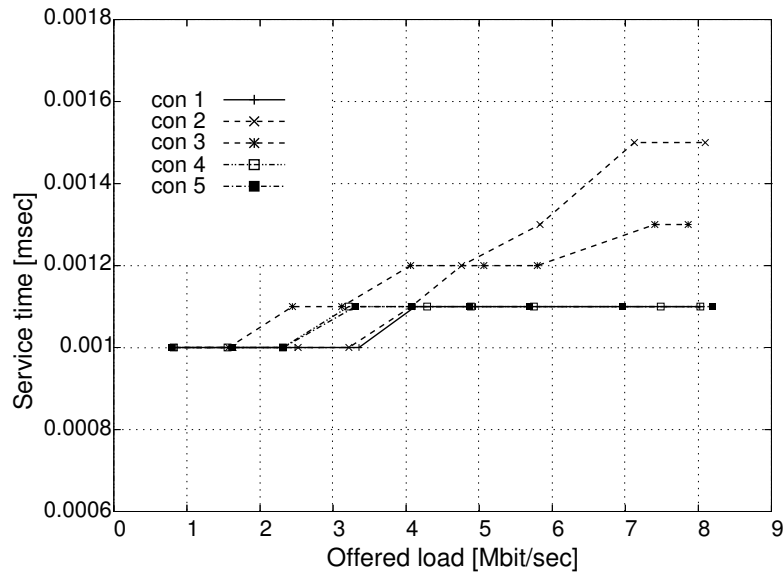


Figure 7.27: Mean service time of successfully transmitted data packets per connection vs. offered load per connection, **with** cch-adaptation. The applied PHY mode is 64QAM 3/4 for data frames and QPSK 1/2 for control frames.

to $1.5\mu\text{sec}$, as a result of collisions induced by MAI.

The benefits of the proposed cch-adaptation algorithm are especially visible from the results presented in Fig. 7.28, where the percentage of retransmitted data frames per connection (referring to the total amount of transmitted data frames) is given. With a suitable selection of the cch, con.

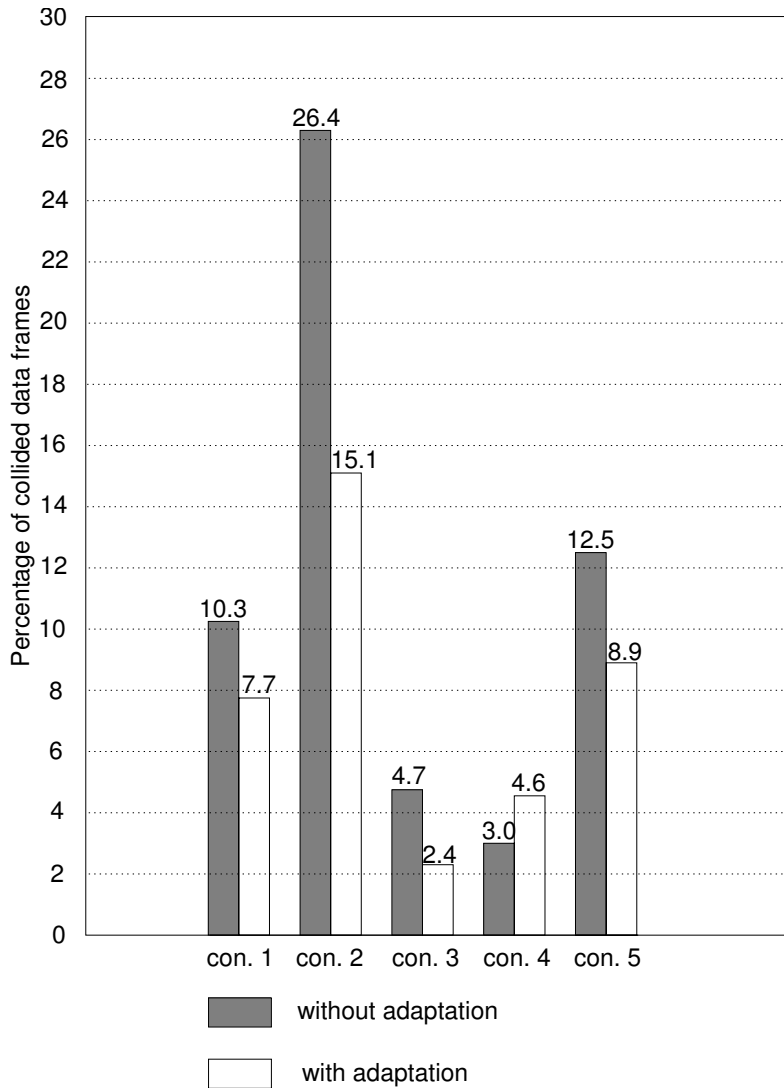


Figure 7.28: Percentage of data frame collisions per connection, **without** and **with** cch-adaptation. The applied PHY mode is 64QAM 3/4 for data frames and QPSK 1/2 for control frames.

2 lowers its retransmission percentage from 26.4% to 15.1%. Additionally, the appropriate cch selection reduces MAI, from which other connections benefit, at a cost of an insignificant raise in retransmission percentage at con. 4 for MS 7.

7.4 Frequency Adaptation - Adaptation to Suitable Frequency Channel

In this section, performance evaluation results of the frequency adaptation method, discussed in Section 5.4, are presented and analyzed. Figure 7.29 shows the simulated scenario consisting of 11 stationary MSs establishing 6 connections in a 10mx10m area, addressing a SOHO scenario. Simulations are performed using the QPSK 1/2 PHY mode (12 Mbit/sec) for control frames and the 64QAM 3/4 PHY mode (54 Mbit/sec) for data frames. The scenario presents a worst case situation with one large distance connection (con. 5) competing to several short connections, which leads to severe near-far-problems. Parallel transmissions of a single MS in more than one cchs are not allowed, in order to focus on the effects of the proposed new frequency channel adaptation method. Further simulation parameters are kept the same as in Table 7.1. The frequency adaptation algorithm is enabled for all transmitters serving one connection.

Connection 1 from MS 1 to MS 2 runs via cch 1, con. 2 between MS 3 and MS 4 is placed in cch 3. MS 5 communicates with MS 6 (con. 3) in cch 4 and connections of MS 7 to both, MS 8 and MS 9 (con. 4) are placed in cch 2. MS 10 uses cch 3 for transmissions to MS 11 (con. 5). The cchs where the MSs transmit their data packets are chosen randomly under the condition that different connections of the same transmitter are placed in the same cch. Data packets are 1024 byte long and they are generated by Poisson traffic load generators with variable mean interarrival time to be able to vary the offered total system load.

In Fig. 7.30 the carried traffic versus the offered system load is given for both cases, enabled and disabled frequency adaptation (FA). When frequency channel adaptation is disabled, the saturation network throughput approaches 28.5 Mbit/sec. According to the analysis given in Section 5.5, Eq. (5.16), the maximum achievable throughput of the system when data frames use the 64QAM 3/4 PHY mode and control packets use QPSK 1/2 is 31.58 Mb/s, for the given data packet length. The 9.75% loss, observed

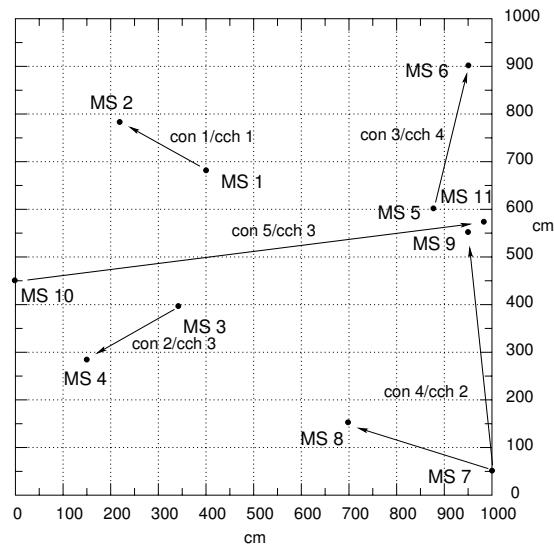


Figure 7.29: The simulated scenario.

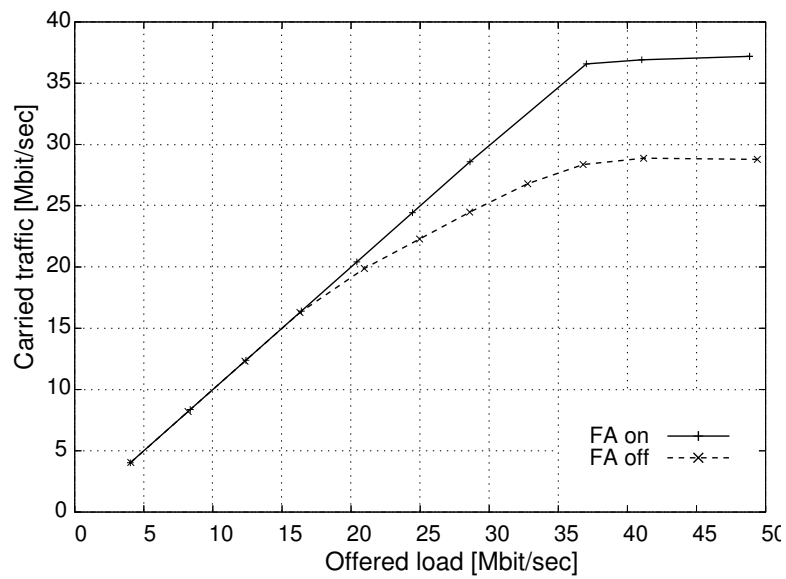


Figure 7.30: System throughput **with** and **without** frequency adaptation vs. offered system load. The applied PHY mode is 64QAM 3/4 for data frames and QPSK 1/2 for control frames.

via comparison to this ideal throughput value, results from the near-far-problem.

With increasing offered load, con. 5 is more and more blocked by the other three connections, where the interference at MS 11 prohibits increasingly the correct reception of data frames. This is illustrated in Fig. 7.31, which presents the carried traffic per connection versus the offered load per connection, when the frequency adaptation algorithm is disabled. From Fig. 7.31 it can be seen that con. 1, con. 3 and con. 4 operate nicely and show a linear rise of throughput with increased offered load. This is an effect of MC-CDMA, which divides the frequency channel in four parallel cchs. Connections 2 and 5, sharing cch 3, can theoretically each achieve half the throughput of the other connections (3.95 Mbit/sec) in the scenario studied. The MAI under heavy load results in con. 5 reaching only 2.8 Mbit/sec carried traffic. The other resources of cch 3 are partly utilized by con. 2, that reaches 4.2 Mbit/sec carried traffic in overload. In Fig. 7.31, the maximum of 7.895 Mbit/sec is not reached by con. 1, con. 3 and con. 4, that do not face near-far-problems, due to mutual interferences and disturbances caused

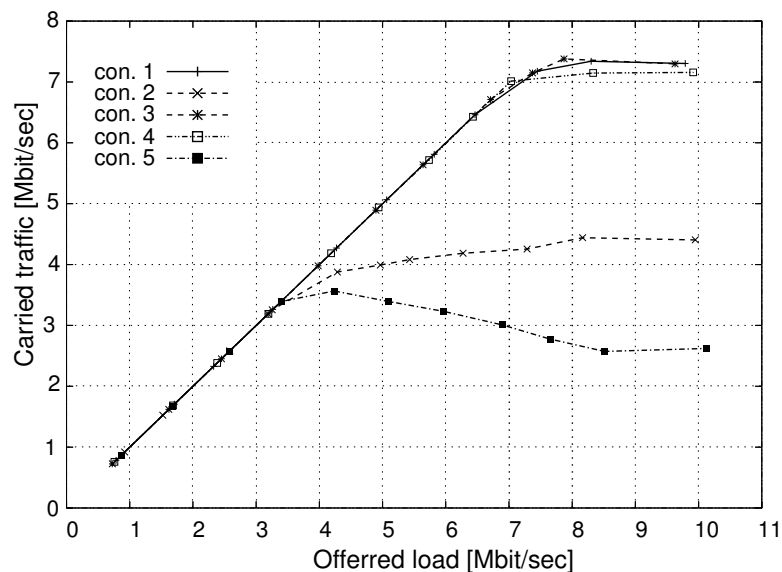


Figure 7.31: Throughput per connection **without** frequency adaptation vs. offered load per connection. The applied PHY mode is 64QAM 3/4 for data frames and QPSK 1/2 for control frames.

by the transmission attempts of other transmitters, especially MS 10.

Figure 7.32 shows the carried traffic per connection over the offered load per connection with frequency adaptation enabled. With frequency adaptation enabled the situation is substantially improved. Connection 5 is diverted to the second frequency channel, thus all connections operate in an efficient manner. Since con. 5 is moved to another frequency channel, the network utilizes now all four cchs in the first channel and one cch in the second. The maximum achievable throughput per cch is a quarter of the frequency channel throughput (see Section 5.5), namely 7.895 Mbit/sec. In a system where 5 cchs are used, the theoretical maximum throughput is $31.58+7.895=39.475$ Mbit/sec. As can be seen in Fig. 7.30, the maximum total carried traffic in the simulated scenario is 37.5 Mbit/sec.

The comparison between Figs. 7.31 and 7.32 underlines the benefits of the frequency adaptation algorithm. With con. 5 operated in another frequency channel, the other four connections can linearly increase their throughput up to 7.2 Mbit/sec, with con. 5 reaching in saturation the maximum of 7.7 Mbit/sec/cch. Since con. 5 is operated as a single connection in

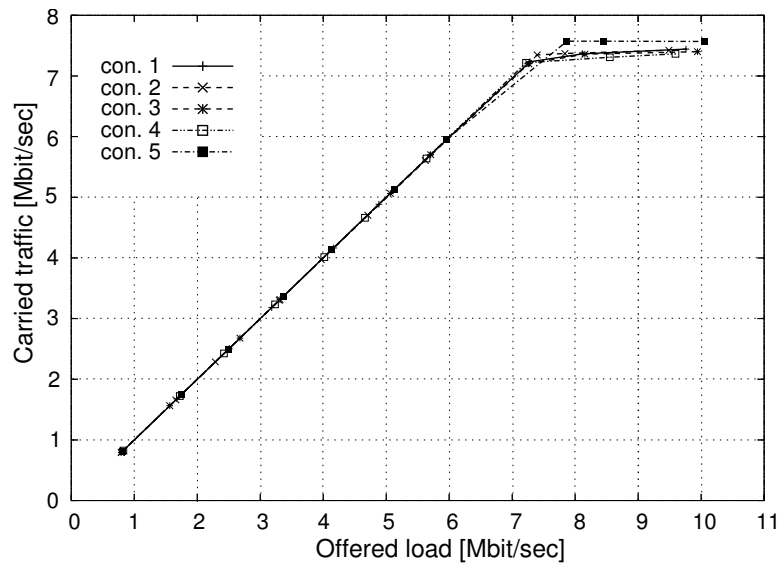


Figure 7.32: Throughput per connection **with** frequency adaptation vs. offered load per connection. The applied PHY mode is 64QAM 3/4 for data frames and QPSK 1/2 for control frames.

the second frequency channel, it avoids small disturbances from concurrent transmissions. In the first frequency channel, where con. 1 to con. 4 are placed, a certain amount of MAI remains, that prohibits the MSs to achieve the theoretical maximum value of 7.895 Mbit/sec/con. (see Section 5.5).

It is worth noting, that all figures referring to results with frequency adaptation enabled present the packet throughput in stationary network operation. The duration until the last frequency change has been performed and no further channel changes occur, is defined as the time duration for the system to become stationary. The network behavior before stationarity is the same as the one when the algorithm is not applied. In stationary operation, the throughput maximizes, the service time minimizes, while the queueing delay reduces. The duration until network stationarity, when applying the adaptation algorithm, depends on the offered load and has random values, as the adaptation algorithm is based on probabilistic input parameters. In the presented simulation set the duration until steady state varies from 1.5 to 6msec.

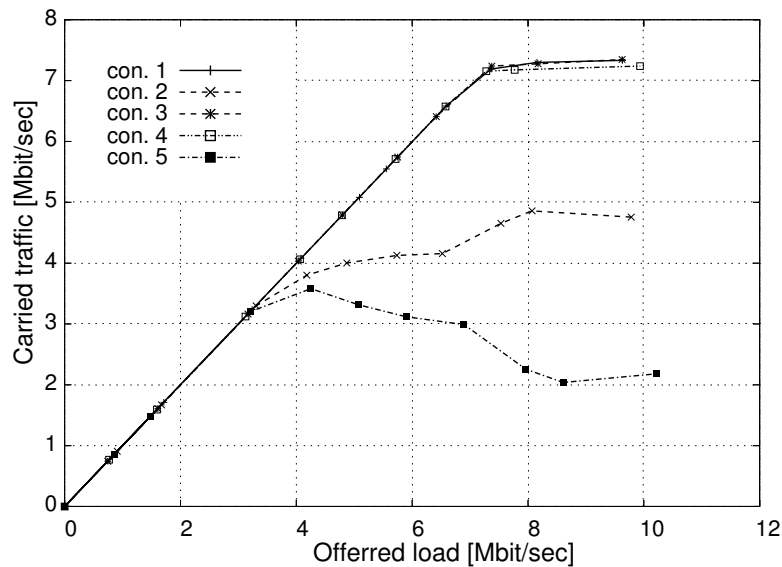


Figure 7.33: Throughput per connection **without** frequency adaptation vs. offered load per connection for PER demand **12%**. The applied PHY mode is 64QAM 3/4 for data frames and QPSK 1/2 for control frames.

Figure 7.33 presents the carried traffic per connection when frequency channel adaptation is disabled. The QoS demand in this simulation is the achievement of 3% PER (target SINR=26) per connection, in contrast to 12% for the results shown in Fig. 7.31. Connection 5 achieves in this case lower throughput, as the number of retransmitted frames is increased, since a lower SINR value is not acceptable. This results in con. 2 benefitting from the lower interference generated by con. 5, thus reaching higher throughput. When frequency channel adaptation is enabled, the system's behavior is the same for both, 12% and 3% PER demand, since con. 5 is operated in another frequency channel. All results presented in the remainder of this section, refer to the case of 12% tolerable PER.

Figure 7.34 depicts the mean queueing delay of all successfully transmitted data packets per connection over the offered load per connection, without frequency adaptation. Looking at con. 2 and 5 which have a different behavior than the other connections, as the load increases from 2.5 to 4.2 Mbit/sec, the queueing delay increases from 1msec to more than 100msec.

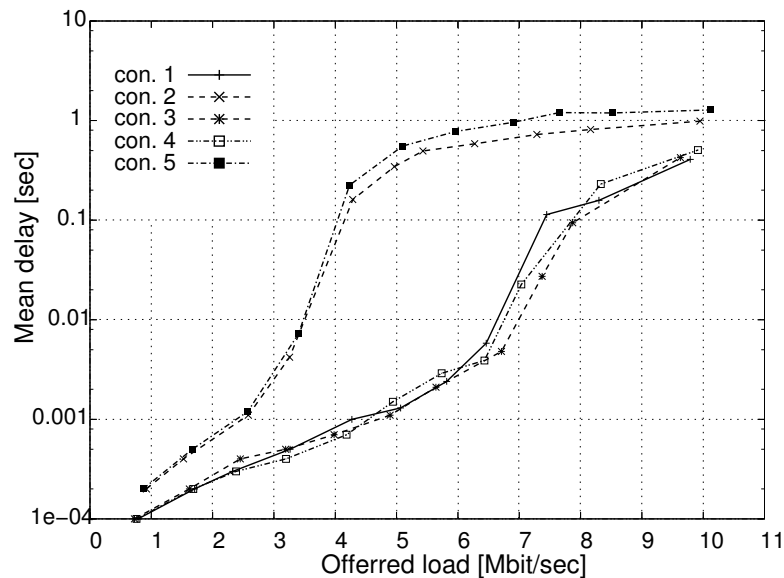


Figure 7.34: Mean queueing delay of successfully transmitted data packets per connection vs. offered load per connection **without** frequency adaptation. The applied PHY mode is 64QAM 3/4 for data frames and QPSK 1/2 for control frames.

This is due to the fact, that the two connections share the same cch, which is offered more traffic load than other cchs in the network and saturates faster. Additionally, con. 5 is disturbed by MAI, see also Fig. 7.31, and it is therefore expected for con. 5, to suffer a high queueing delay, especially for middle and higher offered load, where successful transmissions of con. 2 and con. 5 still occur after some retries using a high CW size.

The mean delay of data packets for con. 2 and con. 5 (and all other connections) has a finite value even in saturation, since the successfully transmitted data packets contribute to delay measurements only and data packets are not dropped after some specific queueing time. Consequently, the few successfully transmitted data packets of con. 5 in saturation, contribute to a high mean delay value, as a result of many frame retransmissions for the same data packet. For all other connections the queueing delay increases approximately exponentially with the load as expected. For offered load higher than 6.5 Mbit/sec/con. the mean queueing delay increases rapidly, since the carried traffic approaches saturation.

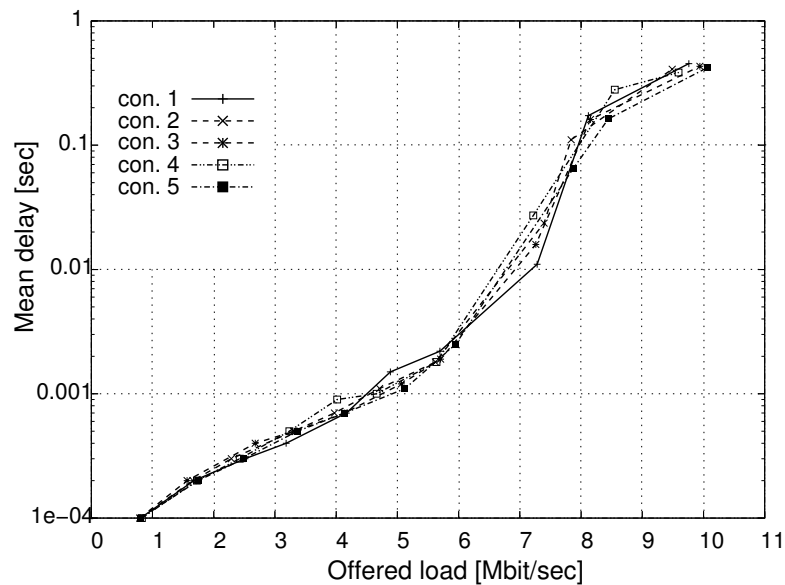


Figure 7.35: Mean queueing delay of successfully transmitted data packets per connection vs. offered load per connection **with** frequency adaptation. The applied PHY mode is 64QAM 3/4 for data frames and QPSK 1/2 for control frames.

In Fig. 7.35, the mean queueing delay under frequency adaptation is presented, showing a progressive increase with the offered load. Compared to the queueing delay without adaptation, two orders of magnitude are gained for con. 2 and con. 5.

Figures 7.36 and 7.37 present the mean service time of successfully transmitted data packets per connection, with frequency adaptation disabled and enabled, respectively. In Fig. 7.36 con. 1, con. 3 and con. 4 have a constant service time of 1msec, that complies with the theoretical values from Section 5.5, Eq. (5.15). For medium and high load some collisions of RTS frames occur at con. 2 and con. 5, as a result of their contention in the same cch 3. This raises the mean service time of con. 2 by 0.2msec. Connection 5 experiences with increasing load continuous increase of its service time, that owes to MAI, in addition to RTS collisions from contention with con. 2. Multiple collisions of RTS frames increase a lot the CW of MS 10. For high load the service time reaches 200% of the value calculated analytically (see Section 5.5, Eq. (5.15)).

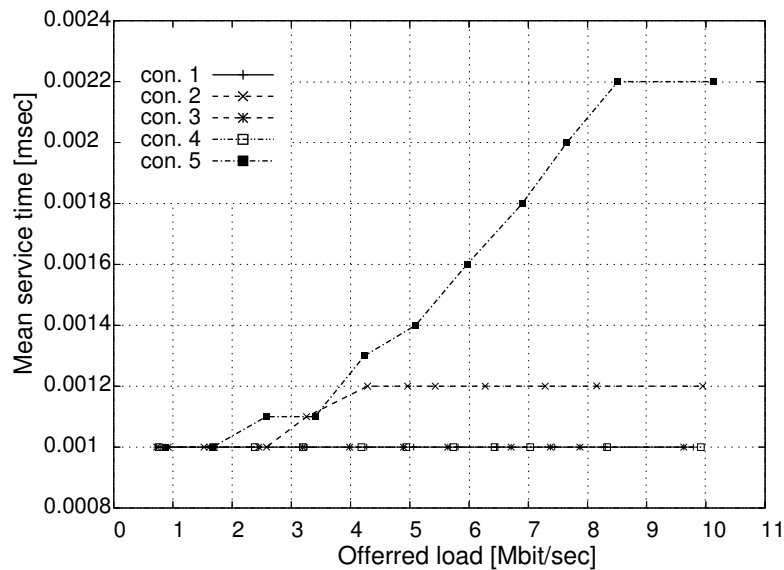


Figure 7.36: Mean service time of successfully transmitted data packets per connection vs. offered load per connection **without** frequency adaptation. The applied PHY mode is 64QAM 3/4 for data packets and QPSK 1/2 for control packets.

7.4. Frequency Adaptation - Adaptation to Suitable Frequency Channel115

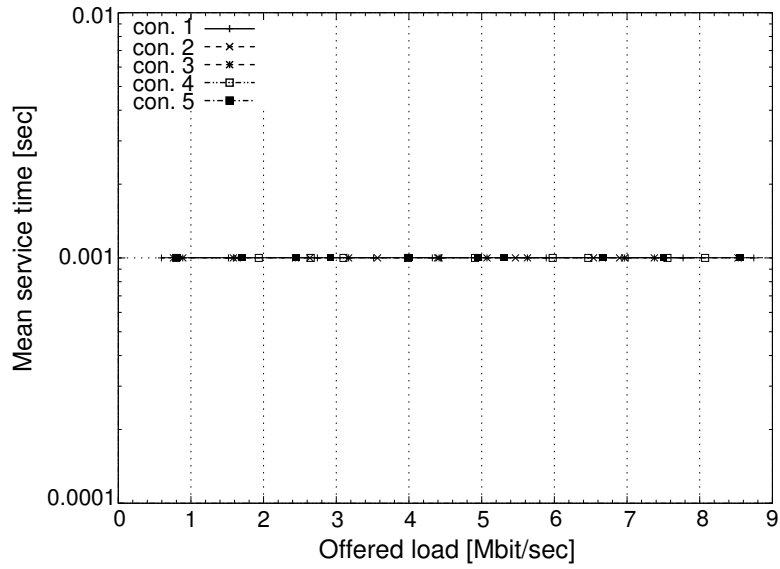


Figure 7.37: Mean service time of successfully transmitted data packets per connection vs. offered load per connection **with** frequency adaptation. The applied PHY mode is 64QAM 3/4 for data packets and QPSK 1/2 for control packets.

In case of frequency channel adaptation enabled (Fig. 7.37), the service time for all connections is constant, equal to the analytically calculated service time of 1.03ms under average backoff (half the size of CW_{min} , namely 3.5 slots), see Section 5.5, as no collisions occur any more. Since near-far-problems are removed, collisions could occur only from competition among the MSs. In the proposed MC-CDMA based system with SF=4 the competition for one cch is reduced by a factor of four. Compared to the IEEE 802.11a standard, in the proposed system, collision probability becomes small, but another frequency channel is needed to overcome near-far-problems, when they occur.

Figure. 7.38 presents the number of collided data and RTS frames per transmitting MS, for 8Mbit/sec/connection offered load. Data frame collisions with frequency adaptation are limited to the period before the steady state is achieved. The enhancement of the network's performance is substantial when frequency adaptation is applied. Especially for con. 5 the improvement is big, where the number of RTS collisions drops from 242 without adaptation to 0 when the proposed adaptation method is applied. What the number of data frame collisions is concerned, the improvement achieved by con. 5, is 99%.

7.5 Conclusion

In this chapter, performance evaluation results of the C-DCF are presented and analyzed. Simulation results for example scenarios comply with the analytical results derived in Section 5.5, and prove both, the effectiveness of the proposed TPC algorithm and of the interference aware cch-adaptation algorithm.

A further improvement of the protocol and the support of long, high capacity connections, is possible using the frequency channel adaptation as proposed in Section 5.4. Simulation results show the promises of this approach, even in worst case scenarios, which allows the MC-CDMA network to approach the analytically calculated maximum throughput and an almost collision free operation.

In Chapter 9, the ability of the frequency adaptation method, to enable the operation of many connections under heavy interference, is further analyzed, where the frequency adaptation method is applied in a large scale scenario comprising 4 subnetworks and 28 active MSs.

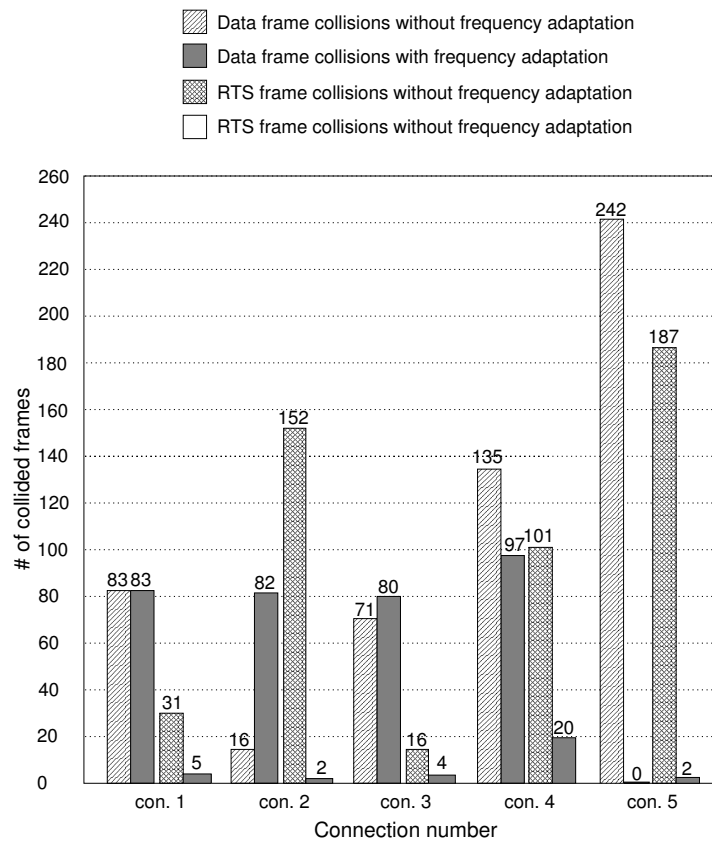


Figure 7.38: Amount of collided data and RTS frames **with** and **without** frequency adaptation. The offered load is 8 Mbit/sec/connection. The applied PHY mode is 64QAM 3/4 for data packets and QPSK 1/2 for control packets.

C-DCF: cch selection on Frame Basis

Content

| | |
|----------------------------------|-----|
| 8.1 Parallel Backoff | 121 |
| 8.2 Smart Backoff | 124 |
| 8.3 Performance Evaluation | 126 |
| 8.4 Prioritized Access | 132 |
| 8.5 Conclusion | 135 |

The application of MC-CDMA in the PHY layer divides the frequency channel in many parallel cchs, separated from each other by different code sequences (spreading codes). In this way, the frequency channel gains a multi-channel structure, which should be taken into consideration in order to optimize the performance of the MAC protocol. In this chapter two different approaches are presented and evaluated, which take advantage of the extra degree of freedom in multi-channel systems, to improve their performance and introduce prioritized access. In the algorithms proposed in this chapter, the selection of the applied spreading sequence per transmitter is performed on frame basis (see Fig. 1.1), introducing an opportunistic usage of the cchs per transmitted frame.

The first MAC protocol improvement, named Parallel Backoff, introduces concurrent, parallel, independent backoff procedures (of equal duration), initiated in a predefined amount of cchs (instead of only one). Since the multiple parallel backoff instances are independent, no restrictions are posed and therefore this algorithm can be also applied in systems where the different channels are divided in (space), frequency or code domain, and the transceiver hardware provides means of monitoring multiple channels in parallel.

The second MAC protocol improvement presented here is an optimization of the backoff procedure for CDMA systems, which is referred to as Smart Backoff. As in CDMA systems with simple modifications of the receiver a MS in idle state can monitor all cchs, the backoff countdown con-

tinues as long as at least one cch is free. The Smart Backoff iterates among all cchs during channel monitoring. This algorithm cannot be effectively extended to be used with multiple frequency channels as it is based on parallel monitoring of all channels and fast switching among them. The delay that would be introduced by a frequency switch in the transceiver of the MS to another channel, would vanish the benefits of Smart Backoff, as channel monitoring over a longer period of time would be needed in order to obtain information about ongoing transmissions in that channel. Parallel monitoring of multiple frequency channels would require multiple transceivers under Smart Backoff increasing the cost of MSs to an unacceptable degree.

The algorithms presented in this chapter for the proposed multi-channel network, combine SS and ALOHA for packet transmission. This combination is known from the spread ALOHA system proposed in [ABRAMSON and LAM (1990)]. In spread ALOHA networks though, "spreading occurs by timely stretching the packet while multiple users are distinguished by the ALOHA contention protocol"[ABRAMSON and LAM (1990)]. Its main focus is the reduction of high peak transmission power through spreading in time domain, by taking advantage of the low duty cycle of an ALOHA network.

The algorithms proposed here are based on MC-CDMA, where concurrent transmissions are separated by different spreading codes and transmitted symbols are detected via correlation with the applied spreading sequence, thus a multi-channel structure is available to the MAC layer. Smart Backoff can be seen as a development of the DS-CDMA slotted ALOHA access for packet *Personal Communication Networks* (PCN), presented in [LIU and EL ZARKI (1994)], where a MS having data to transmit, selects randomly a spreading code and occupies a slot with its packet. With Smart Backoff a MS can change the previously selected slot on a cch (pointed out from the backoff duration), if during its backoff countdown this cch gets blocked by the transmission of another MS. In contrast to this, Parallel Backoff selects the same backoff timer duration for transmission in more than one cchs (found idle during carrier sensing) and initiates the transmission in one or more of the preselected cchs, which are still idle after the backoff countdown has reached zero.

8.1 Parallel Backoff

When applying Parallel Backoff, a MS monitors the cchs for time DIFS to detect the unused ones. It is assumed that MSs in idle state can monitor all cchs by using four correlators to correlate the received signal with all spreading sequences used. Monitoring of the cchs is carried out in PHY layer, by sensing the channel. Accordingly, compared with the standard DCF [802.11A /D7 (1999)], in the proposed MC-CDMA based WLAN each MS supervises separate NAV states for each cch.

The functionality of this extended channel sensing function is summarized in the algorithm of Fig. 8.1, where after monitoring the cchs for time DIFS, the IDs of the idle ones are placed in a list of available cchs. If at least 1 cch is idle, the MS initiates a backoff. The set of the backoff timer is done as in the standard DCF (Chapter 2). For Parallel Backoff, the different backoff instances of a MS don't need to be initiated with the same random value. However, backoff instances using the same backoff duration are advantageous, because parallel transmission via multiple cchs can be initiated when two or more countdowns reach zero at the same time. Parallel transmission stands for bundling cchs, resulting in a higher capacity channel, in which more than one packet can be transmitted at the same time compared to a single cch.

The backoff countdown under Parallel Backoff, in general, is accomplished independently for each cch, as shown in Fig. 8.2 [ORFANOS et al. (2005d)]. Should another MS start a transmission in a cch, the corresponding backoff timer is stopped until the channel becomes idle again. At the same time, the MS proceeds counting down the remaining backoff timers (if any) that are related to still idle cchs until one backoff timer reaches zero. This increases the probability on accessing a cch, thereby reducing the data packet delay.

In case of parallel backoff instances of same backoff duration and for the sense of simplicity, upon detecting more than one idle cch, the MS initiates one backoff instance only, that is valid for all the idle cchs, instead of initializing multiple backoff timers (Fig. 8.1). This solution is applied throughout this work.

In the simplified case of one backoff timer, valid for all idle cchs, the blocked cch is removed from the list of available cchs (Fig. 8.3) and the MS proceeds with the countdown, until the list of available cchs is empty. If all cchs become blocked by other MSs accessing the cchs earlier, the MS

```

for (i=0, i<4, ++i){
  cch_id=i;
  sense_codechannel(cch_id);
  if (cch_id==idle) {
    cch_num= cch_num +1;
    cch_used[cch_id]=true;
  }
}
if (cch_num>0){
  draw_backoff(0,CW);
  backoff_duration=backoff*aSlotTime;
  setTimer(tiEndBackoff, backoff_duration,cch_used[]);
  state(Backoff);
}
else
  state(Wait_for_cch);
}

```

Figure 8.1: Channel sensing with four cchs.

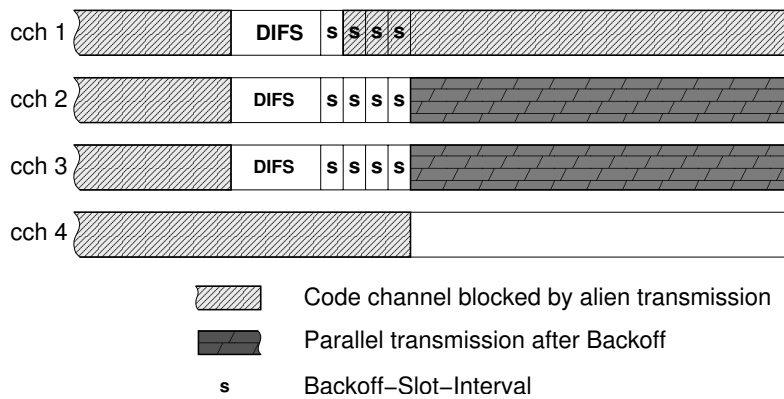


Figure 8.2: Parallel Backoff with parallel transmission in two cchs.

calculates the remaining backoff duration and then again waits for a cch to become idle. When a cch is monitored idle (Fig. 8.3), its corresponding ID is added to the list of available cchs if the list is empty (the MS then is waiting for a free channel), or if the respective cch had been marked by Parallel Backoff as available, when initially setting up the backoff timer for the current data packet transfer.

If more than one backoff timers reach zero at the same slot, the MS may transmit more than one data packet in parallel, like in Fig. 8.2. A prioritization of MSs can be achieved by permitting Parallel Backoff and

```

//Parallel Backoff
event_handler(evChannel_Blocked(cch_id)){
    if (state=Backoff){
        cch_num=cch_num-1;
        cch_used[cch_id]=false;
        if(cch_num>0{
            calculate_remaining_backoff;
            setTimer(tiEndBackoff, remaining_backoff_duration);
            backoff_valid_for(cch_used[]=true);
            state=Backoff;
        }
        else{
            interrupt_backoff;
            calculate_remaining_backoff;
            state=Wait_for_channel;
        }
    }
    else
    ...
}

//Parallel Backoff
event_handler(evChannel_Free(cch_id)){
    if (state=Wait_for_channel){
        cch_num=cch_num+1;
        cch_used[cch_id]=true;
        if(cch_num==0 OR (cch_num==1 AND cch_used(cch_id)==true)){
            setTimer(tiEndBackoff, remaining_backoff_duration);
            state=Backoff;
        }
        else
            state=Wait_for_channel;
    }
    else
    ...
}

```

Figure 8.3: Parallel Backoff: The cases of a blocked cch during countdown and of a free cch after a busy medium.

parallel transmission for prioritized MSs only. Different prioritization levels might be distinguished by specifying the number of parallel backoff counters (1-4) for Parallel Backoff depending on a MS's priority and by specifying the number of parallel cchs permitted for parallel transmission (1, 2 or 4).

The Parallel Backoff algorithm has 3 main advantages:

1. MSs are not transmitting permanently on the same cch, thus leading to a load balance as can be seen from the simulation results in Section 8.3.
2. By transmitting data packets on parallel cchs, prioritized MSs might better achieve their QoS demands, even under high load.
3. The queueing delay of a data packet transfer can be minimized as the Parallel Backoff increases the probability that one backoff timer countdown will reach zero without being interrupted.

Besides these advantages, there is a disadvantage when applying Parallel Backoff namely increased contention: When applying Parallel Backoff, a MS appears in the network as having multiple contention entities, the number of which equals to the number of backoff instances started from this MS. The raised contention level tends to increase the number of collisions in the network and/or limit the performance of other MSs that use a single backoff timer only, unless these MSs don't operate under full load.

8.2 Smart Backoff

Smart-Backoff is an algorithm spanning over many cchs [ORFANOS et al. (2005c)]. It allows a station to switch from the selected idle cch to another idle cch (if available), in case the selected one becomes blocked by another MS. Like in Parallel Backoff, MSs in idle state are assumed able to monitor all cchs and channel monitoring prior to a data packet transmission is done according to the algorithm described in Fig. 8.1.

Under Smart Backoff, the countdown, carried out in steps of $9\mu sec$, of the backoff timer is not stopped by another MS starting transmission, but backoff countdown is continued until the counter expires (Fig. 8.4), or all cchs are found in busy state.

For this purpose, a MSs applying Smart Backoff monitors all cchs during its backoff countdown and marks the moment any other cch is monitored with signal level lower than the threshold defined for an idle channel. If the backoff countdown is stopped by another MS starting a transmission, one

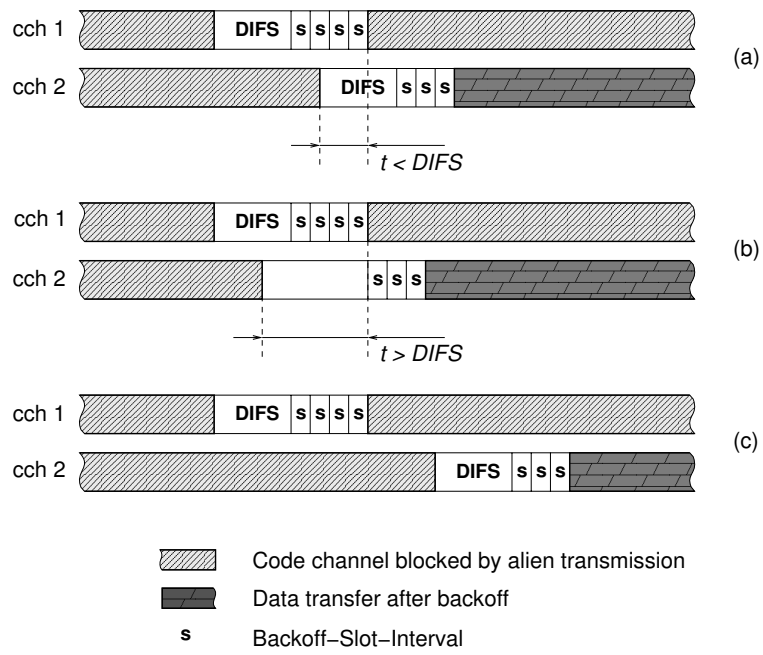


Figure 8.4: Smart Backoff.

of the three cases shown in Fig. 8.4 occurs:

1. Another cch seems to be idle. The MS has to monitor the cch for at least a DIFS interval to determine whether it is idle and then it can continue the countdown of backoff timer in this cch.
2. Another cch was detected idle earlier and the MS can immediately continue to count down its backoff timer for access to this cch.
3. No cch is idle. The MS must wait.

Figure 8.5 presents the Smart Backoff algorithm. For the case a cch is found blocked during countdown, the algorithm is similar to the one of Parallel Backoff, described in Fig. 8.3. The only difference is an update of the list of idle cchs under Smart Backoff, thereby allowing to add new cchs during backoff to the list.

If a cch is sensed idle (Fig. 8.5), while the MS is waiting for a free cch in order to start a transmission, the list of available cchs is updated and backoff countdown starts immediately.

Should more than one cchs be idle, when the backoff countdown is finished, the MS will choose one of them, preferably the one that was idle for the longer time period. The Smart Backoff algorithm may in addition prioritize MSs (like Parallel Backoff (see Section 8.1)) by permitting parallel data packet transmission. As shown in Fig. 8.6, a prioritized MSs is permitted to transmit two or more data packets in parallel if more than one cch is idle after Smart Backoff.

Smart Backoff is a further improvement to Parallel Backoff for CDMA based WLANs as visible in Section 8.3. The contention level is raised too, as described in Section 8.1 for Parallel Backoff.

8.3 Performance Evaluation

In this section the performance of Parallel Backoff and Smart Backoff (with selection of a cch on frame basis) is evaluated and their benefits are exploited by a direct comparison to the standard backoff algorithm (with connection based cch selection, as described in Section 5.1). For this reason, event-driven simulation is used with the parameters specified in Table 7.1. The applied scenario, is the one of Fig. 7.1, comprising 10 MSs pairwise establishing 5 connections in a 8m x 8m area. The QPSK 1/2 PHY mode is used both, for control and data frames.

All MSs are capable of Parallel Backoff, but parallel transmissions are

```

//Smart Backoff
event_handler(evChannel_Free(cch_id)){
  if (state=Wait_for_channel){
    cch_num=cch_num+1;
    cch_used[cch_id]=true;
    setTimer(tiEndBackoff, remaining_backoff_duration);
    state=Backoff;
  }
  else
  ...
}

//Smart Backoff
event_handler(evChannel_Blocked(cch_id)){
  if (state=Backoff){
    cch_num=cch_num-1;
    cch_used[cch_id]=false;
    update_channel_status; //sensing of all cch throughout backoff countdown
    if(cch_num>0{
      calculate_remaining_backoff;
      setTimer(tiEndBackoff, remaining_backoff_duration);
      state=Backoff;
    }
    else if(a_cch_seems_idle){
      interupt_backoff;
      calculate_remaining_backoff;
      state=Wait_for_DIFS;
    }
    else{
      interupt_backoff;
      calculate_remaining_backoff;
      state=Wait_for_channel;
    }
  }
  else
  ...
}

```

Figure 8.5: Smart Backoff: The cases of a free cch after a busy medium and of a blocked cch during countdown.

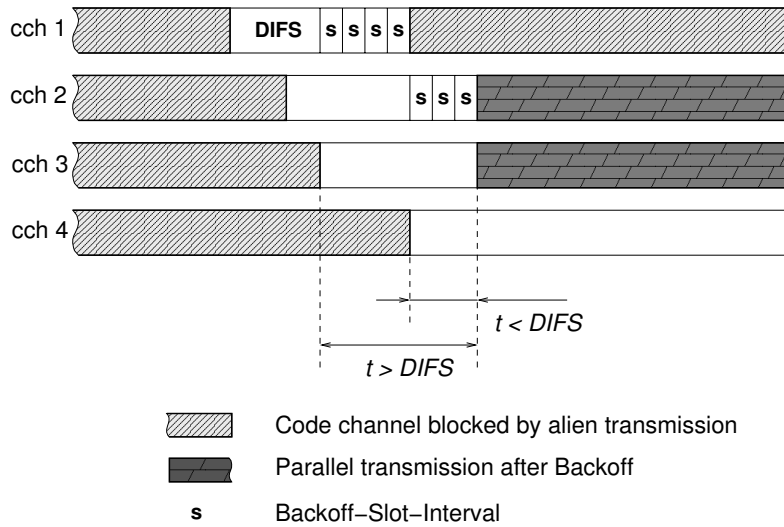


Figure 8.6: Smart Backoff with parallel transmission.

not allowed. The traffic load generators deliver load according to Poisson arrival processes, with the same intensity per connection. Although TPC is applied, receivers are interfered from all other transmitting stations in the scenario. In simulations where connection based cch selection is applied, according to Section 5.1, and Parallel Backoff and Smart Backoff, both, are deactivated, the cchs are randomly chosen by the transmitting MS.

Figure 8.7 shows the carried traffic versus the offered system traffic load for the three algorithms considered: connection oriented cch selection, Parallel Backoff¹ and Smart Backoff¹. For all the algorithms the network reaches under overload condition the same maximum throughput of 10.05 Mbit/sec (Section 5.5).

The benefits of Parallel Backoff and Smart Backoff appear for an offered load higher than 6.25 Mbit/sec, where the network with connection based cch selection enters slowly into saturation. At this value of offered load, the cch serving two out of the 5 connections is saturated (for connection based cch selection), as described in Section 7.1. Further increase of carried traffic is feasible only for the remaining 3 cchs, serving one connection each. The same system under frame oriented cch selection and under Parallel or Smart Backoff shows a linear increase of carried traffic over offered load until 90%

¹Applies frame oriented cch selection.

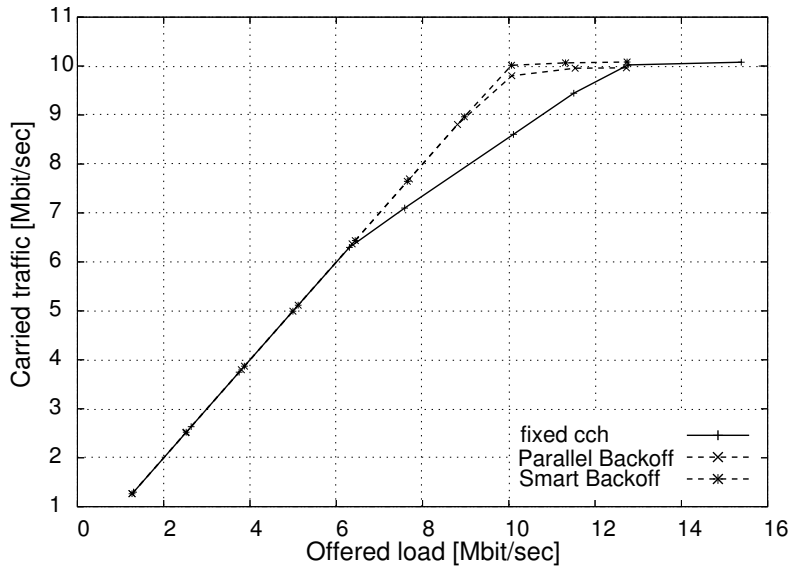


Figure 8.7: System throughput comparison for connection based cch Selection, Parallel Backoff and Smart Backoff. The applied PHY-mode is QPSK 1/2 for both control and data frames.

of load for Parallel Backoff and almost 100% of load for Smart Backoff. The difference between Parallel and Smart Backoff shows the superiority of Smart Backoff towards the Parallel Backoff algorithm.

The differences found in carried traffic can be explained from the observations in Fig. 8.8, where the throughput per connection is shown, for all three backoff algorithms. With connection based cch selection and under high load, con. 1 and con. 4 (see Fig. 7.1), that share the same cch, reach at 1.25 Mbit/sec offered load their throughput, that is 50% of other connections, which each use one cch exclusively, although the system's resources are not completely utilized. This result points out the fact that fairness is missing when assigning a connection to a connection based cch and consequently the system's throughput performance is lower than possible.

Under Parallel and Smart Backoff, Figure 8.8 depicts the benefits for the throughput of con. 1 and con. 4, that are visible when the offered load exceeds 1.25 Mbit/sec/con., since these connections can take advantage of unused resources in the other 3 cchs. The system's resources are now nearly equally distributed among the active connections. When the offered load

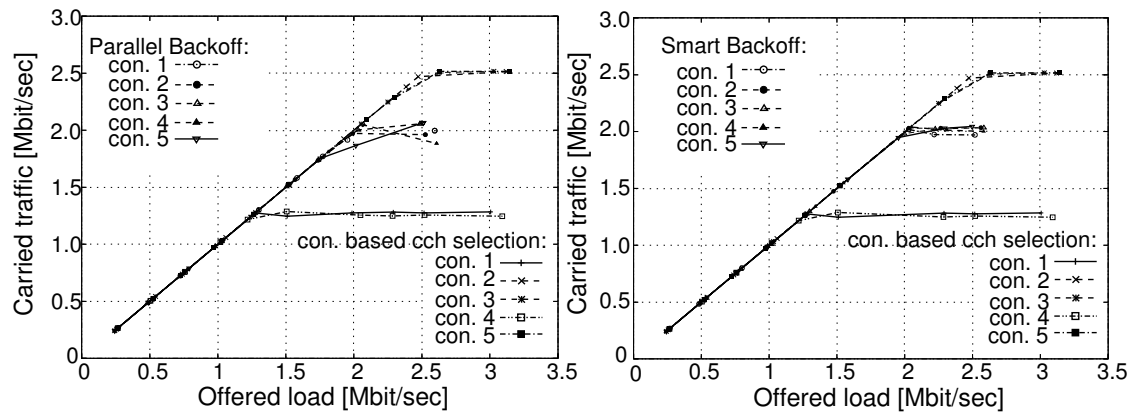


Figure 8.8: Comparison of carried traffic per connection for the three backoff algorithms. Left Parallel Backoff and connection based cch selection, right Smart Backoff and connection based cch selection. The applied PHY-mode is QPSK 1/2 for both control and data frames.

exceeds 1.75 Mbit/sec/connection, the allocation of the system's resources for Parallel Backoff is no longer equal among the MSs, but small unfairness is observed. As soon as two MSs collide, other transmitters take then advantage of their shorter backoff timers and the fact that MSs are bound on the cchs initially selected by Parallel Backoff and gain more data packet transmissions.

Figure 8.9 shows the mean queueing delay of all received data packets over offered load, for the three backoff algorithms. Parallel and Smart Backoff have a clear advantage over connection based cch selection for offered load exceeding 5 Mbit/sec. Beyond saturation (10 Mbit/sec) the delay of Parallel and Smart Backoff's increases dramatically, since it becomes more and more difficult to find a free cch for a data packet transfer. It is worth noting that under Parallel Backoff the mean queueing delay is less than 100 msec, even if the offered load reaches 95% (9.5 Mbit/sec) and the channel is close to saturation, still allowing MSs to support delay sensitive applications. For the same amount of offered load, the queueing delay under Smart Backoff is below 10 msec, underlying the enhanced performance of Smart Backoff compared to Parallel Backoff.

The service time, presented in Fig. 8.10 is about 3.2 msec for all algorithms, in line with the theoretical analysis given in (Section 5.5, Eq. (5.19)),

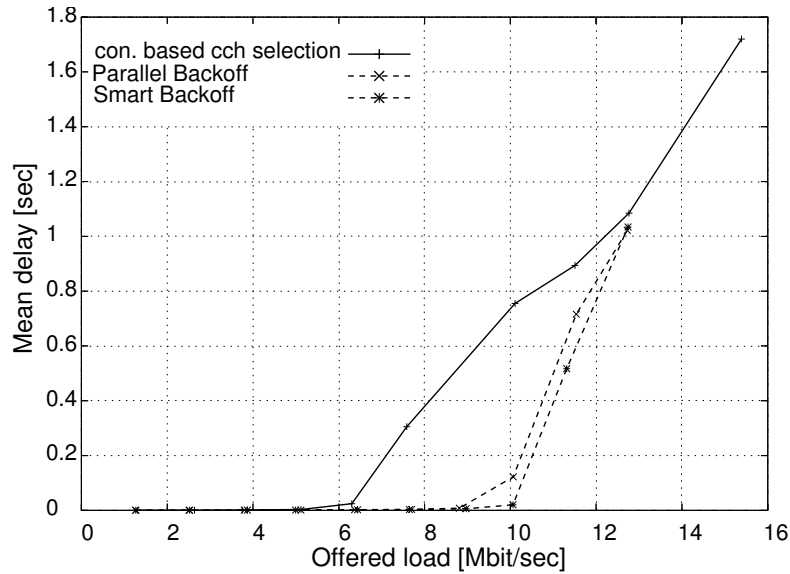


Figure 8.9: Comparison of mean queueing delay for the three backoff algorithms. The applied PHY-mode is QPSK 1/2 for both control and data frames.

and remains constant with increased offered load, since no collisions occur.

A comparison of the three backoff algorithms proposed for the MC-CDMA WLAN, in terms of the queueing delay CDF, shows the differences of the discussed channel access algorithms in the scenario introduced in Fig. 7.1.

Figure 8.11 presents the CDF of the data packet queueing delay under medium load, equivalent to a total system load of 75%. Each connection is offered 1.5Mbit/sec of Poisson load and the QPSK 1/2 PHY mode is applied. Smart Backoff and Parallel Backoff are superior to connection based cch selection, especially in the amount of data packets transmitted without, or with small queueing delay.

Smart Backoff shows a slightly better performance than Parallel Backoff, since it always searches for another free cch when the monitored one gets busy, while Parallel Backoff is fixed to the cchs selected initially (when backoff timer for the current data packet transfer was set).

In Fig. 8.12, the results for the same scenario under higher load equivalent to a system load of 100% are presented. To achieve equal conditions for

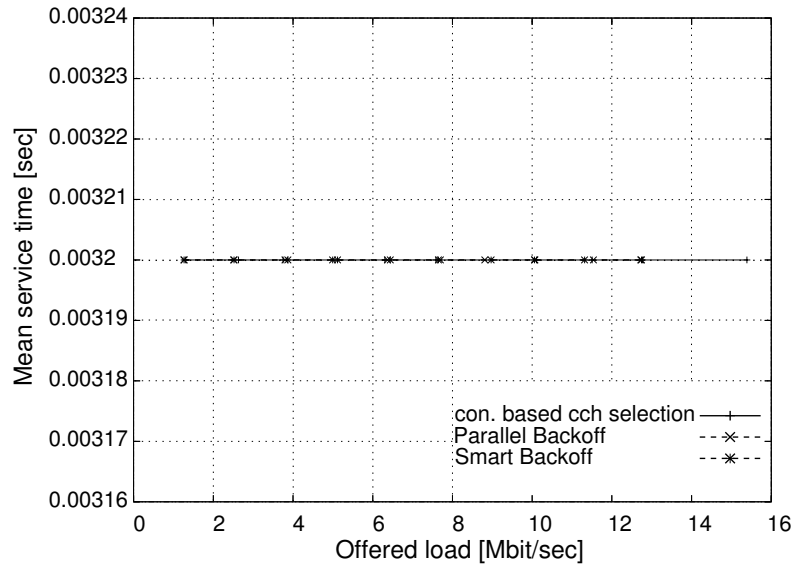


Figure 8.10: Comparison of mean service time for the three backoff algorithms. The applied PHY-mode is QPSK 1/2 for both control and data frames.

the presented comparison results, each transmitting MS is offered 2Mbit/sec of Poisson load under Parallel and Smart Backoff, and for connection based cch allocation the offered load is equal to the cch capacity, divided by the amount of MSs sharing the cch. The superiority of Smart and Parallel Backoff is visible.

8.4 Prioritized Access

In order to investigate the potential of the new algorithms to prioritize a MS in a network, the scenario given in Fig. 7.1 is taken, where the PHY mode used is QPSK 1/2 both, for control and data frames.

Each transmitting MS is assumed to contribute a different amount of traffic from Poisson traffic load generators, as given in Table 8.1. For simulations, where Parallel or Smart Backoff is not used, the connection based cch selection is used. In this case, the used cch per connection is given in Fig. 7.1 and is randomly chosen during an association phase preceding data transmission. MS 3 generates almost 4 Mbit/sec of Poisson load in total for con. 2, and optionally uses Parallel Backoff or Smart Backoff with the ability to

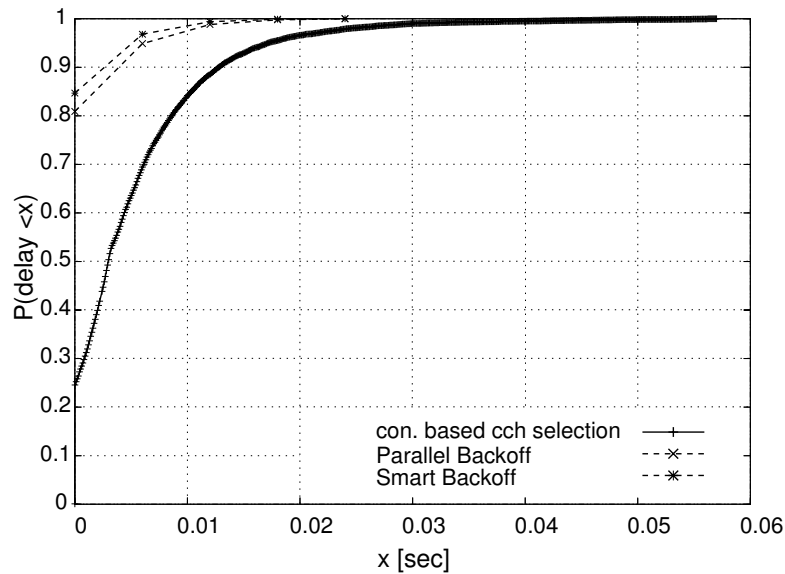


Figure 8.11: CDF of queueing delay under medium system load (1.5 Mbit/sec load per connection). The applied PHY-mode is QPSK 1/2 for both control and data frames.

transmit in two cchs in parallel.

In Table 8.1 the simulation results are presented. When connection based cch selection is used, con. 1 and con. 3 to con. 5 can carry the entire offered load since the capacity of the cch they are bound on is not exceeded. Connection 2 can only successfully transmit almost all generated data packets when using Parallel Backoff, while the application of Smart Backoff allows it to transmit all the generated traffic. With the connection based cch selection, the carried traffic is limited to 2.490 Mbit/sec, corresponding to the maximum capacity of one cch with the applied PHY mode, see Section 5.5. The situation improves with Parallel and Smart Backoff. Now, MS 3 on con. 2 can profit from the non-utilized resources in all 4 cch and carries all traffic generated. The differences in carried traffic between Parallel and Smart Backoff are small.

The advantage of Parallel/ Smart Backoff over connection based cch selection is more evident for the queueing delay. Table 8.2 provides the mean queueing delay per connection gained by simulations. For con. 2, with the prioritized MS 3 as transmitter, the Parallel Backoff algorithm reduces the

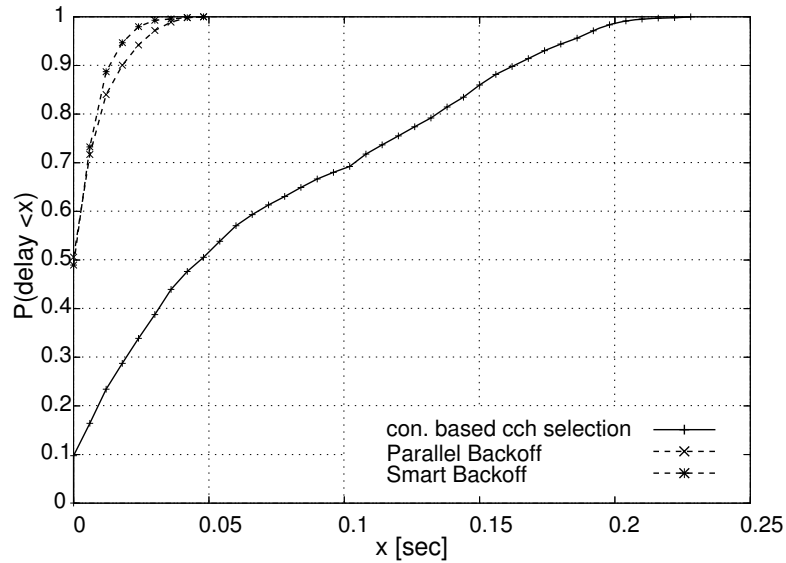


Figure 8.12: CDF of queueing delay under high system load. The applied PHY-mode is QPSK 1/2 for both control and data frames.

Table 8.1: Throughput per connection.

| con. | con. based cch sel. | | Parallel Backoff | | Smart Backoff | |
|------|-------------------------|-------------------------|-------------------------|-------------------------|-------------------------|-------------------------|
| | load [Mbit/sec] offered | load [Mbit/sec] carried | load [Mbit/sec] offered | load [Mbit/sec] carried | load [Mbit/sec] offered | load [Mbit/sec] carried |
| 1 | 0.957 | 0.957 | 1.032 | 1.032 | 1.032 | 1.032 |
| 2 | 3.945 | 2.485 | 3.734 | 3.720 | 3.984 | 3.984 |
| 3 | 1.435 | 1.435 | 1.451 | 1.451 | 1.347 | 1.347 |
| 4 | 0.740 | 0.740 | 0.809 | 0.809 | 0.750 | 0.750 |
| 5 | 1.194 | 1.194 | 1.115 | 1.115 | 1.189 | 1.189 |

queueing delay almost by a factor of 36 (factor 64 for Smart Backoff) and can accomplish strict QoS demands. This has an effect on some of the other connections, that now face more traffic in their cchs, thus their queueing delay is slightly increased, compared to that under connection based cch selection. In general, the network's performance is enhanced under Parallel Backoff or Smart Backoff, on cost of a non-significant increase of mean delay

for low traffic MSs.

Table 8.2: Mean queueing delay per connection.

| | con.con. based cch selection [sec] | Parallel Backoff [sec] | Smart Backoff [sec] |
|---|---------------------------------------|---------------------------|------------------------|
| 1 | 0.0027 | 0.0011 | 0.0012 |
| 2 | 0.9383 | 0.0259 | 0.0147 |
| 3 | 0.0019 | 0.0043 | 0.0022 |
| 4 | 0.0023 | 0.0007 | 0.0007 |
| 5 | 0.0016 | 0.0015 | 0.0019 |

8.5 Conclusion

In this chapter, two MAC protocol extensions, Parallel and Smart Backoff, for cch selection on frame basis were presented, evaluated and compared to the connection based cch selection (see Chapter 5). Besides improving the overall performance and leading to load balancing among the cchs, the proposed algorithms enable bundling of cchs for connections under higher traffic. This is particularly important in CDMA networks, where one cch has only a fraction of the frequency channel capacity available. Additionally, the proposed backoff algorithms avoid to a certain extent the exposed terminal problem (see Section 2.1.6), by allowing MSs the use of another channel, that is idle when a data packet has to be transmitted. In the following chapter, these benefits of Smart Backoff will be exploited in a larger scenario, where higher PHY modes are applied for data transmissions.

It is worth noting that both algorithms can be applied to other multiple access systems as well, and are therefore not bound to CDMA based transmissions. Channel bundling with Parallel Backoff, can also be used to enhance the performance of FDMA based networks.

Cross Layer Optimization of the C-DCF

Content

| | |
|----------------------------------|-----|
| 9.1 Isochronous Medium | 137 |
| 9.2 Performance Evaluation | 139 |
| 9.3 Conclusion | 147 |

Protocol optimization is very important to accomplish the goal of high efficiency. In a CDMA system, where the capacity of the network is limited by interference, optimization should adapt the MAC protocol to PHY layer constraints. Therefore, a cross layer optimization for the C-DCF is suggested in this chapter. The key idea of the optimization is the operation of the network so that the MUDs of the receivers operate at optimum performance, in order to maximize interference suppression.

9.1 Isochronous Packet Transmission

In a MC-CDMA system the frequency channel is divided into cchs by the use of different spreading sequences. In an asynchronous ad-hoc packet based system, like the proposed one, a transmitting MS chooses one cch for transmission. Applying CSMA/CA, each MS transmits its data packet with a certain probability after a cch is detected idle. This method provides a simple multiple access mechanism, but parallel transmissions in different cchs, originating from different MSs are totally asynchronous to each other. Relative delays are randomly distributed in $[0, T_s)$, where T_s is the duration of one multi-carrier symbol. If this delay, which is a measure of asynchronism among transmissions ongoing in parallel could be reduced, then the performance of the MMSE MUD used at the receivers, would enhance. Figure 4.2, gives evidence to this assumption: the SINR at the detector reaches high values, if the relative delay of the interferer to the actual transmitter is small, compared to $T_s/2$. In order to accomplish this, without raising

the system's complexity as would be the case with full synchronization, an isochronous operation is proposed.

Isochronous operation is accomplished if MSs are allowed to start transmissions only at specific time instants, e.g., after the reception of a beacon signal, an RTS or CTS frame. Medium access per cch is proposed to be carried out in a slotted-Aloha manner [KLEINROCK and LAM (1975)], instead of ALOHA [ABRAMSON (1970)] as used so far in this thesis. The transmission time instants are proposed to be multiples of $4\mu\text{sec}$, the duration of a multi-carrier symbol that is the finest time granularity defined at the MAC layer. Accordingly, the medium has a slotted structure, where transmissions are initiated only at the beginning of a slot with $4\mu\text{sec}$ duration. Depending on its length, each frame occupies a different number of slots. This functionality is supported from TSF, a procedure defined in IEEE 802.11 standard to synchronize the local clocks of MSs (Section 2.1.7).

Synchronization of clocks is not enough though, for MSs to keep a common tact of $4\mu\text{sec}$. Since the transmitted frames consist always of an integer multiple of multi-carrier symbols, the backoff time and interframe spaces should be adopted to the $4\mu\text{sec}$ multi-carrier symbol duration, to allow a synchronization on physical layer basis. Therefore, it is proposed to define interframe space durations (SIFS, PIFS, DIFS) as multiples of $4\mu\text{sec}$, as specified in Table 9.1. Furthermore, the slot duration used for the calculation of backoff is proposed to be a multiple of $4\mu\text{sec}$, too.

Table 9.1: Interframe space durations for isochronous network operation.

| Parameter | Proposed duration | IEEE 802.11a |
|-----------|-------------------|-------------------|
| SIFS | $16\mu\text{sec}$ | $16\mu\text{sec}$ |
| PIFS | $24\mu\text{sec}$ | $25\mu\text{sec}$ |
| DIFS | $36\mu\text{sec}$ | $34\mu\text{sec}$ |

The synchronization procedure can be further supported by making use of information gained by the medium sensing function of CSMA/CA networks. A MS in idle that is monitoring the cch can synchronize itself to the tact of an ongoing transmission (Fig. 9.1).

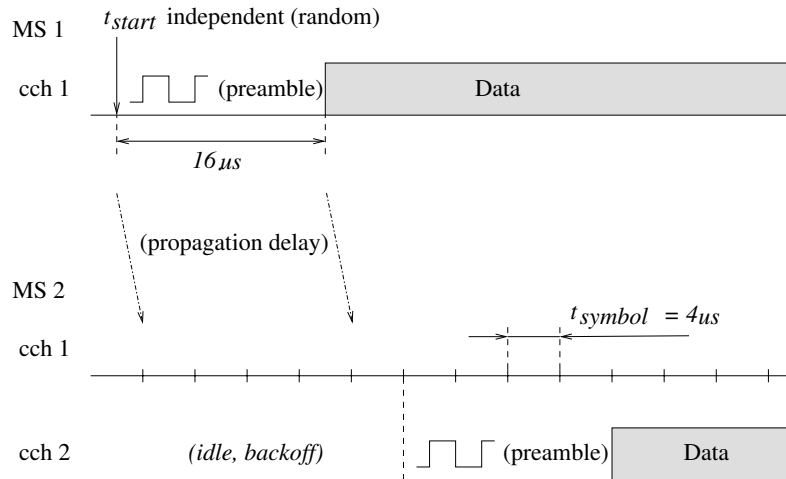


Figure 9.1: The synchronization principle.

From two reasons it is expected that MSs cannot be completely synchronized to each other but will reach quasi-synchronism. First, the propagation delay of both, beacon and the observed transmissions phase, will introduce an error to the slot start time derived. This error is limited in case of a WLAN and *Wireless Personal Area Network* (WPAN), due to the short distance covered with one link. The typical longest distance to be covered in a WPAN with one hop is 20m resulting in a maximum propagation delay of 68psec. For a WLAN 300m equivalent to $1 \mu sec$ might result as error caused by propagation delay. The second reason for imperfect synchronization is that, MSs will not be able to precisely meet the slot start for transmitting, due to hardware constraints. As a consequence, packet transmissions cannot be fully synchronized but are isochronous.

From Fig. (4.2) and the relative analysis in Section 4.3, it is known that a synchronization error in the order of up to 25% ($1 \mu sec$) of the symbol duration ($4 \mu sec$) can nearly perfectly be handled by the MUD. It can therefore be assumed that the good of isochronous operation would be reached with sufficient precision.

9.2 Performance Evaluation

In this section, the performance of the proposed $4 \mu sec$ slot oriented access method is evaluated. For this purpose, a larger scenario, comprising four

subnetworks is considered as depicted in Fig. 9.2. Data packets are assumed 1024 byte long, and traffic load generators deliver Poisson traffic to source MSs. All connections operate the 64QAM 3/4 PHY mode and MSs are capable of Smart Backoff. The other parameters have the values given in Table 7.1, with two modifications:

1. Control frames are transmitted using the BPSK 1/2 PHY mode. This allows the reception of control data under poor channel conditions and enhances the frequency adaptation function, which relies on the correct reception of control frames.
2. CW_{min} is chosen to 31, in order to reduce collision probability during contention and focus on random interference resulting from MAI.

In order to demonstrate the performance enhancement from the proposed cross layer optimization method based on isochronous operation, and provide a comparison among different functions of the protocol, five different

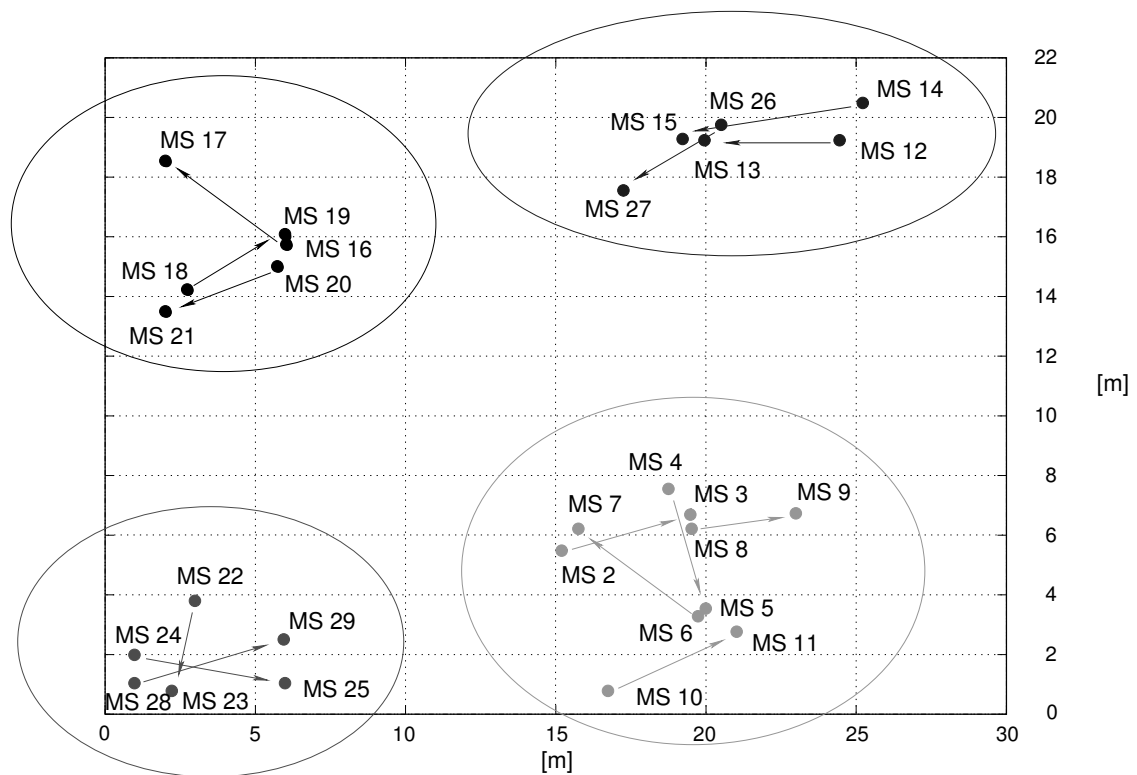


Figure 9.2: The simulated scenario.

operating modes of the subnetworks are analyzed. In each mode, different protocol functions are enabled, but all use Smart Backoff as described in Section 8.2:

- **Mode A**, operates on standard mode as described in Chapters 5 and 8.2, with TPC enabled.
- **Mode B**, applies TPC and cross layer optimization (CL).
- **Mode C**, applies TPC and frequency adaptation (FA)(Section 5.4).
- **Mode D**, applies all three functions together (TPC+ CL+ FA).
- **Mode E** applies different from mode D a new frequency adaptation method (newFA). In this mode the decision for a frequency channel change is made at the transmitter, after 3 consecutive transmissions (RTS or data) without response from the corresponding receiver.

The following assumptions are made for the simulation studies:

- Synchronization error under cross layer optimization is random with a deviation of $\pm 200nsec$ (10% the multi-carrier symbol duration), comprising 110nsec the transmission delay among the two most distant MSs (MS 14 and MS 28) and $\pm 90nsec$ for the oscillators' offset. The error is different for every frame transmission by a MS.
- In case of frequency adaptation, all MSs in all subnetworks initiate transmissions in the same frequency channel. One additional frequency channel is available for the algorithm.

The histogram at Fig. 9.3, shows the carried traffic per MS, for the five operating modes. The poorest performance appears under mode A where TPC is applied only. Transmit power control is not enough to keep the MAI level low enough in a scenario with many MSs operating in close neighborhood. Consequently, the operation of connections using the highest PHY mode, requiring a high SINR value for correct reception is not optimum. The carried traffic increases for most MSs in mode B when cross layer optimization is used in addition to TPC. The improvement reaches from 10% (MS 22) to almost 100% (for MS 14).

In mode C, frequency adaptivity and TPC are used. The carried traffic achieved for all MSs is higher, because of frequency domain available channel adaptation, whereby the resources are doubled to 2 frequency channels and MSs profit in addition from reduced MAI in each frequency channel. A further improvement is achieved for most of the MSs in mode D, applying frequency adaptivity, TPC and cross layer optimization. Only MSs

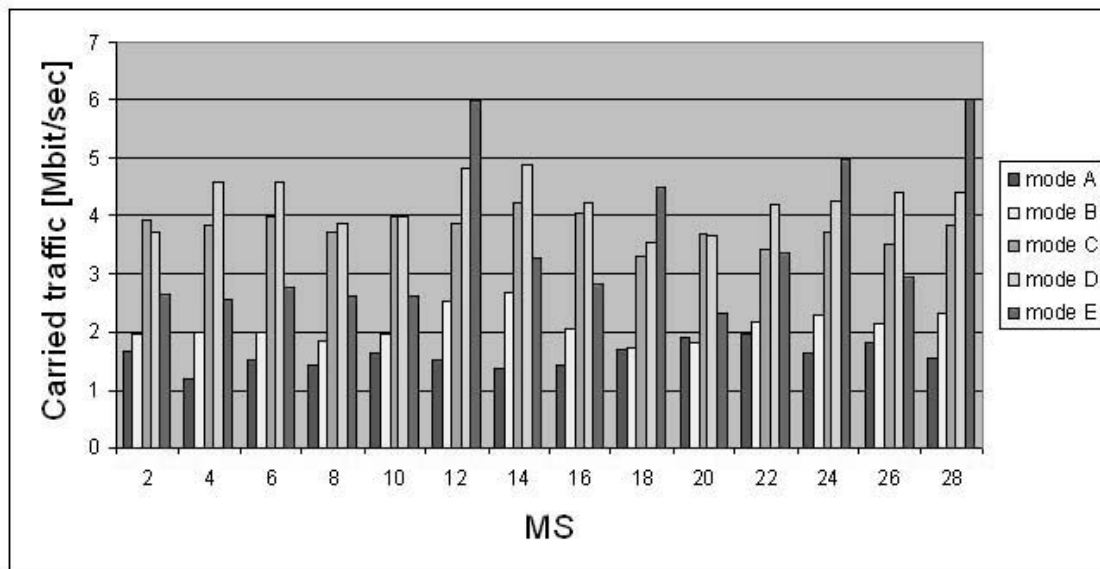


Figure 9.3: The carried traffic per MS, for different operating modes. The applied PHY mode is 64QAM 3/4 for data frames and BPSK 1/2 for control frames.

2 and 20 see a small throughput degradation, whilst the network achieves the maximum throughput, compared to any other operating mode. The achieved MAC protocol efficiency of each operating mode is given in Fig. 9.4. The MAC protocol efficiency is presented as percentage of utilized channel capacity measured at MAC level, normalized to the capacity of one frequency channel. From the results in Fig. 9.4, it is seen that mode D and mode B are almost equivalent, achieving 93.62% and 93.2%, respectively. The superiority of mode D in terms of throughput, results from the use of two frequency channels by the frequency adaptation function. On the other hand, a comparison between mode B and mode C, shows for this WPAN scenario that cross layer optimization (mode B) performs better than frequency adaptation (mode C). Mode E appears, in general to be inferior to mode D.

In Fig. 9.5, the number of RTS collisions per source MS is presented. Mode A shows the worst performance, with a large number of RTS collisions per MS. In all other modes, the number of RTS collisions reduces substantially, with cross layer adaptation (mode B and mode D) achieving better

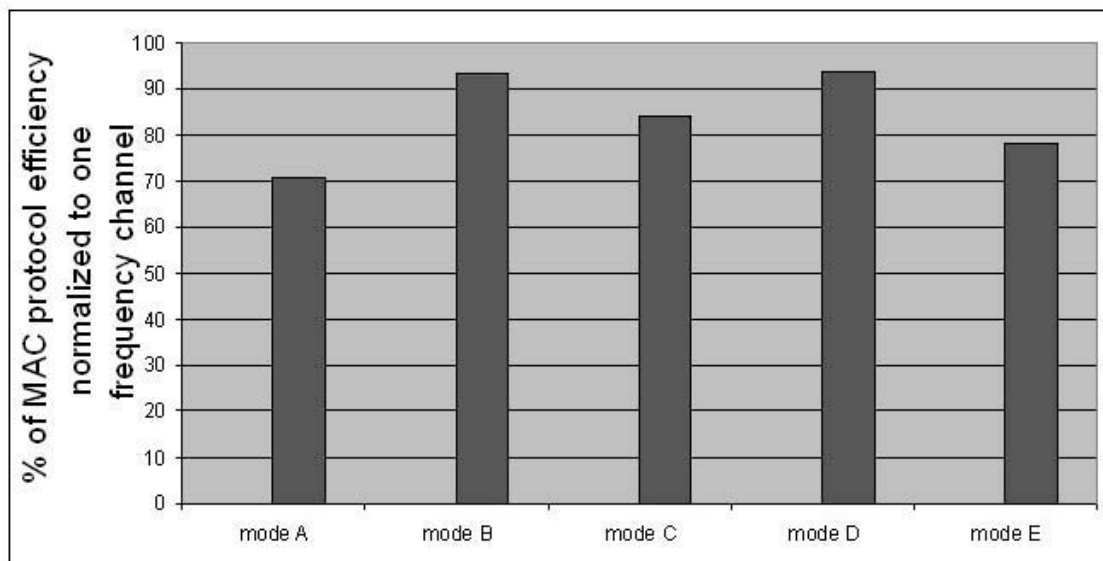


Figure 9.4: Achieved MAC protocol efficiency, for different operating modes. The applied PHY mode is 64QAM 3/4 for data frames and BPSK 1/2 for control frames.

performance than frequency adaptivity (mode C and E).

Figure 9.6 presents the percentage of retransmitted data frames, per source MS. The proposed cross layer optimization combined with TPC and frequency adaptation (mode D), has the best overall performance. Besides the connection between MS 18 and MS 19, facing 19% frame repetition ratio, in all other connections the percentage of repeated data frames is limited to less than 12%.

9.2.1 The impact of cross layer synchronization in larger scenarios

In the following analysis the efficiency of the proposed optimum network operation mode (mode D) is tested in a larger scenario, where the transmission delay increases the synchronization error. The simulated scenario is presented in Fig. 9.7 and is similar to the scenario simulated before (see Fig. 9.2). Despite the increased distances mutual interference among all subnetworks influences transmissions.

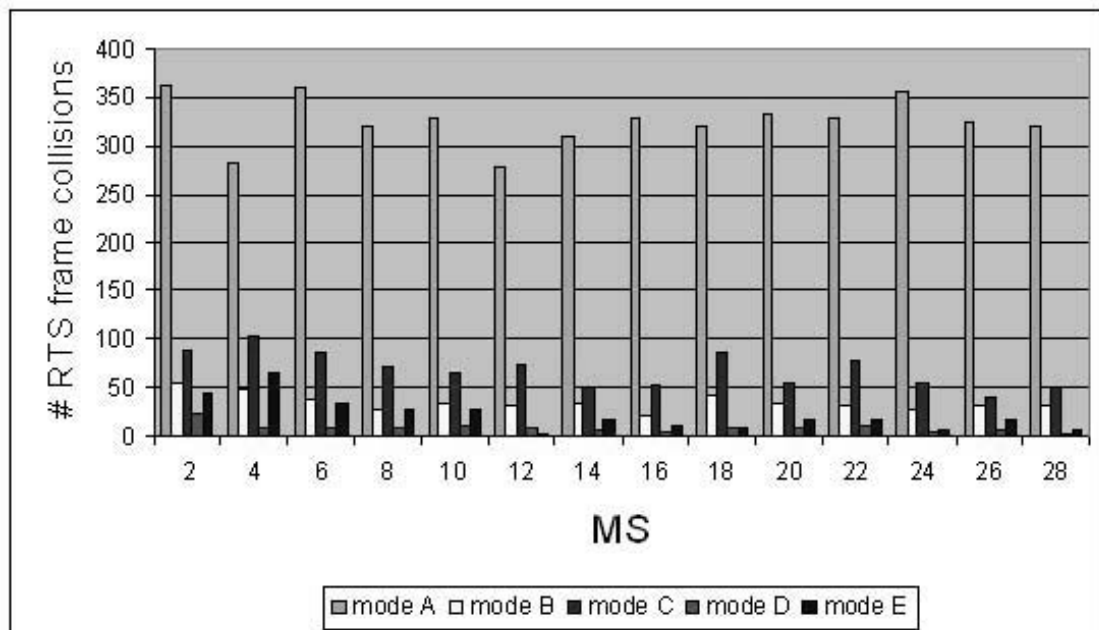


Figure 9.5: Number of RTS collisions per MS, for different operating modes. The applied PHY mode is 64QAM 3/4 for data frames and BPSK 1/2 for control frames.

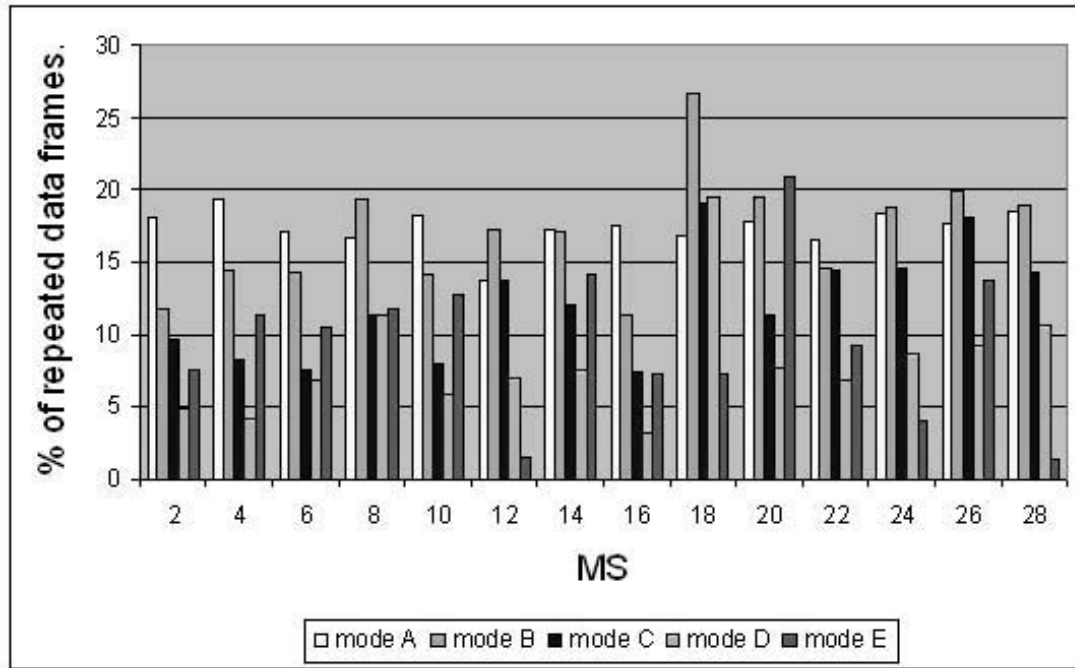


Figure 9.6: Percentage of repeated frames (collisions) per MS, for different operating modes. The applied PHY mode is 64QAM 3/4 for data frames and BPSK 1/2 for control frames.

In order to compensate for the increased pathloss, the maximum allowed transmission power is raised to 23 dBm. The applied PHY modes are BPSK 1/2 for control frames and QPSK 1/2 for the transmission of data frames. All other parameters of the simulation setup have the values given in Table 7.1. The random synchronization error under cross layer optimization is in case of the large area scenario $\pm 460nsec$, comprising 370nsec the transmission delay among the two most distant MSs (MS 14 and MS 28) and $\pm 90nsec$ for the oscillators' offset.

Figure 9.8 presents the carried traffic per source MS for the large area scenario, when operated under both, mode A and the proposed optimum mode D. The application of mode D, not only increases the carried traffic for all MSs in the network, but improves fairness too. The carried traffic under mode D fluctuates 32.35%, between 1.7 Mbit/sec (MS 14) and 2.25 Mbit/sec (MS 12), whilst the fluctuation by mode A is 152.85%, between

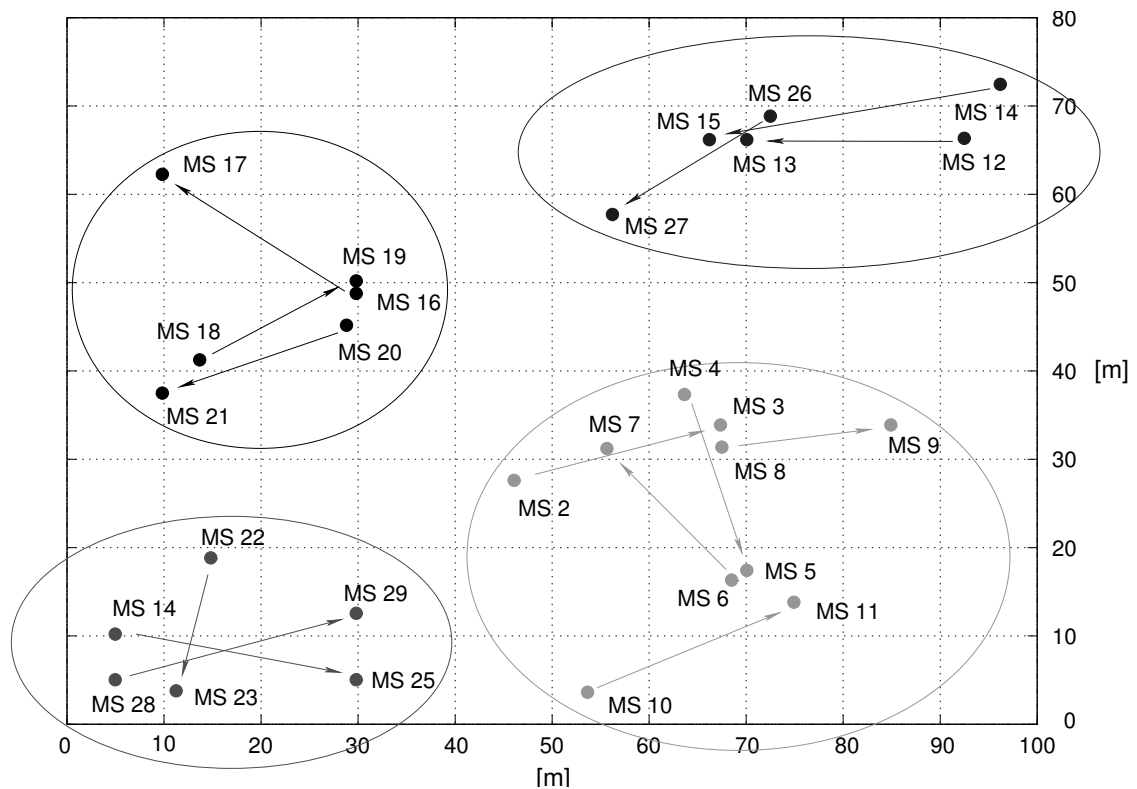


Figure 9.7: The simulated large area scenario.

0.7 Mbit/sec (MS 2) and 1.75 Mbit/sec (MS 12).

In Fig. 9.9, the percentage of retransmitted data frames per source MS is presented, where the efficiency of mode D becomes more evident. The percentage of retransmitted data frames for all MSs is lower than the limit of 12%. Under mode A, the same percentage reaches 23.5% (MS 14).

9.3 Conclusion

A cross layer optimization method has been introduced, and its performance evaluated. By introducing isochronous operation, the MAC protocol can be optimized for the MC-CDMA based network, when using MUD at the receivers. Isochronous operation enhances network performance significantly compared to asynchronous operation, as relative delays among multiuser transmissions are kept low. The proposed improvements, together with frequency adaptation result in good network performance in extended scenarios meeting high QoS demands imposed by the MSs.

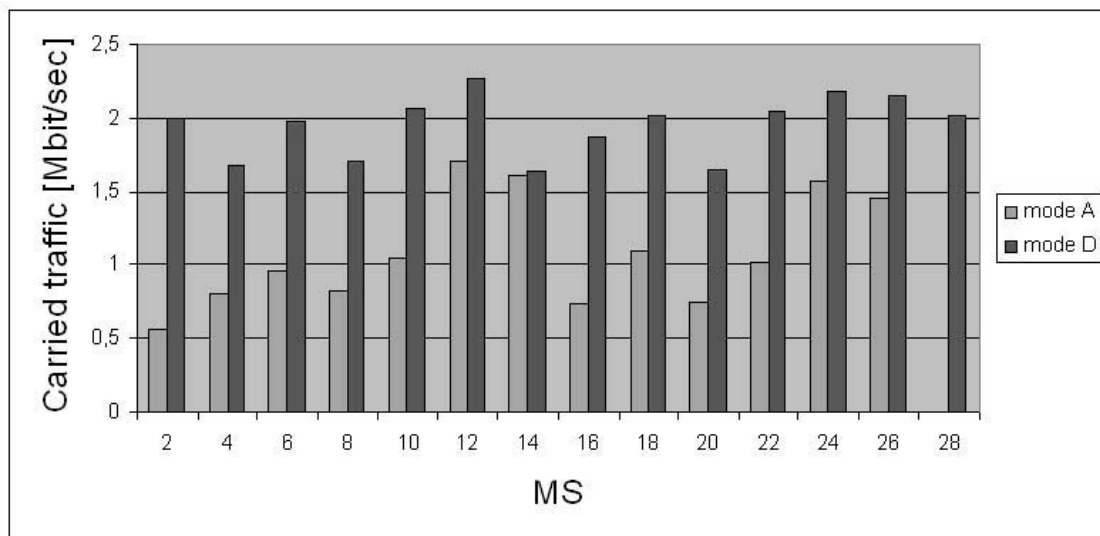


Figure 9.8: The carried traffic per MS, for different operating modes in the large area scenario. The applied PHY mode is QPSK 1/2 for data frames and BPSK 1/2 for control frames.

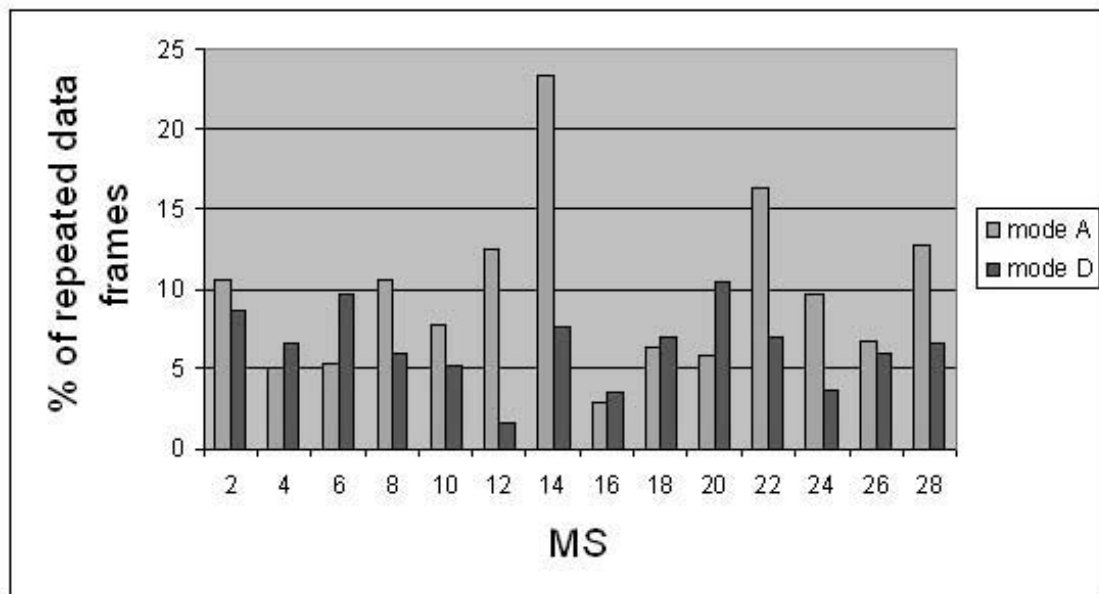


Figure 9.9: Percentage of repeated frames (collisions) per MS, for different operating modes in the large area scenario. The applied PHY mode is QPSK 1/2 for data frames and BPSK 1/2 for control frames.

MAC Extensions for Multihop

Content

| | |
|-----------------------------------|-----|
| 10.1 Multihop MAC Protocol | 150 |
| 10.2 Performance Evaluation | 156 |
| 10.3 Conclusion | 166 |

Besides reducing interference by applying reduced transmitted power, multihop communication is essential for coverage range extension and for the interconnection of (different) subnetworks. Especially in home and office environments, the radio range achievable with WLANs considerably limits the size of the area covered and multihop communication is seen as an important element to provide larger range continuous area coverage.

A multihop connection consists of consecutive links enabling the data transfer between two MSs that are not within mutual radio range. A relaying function is required, providing the needed functionality of an intermediate MS, called forwarding MS (or forwarder), for relaying of data packets to the next node of a multihop connection. Such relaying function can be implemented either in the first, second or third layer of the ISO/OSI reference model. In this chapter the focus is on extension of the MAC layer functionality to support MAC frame packet relaying for the C-DCF proposed for CDMA based WLANs. The relay is assumed to have bridge functionality. Throughout this work the following assumption are made:

- Necessary information from layer three (routing) is known and provided to MAC sublayer.
- Multihop connections of up to 3 hops are considered.
- The same PHY mode is used for all data links in a multihop connection.
- MSs are equipped with one transmitter only.

10.1 Multihop MAC Protocol

The IEEE 802.11 conformant frame exchange in a multihop connection spanning over 3 hops is shown in Fig. 10.1 (solid lines). MS 1 as the initiating node transmits data frames via MS 2 and MS 3 to the final destination MS 4. In this case, every forwarding MS is responsible for the correct transmission in the next hop, dealing with the multihop data packet the same as with its own source data. Signaling of the route is done using the four address fields in the MAC header as follows (see Fig. 2.9):

- Address 1: Contains the source address of the multihop connection (MS 1).
- Address 2: Denotes the first forwarding station (MS 2).
- Address 3: Contains the address of the final receiver. (MS 4).
- Address 4: Specifies the address of the second forwarding station (MS 3).

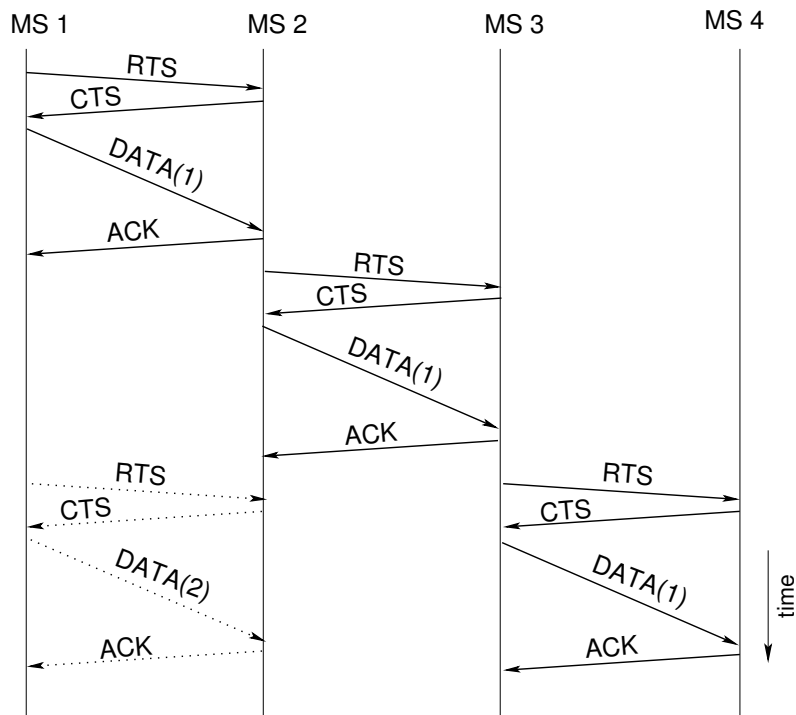


Figure 10.1: Standard multihop transmission.

MS 2 signals the correct reception of a data frame with an ACK and prepares the transmission to MS 3 by starting a handshake cycle to MS 3. A new handshake cycle is started in MS 1 too, and the respective transmission between MS 1 and MS 2 would delay the transmission between MS 2 and MS 3. In order to prioritize packet relaying at MS 2, a deliberate guard interval is introduced for MS 1 that is not specified in IEEE 802.11 (Fig. 10.2). MS 1, being the initiator of the multihop transmission from MS 1 to MS 4, must provide time for forwarding station MS 2 to forward the data packet to MS 3 and therefore must not access the medium for a sufficient long duration called multihop guard interval (the same applies for the transmission from MS 3 to MS 4). After the multihop guard interval has expired, MS 1 may initiate any transmission according to the legacy MAC rules [ACHARYA et al. (2003)]. Depending on the scenario topology and the route chosen, MS 1 might be able to transmit in parallel with MS 3 (dotted lines in Fig. 10.1), using any suitable cch, which would increase overall performance of the multihop transmission and reduce delay.

In order to improve performance, Smart Backoff (Section 8.2) can be used by MSs enabling parallel transmissions in more than one cchs [KWUIMO (2005)]. Especially in case of a forwarding MS serving multiple multihop

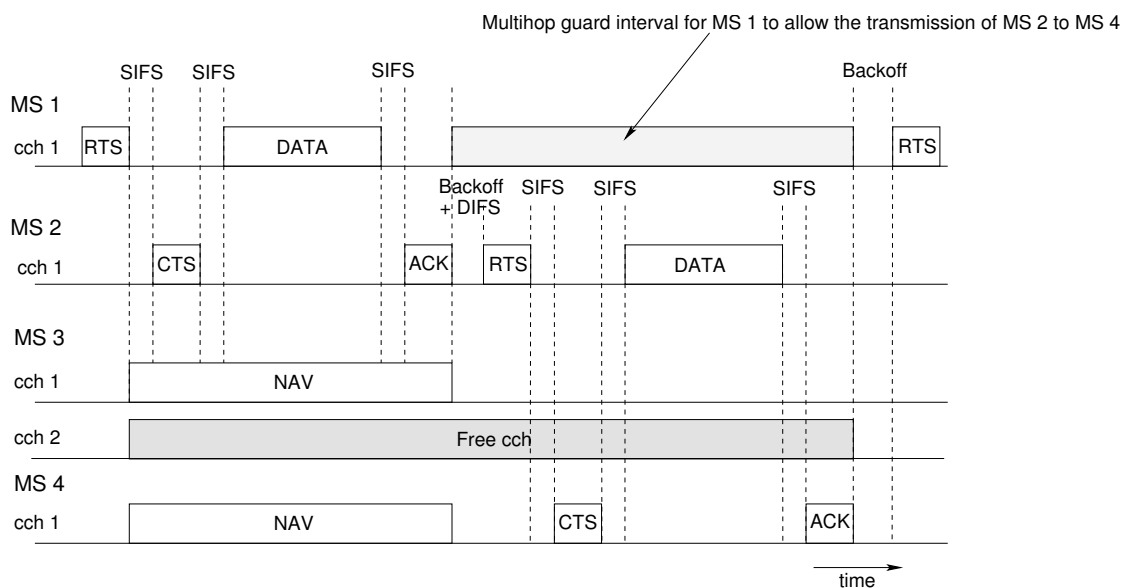


Figure 10.2: The standard NAV problem.

connections, like MS 2 in the star topology of Fig. 10.3, concurrent transmissions like in the link from MS 2 to MS 5 are essential for achieving high network capacity and low queueing delay. It must be noted, that Smart or Parallel Backoff might increase the collision probability of forwarding MSs since contention for medium access is increased as a MS employs CSMA/CA in many cchs in parallel.

Referring to Figs. 10.2 and 10.3, MS 3 will set according to the C-DCF, its NAV timer for the corresponding cch 1 upon receiving the RTS frame from MS 1, or the corresponding CTS from MS 2, for a NAV duration as contained in the RTS (Fig. 10.2), or CTS frames. Smart Backoff would lead MS 3 to another idle cch (cch 2 in Fig. 10.2), where it could continue with its backoff countdown. A concurrent transmission from MS 3 to MS 2 would interfere in this case with the ongoing data transfer from MS 1 to MS 2, since both transmissions address the same receiver (MS 2, Fig. 10.3). To avoid this problem, a cch specific NAV is proposed per MS. According to the cch specific NAV, each MS receiving a RTS and/or a CTS frame, sets its NAV timer for the denoted duration of transmission, on the receive cch, and marks in addition the involved MS(s) as occupied. This precaution prohibits collisions in multihop links, whilst it enables Smart Backoff deployment. Consequently, a source MS intending to transmit a frame to some other (forwarder) MS, first checks whether this MS is currently occupied and then searches for a cch that is not blocked by actual NAV timers supervised by the source MS.

10.1.1 SDL specification of multihop extensions to C-DCF

In this section, the additional functionality in MAC protocol for the support of multihop connections in C-DCF is described. The analysis is based on the star scenario given in Fig. 10.3 and the link between MS 2 and MS 4.

After taking into account the NAV blocked cchs and MSs, the transmitting MS 2 applying Smart Backoff searches for a cch to initiate a transmission. The RTS frame after backoff indicates a new data frame transmission. Figure 10.4 shows the functionality of a MS in idle state when a RTS frame is received. In case the MS that received the RTS frame is the actual recipient of the transmission (MS 4), it prepares the corresponding CTS frame, to be send after SIFS. If the MS is not the recipient (for e.g. MS 5), it sets its NAV timer for the duration encoded in the received RTS, the MSs involved and the cch used for transmission.

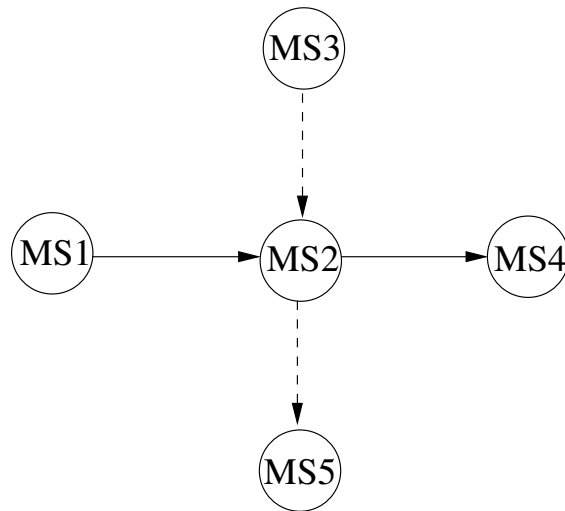


Figure 10.3: Star scenario.

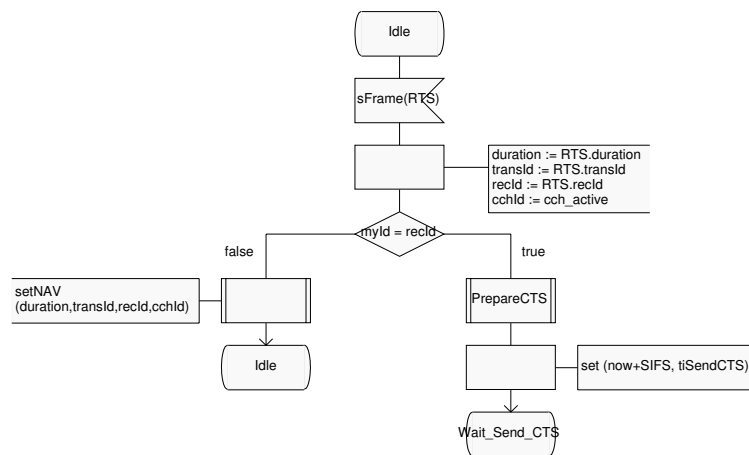


Figure 10.4: Functionality of a MS in idle state receiving RTS.

After receiving the CTS frame, MS 2 transmits the data frame according to the rules of C-DCF, as described in Chapter 5. The data frame is received by MS 4 in state "Wait for Data" (Fig. 10.5), which sets the flag "forwarder" to true if MS 4 is not the end receiver of the data frame and prepares the transmission of the ACK frame.

MS 4 transmits the ACK frame after time SIFS (Fig. 10.6) and prepares a backoff procedure both, when acting as a forwarder to the previously received data frame, or if other data frames in its queues are waiting for transmission. Otherwise, MS 4 switches to idle state.

MS 2, the transmitter of the data frame, receives the ACK from MS 4 in state "Wait for ACK" (Fig. 10.7) and sets a timer with duration equal to the multihop guard interval, if the last transmission was not at the last hop of a multihop connection. Otherwise, MS 4 will proceed with a new backoff timer, if other frames are waiting for transmission, or switch to idle state.

Summarizing the previous analysis on multihop extension of the C-DCF protocol, the following additions should be done to the functionality of MSs in order to enable efficient MAC layer relaying:

- A multihop guard interval, that prevents the transmitting MSs from

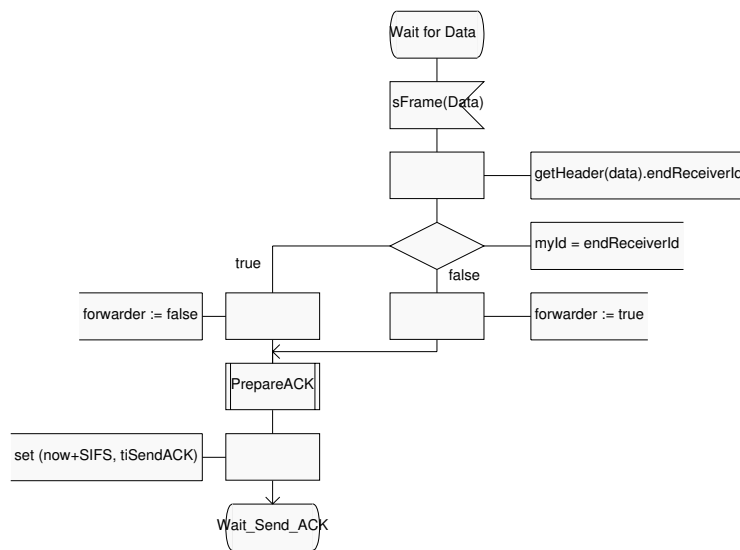


Figure 10.5: Functionality of a MS when a data frame is received.

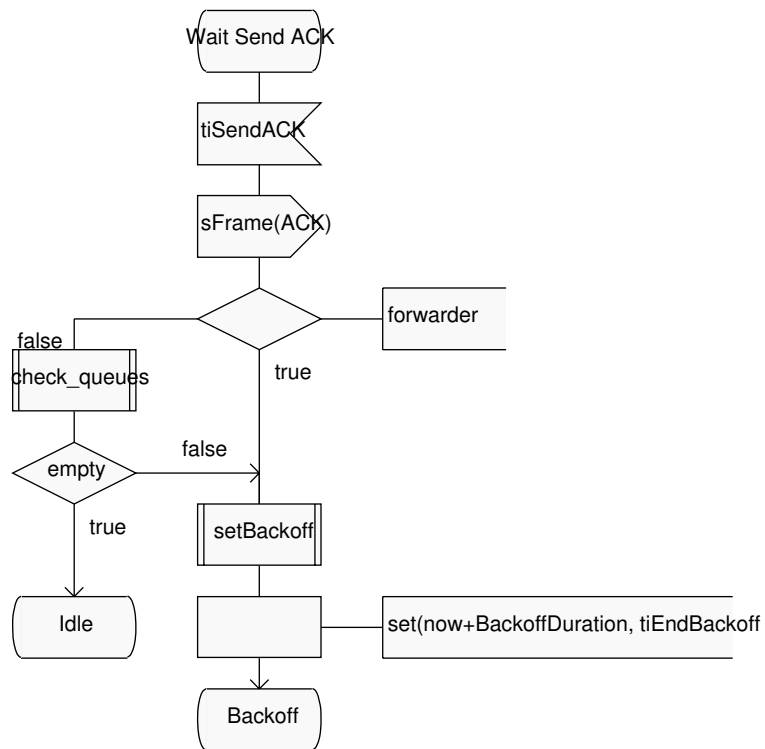


Figure 10.6: Functionality of MS for the transmission of an ACK frame in the multihop protocol.

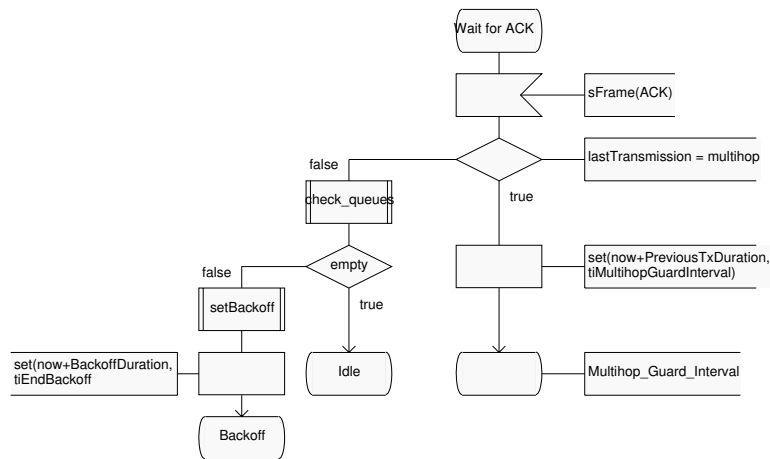


Figure 10.7: Functionality of the transmitting MS after the reception of an ACK for a previously transmitted data frame.

an immediate transmission of the next multihop packet, prioritizes the relaying MS on medium access reducing the end-to-end delay of the multihop connection.

- The use of Smart Backoff by forwarding MSs involved in more than one multihop connections (bottleneck) reduces the medium access time. Furthermore, Smart Backoff enables parallel transmission in many cchs, that increases the available capacity at relaying MSs and reduces the bottleneck effect.
- In multi-channel, multihop environments applying carrier sensing (like the proposed C-DCF), the NAV timer per cch is not enough to secure the transmission after the two way handshake (RTS/CTS), when Smart Backoff is used by transmitting MSs. The cch specific NAV per cch and MS proposed in this chapter is then necessary.

10.2 Performance Evaluation

10.2.1 The Bottleneck Case

In the following, performance evaluation results of the proposed multihop protocol are presented. At first, the protocol's behavior in a bottleneck

scenario is analyzed. A network topology as described in Fig. 10.8 is studied, where MS 2 is simultaneously the forwarding MS for the connection MS 1 to MS 3 (con. 1) and is the initiator for con. 2. Both transmitting MSs are assumed to be Smart Backoff capable, and able to operate in two cchs in parallel. Traffic generators generating Poisson load of variable intensity are used. The other simulation parameter vales are given in Table 7.1. For all frame transmissions the QPSK 1/2 PHY mode is used, and TPC is deactivated.

A value $CW_{min}=31$ is used throughout the multihop investigations performed. For the QPSK 1/2 PHY mode and 1024 Byte long data packets, the net throughput at MAC layer can be calculated, similarly to the calculations presented in Section 5.5, to 9.8 Mbit/sec. A higher CW value does reduce contention of MSs during medium access and contributes significantly to collision avoidance when more than one multihop connection use the same forwarding MS making it a bottleneck. However, the delay is increased by this.

Fig. 10.9 presents the achieved carried traffic per connection over the offered load. For both connections, carried traffic per connection raises linearly with offered load, up to a load of 1,1 Mbit/sec. With further increased load the carried traffic of con. 2 raises further, becoming privileged to con. 1 whose carried traffic drops.

The advantage of con. 2 owes to the forwarding station MS 2 and its capability of parallel transmission. Each time MS 1 transmits a data packet to MS 2, MS 1 defers for a certain time, in order to give MS 2 the opportunity to forward the data packet to MS 3. Due to parallel transmission in two cchs

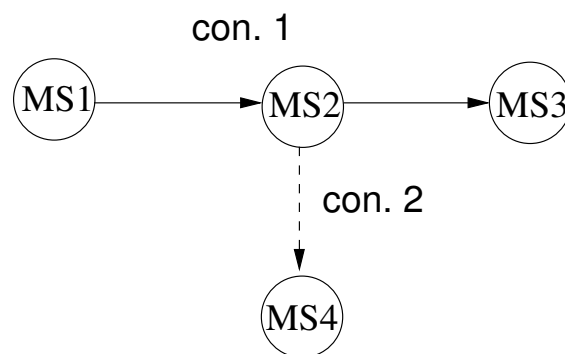


Figure 10.8: The bottleneck scenario.

and Smart Backoff, MS 2 can then transmit two data packets in parallel. Additionally, when MS 1 has a new data packet to transmit, it competes with MS 2 for medium access.

The total carried traffic is 2.4 Mbit/sec, which is close to the capacity of a single cch for the used PHY mode. In the scenario of Fig. 10.8 throughput is achieved, in both connections, when a data packet is transmitted from MS2. In a fair contention between MS 1 and MS 2, each station would transmit 50% of the time, then blocking transmission of the other MS. Thus MS 2 would use in overload 50% of the capacity of two cchs, which equals the capacity of 1 cch.

Figure 10.10 presents the results for the cumulative queueing delay per connection, that is is defined as the sum of queueing delay of a frame in consecutive hops. For both connections, cumulative queueing delay raises similarly with offered load. Con. 2 achieves lower delay since it uses a one hop link only.

The advantage of Smart-Backoff applied in multihop is demonstrated in Fig. 10.11, presenting the CDF of end-to-end service time per connection for the bottleneck scenario compared to connection based cch selection. For

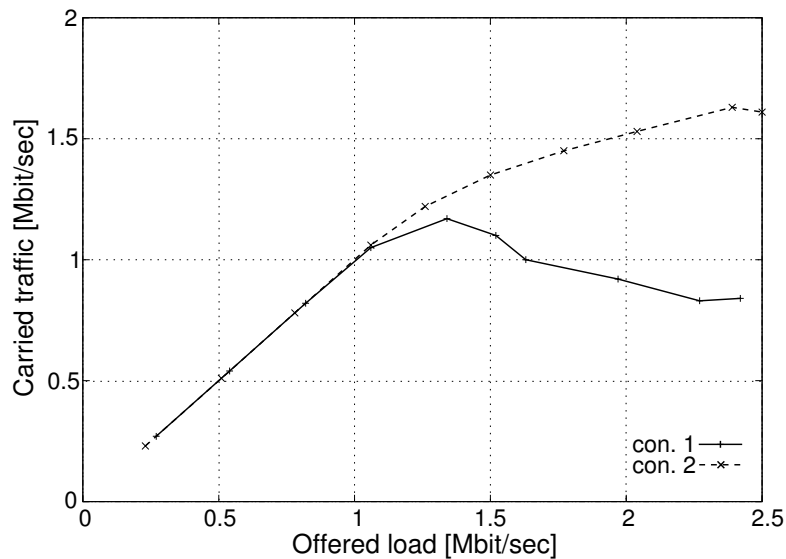


Figure 10.9: Throughput sharing in bottleneck scenario (Fig. 10.8). The applied PHY mode is QPSK 1/2 for both, control and data frames.

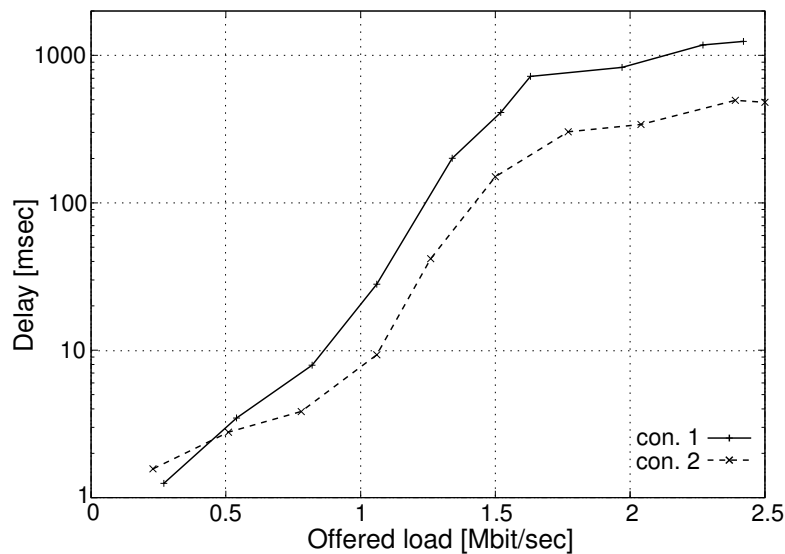


Figure 10.10: Mean cumulative queuing delay per connection in bottleneck scenario (Fig. 10.8). The applied PHY mode is QPSK 1/2 for both, control and data frames.

an offered load per connection of 1.25 Mbit/sec, the maximum end-to-end service time for con. 2 is limited with Smart Backoff to 12msec, but 65msec appears with connection based cch selection, whilst the improvement from using Smart Backoff for con. 1 is almost 1sec. It can be concluded that in multihop networks Smart Backoff should be applied.

10.2.2 Multihop Network Performance Study

In this section a multihop network scenario as shown in Fig. 10.12 is studied. Besides a bottleneck station (MS 7), the scenario contains three multihop connections with 2 or 3 hops and a direct link (con. 4). The same simulation parameters are taken as used in the bottleneck scenario (7.1). All transmitting MSs are capable of Smart Backoff and parallel transmission in two cchs is allowed for MS 7, that is offered the highest traffic load. End-to-end connections are named as follows: connection between MS 2 and MS 4 is referred to as con. 1, between MS 5 and MS 9 as con. 2, between MS 6 and MS 10 as con. 3 and between MS 11 and MS 12 as con. 4.

Figure 10.13 presents the carried traffic per connection versus the offered

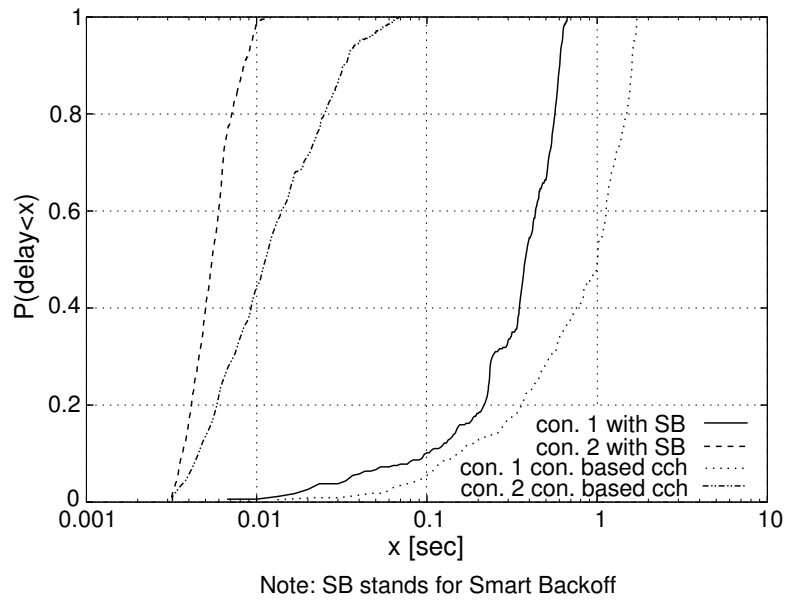


Figure 10.11: CDF of end-to-end service time per connection in bottleneck scenario (Fig. 10.8). Comparison of connection based cch selection and Smart Backoff for 1.25 Mbit/sec offered load per connection. The applied PHY mode is QPSK 1/2 for both, control and data frames.

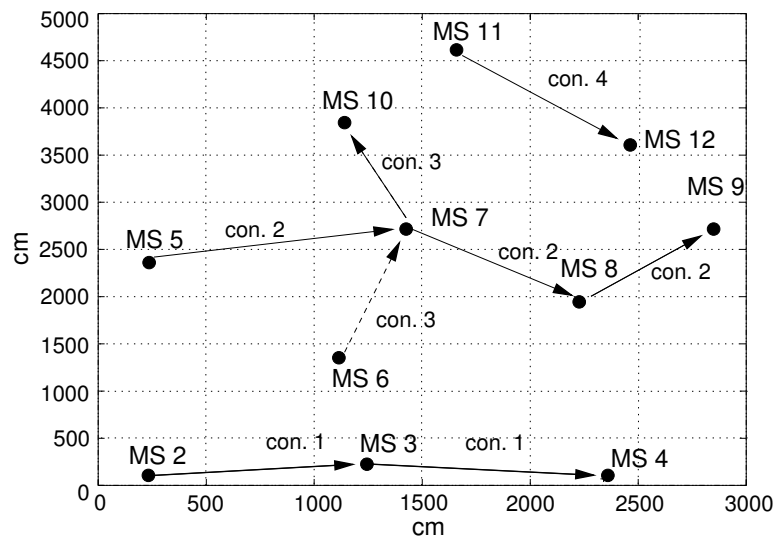


Figure 10.12: The simulated scenario for multihop transmissions.

load. Con. 4 approaches in saturation the maximum cch MAC level capacity for the applied PHY mode, namely 2.5 Mbit/sec (a quarter of the system's capacity, see Eq. (5.20)). The 2 hop con. 1 reaches an end-to-end carried traffic of 1.2 Mbit/sec, that corresponds to about half the cch capacity. The achieved maximum carried traffic for the three hop con. 2 and two hop con. 3 is about 0.8 Mbit/sec for each and is limited by the common forwarding station (MS 7), that is a bottleneck and defines the throughput in con. 2 and con. 3.

MS 7 competes for channel access with the two transmitters MS 5 and MS 6 and transmits in 1/3 of the time, using in ideal case two cchs (MS 7 is the only MS allowed to transmit in parallel in two cchs). The two other cchs are used by con. 1 and con. 2. Consequently, the throughput at MS 7 is 1/3 of the aggregated capacity of two cchs: $1/3(2 \times 2.49 \text{ Mbit/sec})$, averaging to 1.66 Mbit/sec. This throughput at MS 7 is equally divided among con. 2 and con. 3, each achieving 0.83 Mbit/sec in the ideal case, where no collisions are considered.

Figure 10.14 presents the mean end-to-end queueing delay per connection, that comprises the queueing delay at all sequential queues for a specific data packet on a specific connection. Results comply with the above throughput analysis: Multihop connections, in general, face for a given load

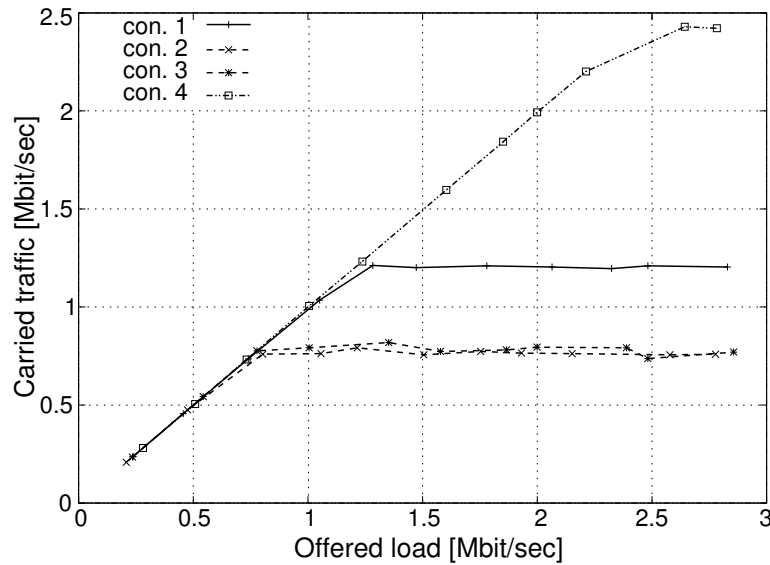


Figure 10.13: Carried end-to-end traffic per multihop connection vs. offered load. The applied PHY mode is QPSK 1/2 for both, control and data frames.

a higher end-to-end queueing delay than single hop connections. The one hop con. 4 achieves the lowest end-to-end queueing delay, whilst con. 3 and con. 2 suffer from high end-to-end queueing delay, rapidly raising with offered load.

In Figs. 10.15 and 10.16, the CDFs of queueing delay per hop are presented, for 0.75 and 1.25 Mbit/sec offered load per connection, respectively. The offered load of 0.75 Mbit/sec/connection approaches the saturation load of con. 2 and con. 3 that achieve the lowest carried traffic. The highest queueing delay comprises 200msec for MS 5 on end-to-end con. 2. Its queueing delay distribution is similar to the one of MS 6 on end-to-end on. 3, since both MSs are the sources of multihop connections sharing the same bottleneck forwarding station MS 7. Furthermore, the multihop guard intervals of MS 5 and MS 6 prohibit after a successful data packet transfer the immediate transmission of the next data packet, raising its delay in the queue. Collisions occurring among MS 5 and MS 6 further increase the delay. The second highest end-to-end queueing delay is achieved by MS 2, owing to the multihop guard interval for prioritization of forwarding station

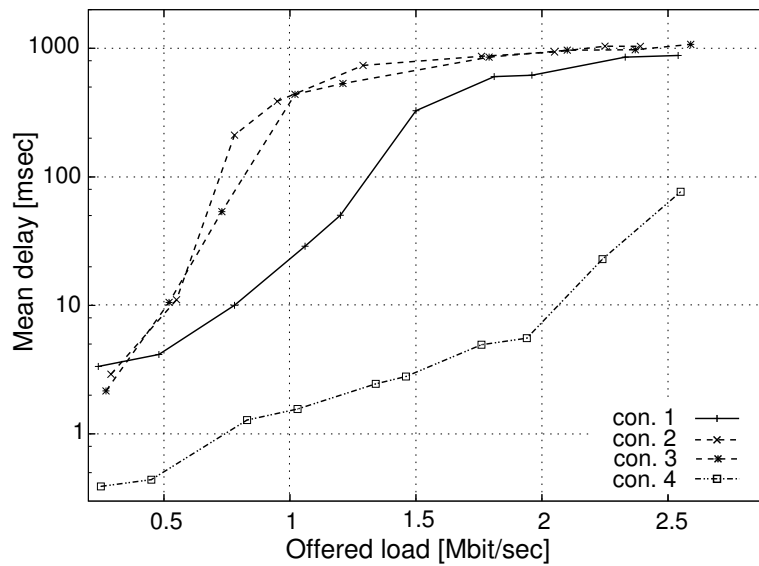


Figure 10.14: Mean end-to-end queueing delay per multihop connection vs. offered load. The applied PHY mode is QPSK 1/2 for both, control and data frames.

MS 3. The direct con. 4 between MS 11 and MS 12 follows, with better queueing delay performance. In this case, queueing delay is affected by the ability of Smart Backoff to detect a free cch.

Queueing delay distributions of the hop between MS 7 and MS 8, and the hop between MS 7 and MS 10, are quite similar. The 3.1msec stepwise raise of queueing delay at 63% and 73% respectively, results from the contention between MS 7 and MS 5 or MS 6 and the guard intervals of length $3253.5\mu\text{sec}$ applied there (Eq. (5.19)).

Best queueing delay performance is achieved at MS 3 and MS 8, which neither apply the multihop guard interval, since they serve the final hops of the respective con. 1 and con. 2, nor participate in any other multihop connection. Particularly, MS 8 can transmit concurrently with MS 5 even in the same cch.

Figure 10.16 presents the CDFs of queueing delay, for an 1.25 Mbit/sec offered load per connection. The relative performances of the connections are similar as under lower load but with higher end-to-end queueing delay for MS 5 and MS 6, which are now in overload. Additionally, MS 2 now

experiences much higher end-to-end queuing delay, since the offered load is chosen such that the saturation of con. 1 is reached (but not the saturation of MS 6).

The CDF of end-to-end delay, measured as the delay between the arrival of a data packet in the network and the reception of the ACK at the last hop, is depicted in Fig. 10.17, for 0.75 Mbit/sec offered load per connection. For con. 2 and con. 3, the end-to-end delay has a similar distribution, due to the common forwarding station MS 7. The reason for the small difference between the two CDFs is the one more hop at con. 2. Similar results are shown in Fig. 10.18, presenting the end-to-end delay for 1.25 Mbit/sec offered load per connection. The network operates in saturation and the high offered load introduces high end-to-end delay for data transfer.

10.2.3 Simulative Comparison with IEEE 802.11 DCF

In order to demonstrate the efficiency of the proposed multihop extensions for C-DCF MAC protocol, a direct comparison with IEEE 802.11 DCF is performed. The standard DCF has been extended to support multihop

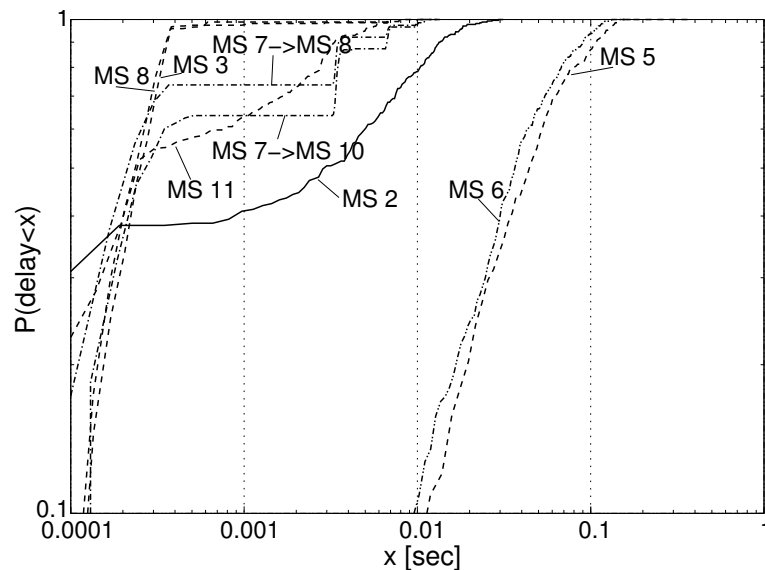


Figure 10.15: CDF of queuing delay per hop for 0.75 Mbit/sec offered load per connection. The applied PHY mode is QPSK 1/2 for both, control and data frames.

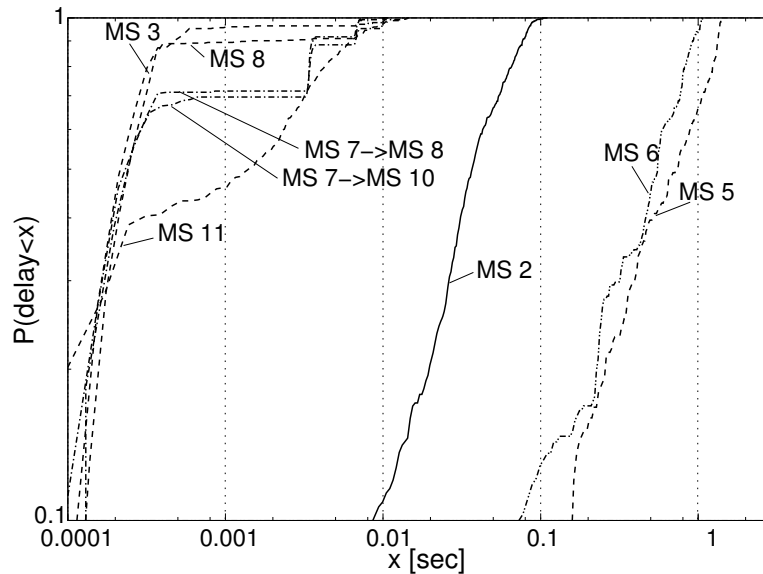


Figure 10.16: CDF of queuing delay per hop for 1.25 Mbit/sec offered load per connection. The applied PHY mode is QPSK 1/2 for both, control and data frames.

connections, in a way that each intermediate MS forwards received multihop data frames following the same rules as with own data. It is assumed that the route is known.

The scenario used for comparison is the one of Fig. 10.12. The generated load type is CBR and QPSK 1/2 is the applied PHY mode for both, control and data frames, latter with payload 1024 Bytes. All other parameters are set to the values given in Table 7.1. In case of C-DCF, Smart Backoff is used by all transmitting MSs to exploit spacial diversity for links in sufficient distance.

Figure 10.19 presents the carried end-to-end traffic per multihop connection with the offered load per connection, for both MAC protocols, DCF and C-DCF. The performance of C-DCF is better for every connection as a result of higher capacity (see Section 5.5) and reduced connection due to the 4 available cchs. Additionally, the performance of C-DCF is enhanced by protocol characteristics such as the multihop guard interval, Smart Backoff with parallel transmission in 2 cchs and reduction of CW to half after collision resolution (see Section 5.1.4). Further, in C-DCF and for middle and

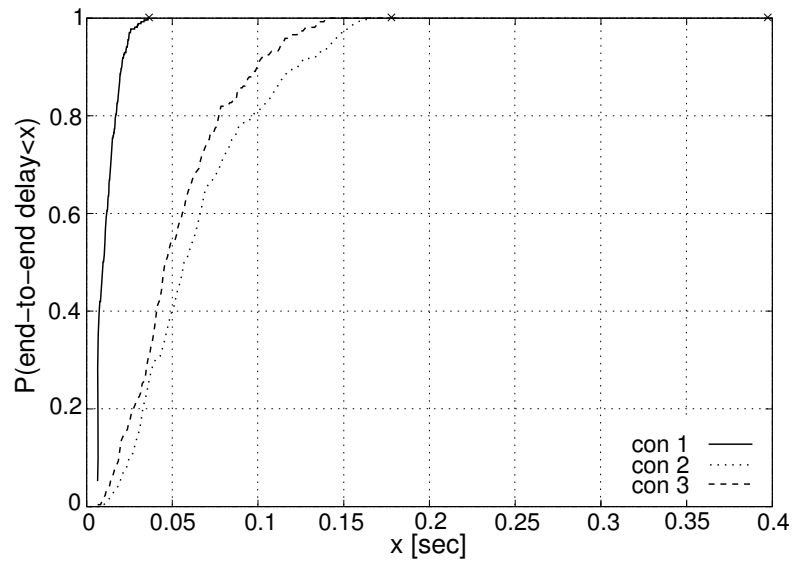


Figure 10.17: CDF of end-to-end delay per multihop connection for 0.75 Mbit/sec offered load per connection. The applied PHY mode is QPSK 1/2 for both, control and data frames.

high offered load especially, con. 2 and con. 3 sharing the same forwarding MS in the first hop (MS 7), carry almost the same amount of traffic, while with DCF fairness on medium access is not achieved.

Similar to the difference in carried traffic, the performance of C-DCF is superior when comparing the delays. In Fig. 10.20 the complementary CDF of end-to-end delay per multihop connection for DCF and C-DCF is presented with 0.75 Mbit/sec/con CBR offered load. The difference of measured delay is for every connection at least an order of magnitude in favor of C-DCF.

10.3 Conclusion

An efficient forwarding method for the C-DCF is proposed. Performance evaluation results show the ability of the multihop network to achieve an overall good performance. Using Smart Backoff, forwarding MSs, which participate in more than one multihop connection can improve their performance, and achieve higher throughput. Technical solutions proposed in this

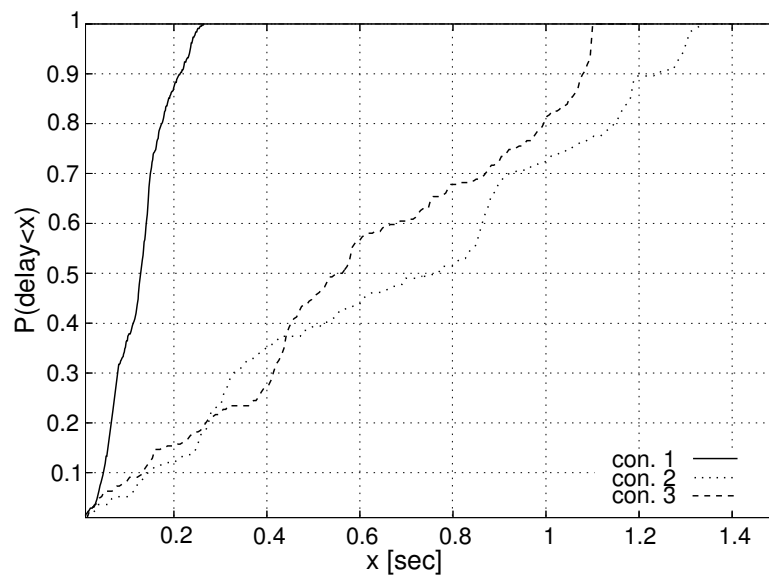


Figure 10.18: CDF of end-to-end delay per multihop connection for 1.25 Mbit/sec offered load per connection. The applied PHY mode is QPSK 1/2 for both, control and data frames.

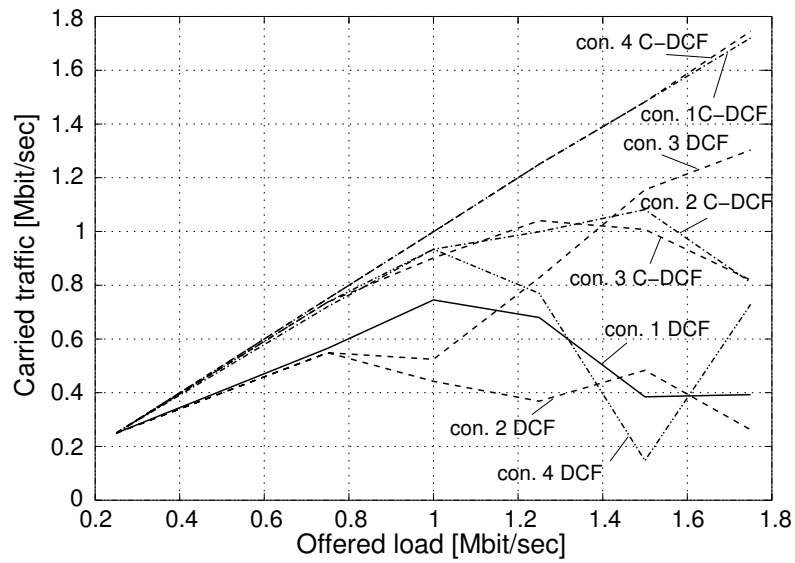


Figure 10.19: Carried end-to-end per multihop connection for DCF and C-DCF. The applied PHY mode is QPSK 1/2 for both, control and data frames.

chapter for the realization of relays, such as the NAV timer per MS and cch, can be adopted from other wireless systems with multi-channel structure, which don't necessarily use MC-CDMA.

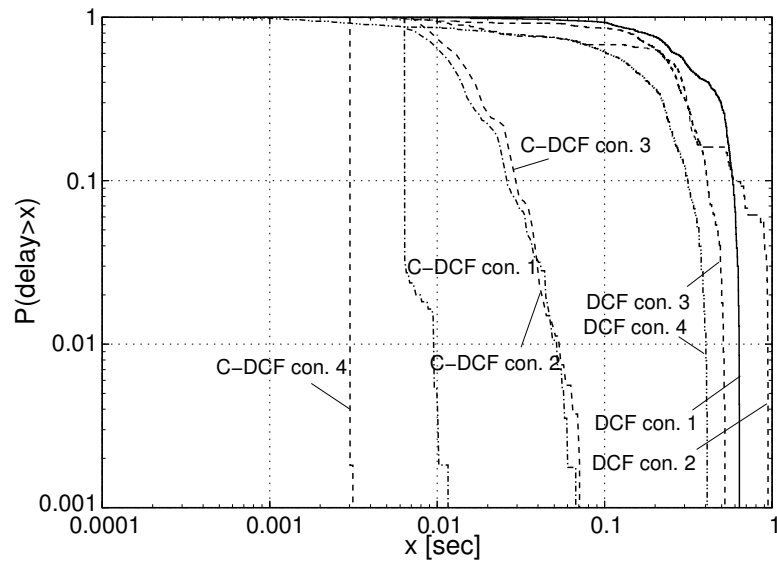


Figure 10.20: Complementary CDF of end-to-end delay per multihop connection for DCF and C-DCF. The offered load is CBR, 0.75 Mbit/sec/con and the applied PHY mode is QPSK 1/2 for both, control and data frames.

Centralized Mode of the C-DCF

Content

| | |
|---------------------------------------|-----|
| 11.1 The Contention Free Period | 171 |
| 11.2 Capacity Anylysis | 174 |
| 11.3 Performance Evaluation | 178 |
| 11.4 Conclusion | 183 |

In many cases, W-LANs are interconnected over an Ethernet backbone network, that is connected to the Internet. For that purpose, at least one MS in each W-LAN network, the so called AP, must participate in both, the wireless and wired communication system. APs typically carry a large fraction of networks traffic, and can therefore be prioritized over other MSs, or even control the networks resources. In the latter case, a centralized network is operated.

Besides the drawbacks of higher cost, and the need to plan a deployment, centralized networks outperform decentralized ones. Since every MSs has to apply for resource grant at the AP, the AP has an overview of the network load situation and can consequently schedule the available resources according to the needs of MSs. Moreover, it can avoid collisions, and near-far-problems by proper scheduling of transmissions or even schedule parallel transmission on the same or different cchs and at the same time for different connections, if the network topology (interference situation) allows this. Furthermore, in centralized networks overhead is reduced, as network coordination is done by the AP.

In this chapter, an extension of the C-DCF is introduced for the operation in centralized mode.

11.1 The Contention Free Period

The decentrally controlled MAC protocol is periodic in operation based in periodic beacon transmissions. The interval starting with the transmission

of a beacon has a duration equal to TBTT. It is called a superframe and comprises the basic element of the centrally controlled mode. In the presence of an AP, the network operation within a superframe is divided in two phases: CP and CFP. During CP, network is under decentral control operation following the rules of C-DCF as described in Chapter 5- during CFP the AP has central control over the network. Division of available resources is done in both, time and code domains, according to the information contained in the beacon that is broadcasted by the AP to all cchs. An example is given in Fig. 11.1, where a CP is operated in cch 3 and cch 4 for 60% of the superframe duration and cch 1 and cch 2 are operated 100% in CFP.

In centralized mode the AP transmits the first beacon immediately after its initialization, and signals the network's operation characteristics. Besides the information contained in the IEEE 802.11a beacon, the AP specifies for each cch the duration of the CFP that follows immediately after the beacon (Fig. 11.2), similar to IEEE 802.11e [802.11E /D9 (2004)]. Such a cch-specific allocation of CFP and CP durations adds flexibility compared to an allocation in the network. MSs, initiating a new connection may use the

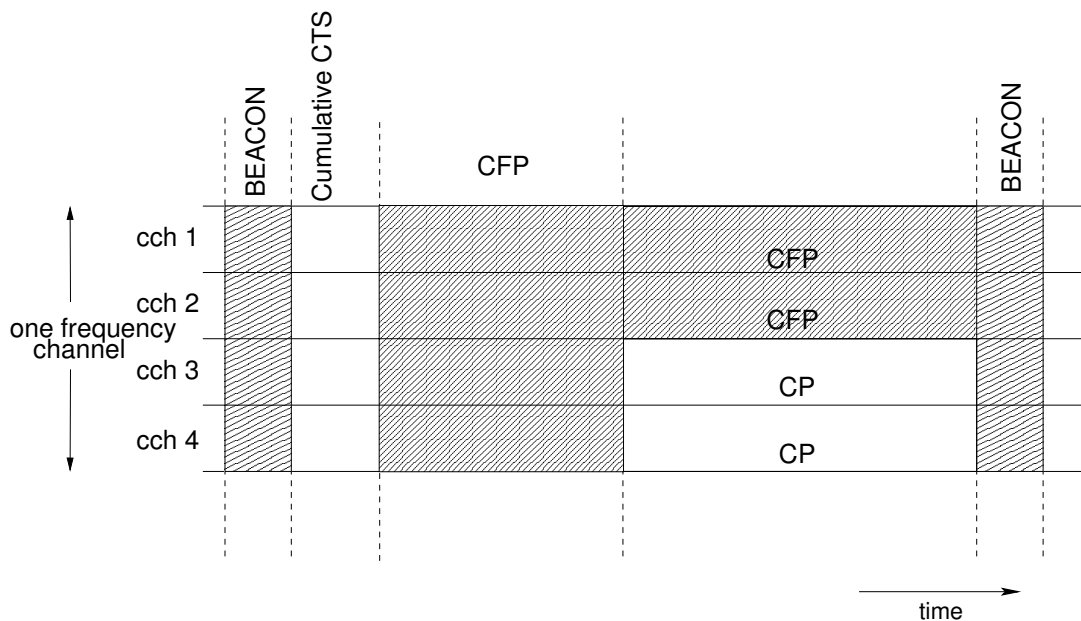


Figure 11.1: Centralized mode functionality of the protocol.

CP for their first transmission, thus reducing delay until they are granted resources for CFP in response to their request. MSs with low load, or serving best effort traffic may operate in CP continuously. The total duration of CFP per cch depends on the network traffic and can be adjusted by the AP in every superframe.

MSs may request resources for transmission during CFP, by sending a *Ready To Send application* (RTSapp) frame (Fig. 11.3) to the AP during CP according to the C-DCF access rules. RTSapp contains either the amount of data to be transmitted or a request for transmission according to a traffic class. A traffic class specifies a transmission rate [HEIER (2003)] or maximum tolerable delay [802.11E /D9 (2004)], which guide the AP to appropriately schedule transmissions for this MS.

A beacon transmission is followed, after a guard interval of one slot, by the transmission of the *Clear To Send cumulative* (CTS_{cum}) frame (Fig. 11.4). Like the beacon, CTS_{cum} is transmitted in parallel via all cchs, and contains information for the forthcoming transmissions during CFP in each cch, the so called access grants. An access grant contains the addresses of the transmitters in the order of transmission within a superframe and may be different for every cch. Alternatively, the access grant may contain connection identifiers. An extra byte in CTS_{cum} signals the periodic repetition of the cch allocation within a superframe, valid until the end of the superframe and the period duration, in order to reduce overhead.

To further reduce overhead, address compression may be applied in cen-

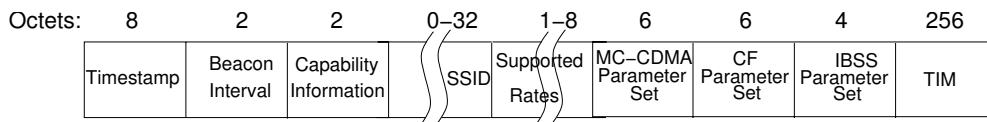


Figure 11.2: Beacon for centralized mode.

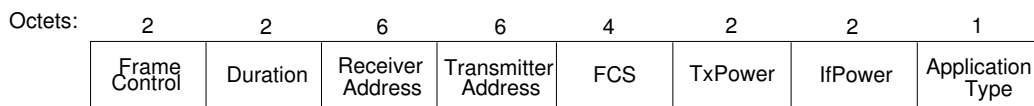


Figure 11.3: RTSapp for centralized mode.

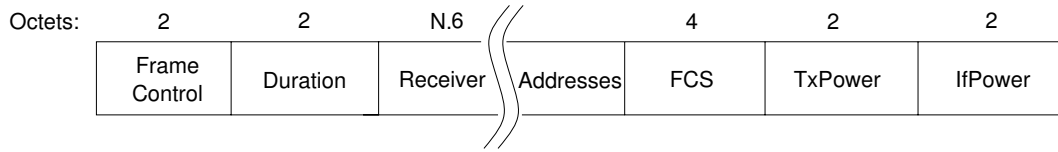


Figure 11.4: CTScum for centralized mode.

tralized mode. MSs, upon association with the AP, get a unique one byte long address that is used as an identifier. One byte is enough to support 255 MSs in a network controlled by one AP. Together with the network identifier, it provides a unique address to each MS. The number of MAC addresses can be reduced to three (from 4 in the standard [802.11 (1999)]), namely the source, destination and subnetwork address, as long as no multihop function is permitted.

The CTScum frame finalizes the broadcast transmission phase and CFP follows, Fig. 11.5. According to the access grants, MSs start direct link transmissions in the assigned cchs in the order specified by the CTScum frame. The correct reception of a data frame is acknowledged with an ACK frame, transmitted after time SIFS. An ACK might be followed by SIFS, if fragmentation is permitted before the next data frame follows, in order to allow consecutive transmissions of data frames from the same MS.

As shown in Fig. 11.5, CFP ends after 40% of superframe duration in cchs 2 and 4. CP operation follows. According to the TBTT announced in the last beacon frame, the AP sends the beacon, after having sensed the channel for free for a duration PIFS. In order to avoid collisions with beacon, resource grants for CFP consider the TBTT, and MSs operating in CP, which received the previous beacon, must end all transmissions when TBTT approaches [KUMAR (2005)]. Channel monitoring for duration PIFS, by the AP, prior to beacon retransmission is still necessary, to ensure collision avoidance between the beacon and transmissions in CP from MSs with large clock drifts.

11.2 Capacity Analysis and Comparison with IEEE 802.11e

The maximum achievable throughput during CFP in C-DCF and IEEE 802.11e is calculated in the following.

Within a superframe that does not contain any CP, the following frames

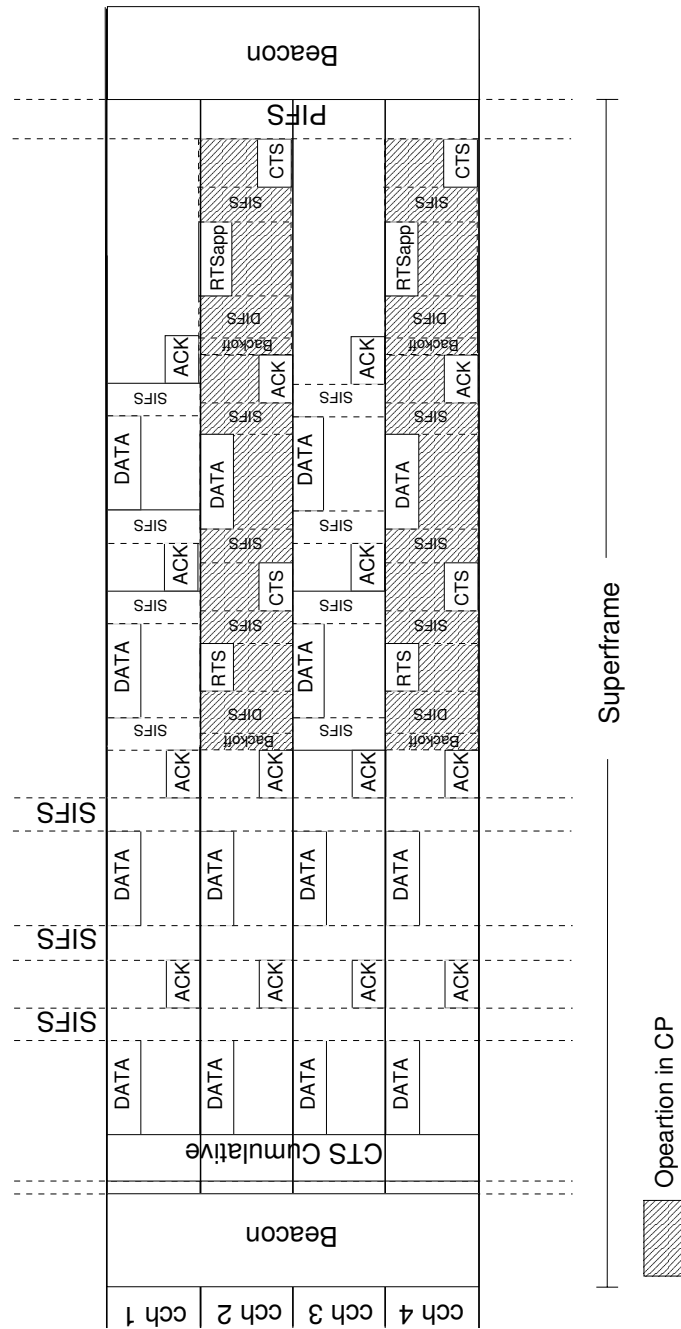


Figure 11.5: Data transmission in CP and CFP.

are transmitted per cch:

$$\begin{aligned} \text{Super frame} = & \text{Beacon} + \text{aSlotTime} + \text{CTScum} + N_p(\text{SIFS} + \\ & \text{DATA} + \text{SIFS} + \text{ACK}) + \text{PIFS} \end{aligned} \quad (11.1)$$

where N_p denotes the number of data frames transmitted in one superframe per cch and data frames are assumed completely filled with user data. The duration of a superframe can be then calculated, according to the parameters in Table 11.1, taken from the standard [802.11 (1999)].

Table 11.1: CFP parameters.

| Parameter | Value |
|-----------|-------------------|
| aSlotTime | $9\mu\text{sec}$ |
| SIFS | $16\mu\text{sec}$ |
| PIFS | $25\mu\text{sec}$ |

The MAC frames for data and ACK are specified in the standard, [802.11 (1999)], whilst the extended beacon and CTScum frame are described in Section 11.1. Mapping of MAC frames to PHY layer frames, follows the same rules as specified for CP (Section 2.2.2). For the present analysis the worst case is considered where subsequent data frames originate from different transmitters, thus a synchronization preamble in front of each frame is necessary. Assuming that all control frames are transmitted with QPSK 1/2 and data frames with the 64QAM 3/4 PHY modes, the superframe duration is:

$$\Delta T_{SF} = 338 + 4 \left\lceil \frac{94 + 8N_p}{48} \right\rceil + 776N_p [\mu\text{sec}] \quad (11.2)$$

In case of [802.11E /D9 (2004)], where subsequent data frames are completely filled with user data and originate from different transmitters (as for C-DCF), the following frame transmissions take place within a superframe completely occupied by Controlled Access Phase (CAP)s from Hybrid Coordinator (HC):

$$\begin{aligned} \text{Super frame.11e} = & \text{Beacon} + N_{p11e}(\text{PIFS} + \text{QoS} - \text{CF} - \text{Poll} + \\ & \text{SIFS} + \text{DATA} + \text{SIFS} + \text{ACK}) + \text{PIFS} \end{aligned} \quad (11.3)$$

where N_{p11e} denotes the number of CAPs in the superframe.

In Eq.(11.3) the assumption has been made that transmission requests are already known to HC and enough to cover the whole superframe duration. The duration of PIFS, and the frame structure of Beacon and *Quality of Service-Contention Free-Poll* (QoS-CF-Poll) are described in [802.11E/D9 (2004)]. Consequently the duration of the IEEE 802.11e superframe can be calculated, when 1024 Byte long data packets are considered and the applied PHY mode is QPSK 1/2 for control and 64QAM 3/4 for data frames:

$$\Delta T_{SF11e} = 285 + N_{p11e}313[\mu sec] \quad (11.4)$$

For different values of ΔT_{SF} , N_p , ΔT_{SF11e} and N_{p11e} the achievable throughput for both, C-DCF centralized mode and IEEE 802.11e, according to Eqs. (11.2) and (11.4) respectively, is presented in Table 11.2.

Table 11.2: CFP Throughput vs. superframe length for 1024 byte long data packets.

| Superframe length | C-DCF Max. theoretical Throughput on 4 cchs | IEEE 802.11e |
|-------------------|---|----------------|
| 20msec | 40.96 Mbit/sec | 25.39 Mbit/sec |
| 40msec | 40.96 Mbit/sec | 25.80 Mbit/sec |
| 100msec | 41.61 Mbit/sec | 26.05 Mbit/sec |

The results in Table 11.2 show the high efficiency achieved by C-DCF centralized mode, which is up to 60% higher than the efficiency of IEEE 802.11e.

Equation (11.2) is valid only when operating the whole superframe in CFP. The throughput for the centralized mode, a mixed operation of CFP and CP which gives more flexibility to the network, depends on both, the superframe duration and the percentage duration of CP and CFP. The maximum throughput for the decentralized protocol has been calculated in Section 5.5, Eq. (5.16) to 31.58 Mbit /sec for 1KByte long data frames without considering beacon transmissions. With periodic beacon transmissions every 100msec (superframe duration), the maximum throughput during CP

reduces to 31.46 Mbit/sec. Consequently, for the example given in Fig. 11.5, with 60% CP on two out of four cchs, 100msec superframe duration and 1024 byte long data packets, the total maximum throughput is 38.6 Mbit/sec.

11.3 Performance Evaluation

In this section, performance evaluation results of the proposed centralized mode are presented. For this purpose, the scenario of Fig. 11.6 was simulated. It comprises one AP and 16 MSs around it, operating 8 direct link connections named con. 1 to con. 8. Simulation parameters used are given in Table 7.1, and CP operation covers 60% of the 100msec superframe duration in cch 2, and cch 4, as depicted in Fig. 11.5. Control frames are transmitted with QPSK 1/2, data frames with the 64QAM 3/4 PHY mode. Poisson traffic load generators are applied at each MS.

The focus of the analysis is on MSs that either are transmitting in CFP only, and on MSs with mixed transmissions in CFP and CP. For transmissions during CP only, network characteristics are the same under C-DCF as analyzed in Chapter 7. In the following analysis, two sets of MSs are distinguished:

- In set A: MSs are of same priority and transmit during both, CFP and CP.
- In set B: Prioritized MSs transmit exclusively in CFP, whilst other MSs transmit in both phases, CFP and CP. Prioritized MSs are: MS 10, MS 12, MS 14 and MS 16, the respective connections are con. 4, con. 5, con. 6 and con. 7.

Figure 11.7 presents the carried system traffic versus the offered load. The three graphs correspond to throughput of MSs transmitting only in CP, the throughput of MSs transmitting exclusively in CFP and the total system throughput, which raises linearly with the offered load until 28 Mbit/sec, where saturation is reached for CP. Maximum values for throughput are reached in overload, due to Poisson traffic sources, and for CFP comply with the analytical results. The maximum throughput during CP, is 32.5 Mbit/sec and 3.3% higher than the analytically calculated upper bound of 31.46 Mbit/sec (see Section 11.2), which owes to channel re-use of the same cch in this scenario.

The carried traffic for each connection is presented in Fig. 11.8. Like the

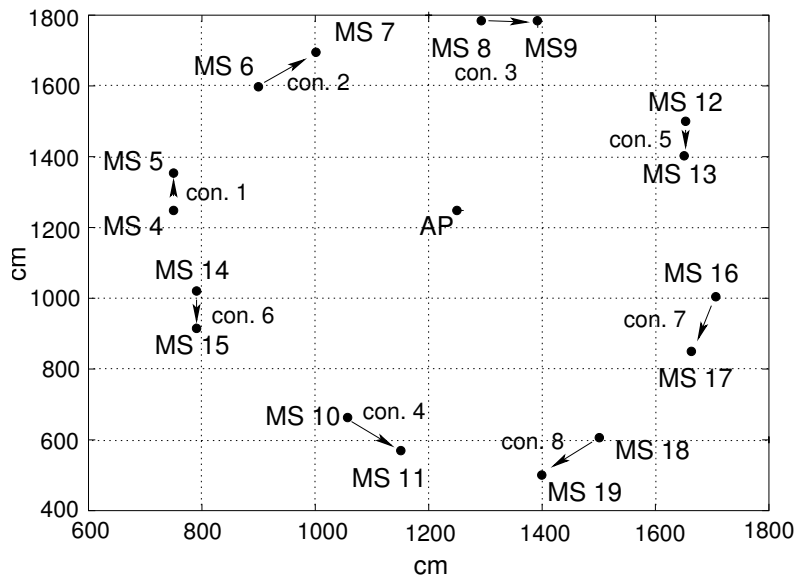


Figure 11.6: Simulated scenario with AP controlling channel access.

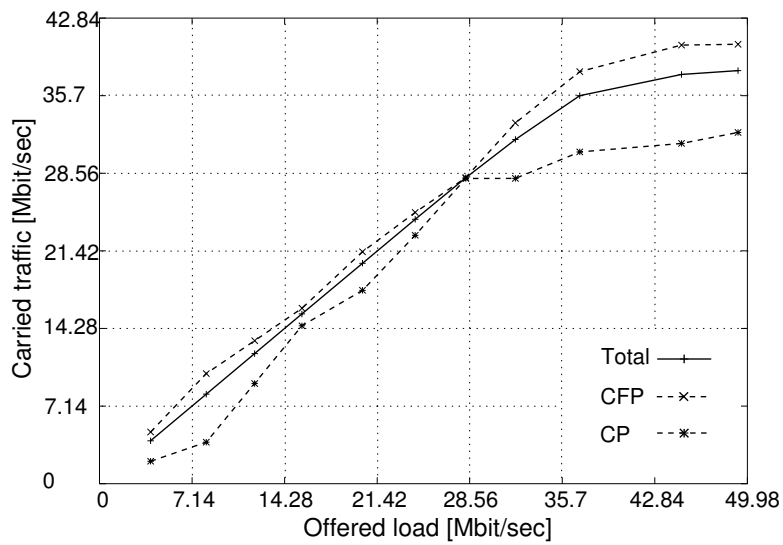


Figure 11.7: Carried traffic in the network for the two operating modes and total carried traffic. The applied PHY mode is 64QAM 3/4 for data frames and QPSK 1/2 for control frames.

total carried traffic, carried traffic of each connection shows a linear raise with offered load up to saturation load, which is different for the two sets. The throughput per connection is the same for all connections in set A, as they share operation in CFP and in CP. For set B, connections operating only in CFP, achieve the highest throughput (more than 5 Mbit/sec), which is on average almost 14% more, than the throughput of connections in mixed operation.

An analogous behavior is observed for mean delays. Figure 11.9 presents the mean queueing delay of data packets per connection over the offered load. Queueing delay is for both sets lower than 10msec for load up to 4 Mbit/sec/transmitter, which corresponds to a network load of 32 Mbit/sec. For higher loads, saturation begins and queueing delay increases rapidly, exceeding 100msec in overload. The break point in the queueing delay curves, i.e. the point where a steep raise of queueing delay starts, depends on the applied set and operating mode. It corresponds to the amount of offered load that brings the network to saturation, according to Fig. 11.8. The best queueing delay performance is observed for MSs operating in CFP only, while the queueing delay for mixed operation in set A is equal for all MSs since no priorities are considered.

Figure 11.10 shows the mean service time per connection, as a function of

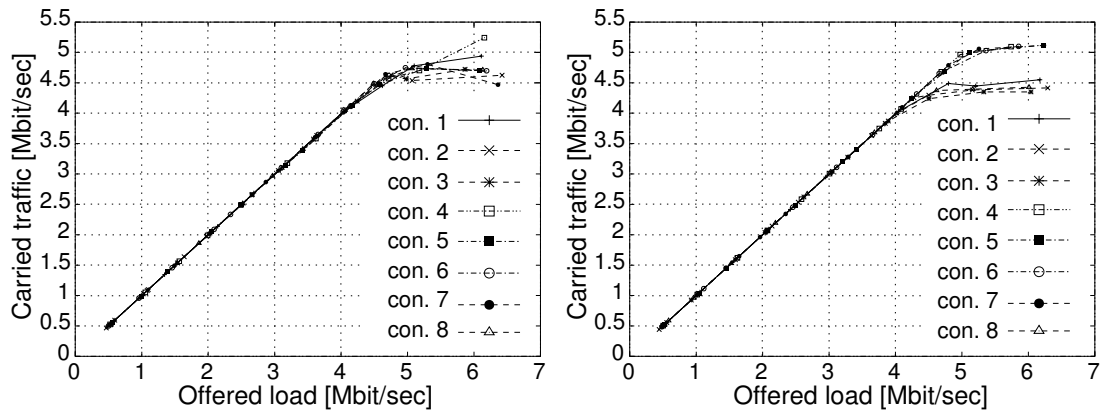


Figure 11.8: Carried traffic per connection over offered load for the centralized mode. Left for set A, right for set B. The applied PHY mode is 64QAM 3/4 for data frames and QPSK 1/2 for control frames.

offered load. It must be noted that for CFP, service time measurement starts with the transmission of data packet and ends with the reception of the corresponding ACK. For set B, the mean service time comprises 0.76msec for CFP transmissions and 0.9msec for the mixed case. The absence of collisions contributes to a constant service time independent of offered load. For set A a jitter of $60\mu\text{sec}$ is observed owing to the random duration of backoff timer and the ratio of frames transmitted in CP to those transmitted in CFP. In set A, all MSs experience approximately the same mean service time, as all of them transmit in a mixed mode.

Figure 11.11 presents the CDF of queueing delay for 2.8 Mbit/sec offered load per connection for set B. MSs face different network performance, depending on their priority. With probability 90% the queueing delay is limited to less than 11.5msec for all MSs underlying the QoS support ability of the centralized mode. Maximum values of queueing delay average to 18msec for CFP transmissions and 25msec for MSs in mixed operation (for con. 1, con. 2, con. 3, con. 8).

The influence of different percentages of CP duration in the superframe on queueing delay of MS 6, is presented in Fig. 11.12. The mean offered Poisson load in this case is 2.8 Mbit/sec, and MS 6 transmits both, during CP and CFP. The best queueing delay distribution is achieved without CP operation (CP 0%), where a maximum queueing delay of 11msec is mea-

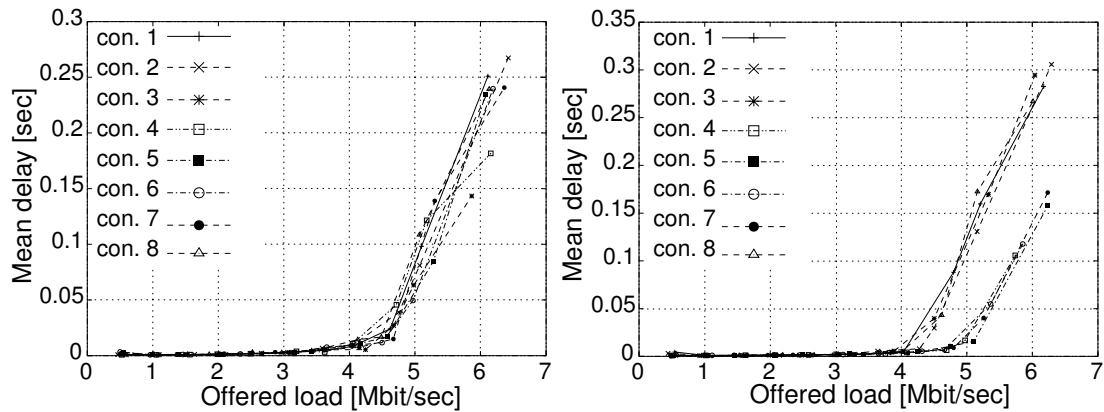


Figure 11.9: Mean queueing delay over the offered load for the centralized mode. Left for set A, right for set B. The applied PHY mode is 64QAM 3/4 for data frames and QPSK 1/2 for control frames.

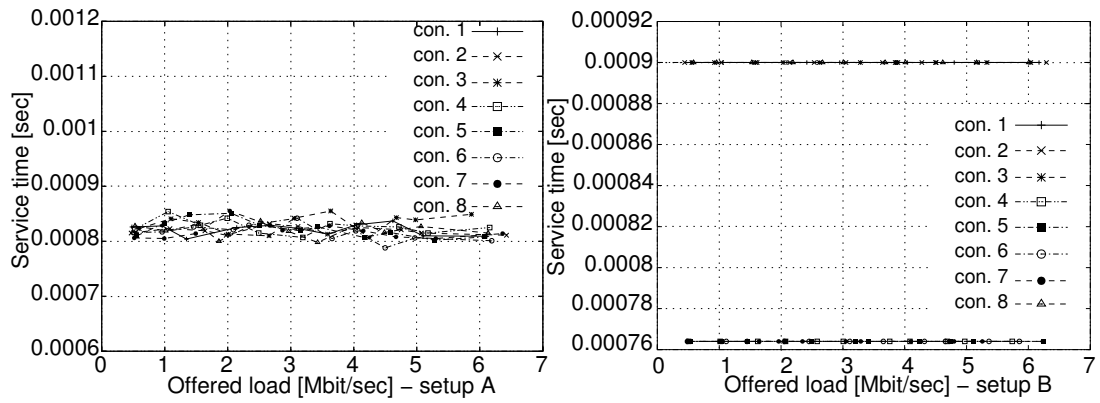


Figure 11.10: Mean service time over the offered load for the centralized mode. Left for set A, right for set B. The applied PHY mode is 64QAM 3/4 for data frames and QPSK 1/2 for control frames.

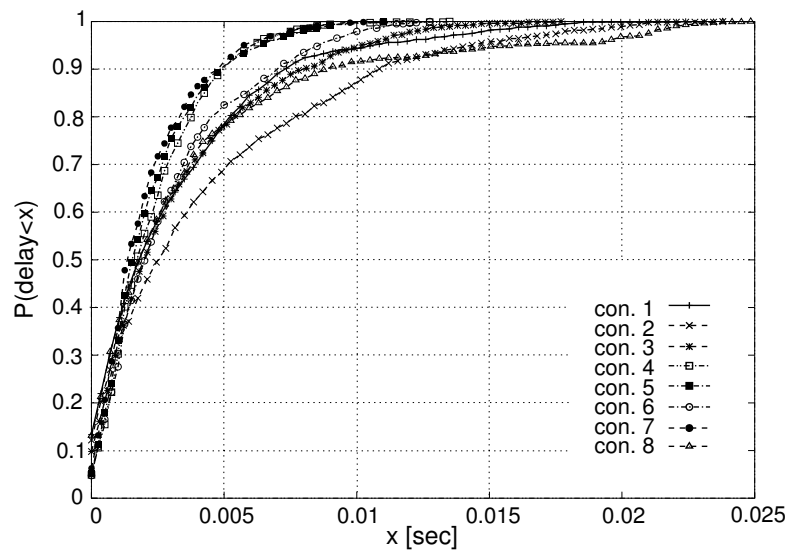


Figure 11.11: CDF of queuing delay per MS with 2.8 Mbit/sec/MS Poisson distributed offered load. The applied PHY mode is 64QAM 3/4 for data frames and QPSK 1/2 for control frames.

sured. With larger CP percentage duration the queueing delay increases, and reaches its maximum for 100% CP operation. In this case the maximum queueing delay is 28msec.

11.4 Conclusion

A centralized operating mode for the C-DCF is presented. Extensive simulation results show its performance and ability to support QoS. Channel bandwidth division in 4 parallel cchs enables operation of CFP and CP in parallel on the same radio channel, which is an important option for supporting different communication needs in a network, e.g. multihop. In future systems with variable SF, a fraction of the available cchs could be reserved for signaling and transmissions using CP. Such a channel is advantageous for the following reasons:

- Since any MS can use the signalling cchs for sending an access request for CFP at any time, access delay reduces.

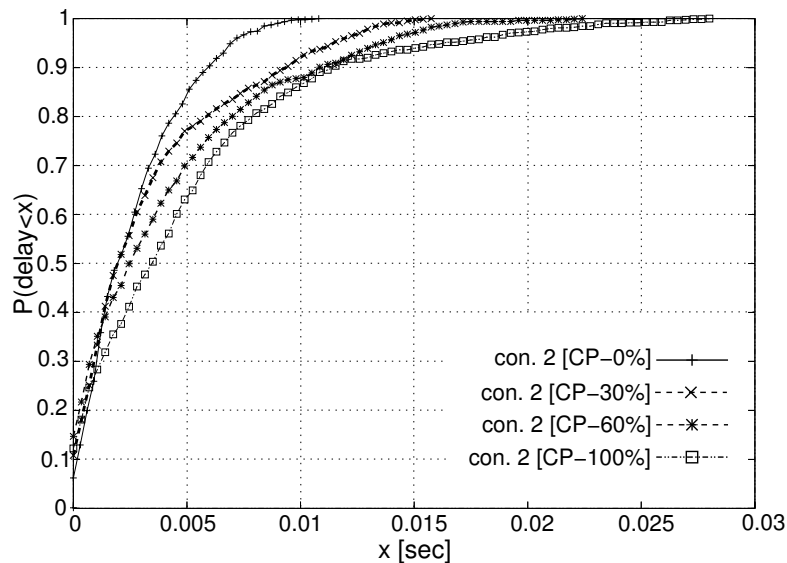


Figure 11.12: CDF of queueing delay at MS 6, in different proportions of mixed operation. The applied PHY mode is 64QAM 3/4 for data frames and QPSK 1/2 for control frames.

- Unpredictable beacon delays and collisions from the operation of CP and CFP on the same channel as mentioned in [Ni et al. (2004)] can be avoided, since separation between CP and CFP takes place in code domain, rather than the TDM method of IEEE 802.11a/e.
- MSs with high QoS requirements may transmit exclusively in CFP, where transmission delays can be guaranteed.

Conclusion

In this thesis, new protocols for next generation indoor W-LANs based on MC-CDMA are proposed and their performance evaluated, by means of stochastic event driven simulation. The introduced protocols aim at achieving high MAC protocol efficiency and support of QoS. For this purpose, solutions to technical problems for the realization of MC-CDMA based protocols are provided and adaptation rules are designed to allow good operation of the wireless system under the conditions of real operation scenarios.

After an overview of different CDMA techniques, the functionality of MC-CDMA is discussed and compared with that of MC DS-SS as well as with the functionality of OFDM. MC-CDMA combines the robustness of OFDM, with the diversity of frequency spreading at a reasonably low complexity. Consequently, the performance of MC-CDMA is studied with respect to an asynchronous transmission system. Assuming the use of MMSE MUD at the receivers and the application of the $K=7$ convolutional encoder/decoder, link level results are generated that serve for the evaluation of both, the new transmission technique, and the link quality as a basis for protocol performance simulation studies. To evaluate the link quality the air interface for SINR calculation is carefully modelled, taking into account the emissions per cch and the relative delays of asynchronous transmissions of concurrent MSs transmitting in parallel. This is necessary in order to model accurately MAI on MC-CDMA based systems.

The main focus of this thesis is on the MAC sublayer. The MAC protocol proposed, for the support of MC-CDMA, is a modification of the IEEE 802.11a MAC, namely C-DCF. The achievable throughput has been analytically calculated, and direct comparison shows its superiority to an OFDM based system, owing mainly to the longer duration of spread data frames compared to protocol guard intervals and control frames duration. It must be noted that protocol guard intervals are a limiting factor for throughput when broader channels are considered. This makes the use of MC-CDMA inevitable for the emerging wireless systems aiming at a net throughput of

1Gbit/sec and more.

The proposed TPC algorithm based on an improved handshake contributes much to a good network performance, since it fast adapts to the environment conditions. TPC is an important feature for CDMA networks, because their capacity is limited by interference, namely by the receivers ability to decode the intended signal from the received one. Therefore, TPC is assumed based on an interference estimate of the receiver, established with the help of MUD. Transmission power fluctuations due to short term fading and small fluctuations of MAI can be controlled by:

1. Power adjustment not only based on the last interference estimate, but taking earlier estimates into account, too.
2. Power adjustment 2-3dB higher than necessary to achieve the required SINR value.

Especially for wireless decentrally controlled networks, where an optimum power adjustment for all transmitting MSs is not always possible, it has been demonstrated that TPC should be combined with adaptation rules, that avoid link failure due to high MAI. For this purpose, the improved handshake algorithm is proposed in this thesis, based on the two way handshake protocol (RTS/CTS) prior to the data transmission. The key idea is to control connections that interfere too much with each other, when operating at the same time in the same cch, so that they time-share the cch.

Performance parameters used to evaluate the proposed protocols and algorithms are the achieved throughput as well as the data packet queueing delay and transmission time per active connection. Since MAI may prevent the proper reception of data at a MS, it is essential to observe the performance of each receiver separately. This allows also a finer granularity of the conclusions concerning the effectiveness of the proposed protocol algorithms.

In order to increase the network capacity, the frequency adaptation method is proposed as supplement to the C-DCF protocol. According to this method, long distance connections, that suffer from high MAI due to concurrent transmissions of other MSs, are diverted to operate in other frequency channels. Simulation results confirm the effectiveness of this method.

The C-DCF protocol is further improved by introducing new backoff algorithms, comprising Parallel and Smart Backoff, that optimize the protocol for the support of a multi-channel cch structure. These algorithms

allow each transmitter to reselect the cch used for transmission of the next data frame, thus leading to an opportunistic cch usage. Furthermore, parallel transmission in more than one cch becomes possible. Two benefits of these backoff algorithms are the support of prioritized access to MSs (that consequently achieve lower delays), and load balancing among the different cchs.

A cross layer optimization is also proposed. Based on the performance of the MUD, that is very dependable on the relative delays of concurrent transmissions in different cchs, a new parameter set for the MAC protocol is applied, that allows the asynchronous system to operate in an isochronous mode. Performance improves substantially by using this simple arrangement.

Multihop connections are essential for W-LANs, used not only for coverage extension, but also as a method to reduce interference. The protocol has been extended for that with the needed functionality, and technical solutions for the realization of relays have been proposed in this thesis.

The centralized operation mode, is another feature of the proposed protocol, that can be operated based on an AP. The AP can control the traffic and schedule the network resources among the transmitting MSs according to their traffic needs. Accordingly, high QoS characteristics are achieved from the centrally controlled network.

The protocols and algorithms presented in this thesis have the potential to further be improved in future work. Examples for these are the use of carrier interferometry codes to enhance the capacity, and the use of higher spreading factors in broader channels, that lower the contention on medium access further and improve the ratio of data packet transmission duration to protocol overhead, with positive impact on efficiency.

Derivation of a Closed Form Expression for the Demodulator Outputs

In an synchronous system, assuming $\tau_1 = 0 \leq \tau_2 \leq \tau_3 \leq \tau_4$, the demodulator outputs y_n , for the i -th symbol ($b_1(i)$) of the considered user 1, are subject to MAI from two successive symbols of other active users (Fig. A.1).

The demodulator output at the n -th branch corresponding to the n -th subcarrier (Eq. (4.4)) can be expressed as [YI et al. (2003)]:

$$y_n = \sum_{k=1}^K \sqrt{a_k} [p_{nk} b_k(i) + p'_{nk} b_k(i-1)] + z_n \quad (\text{A.1})$$

with:

$$p_{nk} = \frac{1}{T} \sum_{m=1}^{M_s} c_{km} h_{km} e^{-j2\pi n \tau_k / T} \int_{\tau_k}^T e^{j2\pi(m-n)t/T} dt \quad (\text{A.2})$$

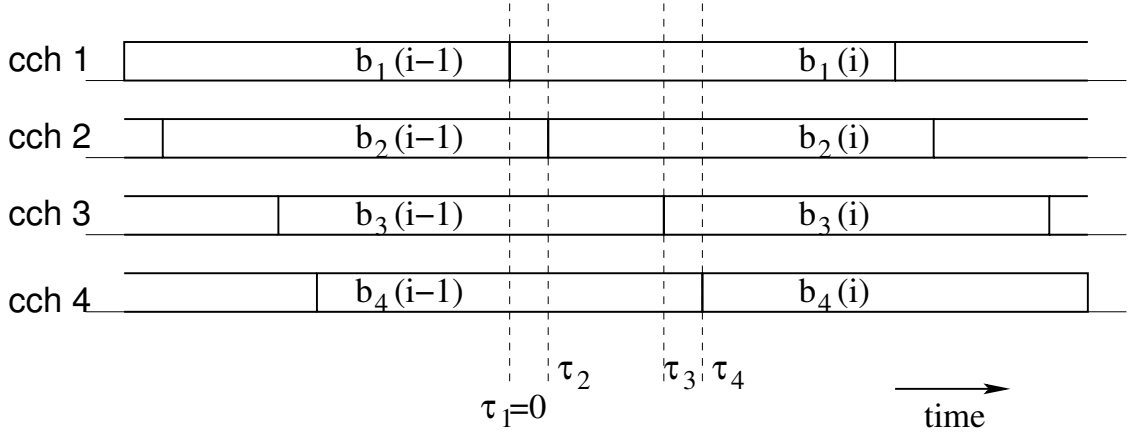


Figure A.1: Relative delays of different users' symbols.

$$p'_{nk} = \frac{1}{T} \sum_{m=1}^{M_s} c_{km} h_{km} e^{-j2\pi n \tau_k / T} \int_0^{\tau_k} e^{j2\pi(m-n)t/T} dt \quad (\text{A.3})$$

$$z_n = \frac{1}{T} \int_0^T \eta(t) e^{-2\pi n t / T} dt \quad (\text{A.4})$$

Since Eq. (A.2) and Eq. (A.3) differ only in the integration limits, one form for the general case can be developed, with lower limit a , and higher limit b :

$$p_{nk} = \begin{cases} \sum_{m=1}^{M_s} \frac{c_{km} \beta_{km}}{\pi(m-n)} \sin \left[\frac{\pi(m-n)(b-a)}{T} \right] (\cos A - j \sin A) & m \neq n, \\ \sum_{m=1}^{M_s} \frac{c_{km} \beta_{km} (b-a)}{T} (\cos B - j \sin B) & m = n \end{cases} \quad (\text{A.5})$$

with:

$$A = \left[\left(\frac{2\pi n \tau_k}{T} \right) - \phi_{km} - \frac{\pi(m-n)(b+a)}{T} \right] \quad (\text{A.6})$$

$$B = \left[\left(\frac{2\pi n \tau_k}{T} \right) - \phi_{km} \right] \quad (\text{A.7})$$

In [YI et al. (2003)] Eq. (A.1) is expanded to a linear set of equations for all demodulator outputs, which in matrix notation is:

$$\mathbf{y} = \mathbf{P} \mathbf{A} \mathbf{b} + \mathbf{z} \quad (\text{A.8})$$

where:

$$\begin{aligned} \mathbf{y} &= [y_1, \dots, y_k]^T \\ \mathbf{A} &= \text{diag}[\sqrt{a_1}, \dots, \sqrt{a_k}, \sqrt{a_1}, \dots, \sqrt{a_k}] \\ \mathbf{b} &= [b_1(i-1), \dots, b_k(i-1), b_1(i), \dots, b_k(i)] \\ \mathbf{P} &= [p'_{nk}, p_{nk}] \\ \mathbf{z} &= [z_1, \dots, z_n] \end{aligned} \quad (\text{A.9})$$

From the above equations, an expression for the SINR at the receiver is derived in [YI et al. (2003)], which is used in the analysis of the MC-CDMA PHY layer performance in Chapter 4.

LIST OF FIGURES

| | | |
|------|--|----|
| 1.1 | Overview of the C-DCF functions for codechannel selection. | 3 |
| 2.1 | ISO/OSI equivalent of IEEE 802.11. | 8 |
| 2.2 | Distributed Coordination Function. | 11 |
| 2.3 | Setting NAV according to RTS/CTS control frames. | 12 |
| 2.4 | Hidden and exposed station problem in IEEE 802.11a. | 13 |
| 2.5 | Point Coordination Function. | 15 |
| 2.6 | Beacon frame format. | 16 |
| 2.7 | RTS frame format. | 16 |
| 2.8 | CTS frame format. | 17 |
| 2.9 | Data frame format. | 17 |
| 2.10 | Frequency representation of orthogonal, unmodulated OFDM subcarriers. | 18 |
| 2.11 | PHY frame format. | 20 |
| 3.1 | Multiplex schemes. | 22 |
| 3.2 | Direct Sequence-Code Division Multiple Access. | 24 |
| 3.3 | Multi-Carrier Code Division Multiple Access. | 25 |
| 3.4 | Multi-Carrier DS-CDMA. | 26 |
| 3.5 | MC-CDMA transmitter. | 27 |
| 3.6 | MC-CDMA receiver. | 29 |
| 4.1 | MUD performance with 4 active users and $SF = 4$ | 38 |
| 4.2 | SINR at the detector vs. relative delay of interferer to trans- mitter and spreading factor 4. | 40 |
| 4.3 | Theoretical PER for a 1514 byte long packet. The solid lines refer to a multi-carrier system with $a_{CP} = 80\%$. Dashed lines refer to a single carrier system without cyclic prefix. | 41 |
| 4.4 | PER vs. E_{av}/N_0 for different packet sizes. | 42 |
| 5.1 | CSMA/CA on four cchs. | 48 |
| 5.2 | Extended RTS frame format. | 51 |

| | | |
|------|---|----|
| 5.3 | Extended CTS frame format. | 51 |
| 5.4 | The TPC method. | 53 |
| 5.5 | Selection of another cch, after collision, increases the possibility of successful retransmission. | 56 |
| 5.6 | Practical application scenario of the improved handshake. . . | 57 |
| 5.7 | Improved handshake algorithm. The SDL diagram shows the case for a missing CTS, but applies equally to a missing ACK. | 58 |
| 5.8 | The frequency adaptation algorithm. | 62 |
| 5.9 | A transmission window. | 64 |
| 5.10 | MAC protocol efficiency comparison for different PHY modes. The MAC protocol efficiency is defined as the percentage of net MAC throughput to the channel capacity at the PHY mode used for data frame transmission | 67 |
| 5.11 | MAC protocol efficiency comparison for different data packet sizes. | 68 |
| 5.12 | MAC protocol efficiency comparison for different data packet sizes and PHY modes. | 70 |
| 6.1 | The MACNET2 simulation tool. | 72 |
| 6.2 | Event driven channel model for interference calculation. . . . | 75 |
| 6.3 | Mean interference calculation. | 76 |
| 6.4 | Simulated and analytically calculated throughput. | 77 |
| 7.1 | Elementary simulation scenario. | 81 |
| 7.2 | Achievable system throughput and throughput per cch for 512 byte long data packets, applying the QPSK 1/2 PHY mode for both control and data frames. | 82 |
| 7.3 | Achievable system throughput and throughput per cch for 1024 byte long data packets, applying the QPSK 1/2 PHY mode for both control and data frames. | 83 |
| 7.4 | Mean queueing delay over all transmitted data packets for 512 and 1024 byte long data packets, applying the QPSK 1/2 PHY mode for both control and data frames. | 84 |
| 7.5 | Mean queueing delay per connection for 512 and 1024 byte long data packets, applying the QPSK 1/2 PHY mode for both control and data frames. | 85 |

| | | |
|------|--|----|
| 7.6 | Mean service time over all transmitted data packets for 512 and 1024 byte long packets, applying the QPSK 1/2 PHY mode for both control and data frames. | 86 |
| 7.7 | CDF of data packet queueing delay in the network at different load. The applied PHY-mode is QPSK 1/2 for both control and data frames. | 87 |
| 7.8 | CDF of data packet queueing delay at MS 8 with two MPEG streams. The applied PHY-mode is QPSK 1/2 for both control and data frames. | 88 |
| 7.9 | CDF of data packet queueing delay for con. 2 in the wideband channel, built by LRE algorithm. The applied PHY-mode is 16QAM 1/2 for control and 64QAM 3/4 data frames. | 89 |
| 7.10 | Simulated scenario for TPC analysis. | 90 |
| 7.11 | System throughput with and without TPC. The applied PHY-mode is QPSK 1/2 for both control and data frames. | 91 |
| 7.12 | Throughput per cch without TPC. The applied PHY-mode is QPSK 1/2 for both control and data frames. | 92 |
| 7.13 | Throughput per cch with TPC. The applied PHY-mode is QPSK 1/2 for both control and data frames. | 92 |
| 7.14 | Mean queueing delay per transmitting MS without TPC. The applied PHY-mode is QPSK 1/2 for both control and data frames. | 94 |
| 7.15 | Mean queueing delay per transmitting MS with TPC. The applied PHY-mode is QPSK 1/2 for both control and data frames. | 94 |
| 7.16 | Mean service time per transmitting MS without TPC. The applied PHY-mode is QPSK 1/2 for both control and data frames. | 95 |
| 7.17 | Mean service time per transmitting MS with TPC. The applied PHY-mode is QPSK 1/2 for both control and data frames. | 95 |
| 7.18 | CDF of queueing delay with and without TPC. The applied PHY-mode is QPSK 1/2 for both control and data frames. | 96 |
| 7.19 | CDF of queueing delay for different weights in mean interference calculation. The applied PHY-mode is QPSK 1/2 for both control and data frames. | 97 |
| 7.20 | Simulation scenario for the improved handshake evaluation. | 98 |

| | | |
|------|--|-----|
| 7.21 | System throughput with and without adaptation to suitable cch vs. offered system load. The applied PHY mode is 64QAM 3/4 for data frames and QPSK 1/2 for control frames. | 99 |
| 7.22 | Throughput per connection without cch-adaptation vs. offered load per connection. The applied PHY mode is 64QAM 3/4 for data frames and QPSK 1/2 for control frames. | 100 |
| 7.23 | Throughput per connection with cch-adaptation vs. offered load per connection. The applied PHY mode is 64QAM 3/4 for data frames and QPSK 1/2 for control frames. | 101 |
| 7.24 | Mean queueing delay of successfully transmitted data packets per connection vs. offered load per connection, without cch-adaptation. The applied PHY mode is 64QAM 3/4 for data frames and QPSK 1/2 for control frames. | 102 |
| 7.25 | Mean queueing delay of successfully transmitted data packets per connection vs. offered load per connection, with cch-adaptation. The applied PHY mode is 64QAM 3/4 for data frames and QPSK 1/2 for control frames. | 103 |
| 7.26 | Mean service time of successfully transmitted data packets per connection vs. offered load per connection, without cch-adaptation. The applied PHY mode is 64QAM 3/4 for data frames and QPSK 1/2 for control frames. | 104 |
| 7.27 | Mean service time of successfully transmitted data packets per connection vs. offered load per connection, with cch-adaptation. The applied PHY mode is 64QAM 3/4 for data frames and QPSK 1/2 for control frames. | 105 |
| 7.28 | Percentage of data frame collisions per connection, without and with cch-adaptation. The applied PHY mode is 64QAM 3/4 for data frames and QPSK 1/2 for control frames. | 106 |
| 7.29 | The simulated scenario. | 108 |
| 7.30 | System throughput with and without frequency adaptation vs. offered system load. The applied PHY mode is 64QAM 3/4 for data frames and QPSK 1/2 for control frames. | 108 |
| 7.31 | Throughput per connection without frequency adaptation vs. offered load per connection. The applied PHY mode is 64QAM 3/4 for data frames and QPSK 1/2 for control frames. | 109 |
| 7.32 | Throughput per connection with frequency adaptation vs. offered load per connection. The applied PHY mode is 64QAM 3/4 for data frames and QPSK 1/2 for control frames. | 110 |

| | | |
|------|---|-----|
| 7.33 | Throughput per connection without frequency adaptation vs. offered load per connection for PER demand 12% . The applied PHY mode is 64QAM 3/4 for data frames and QPSK 1/2 for control frames. | 111 |
| 7.34 | Mean queueing delay of successfully transmitted data packets per connection vs. offered load per connection without frequency adaptation. The applied PHY mode is 64QAM 3/4 for data frames and QPSK 1/2 for control frames. | 112 |
| 7.35 | Mean queueing delay of successfully transmitted data packets per connection vs. offered load per connection with frequency adaptation. The applied PHY mode is 64QAM 3/4 for data frames and QPSK 1/2 for control frames. | 113 |
| 7.36 | Mean service time of successfully transmitted data packets per connection vs. offered load per connection without frequency adaptation. The applied PHY mode is 64QAM 3/4 for data packets and QPSK 1/2 for control packets. | 114 |
| 7.37 | Mean service time of successfully transmitted data packets per connection vs. offered load per connection with frequency adaptation. The applied PHY mode is 64QAM 3/4 for data packets and QPSK 1/2 for control packets. | 115 |
| 7.38 | Amount of collided data and RTS frames with and without frequency adaptation. The offered load is 8 Mbit/sec/connection. The applied PHY mode is 64QAM 3/4 for data packets and QPSK 1/2 for control packets. | 117 |
| 8.1 | Channel sensing with four cchs. | 122 |
| 8.2 | Parallel Backoff with parallel transmission in two cchs. | 122 |
| 8.3 | Parallel Backoff: The cases of a blocked cch during countdown and of a free cch after a busy medium. | 123 |
| 8.4 | Smart Backoff. | 125 |
| 8.5 | Smart Backoff: The cases of a free cch after a busy medium and of a blocked cch during countdown. | 127 |
| 8.6 | Smart Backoff with parallel transmission. | 128 |
| 8.7 | System throughput comparison for connection based cch Selection, Parallel Backoff and Smart Backoff. The applied PHY-mode is QPSK 1/2 for both control and data frames. | 129 |

| | | |
|------|---|-----|
| 8.8 | Comparison of carried traffic per connection for the three backoff algorithms. Left Parallel Backoff and connection based cch selection, right Smart Backoff and connection based cch selection. The applied PHY-mode is QPSK 1/2 for both control and data frames. | 130 |
| 8.9 | Comparison of mean queueing delay for the three backoff algorithms. The applied PHY-mode is QPSK 1/2 for both control and data frames. | 131 |
| 8.10 | Comparison of mean service time for the three backoff algorithms. The applied PHY-mode is QPSK 1/2 for both control and data frames. | 132 |
| 8.11 | CDF of queueing delay under medium system load (1.5 Mbit/sec load per connection). The applied PHY-mode is QPSK 1/2 for both control and data frames. | 133 |
| 8.12 | CDF of queueing delay under high system load. The applied PHY-mode is QPSK 1/2 for both control and data frames. | 134 |
| 9.1 | The synchronization principle. | 139 |
| 9.2 | The simulated scenario. | 140 |
| 9.3 | The carried traffic per MS, for different operating modes. The applied PHY mode is 64QAM 3/4 for data frames and BPSK 1/2 for control frames. | 142 |
| 9.4 | Achieved MAC protocol efficiency, for different operating modes. The applied PHY mode is 64QAM 3/4 for data frames and BPSK 1/2 for control frames. | 143 |
| 9.5 | Number of RTS collisions per MS, for different operating modes. The applied PHY mode is 64QAM 3/4 for data frames and BPSK 1/2 for control frames. | 144 |
| 9.6 | Percentage of repeated frames (collisions) per MS, for different operating modes. The applied PHY mode is 64QAM 3/4 for data frames and BPSK 1/2 for control frames. | 145 |
| 9.7 | The simulated large area scenario. | 146 |
| 9.8 | The carried traffic per MS, for different operating modes in the large area scenario. The applied PHY mode is QPSK 1/2 for data frames and BPSK 1/2 for control frames. | 147 |

| | | |
|-------|---|-----|
| 9.9 | Percentage of repeated frames (collisions) per MS, for different operating modes in the large area scenario. The applied PHY mode is QPSK 1/2 for data frames and BPSK 1/2 for control frames. | 148 |
| 10.1 | Standard multihop transmission. | 150 |
| 10.2 | The standard NAV problem. | 151 |
| 10.3 | Star scenario. | 153 |
| 10.4 | Functionality of a MS in idle state receiving RTS. | 153 |
| 10.5 | Functionality of a MS when a data frame is received. | 154 |
| 10.6 | Functionality of MS for the transmission of an ACK frame in the multihop protocol. | 155 |
| 10.7 | Functionality of the transmitting MS after the reception of an ACK for a previously transmitted data frame. | 156 |
| 10.8 | The bottleneck scenario. | 157 |
| 10.9 | Throughput sharing in bottleneck scenario (Fig. 10.8). The applied PHY mode is QPSK 1/2 for both, control and data frames. | 158 |
| 10.10 | Mean cumulative queueing delay per connection in bottleneck scenario (Fig. 10.8). The applied PHY mode is QPSK 1/2 for both, control and data frames. | 159 |
| 10.11 | CDF of end-to-end service time per connection in bottleneck scenario (Fig. 10.8). Comparison of connection based cch selection and Smart Backoff for 1.25 Mbit/sec offered load per connection. The applied PHY mode is QPSK 1/2 for both, control and data frames. | 160 |
| 10.12 | The simulated scenario for multihop transmissions. | 161 |
| 10.13 | Carried end-to-end traffic per multihop connection vs. offered load. The applied PHY mode is QPSK 1/2 for both, control and data frames. | 162 |
| 10.14 | Mean end-to-end queueing delay per multihop connection vs. offered load. The applied PHY mode is QPSK 1/2 for both, control and data frames. | 163 |
| 10.15 | CDF of queueing delay per hop for 0.75 Mbit/sec offered load per connection. The applied PHY mode is QPSK 1/2 for both, control and data frames. | 164 |

| | | |
|-------|---|-----|
| 10.16 | CDF of queueing delay per hop for 1.25 Mbit/sec offered load per connection. The applied PHY mode is QPSK 1/2 for both, control and data frames. | 165 |
| 10.17 | CDF of end-to-end delay per multihop connection for 0.75 Mbit/sec offered load per connection. The applied PHY mode is QPSK 1/2 for both, control and data frames. | 166 |
| 10.18 | CDF of end-to-end delay per multihop connection for 1.25 Mbit/sec offered load per connection. The applied PHY mode is QPSK 1/2 for both, control and data frames. | 167 |
| 10.19 | Carried end-to-end per multihop connection for DCF and C-DCF. The applied PHY mode is QPSK 1/2 for both, control and data frames. | 168 |
| 10.20 | Complementary CDF of end-to-end delay per multihop connection for DCF and C-DCF. The offered load is CBR, 0.75 Mbit/sec/con and the applied PHY mode is QPSK 1/2 for both, control and data frames. | 169 |
| 11.1 | Centralized mode functionality of the protocol. | 172 |
| 11.2 | Beacon for centralized mode. | 173 |
| 11.3 | RTSapp for centralized mode. | 173 |
| 11.4 | CTScum for centralized mode. | 174 |
| 11.5 | Data transmission in CP and CFP. | 175 |
| 11.6 | Simulated scenario with AP controlling channel access. | 179 |
| 11.7 | Carried traffic in the network for the two operating modes and total carried traffic. The applied PHY mode is 64QAM 3/4 for data frames and QPSK 1/2 for control frames. | 179 |
| 11.8 | Carried traffic per connection over offered load for the centralized mode. Left for set A, right for set B. The applied PHY mode is 64QAM 3/4 for data frames and QPSK 1/2 for control frames. | 180 |
| 11.9 | Mean queueing delay over the offered load for the centralized mode. Left for set A, right for set B. The applied PHY mode is 64QAM 3/4 for data frames and QPSK 1/2 for control frames. | 181 |
| 11.10 | Mean service time over the offered load for the centralized mode. Left for set A, right for set B. The applied PHY mode is 64QAM 3/4 for data frames and QPSK 1/2 for control frames. | 182 |

11.11 CDF of queueing delay per MS with 2.8 Mbit/sec/MS Poisson distributed offered load. The applied PHY mode is 64QAM 3/4 for data frames and QPSK 1/2 for control frames. 182

11.12 CDF of queueing delay at MS 6, in different proportions of mixed operation. The applied PHY mode is 64QAM 3/4 for data frames and QPSK 1/2 for control frames. 183

A.1 Relative delays of different users' symbols. 189

LIST OF TABLES

| | | |
|------|--|-----|
| 2.1 | IEEE 802.11a PHY layer parameters. | 19 |
| 2.2 | U-NII Frequency bands and allowed emissions. | 20 |
| 4.1 | Distance spectra. | 36 |
| 4.2 | PHY modes. | 37 |
| 4.3 | PHY layer parameters. | 38 |
| 5.1 | Number of multi-carrier symbols per frame. | 65 |
| 5.2 | Durations. | 66 |
| 5.3 | Parameters of the wideband channel for high speed WLANs at 5.25 GHz. | 68 |
| 5.4 | Values of interframe spaces adopted to the wideband channel. | 69 |
| 7.1 | Simulation parameters. | 80 |
| 8.1 | Throughput per connection. | 134 |
| 8.2 | Mean queueing delay per connection. | 135 |
| 9.1 | Interframe space durations for isochronous network operation. | 138 |
| 11.1 | CFP parameters. | 176 |
| 11.2 | CFP Throughput vs. superframe length for 1024 byte long data packets. | 177 |
| B.1 | Index of used mathematical symbols | 205 |

GLOSSARY

- Rayleigh fading** The type of fading, where the magnitude of the received complex envelope follows the Rayleigh distribution at any time. This is the case in scattering environments without a *Line of Sight* (LoS) component. In this case the composite signal consists of a large number of plane waves and both the real and imaginary part of the received complex envelope are independent, identically distributed, zero-mean Gaussian random variables.
- Q-function** $Q(x)$ is defined as the probability that a Gaussian random variable X , with zero mean and unit variance, exceeds the value of x .
- Normalized frequency offset** The ratio of the maximum oscillator offset to the subcarrier spacing.

NOMENCLATURE

Table B.1: Index of used mathematical symbols

| Mathematical symbol | Area | Page | Meaning |
|---------------------|----------------|------|---|
| d_{free} | Modulation | 36 | Free distance of the convolutional code |
| $b_k(i)$ | Modulation | 32 | k-th user's i-th modulated symbol |
| M_s | Modulation | 32 | Number of subcarriers |
| SF | Modulation | 32 | Spreading factor |
| K | Modulation | 32 | Number of active users |
| a_k | Modulation | 32 | Transmission power of user k |
| $p(t)$ | Modulation | 32 | Rectangular pulse over $[0, T)$ |
| g_1, g_2 | Channel coding | 34 | Generator polynoms of the convolutional code |
| T | Modulation | 32 | Multi-carrier symbol duration |
| τ_k | Modulation | 32 | Relative delay of user k to the reference user |
| $\eta(t)$ | Modulation | 32 | Gaussian noise |
| β_{km} | Modulation | 33 | Rayleigh distributed random amplitude for the k-th user at the m-th subcarrier |
| ϕ_{km} | Modulation | 33 | Uniform distributed random phase coefficient for the k-th user at the m-th subcarrier |
| y_n | Modulation | 33 | Demodulator output at the n-th subcarrier |
| w_m | Modulation | 33 | MUD weight for the m-th subcarrier |
| T_s | Modulation | 34 | Duration of multi-carrier symbol without cyclic prefix |
| T_{CP} | Modulation | 34 | Cyclic prefix duration |
| a_{CP} | Modulation | 34 | Power reduction factor due to cyclic prefix |
| M | Modulation | 35 | Modulation order |
| E_{av} | Modulation | 35 | Energy per bit |

Continued in next page

Table B.1: Index of used mathematical symbols*Continued from previous page*

| Mathematical symbol | Area | Page | Meaning |
|----------------------------|---------------------|-------------|---|
| N_0 | Modulation | 35 | Noise power |
| P_b | Channel coding | 35 | BER |
| $P_e^m(L)$ | Channel coding | 35 | PER upper bound for packet length L |
| L_b | Channel coding | 35 | Packet length in bits |
| P_u^m | Channel coding | 35 | First event error probability |
| a_d | Channel coding | 36 | Total number of errors with weight d |
| P_d | Channel coding | 36 | Probability of error on the pairwise comparison of paths which differ in d bits |
| P_c | Modulation | 39 | Carrier strength at the receiver |
| P_I | Modulation | 39 | Total interference power at the receiver |
| G_{sp} | Modulation | 39 | Spreading gain |
| p'_{nk} | Multiuser Detection | 189 | Contribution of the k-th user's (i-1)-th symbol to the signal received at the n-th subcarrier |
| p_{nk} | Multiuser Detection | 189 | Contribution of the k-th user's i-th symbol to the signal received at the n-th subcarrier |
| z_n | Multiuser Detection | 189 | Gaussian noise samples at the n-th demodulator output |
| \mathbf{y} | Multiuser Detection | 190 | Matrix of demodulator outputs |
| \mathbf{A} | Multiuser Detection | 190 | Matrix of users' transmission power |
| \mathbf{b} | Multiuser Detection | 190 | Matrix of users' symbols |
| \mathbf{P} | Multiuser Detection | 190 | Matrix, input to Multiuser detector |
| \mathbf{z} | Multiuser Detection | 190 | Matrix of Gaussian noise samples at the demodulator outputs |
| CW | MAC | 10 | Contention window value |
| CW_{min} | MAC | 10 | Contention window minimum value |
| CW_{max} | MAC | 10 | Contention window maximum value |

Continued in next page

Table B.1: Index of used mathematical symbols*Continued from previous page*

| Mathematical symbol | Area | Page | Meaning |
|---------------------|---------------|------|---|
| gt | Channel model | 74 | Transmitter antenna gain in dB |
| gr | Channel model | 74 | Receiver antenna gain in dB |
| λ | Channel model | 74 | Wavelength in meters |
| γ | Channel model | 74 | Path loss factor |
| d | Channel model | 74 | Distance between two MS in m |
| N_c | Spreading | 23 | Number of chips |
| T_b | Modulation | 17 | Duration of modulation pulse |
| B | Spreading | 28 | Matrix of users' symbols |
| C | Spreading | 28 | Spreading matrix |
| S | Spreading | 28 | Matrix of subcarrier symbols in downlink MC-CDMA |
| $c_k(i)$ | Spreading | 28 | i-th element of k-th spreading sequence |
| s_k | Spreading | 28 | composite symbol at the k-th subcarrier |
| $maxSINR$ | Power control | 55 | Maximum achievable SINR under the current interference situation of the receiver |
| P_{IF}^{MSk} | Power control | 55 | Estimated interference at MS k |
| $maxP_{TX}$ | Power control | 55 | Maximum allowed transmission power |
| P_{TX}^{MSk} | Power control | 55 | Transmission power used from MS k |
| $minSINR$ | Power control | 55 | Minimum SINR required for the use of a specific PHY-mode |
| L | Power control | 74 | Pathloss |
| P_{RX}^{RTS} | Power control | 55 | Receive power for RTS frame |
| P_{RX}^{CTS} | Power control | 55 | Receive power for CTS frame |
| P_{MeanIF} | Power control | 55 | Mean interference estimate of a MS |
| P_{LastIF} | Power control | 55 | Last interference estimate of a MS |
| a_{IF} | Power control | 51 | Weight for the contribution of the latest interference estimate to total estimate of a MS |
| B_{TS} | Backoff | 59 | Number of backoff slots |
| N_s | PHY | 65 | Number of multi-carrier symbols required for the transmission of a frame |

Continued in next page

Table B.1: Index of used mathematical symbols*Continued from previous page*

| Mathematical symbol | Area | Page | Meaning |
|----------------------------|-------------|-------------|--|
| N_b | PHY | 64 | Number of data bits per multi-carrier symbol |
| N_p | MAC | 176 | Number of data packets per superframe and code channel in C-DCF centralized mode |
| ΔT_{SF} | MAC | 176 | Duration of a superframe in C-DCF centralized mode |
| N_{p11e} | MAC | 177 | Number of data packets per superframe and code channel in IEEE 802.11e |
| ΔT_{SF11e} | MAC | 177 | Duration of a superframe in IEEE 802.11e |

LIST OF ABBREVIATIONS

| | | | |
|-------|--|---------|--|
| 3GPP | 3rd <u>G</u> eneration <u>P</u> artnership <u>P</u> roject | CDF | <u>C</u> umulative <u>D</u> istribution <u>F</u> unction |
| ABMT | <u>A</u> achener <u>B</u> eiträge zur <u>M</u> obil- und <u>T</u> elekommunikation | CF | <u>C</u> ontention <u>F</u> ree |
| ACK | <u>A</u> cknowledgement | CFP | <u>C</u> ontention <u>F</u> ree <u>P</u> eriod |
| ADT | <u>A</u> bstract <u>D</u> ata <u>T</u> ypes | CP | <u>C</u> yclic <u>P</u> refix |
| APs | <u>A</u> ccess <u>P</u> oints | CP | <u>C</u> ontention <u>P</u> eriod |
| AP | <u>A</u> ccess <u>P</u> oint | CRC | <u>C</u> yclic <u>R</u> edundancy <u>C</u> heck |
| AWGN | <u>A</u> dditive <u>W</u> hite <u>G</u> aussian <u>N</u> oise | CSMA/CA | <u>C</u> arrier <u>S</u> ense <u>M</u> ultiple <u>A</u> ccess with <u>C</u> ollision <u>A</u> voidance |
| BPSK | <u>B</u> inary <u>P</u> hase <u>S</u> hift <u>K</u> eying | CTS | <u>C</u> lear <u>T</u> o <u>S</u> end |
| BER | <u>B</u> it <u>E</u> rror <u>R</u> ate | CTScum | <u>C</u> lear <u>T</u> o <u>S</u> end cumulative |
| BRAN | <u>B</u> roadband <u>R</u> adio <u>A</u> ccess <u>N</u> etwork | CW | <u>C</u> ontention <u>W</u> indow |
| BSS | <u>B</u> asic <u>S</u> ervice <u>S</u> et | DA | <u>D</u> estination <u>A</u> ddress |
| BSSID | <u>B</u> asic <u>S</u> ervice <u>S</u> et <u>I</u> Dentification | DCF | <u>D</u> istributed <u>C</u> oordination <u>F</u> unction |
| C-DCF | <u>C</u> oded- <u>D</u> istributed <u>C</u> oordination <u>F</u> unction | DIFS | <u>D</u> istributed <u>C</u> oordination <u>F</u> unction |
| CA | <u>C</u> ollision <u>A</u> voidance | | <u>I</u> nter <u>F</u> rame <u>S</u> pace |
| CAP | <u>C</u> ontrolled <u>A</u> ccess <u>P</u> hase | DLC | <u>D</u> ata <u>L</u> ink <u>C</u> ontrol |
| CBR | <u>C</u> onstant <u>B</u> it <u>R</u> ate | DS | <u>D</u> irect <u>S</u> equene |
| cch | <u>c</u> ode <u>ch</u> annel | DS-CDMA | <u>D</u> irect <u>S</u> equene- <u>C</u> ode <u>D</u> ivision <u>M</u> ultiple |
| cchs | <u>c</u> ode <u>ch</u> annels | | <u>A</u> ccess |
| CDM | <u>C</u> ode <u>D</u> ivision <u>M</u> ultiplex | DS-SS | <u>D</u> irect <u>S</u> equene- <u>S</u> pread <u>S</u> pectrum |
| CDMA | <u>C</u> ode <u>D</u> ivision <u>M</u> ultiple <u>A</u> ccess | | |

| | | | |
|-------|---|------------|---|
| EDCA | <u>E</u> nhanced <u>D</u> istributed <u>C</u> hannel <u>A</u> ccess | ISO | <u>I</u> nternational <u>S</u> tandards <u>O</u> rganization |
| EIFS | <u>E</u> xtended <u>I</u> nter <u>F</u> rame <u>S</u> pace | LoS | <u>L</u> ine of <u>S</u> ight |
| ESS | <u>E</u> xtended <u>S</u> ervice <u>S</u> et | LRC | <u>L</u> ong <u>R</u> etry <u>C</u> ounter |
| ETSI | <u>E</u> uropean <u>T</u> elecommunications <u>S</u> tandards <u>I</u> nstitute | LRE | <u>L</u> imited <u>R</u> elative <u>E</u> rror |
| FCS | <u>F</u> rame <u>C</u> heck <u>S</u> equence | MAC | <u>M</u> edium <u>A</u> ccess <u>C</u> ontrol |
| FDM | <u>F</u> requency <u>D</u> ivision <u>M</u> ultiplex | MAI | <u>M</u> ultiple <u>A</u> ccess <u>I</u> nterference |
| FDMA | <u>F</u> requency <u>D</u> ivision <u>M</u> ultiple <u>A</u> ccess | MC | <u>M</u> ulti- <u>C</u> arrier |
| FFT | <u>F</u> ast <u>F</u> ourier <u>T</u> ransform | MC-CDMA | <u>M</u> ulti- <u>C</u> arrier <u>C</u> ode <u>D</u> ivision <u>M</u> ultiple <u>A</u> ccess |
| FH-SS | <u>F</u> requency <u>H</u> opping- <u>S</u> pread <u>S</u> pectrum | MC DS-CDMA | <u>M</u> ulti- <u>C</u> arrier <u>D</u> irect <u>S</u> equence <u>C</u> ode <u>D</u> ivision <u>M</u> ultiple <u>A</u> ccess |
| GSM | <u>G</u> lobal <u>S</u> ystem for <u>M</u> obile <u>C</u> ommunication | MMSE | <u>M</u> inimum <u>M</u> ean <u>S</u> quare <u>E</u> rror |
| HC | <u>H</u> ybrid <u>C</u> oordinator | MPEG | <u>M</u> oving <u>P</u> icture <u>E</u> xperts <u>G</u> roup |
| IBSS | <u>I</u> ndependent <u>B</u> asic <u>S</u> ervice <u>S</u> et | MS | <u>M</u> obile <u>S</u> tation |
| ICI | <u>I</u> nter <u>C</u> arrier <u>I</u> nterference | MSs | <u>M</u> obile <u>S</u> tations |
| ID | <u>I</u> Dentification | MSDU | <u>M</u> AC sublayer <u>S</u> ervice <u>D</u> ata <u>U</u> nit |
| IEEE | <u>I</u> nstitute of <u>E</u> lectrical and <u>E</u> lectronics <u>E</u> ngineers | MUD | <u>M</u> ultiuser <u>D</u> etector |
| IFFT | <u>I</u> nverse <u>F</u> ast <u>F</u> ourier <u>T</u> ransform | NAV | <u>N</u> etwork <u>A</u> llocation <u>V</u> ector |
| IFS | <u>I</u> nter <u>F</u> rame <u>S</u> paces | OFDM | <u>O</u> rthogonal <u>F</u> requency <u>D</u> ivision <u>M</u> ultiplexing |
| IS | <u>I</u> nter <u>F</u> rame <u>S</u> pace | OFDMA | <u>O</u> rthogonal <u>F</u> requency <u>D</u> ivision <u>M</u> ultiple <u>A</u> ccess |
| ISI | <u>I</u> nter- <u>S</u> ymbol <u>I</u> nterference | OSI | <u>O</u> pen <u>S</u> ystems <u>I</u> nterconnection |
| ISM | <u>I</u> ndustrial <u>S</u> cientific and <u>M</u> edical bands | PC | <u>P</u> oint <u>C</u> oordinator |

| | | | |
|-------------|--|---------|---|
| PCF | <u>P</u> oint <u>C</u> oordination <u>F</u> unction | SER | <u>S</u> ymbol <u>E</u> rror <u>R</u> ate |
| PCN | <u>P</u> ersonal <u>C</u> ommunication <u>N</u> etworks | SF | <u>S</u> preading <u>F</u> actor |
| PDU | <u>P</u> rotocol <u>D</u> ata <u>U</u> nit | SIC | <u>S</u> uccessive <u>I</u> nterference <u>C</u> ancellation |
| PER | <u>P</u> acket <u>E</u> rror <u>R</u> ate | SIFS | <u>S</u> hort <u>I</u> nter <u>F</u> rame <u>S</u> pace |
| PHY | <u>P</u> hysical <u>L</u> ayer | SINR | <u>S</u> ignal to <u>I</u> nterference and <u>N</u> oise <u>R</u> atio |
| PIC | <u>P</u> arallel <u>I</u> nterference <u>C</u> ancellation | SOHO | <u>S</u> mall <u>O</u> ffice/ <u>H</u> ome <u>O</u> ffice |
| PIFS | <u>P</u> oint <u>C</u> oordination <u>F</u> unction <u>I</u> nterframe <u>S</u> pace | SPEETCL | <u>S</u> DL <u>P</u> erformance <u>E</u> valuation <u>T</u> ool <u>C</u> lass <u>L</u> ibrary |
| PLCP | <u>P</u> hysical <u>L</u> ayer <u>C</u> onvergence <u>P</u> rotocol | SRC | <u>S</u> hort <u>R</u> etry <u>C</u> ounter |
| PMD | <u>P</u> hysical <u>M</u> edium <u>D</u> ependent | SSID | <u>S</u> ervice <u>S</u> et <u>I</u> dentification |
| PN | <u>P</u> seudo <u>N</u> oise | SS | <u>S</u> pread <u>S</u> pectrum |
| PSK | <u>P</u> hase <u>S</u> hift <u>K</u> eysing | TBTT | <u>T</u> arget <u>B</u> eacon <u>T</u> ransmission <u>T</u> ime |
| QAM | <u>Q</u> uadrature <u>A</u> mplitude <u>M</u> odulation | TDM | <u>T</u> ime <u>D</u> ivision <u>M</u> ultiplex |
| QoS | <u>Q</u> uality of <u>S</u> ervice | TDMA | <u>T</u> ime <u>D</u> ivision <u>M</u> ultiple <u>A</u> ccess |
| QoS-CF-Poll | <u>Q</u> uality of <u>S</u> ervice- <u>C</u> ontention <u>F</u> ree- <u>P</u> oll | TPC | <u>T</u> ransmit <u>P</u> ower <u>C</u> ontrol |
| QPSK | <u>Q</u> uaternary <u>P</u> hase <u>S</u> hift <u>K</u> eysing | TP | <u>T</u> ransmit <u>P</u> ower |
| RF | <u>R</u> adio <u>F</u> requency | TSF | <u>T</u> ime <u>S</u> ynchronization <u>F</u> unction |
| RTS | <u>R</u> eady <u>T</u> o <u>S</u> end | UMTS | <u>U</u> niversal <u>M</u> obile <u>T</u> elecommunication <u>S</u> ystem |
| RTSapp | <u>R</u> eady <u>T</u> o <u>S</u> end application | U-NII | <u>U</u> nlicensed- <u>N</u> ational <u>I</u> nformation <u>I</u> nfrastructure |
| SA | <u>S</u> ource <u>A</u> ddress | W-CDMA | <u>W</u> ideband- <u>C</u> ode <u>D</u> ivision <u>M</u> ultiple <u>A</u> ccess |
| SAP | <u>S</u> ervice <u>A</u> ccess <u>P</u> oint | | |
| SDL | <u>S</u> pecification and <u>D</u> escription <u>L</u> anguage | | |
| SDU | <u>S</u> ervice <u>D</u> ata <u>U</u> nit | | |
| SDM | <u>S</u> pace <u>D</u> ivision <u>M</u> ultiplex | | |

| | | | |
|--------|---|------|--|
| WIGWAM | <u>W</u> ireless <u>G</u> igabit <u>w</u> ith <u>A</u> dvanced <u>M</u> ultimedia Support | | <u>N</u> etwork |
| WPAN | <u>W</u> ireless <u>P</u> ersonal <u>A</u> rea | WLAN | <u>W</u> ireless <u>L</u> ocal <u>A</u> rea <u>N</u> etwork |

LIST OF UNPUBLISHED DOCUMENTS

This list refers, in contrary to the bibliography, to unpublished documents. It consists of references to diploma and student project thesis, which represent a decisive part of this dissertation and have been supervised by the author himself at the chair of Communication Networks.

- W. BUTSCH. *Adaptive MAC-Protocol with QoS Consideration for MultiCarrier-CDMA based W-LANs*. Diploma thesis, Aachen University, Chair of Communication Networks, Juni 2004. Cited on p. 61.
- E.-S. KUMAR. *Development of a Centralized Mode for MC-CDMA Wireless LANs Supporting Quality of Service*. Mastersthesis, Aachen University, Chair of Communication Networks, October 2005. Cited on p. 174.
- A. KWUIMO. *Multihop Extension of MC-CDMA based IEEE 802.11 W-LANs*. Diploma thesis, Aachen University, Chair of Communication Networks, October 2005. Cited on p. 151.
- L. LIU. *Performance Evaluation of MC-CDMA in Rayleigh Fading Channels*. Student project thesis, Aachen University, Chair of Communication Networks, January 2003a. Cited on p. 28.
- L. LIU. *Simulative Performance Evaluation of MultiCarrier-CDMA based W-LAN*. Mastersthesis, Aachen University, Chair of Communication Networks, September 2003b. Cited on p. 44.
- H. SIRIN. *Implementation and simulative Evaluation of Power Adjustment in MultiCarrier-CDMA based W-LAN*. Student project thesis, Aachen University, Chair of Communication Networks, February 2004. Cited on p. 50.

BIBLIOGRAPHY

- 3GPP TS 25.301. *Radio Interface Protocol Architecture*. Technical Specification V5.0.0, Release 4, 3rd Generation Partnership Project, Technical Specification Group Radio Access Network, March 2002. Cited on p. 23.
- STD. 802.11. *Wireless LAN Medium Access Control (MAC) and physical layer (PHY) specifications: Wireless LAN Medium Access Control (MAC) and physical layer (PHY) specifications, Technical Specification, IEEE LAN/MAN Standard Comitee*. IEEE, July 1999. Cited on p. 8, 10, 16, 174, 176.
- STD. 802.11A /D7. *Wireless LAN Medium Access Control (MAC) and physical layer (PHY) specifications: High Speed Physical Layer in the 5GHz band. Draft Supplement to IEEE 802.11-1999, Technical Specification, IEEE LAN/MAN Standard Comitee*. IEEE, July 1999. Cited on p. 1, 3, 8, 21, 34, 35, 37, 39, 43, 65, 69, 121.
- STD. 802.11E /D9. *Wireless LAN Medium Access Control (MAC) and physical layer (PHY) specifications: Medium Access Control (MAC) Enhancements for Quality of Service (QoS), Technical Specification, IEEE LAN/MAN Standard Comitee*. IEEE, August 2004. Cited on p. 21, 37, 59, 172, 173, 176, 177.
- STD. 802.11G. *Wireless LAN Medium Access Control (MAC) and physical layer (PHY) specifications: Amendment 4: Further Higher Data Rate Extension in the 2.4 GHz Band, IEEE Computer Society, Sponsored by LAN/MAN Standards Committee*. IEEE, June 2003. Cited on p. 1, 8.
- STD. 802.11H /D2.0. *Wireless LAN Medium Access Control (MAC) and physical layer (PHY) specifications: Spectrum and Transmit Power Management extensions in the 5 GHz Band in Europe, IEEE Computer Society, Sponsored by LAN/MAN Standards Committee*. IEEE, June 2003. Cited on p. 46.
- N. ABRAMSON. *The ALOHA system - Another alternative for computer communications*. In *Proceedings of American Federation of Information Processing Societies (AFIPS) Conference*, Band 37, S. 281–285, 1970. Cited on p. 138.
- N. ABRAMSON and S. LAM. *VSAT Data Networks*, Bd. 78. S. 1267–1274, 1990. Cited on p. 120.

- A. ACHARYA, A. MISRA and S. BANSAL. *High-Performance Architectures for IP-Based Multihop 802.11 Networks*. *Wireless Communications*, S. 22–28, October 2003. Cited on p. 151.
- S. AGARWAL, S.V. KRISHNAMURTHY, R.K. KATZ and S.K. DAO. *Distributed Power Control in Ad-Hoc Wireless Networks*. In *Proceedings of the Personal Indoor Radio Communications Conference, IEEE PIMRC'01*, S. 59–66, 2001. Cited on p. 49, 50.
- AIXCOM. *Formale Spezifikation und Leistungsbewertung von Protokollen*. Available over www at <http://www.aixcom.com/Produkte/Speet>, 2002. Cited on p. 71, 73.
- I. AKYILDIZ, J. MCNAIR, L.C. MARTORELL, R. PUIGJANER and Y. YESHA. *Medium Access Control Protocols for Multimedia Traffic in Wireless Networks*. *Network*, S. 39–47, July/August 1999. Cited on p. 74.
- J. ANDREWS and T. MENG. *Performance of Multicarrier CDMA with Successive Interference Cancellation in a Multipath Fading Channel*. *Trans. on Communications*, Bd. 52, S. 811–822, May 2004. Cited on p. 60.
- N. BENVENUTO and P. BISAGLIA. *Parallel and successive interference cancellation for MC-CDMA and their near-far resistance*. In *The 58th Semiannual Vehicular Technology Conference, VTC 2003 Fall*, 2003. IEEE. Cited on p. 60.
- I. COSOVIC. *Uplink Multi-Carrier CDMA Mobile Radio Systems*. Media-graf, 2005, ISBN 86-7658-008-1. Cited on p. 31, 41.
- J.-H. DENG and T.-S. LEE. *An iterative Maximum SINR Receiver for Multicarrier CDMA Systems over a Multipath Fading Channel With Frequency Offset*. *Trans. on Communications*, Bd. 51, S. 560–569, May 2003. Cited on p. 60.
- A. DUEL-HALLEN, J. HOLTZMAN and Z. ZVONAR. *Multiuser Detection for CDMA Systems*, Bd. 2. S. 46–58, 1995. Cited on p. 50.
- J.-P. EBERT and A. WOLISZ. *Combined Tuning of RF Power and Medium Access Control for WLANs*. *Mobile Networks and Applications*, Bd. 5, September 2001. Cited on p. 49.
- F.H.P. FITZEK and M. REISSLEIN. *MPEG-4 and H.263 Video Traces for Network Performance Evaluation*. *Network*, Bd. 15, S. 40–54, Nov./Dec. 2001. Cited on p. 74.
- P. FRENGER, P. ORTEN and T. OTTOSON. *Convolutional codes with optimum distance spectrum*. *Communications Letters*, Bd. 3, S. 317–319, November 1999. Cited on p. 35.

- L. HANZO, M. MÜNSTER, B.-J. CHOI and KELLER T.. *OFDM and MC-CDMA for Broadband Multi-User Communications, WLANs and Broadcasting*. John Willey and Sons Ltd., Chichester, West Sussex, England, 2003a, ISBN 0-470-85879-6. Cited on p. 32.
- L. HANZO, L.-L. YANG, E.-L. KUAN and YEN K.. *Single- and Multi-Carrier DS-CDMA, Multi-User Detection, Space-Time Spreading, Synchronization and Standards*. John Willey and Sons Ltd., Chichester, West Sussex, England, 2003b, ISBN 0-470-86309-9. Cited on p. 32.
- S. HARA and R. PRASAD. *Overview of MC-CDMA*. *Communications Magazine*, Bd. 35, S. 104–108, April 1997. Cited on p. 25, 27, 33.
- S. HARA and R.. PRASAD. *Design and Performance of Multicarrier CDMA System in Frequency-Selective Rayleigh Fading Channels*. *Transactions on Vehicular Technology*, Bd. 48, S. 1584–1595, Sept 1999. Cited on p. 27.
- S. HEIER. *Leistungsbewertung der UMTS Funkschnittstelle*. Dissertation, Aachen University, 2003, ISBN 3-86073-167-9. Cited on p. 24, 173.
- A. HETTICH. *Leistungsbewertung des Standards HIPERLAN/2 und IEEE 802.11 für drahtlose lokale Netze*. Dissertation, Aachen University, 2001, ISBN 3-86073-824-0. Cited on p. 15.
- HIPERLAN2. *Hiperlan Type 2, Functional Specification Part 1 - Physical (PHY) layer. DraftDTS/BRAN030003-1*. ETSI BRAN, Sophia Antipolis, France, 1999, ISBN -. Cited on p. 21, 37.
- M. JANKIRAMAN and R. PRASAD. *A Novel Solution to Wireless Multimedia Application: the Hybrid OFDM/CDMA/SFH Approach*. In *Proceedings of IEEE Personal Indoor Mobile Radio Communications, PIMRC 2000*, S. 212–215, Feb. 2000. Cited on p. 31.
- E.-S. JUNG and N.H. VAIDYA. *An Energy Efficient MAC Protocol for Wireless LANs*. In *Proceedings of the Conference on Computer Communications, IEEE INFOCOM'02*, New York City, NY, 2002. Cited on p. 49.
- L. KLEINROCK and S. LAM. *Packet Switching in a Multiple Broadcast Channel: Performance Evaluation*, Bd. 23. S. 410–423, 1975. Cited on p. 138.
- J. LINDNER. *MC-CDMA and its Relation to General Multiuser/Multisubchannel Transmission Systems*, Bd. 1. S. 115–121, September 1996. Cited on p. 2.
- J.-P. LINNARTZ. *Performance Analysis of Synchronous MC-CDMA in Mobile Rayleigh Channel With Both Delay and Doppler Spreads*. *Transac-*

- tions on Vehicular Technology*, Bd. 50, S. 1375–1387, November 2001. Cited on p. 2, 26.
- Z. LIU and M. EL ZARKI. *Performance Analysis of DS-CDMA with Slotted ALOHA Random Access for Packet PCNs*. In *The 5th Annual IEEE International Symposium on Personal Indoor and Mobile Radio Communications*, Sep. 1994. Cited on p. 120.
- S. MANGOLD. *Analysis of IEEE 802.11 and Application of Game Models for Support of Quality-of-Service in Coexisting Wireless Networks*. Dissertation, Aachen University, 2003, ISBN 3-86073-985-9. Cited on p. 10, 46.
- C.R. NASSAR, B. NATARAJAN, Z. WU, WIEGANDT D., S.A. ZEKAVAT and S. SHATTIL. *Multi-Carrier Technologies for Wireless Communication*. Kluwer Academic Publishers, 2002, ISBN 0-7923-7618-8. Cited on p. 25.
- Q. NI, L. ROMDHANI and T. TURLETTI. *A Survey of QoS Enhancements for IEEE 802.11 Wireless LAN*, Bd. 4. S. 547–566, 2004. Cited on p. 184.
- G. ORFANOS, J. HABETHA and W. BUTSCH. *Efficient Power Control for MC-CDMA based W-LANs*. In *Proceedings of 11th European Wireless Conference 2005*, Band 1, S. 365–371, Nicosia, Cyprus, Apr 2005a. ISBN 3-8007-2886-9. Cited on p. 51.
- G. ORFANOS, J. HABETHA and W. BUTSCH. *Error Probabilities for Radio Transmissions in MC-CDMA Wireless LANs*. In *Proceedings of the 65th IEEE Vehicular Technology Conference, VTC Spring 2005*, Stockholm, Sweden, May 2005b. ISBN 0-7803-8888-7. Cited on p. 36, 99.
- G. ORFANOS, J. HABETHA and W. BUTSCH. *A new Distributed Coordination Function Adapted to Mc-CDMA based W-LANs*. In *Proceedings of 11th European Wireless Conference 2005*, Band 1, S. 372–377, Nicosia, Cyprus, Apr 2005c. ISBN 3-8007-2886-9. Cited on p. 124.
- G. ORFANOS, J. HABETHA and W. BUTSCH. *A new Distributed Coordination Function for W-LANs with multiple channel structure*. In *Proceedings of 14th IST Mobile & Wireless Communications Summit*, Dresden, Germany, Jun 2005d. Cited on p. 121.
- G. ORFANOS, J. HABETHA and L. LIU. *MC-CDMA based IEEE 802.11 Wireless LAN*. In *Proceedings of the Twelfth IEEE International Symposium on Modeling, Analysis, and Simulation of Computer and Telecommunication Systems, MASCOTS 2004*, S. 400–405, Volendam, Holland, Oct 2004a. ISBN 0-7695-2251-3. Cited on p. 41.
- G. ORFANOS, J. HABETHA and L. LIU. *A Modified IEEE 802.11 MAC Protocol for MC-CDMA*. In *Proceedings of the 1st ACM International Work-*

- shop on Evaluation of Wireless Ad Hoc, Sensor and Ubiquitous Networks PE-WASUN 2004*, S. 52–55, Venice, Italy, Oct 2004b. ISBN 1-58113-959-4. Cited on p. 45.
- G. ORFANOS, B. WALKE, W. BUTSCH and H.-J. REUMERMAN. *An Adaptive MAC Protocol for MC-CDMA Adhoc Wireless LANs*. In *The 16th Annual IEEE International Symposium on Personal Indoor and Mobile Radio Communications*, Berlin, Germany, Sept 2005e. ISBN 3-8007-2909-1. Cited on p. 61.
- G. ORFANOS, B. WALKE, J.-W. JANSEN and H.-J. REUMERMAN. *Interference Aware Adaptive MAC Protocol for MC-CDMA Adhoc Wireless LANs*. In *The 16th Annual IEEE International Symposium on Personal Indoor and Mobile Radio Communications*, Berlin, Germany, Sept 2005f. ISBN 3-8007-2909-1. Cited on p. 55.
- J. PEETZ. *Multihop-Ad-Hoc-Kommunikation mit dynamischer Frequenzwahl, Leistungssteuerung, und Ratenanpassung für drahtlose Netze im 5GHz Band*. Dissertation, Aachen, February 2003, ISBN 3-86073-984-0. Cited on p. 71.
- A. PERSSON. *On Convolutional Codes and Multi-Carrier Techniques for CDMA Systems*. Dissertation, Communication Systems Group, Department of Signals and Systems, School of Electrical Engineering, Chalmers University of Technology, Göteborg, Sweden, 2002. Cited on p. 26.
- H. V. POOR and S. VERDU. *Probability of Error in MMSE Multiuser Detection*, Bd. 43. S. 858–871, 1997. Cited on p. 31.
- R. PRASAD. *CDMA for Wireless Personal Communications*. Artech house Publishers, 1996, ISBN 0-89006-571-3. Cited on p. 21.
- J. PROAKIS. *Digital Communications*. McGraw-Hill, 2001, ISBN 0-07-232111-3. Cited on p. 34, 35, 36.
- D. QIAO, S. CHOI, A. JAIN and K. SHIN. *Adaptive Transmit Power Control in IEEE 802.11a Wireless LANs*. In *Proceedings of the 57th Semiannual Vehicular Technology Conference, IEEE VTC 2003 Spring*, April 2003. Cited on p. 50.
- F. SCHREIBER. *Effective Control of Simulation Runs by a New Evaluation Algorithm for Correlated Random Sequences*. *AEÜ International Journal of Electronics and Communications*, Bd. 42, S. 347–354, 1988. Cited on p. 89.
- T. SIMUNIC, L. BENINI, P. GLYNN and G. DEMICHELII. *Dynamic Power Management for Portable Systems*. In *Proceedings of the ACM Annual*

- International Conference on Mobile Computing and Networking, Mobi-com'00*, Boston, MA, August 2000. Cited on p. 49.
- N.-O. SONG, B.-J. KWAK, JABIN SONG and MILLER M.E.. *Enhancement of IEEE 802.11 distributed coordination function with exponential increase exponential decrease backoff algorithm*. In *Proceedings of the 57th Semiannual Vehicular Technology Conference, IEEE VTC 2003 Spring*, S. 2775–2778, April 2003. Cited on p. 46.
- G. STUEBER. *Principles of mobile communication*. Kluwer Academic Publishers, 2001, ISBN 0-7923-7998-5. Cited on p. 33, 36.
- A. TANENBAUM. *Computer Networks*. Prentice Hall PTR, 1996, ISBN 0-13-349945-6. Cited on p. 9.
- F. TUFVESSON. *Design of wireless communication systems-issues on synchronization, channel estimation and multi-carrier systems*. Dissertation, 2000, ISBN -. Cited on p. 34, 36.
- S. VERDU. *Optimum Multiuser Asymptotic Efficiency*, Bd. 34. S. 890–897, 1986. Cited on p. 31.
- B. WALKE. *Mobilfunknetze und ihre Protokolle*, Band 1. <http://www.teubner.de>, TEUBNER B.G., Stuttgart, 535 Seiten, ISBN 3-519-16430-0, 2000. Cited on p. 22.
- K. WANG, P. ZONG and Y. BAR-NESS. *A reduced complexity partial sampling MMSE receiver for asynchronous MC-CDMA systems*. In *Proceedings of GLOBECOM 2001*, 2001. Cited on p. 31, 33, 34, 60.
- Y. XIAODONG and H.H. FAN. *Near-far resistance of multicarrier CDMA systems*. *Signal Processing Letters*, Bd. 11, S. 212–215, February 2004. Cited on p. 59.
- N. YEE and J.-P. LINNARTZ. *Multi-Carrier CDMA in an Indoor Wireless Radio Channel*. Technical Memorandum UCB/ERL M94/6, University of California, 1994a. Cited on p. 21.
- N. YEE and J.-P. LINNARTZ. *Wiener filtering of multi-carrier CDMA in Rayleigh fading channel*. In *Proceedings of 5th IEEE International Symposium on Personal, Indoor and Mobile Radio Communications, 1994*, S. 18–23, The Hague, Netherlands, Sept 1994b. ISBN 90-5199-193-2. Cited on p. 28.
- N. YEE, J.-P. LINNARTZ and G. FETTWEIS. *Multicarrier CDMA in Indoor Wireless Radio Networks*. In *Proceedings of Personal Indoor Mobile Radio Communications, PIMRC 1993*, S. 109–113, Yokohame, Japan, Sept 1993. Cited on p. 27.

- S. YI, C. TSIMENIDIS, O. HINTON and O. SHARIF. *Adaptive minimum bit error rate multi-user detection for asynchronous MC-CDMA systems in frequency selective rayleigh fading channels*. In *Proc. IEEE PIMRC 2003*, 2003. Cited on p. 33, 60, 189, 190.
- Y. ZANG, L. STIBOR, G. ORFANOS, S. GUO and H.-J. REUMERMAN. *An Error Model for Inter-Vehicle Communication in Highway Scenario at 5.9GHz*. In *Proceedings of the 2nd ACM International Workshop on Evaluation of Wireless Ad Hoc, Sensor and Ubiquitous Networks PE-WASUN 2005*, Montreal, Qc. Canada, Oct 2005. ISBN 1-59593-182-1. Cited on p. .
- R. ZHAO, B. WALKE, M. EINHAUS and G. ORFANOS. *A Primary Adaptation of the W-CHAMB Protocol for Gigabit WPANs*. In *The 16th Annual IEEE International Symposium on Personal Indoor and Mobile Radio Communications*, Berlin, Germany, Sept 2005. ISBN 3-8007-2909-1. Cited on p. .

INDEX

Normally printed entries are related to the mentions in text. Italic entries represent the full form of abbreviations referred in the text, cf. the list of abbreviations on page 209.

Symbols

3GPP 23
3rd Generation Partnership Project ..
see 3GPP

A

Abstract Data Type see ADT
Access Point see AP
Access Points see APs
ACK .. 10, 16, 51, 55, 57, 69, 84, 151,
154, 174, 181
Acknowledgement see ACK
ADT 71, 73
AP ... 6, 14, 15, 97, 171–174, 178, 187
APs 4, 7

B

C

C-DCF . 4, 43, 46, 61, 68, 69, 71, 72,
79, 81, 88, 89, 116, 137, 149,
152, 154, 156, 164–166, 171–174,
176–178, 183, 185, 186
CA 10, 55
CAP 176, 177
Carrier Sense Multiple
Access/Collision Avoidance .. see
CSMA/CA
CBR 85, 165, 166

cch 4–6, 31, 43–47, 49–51, 57, 59, 60,
71, 74, 76, 79, 81–84, 91, 99,
100, 102, 104, 106, 107, 109, 113,
114, 119–124, 126–135, 137, 138,
151, 152, 156–161, 163, 165,
171–174, 176, 178, 183, 186
cchs 2
CDF 73, 85–89, 93, 96, 97, 131, 133,
134, 158, 160, 162–167, 181–183
CDM 22, 23
CDMA .. 1, 2, 21, 23, 25, 45, 49, 59,
119, 126, 135, 137, 149, 185, 186
Centralized mode of the C-DCF
171–184
CF 15
CFP 5, 9, 15, 172–174, 177, 178, 180,
181, 183, 184
Clear To Send see *CTS*
Ba Clear To Send cumulative see
CTScum
code channel see *cch*
code channels see *cchs*
Code Division Multiple Access ... see
CDMA
Code Division Multiplex ... see *CDM*
Coded-Distributed Coordination
Function 43
Coded-Distributed Coordination
Function see *C-DCF*
Collision Avoidance see *CA*
Conclusion 185

- Constant Bit Rate see *CBR*
- Contention Free see *CF*
- Contention Free Period see *CFP*
- Contention Period see *CP²*
- Contention Window see *CW*
- Controlled Access Phase see *CAP*
- CP* 28
- CP²* ... 5, 15, 172–174, 176–178, 180, 181, 183, 184
- CRC* 16
- Cross layer optimization of the C-DCF* 137–147
- CSMA/CA* 9, 55, 137, 138, 152
- CTS* ... 12, 13, 15, 16, 46, 47, 49–52, 54, 55, 57, 61, 63, 69, 138, 152, 154, 156, 186
- CTScum* 173, 174
- Cumulative Distribution Function see *CDF*
- CW* 10, 57, 59, 61, 81, 113, 165
- Cyclic Prefic see *CP*
- Cyclic Redundancy Check .. see *CRC*
- D**
- DA* 16
- Data Link Control see *DLC*
- DCF* 3, 4, 7–9, 11, 14–16, 19, 43–45, 59, 69, 121, 164–166
- Derivation of a closed form expression for the demodulator outputs* 189
- Destination Address see *DA*
- DIFS* 9, 11, 16, 45, 64, 121, 126, 138
- Direct Sequence see *DS*
- Direct Sequence-Code Division Multiple Access .. see *DS-CDMA*
- Direct Sequence-Spread Spectrum see *DS-SS*
- Distributed Coordination Function ... see *DCF*
- Distributed Coordination Function Interframe Space see *DIFS*
- DLC* 7
- DS-CDMA* ... 21, 23, 24, 26, 27, 120
- DS-SS* 8
- DS* 23
- E**
- EDCA* 59
- EIFS* 9
- Enhanced Distributed Channel Access see *EDCA*
- ESS* 7
- ETSI* 37
- European Telecommunications Standards Institute see *ETSI*
- Evaluation of the MC-CDMA physical layer performance* 31–41
- Extended Interframe Space . see *EIFS*
- Extended Service Set see *ESS*
- Extension for multihop* 168
- F**
- Fast Fourier Transform see *FFT*
- FCS* 9, 16
- FDM* 22
- FDMA* 2, 24, 135
- FFT* 19, 26, 28, 33
- FH-SS* 8
- Frame Check Sequence see *FCS*
- Frequency Division Multiple Access .. see *FDMA*
- Frequency Division Multiplex see *FDM*
- Frequency Hopping-Spread Spectrum . see *FH-SS*
- G**
- Glossary* 203
- H**
- HC* 176, 177
- Hybrid Coordinator see *HC*

- I**
- IBSS* 7, 14
 - ICI* 18
 - ID* 63
 - Identification see *ID*
 - IEEE 802.11a* 7–20
 - IEEE* 37, 40, 41
 - IFFT* 18, 25, 27
 - IFS* 9, 69
 - Independent Basic Service Set see *IBSS*
 - Industrial Scientific and Medical bands
see *ISM*
 - Institute of Electrical and Electronics
Engineers see *IEEE*
 - Inter-Symbol Infrference see *ISI*
 - InterCarrier Interference see *ICI*
 - Interframe Spaces see *IFS*
 - International Standards Organization
see *ISO*
 - Introduction* 1
 - Inverse Fast Fourier Transform ... see
IFFT
 - ISI* 17, 19, 28, 34, 37
 - ISM* 8
 - ISO* 73
- L**
- Limited Relative Error see *LRE*
 - Line of Sight see *LoS*
 - Long Retry Counter see *LRC*
 - LoS* 203
 - LRC* 11
 - LRE* 89
- M**
- MAC Extensions for Multihop* ... 149
 - MAC sublayer Service Data Unit . see
MSDU
 - MAC* 1–3, 5, 7, 9, 12, 15, 16, 20, 41,
43, 45, 46, 52, 55, 60, 61, 65–67,
69, 71, 72, 79, 87–90, 119, 120,
135, 137, 138, 143, 147, 149, 151,
152, 154, 157, 161, 164, 165, 171,
174, 185
 - MAI* .. 2, 4, 5, 24, 29, 31, 33, 37, 39,
49, 59, 71, 74, 79, 89, 90, 97,
100, 102, 104, 106, 107, 109, 111,
113, 114, 140, 141, 185, 186, 189
 - MC DS-CDMA* 25–27, 185
 - MC-CDMA* . 2, 3, 5, 6, 21, 25–28, 31,
32, 34, 37, 40, 41, 43, 44, 46, 47,
49, 50, 64–66, 69, 71, 72, 79, 81,
116, 119–121, 131, 137, 147, 185,
190
 - MC* 2
 - Medium Access Control see *MAC*
 - Minimum Mean Square Error see
MMSE
 - MMSE* 3, 31, 33, 59, 60, 74, 137, 185
 - Mobile Station see *MS*
 - Mobile Stations see *MSs*
 - Moving Picture Experts Group ... see
MPEG
 - MPEG* 74, 86, 87
 - MS* . 5, 7, 9–16, 24, 32, 43–47, 49–52,
54–57, 60, 62, 74, 79, 82, 84, 91,
96, 99, 107, 111, 116, 119–122,
124, 126, 128, 130, 132, 133, 135,
137–141, 143, 144, 146, 147, 149,
152, 154, 156–158, 161–163, 165,
166, 173, 174, 178, 181, 184, 185
 - MSDU* 81–84, 86, 87
 - MSs* 2
 - MUD* . 2, 3, 5, 29, 31, 33, 37, 39, 46,
49, 50, 74, 137, 139, 147,
185–187
 - Multi-Carrier see *MC*
 - Multi-Carrier Code Division Multiple
Access* 21–29
 - Multi-Carrier Code Division Multiple
Access see *MC-CDMA*

- Multi-Carrier Direct Sequence-Code
Division Multiple Access *see* *MC DS-CDMA*
- Multiple Access Interference *see* *MAI*
- Multisuser Detector *see* *MUD*
- N**
- NAV* 12, 15, 16, 45, 47, 121, 152, 156
- Network Allocation Vector .. *see* *NAV*
- New Backoff Procedures* 119–135
- Normalized frequency offset* 203
- O**
- OFDM* 2–4, 9, 17–19, 21, 25, 26, 28, 34, 35, 37, 45, 49, 64–66, 69, 72, 185
- OFDMA* 28
- Open Systems Interconnection *see* *OSI*
- Orthogonal Frequency Division
Multiple Access *see* *OFDMA*
- Orthogonal Frequency Division
Multiplexing *see* *OFDM*
- OSI* 73
- P**
- Packet Error Rate *see* *PER*
- Parallel Interference Cancellation . *see* *PIC*
- PC* 14, 15
- PCF* 7–9, 14, 15, 17
- PCN* 120
- PDU* 73, 76
- PER* 34, 39, 40, 76, 112
- Performance evaluation of C-DCF* 79
- Performance evaluation of the C-DCF* 116
- Personal Communication Networks ... *see* *PCN*
- Pha
- Q**
- Q-function 203
- QAM 34, 35, 60
- QoS-CF-Poll 177
- QoS .. 1, 5, 8, 54, 59, 60, 74, 102, 104, 112, 124, 134, 147, 181, 183–185, 187
- QPSK . 35, 39, 40, 60, 79, 82, 91, 107, 146, 157, 165
- Quadrature Amplitude Modulation* *see* QAM
- Quality of Service* *see* QoS
- Quality of Service-Contention Free-Poll* *see* QoS-CF-Poll
- Quaternary Phase Shift Keying* ... *see* QPSK
- R**
- Radio Frequency* *see* RF
- Rayleigh fading 203
- Ready To Send* *see* RTS
- Ready To Send application* *see* RTSapp
- RF 9
- RTS . 11–16, 46, 47, 49–52, 55, 57, 61, 64, 69, 81, 84, 114, 116, 138, 143, 152, 156, 186
- RTSapp 173
- S**
- SA 16
- SAP 20
- SDL Performance Evaluation Tool Class Library* *see* SPEETCL
- SDL 71–73
- SDM 22, 23
- SDU 16, 20, 65, 73
- SER 35
- Service Access Point* *see* SAP
- Service Data Unit* *see* SDU
- Service Set Identification* ... *see* SSID

- SF 23, 26, 29, 32, 46, 67, 183
Short Interframe Space see SIFS
Short Retry Counter see SRC
 SIC 60
 SIFS . 9, 10, 12, 15, 16, 138, 152, 154, 174
Signal to Interference and Noise Ratio see SINR
 SINR 31, 33, 34, 39, 40, 49–51, 54, 60, 61, 63, 74, 76, 90, 112, 141, 185, 190
Small Office Home Office . see SOHO
 SOHO 51, 79, 84, 107
Source Address see SA
Space Division Multiplex ... see SDM
Specification and Description Language see SDL
 SPEETCL 73
Spread Spectrum see SS
Spreading Factor see SF
 SRC 11
 SS 6, 120
 SSID 17
Successive Interference Cancellation .. see SIC
Symbol Error Rate see SER
- T**
- Target Beacon Transmission Time* see TBTT
 TBTT 14, 17, 172, 174
 TDM 22, 184
 TDMA 2, 9, 24
 The MACNET2 simulation tool 71–77
- Time Division Multiple Access* see TDMA
Time Division Multiplex ... see TDM
Time Synchronization Function ... see TSF
 TP 52
 TPC . 4, 46, 49–52, 61, 91, 93, 96, 97, 116, 128, 141, 144, 157, 186
Transmit Power see TP
Transmit Power Control see TPC
 TSF 14, 16, 138
- U**
- U-NII 8, 19
 UMTS 21, 23, 44
Universal Mobile Telecommunication System see UMTS
Unlicensed-National Information Infrastructure see U-NII
- W**
- W-CDMA 2, 23
Wideband-Code Division Multiple Access see W-CDMA
 WIGWAM 67, 88
Wireless Gigabit with Advanced Multimedia Support see WIGWAM
Wireless Local Area Network see WLAN
Wireless Personal Area Network .. see WPAN
- WLAN 1–7, 17, 21, 37, 40, 41, 43, 44, 67, 68, 71, 121, 126, 131, 139, 149
 WPAN 139, 143

CURRICULUM VITAE

Family name, Name Orfanos, Georgios

Date of birth 04.May.1976

Place of birth Athens, Greece

Nationality Greek

Studies:

1982–1988 Primary School

1988–1994 Gymnasium, German School of Thessaloniki

10/1995–09/2000 Studies, Aristoteles University of Thessaloniki, Polytechnic School, Faculty of Electrical and Computer Engineers, major in Telecommunications

12/2000–05/2006 Research assistant in Chair of Communication Networks, RWTH Aachen

ACKNOWLEDGEMENT

This thesis results from my work as research assistant at the Chair of Communication Networks at the RWTH Aachen University, Germany.

I would like to express my appreciation and special thanks to Prof. Dr.-Ing. Bernhard Walke, for whom I had the pleasure to work towards my PhD, for his friendly support and advices throughout these years.

Very special thanks go to my colleague Dipl.-Ing. Jelena Mirkovic for our cooperation, for checking this thesis and making valuable comments.

Further, I would like to thank all my colleagues at the Chair of Communication Networks, particularly Msc. Rui Zhao, Dipl.-Ing. Guido Hiertz and Dr.-Ing. Christian Becker for our fruitful discussions.

Sincere thanks go to my students Moez Ur Rehmann, Masud Tahir, Liu Ling, Hamza Sirin, Willi Butsch, Jan Wilem Jansen, Aurelien Kwuimo and Sumil Kumar Emmadi who contributed to my research during their studies at the chair.

Finally, I would like to thank my parents and my sister for their continuous support and love throughout my life.

Aachen, June 2006

Georgios Orfanos